# EFFECTS OF PATTERN AND PROCESS INTERACTIONS UPON LATERAL WATER AND MATTER FLUXES IN AGRICULTURAL LANDSCAPES

Habilitationsschrift zur Erlangung
der Lehrbefähigung im Fach Geographie
an der Mathematisch-Naturwissenschaftlichen
Fakultät der Universität zu Köln

vorgelegt von
Dr. Peter Fiener
aus Bonn

Köln 2009

CONTENTS

# FOREWORD

Attempting to understand the world around us has been fascinating mankind for millennia and is part of our human nature. However, human interest in investigating the environment is not solely based upon scientific interest, but is rather mainly a result of the need to utilize environmental resources. Thus, human impacts upon the environment have strongly changed the environment, its function and character. Amongst these impacts, human use and abuse of soils as a major environmental resource in agriculture is one of the most widespread and long-lasting. One vital problem (among many) that must be solved is how to maintain high agricultural productivity as a basis for living for a growing population without (irreversibly) damaging the environment at the same time. The environment is a very complex system and hence it is challenging to understand the sometimes subtle and unexpected interrelationships of its components and to recognize that stress in one area may have far-reaching effects in other areas. The fascination of this complexity, but also the optimism that with an improved understanding of the system at least some of the environmental problems resulting from modern agriculture can be mitigated and a more sustainable use can be established, is a fundamental motivation of my own research that focuses on lateral water and matter fluxes in agricultural landscapes.

Sustainable use of soil resources requires understanding of water and matter fluxes in agro-ecosystems. Particularly lateral fluxes are of great importance, since these fluxes result in the typically (often) irreversible translocation of matter and cause severe off-site damages. The manifold inactions and feedbacks of the involved processes and the large human impact upon this system require a holistic approach. Therefore, I have highly appreciated the opportunity of having been able to work in geographical, agronomical and hydrological research groups and being involved in several multidisciplinary research projects that inspire an interdisciplinary way of thinking. Hence, I want to express my thanks to all the members of the working and project groups in Cologne, Freising, Munich and Leuven for the inspiring discussions and interesting ideas that contributed to my own research. I am particularly grateful to my co-authors, namely Karl Auerswald, Richard Dikau, Verena Dlugoß, Gerard Govers, Max Kainz, Karl Schneider, Hendrik Van Hemelryck, Kristof Van Oost, and Stephan Weigand. Moreover, I am indebted to all the Ph.D. students, student research assistants, technical staff, and the land owners and farmers for their support and the opportunity for extensive field work.

Special thanks go to the two principal supporters of my habilitation project. This is on the one hand Karl Schneider who gave me the opportunity and the support to realize my own research ideas within his working group in Cologne. On the other hand this is Karl Auers-

wald, the person who set the ground for my scientific career and who is still an important source of inspiring open-minded scientific discussion.

The scientific activities presented here were embedded in and/or supported by the following research projects: (1) The “Munich research alliance on agro-ecosystems” (“Forschungsverbund Agrarökosysteme München”; BMBF 0339370 and Bavarian State Ministry for Science, Research and Arts), (2) the project “Soil redistribution in agricultural landscapes – source or sink of $CO_2$?” (DFG-FI 1216/4-1), (3) the project “Effects of land use and management on runoff generation and concentration in small agricultural watersheds” (DFG-DI 639/1-1), (4) the project “Effective modeling of water erosion in agricultural landscapes” (Katholieke Universiteit Leuven) and (5) the SFB/TR 32 “Pattern in Soil-Vegetation-Atmosphere Systems: Monitoring, Modelling, and Data Assimilation”. Therefore, the financial support through the German Research Agency (DFG), the German Federal Ministry of Education and Research (BMBF), the Bavarian State Ministry for Science, Research and Arts, and the Katholieke Universiteit Leuven is gratefully acknowledged.

Finally, much love and many thanks go to my always encouraging wife and children without whose quiet and undying support over the years none of this would have been possible.

# INTRODUCTION

The lateral movement of water and matter through agricultural landscapes has been intensively investigated on different spatial and temporal scales throughout the last decades in various disciplines. For example in agronomy, focusing mainly on the plot scale (e.g. Léonard et al., 2006; Wischmeier and Smith, 1960), geomorphology focusing on long-term sediment fluxes in mesoscale to macroscale watersheds using data from colluvial and alluvial deposits (e.g. Hoffmann et al., 2007; Phillips, 1991), and hydrology dealing with storm runoff generation (e.g. Bronstert et al., 2002; Fohrer et al., 2001) as well as water quality issues on various scales (e.g. Parson et al., 2001; Sharpley et al., 1985). Amongst others, the topicality of lateral water and matter fluxes in agricultural landscapes is underlined in the European Water Framework Directive (Directive 2000/60/EC of the European Parliament and of the Council establishing a framework for the Community action in the field of water policy) and in the scientific debate about the importance of lateral soil carbon redistribution within the global carbon cycle (e.g. Kuhn et al., 2009; Lal, 2003; Van Oost et al., 2007).

To analyze and better understand the nature of water and matter fluxes in landscapes, a growing interest in understanding pattern and process interactions developed. Patterns can be defined as observations that have a structure, which is significantly different from a random process realization. Hence patterns contain information on the mechanisms or processes from which they emerge (Grimm et al., 2005). Especially in landscape ecology, there is a long tradition in evaluating the effect of spatio-temporal patterns in landscapes on ecological functions, e.g. connectivity of habitats (e.g. Turner, 1989; Wiens, 1976). The importance of spatio-temporal patterns was also emphasized in hydrological watershed and erosion research. This has been exemplarily documented by the fundamental book on patterns and catchment hydrology edited by Grayson and Blöschl (2000) and a recent special issue of Earth Surface Processes and Landforms entitled “Soil erosion patterns: evolution, spatio-temporal dynamics and connectivity” edited by Helming et al. (2005). Their results can be summarized and underlined by the hydrologic synthesis of Blöschl (2006) stating “It is patterns, patterns, and more patterns, all of them viewed as puzzles that require explanation, interpretation and quantification”.

In agricultural landscapes, man-made spatial patterns in land use and (asynchronous) temporal patterns in management of single fields substantially affect lateral water and matter fluxes. Analyzing and understanding these fluxes requires a holistic, interdisciplinary research approach utilizing knowledge and methods from geography, agronomy (including agro-economics) as well as several other scientific disciplines, such as hydrology, geomorphology and soil sciences. Such research is challenging, but may prepare the ground to better

balance different aspects of agro-ecosystem functions and services highly required under a growing population.

Experimental research upon lateral water and matter fluxes is typically done either as plot experiments focusing on individual processes or on watersheds researching the internal sum of processes. Both approaches have their drawbacks: Plot experiments create highly artificial conditions that cannot be directly transferred to a whole watershed; in watershed-scale experiments, the internal dynamics of lateral fluxes are typically unknown. Controlled watershed-scale experiments are understood here as an experimental setup, which combine both, the measurement of internal pattern-process interactions and the integral watershed response. The measurement design therefore has to ensure that typical agronomic management operations are practiced and, at the same time, that the measurements do not affect the site properties. In order to study event driven processes, such watershed monitoring must be continuous and sufficiently long, which is especially true for lateral water and matter fluxes, since these are often dominated by single, rare rain events occurring under specific field conditions. However, as some processes cannot be measured in-situ without destructive methods or without affecting agronomic practice, such long-term monitoring has to be combined with detailed process studies outside the watersheds or under laboratory conditions, e.g. measuring phosphorus leakage from mulch cover without soil-mulch interaction.

Moreover, modeling approaches should be applied or developed to scrutinize and extend our process understanding. Modeling tools are also essential to understand patterns in agricultural landscapes, e.g. in soil properties, emerging from slow processes, which in practice cannot be measured in continuous experiments.

Besides a need for an improved understanding of watershed internal pattern-process interactions, which should be the basis for the planning of any control measures for lateral fluxes within a watershed, there is a need to up-scale such results to the regional or even continental scale. In general, the issue of up-scaling of lateral water and matter fluxes has been addressed in numerous (modeling) studies and review papers (e.g. Blöschl and Sivapalan, 1995; Le Bissonnais et al., 1998). Amongst others, two important and still unresolved problems arise, especially if land use and management substantially affect lateral water and matter fluxes and/or if soil and water conservation planning is addressed. (i) The data basis used to develop and test land use and management effects on lateral water and matter fluxes is often insufficient in case of large scale models, and (ii) even more serious is the substantial lack of adequate model input data regarding spatio-temporal patterns in land use and land management.

Against this background, the general objective of the study presented here is to evaluate pattern-process interactions affecting water and matter fluxes in environments dominated by

man-made patterns in land use and processes often affected by management operations. The series of publication, which forms the basis of this thesis, follows this general objective by utilizing mostly continuous, controlled, 'real world' watershed-scale data in combination with detailed process studies and process-oriented modeling. Moreover, up-scaling studies to the regional scale are included. The spatial scales addressed in this work range from the scale of soil aggregates (lower left in Figure 1) to the regional scale (upper right in Figure 1), the temporal scales range from minutes to decades. As indicated in Figure 1, the different temporal and special scales addressed in the different publications are not separated but highly intertwined.

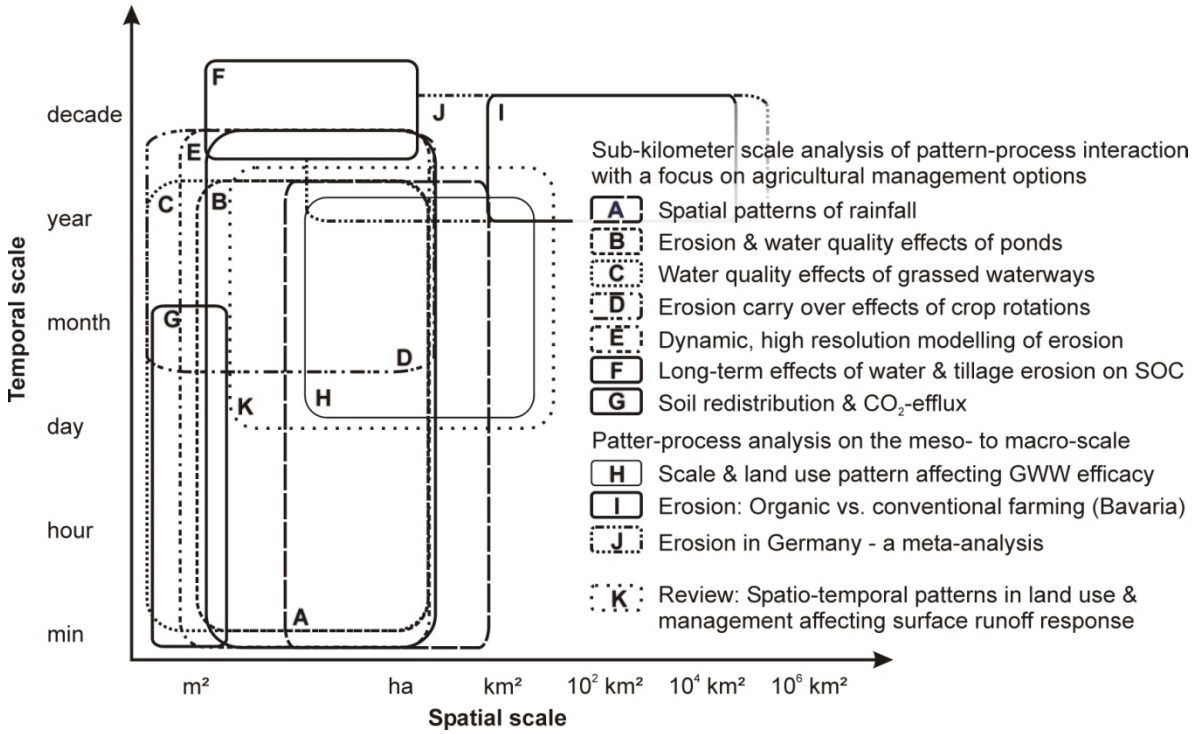


**Figure 1. Schematic overview of spatial and temporal scales of all presented manuscripts.**

The specific aims of these studies can be summarized as follows:

(i) To experimentally determine lateral water and matter fluxes as affected by spatial patterns in land use and temporal patterns in land management, with a special focus on soil and water conservation measures. Experiments were performed using continuous measurements within controlled watersheds, thus integrating process-oriented with temporally and spatially integrating measurements. These studies bridge the gap between plot studies focusing on small scale processes and hydrological watershed studies (chapters 1-4).

(ii) To analyze existing patterns in agricultural landscapes and to evaluate the processes from which these emerge, by combining the measured patterns of soil properties and pools with modeling and detailed flux studies (chapters 5-6).

(iii) To combine existing, improved or newly developed modeling approaches with high resolution data to improve our system understanding on the sub-kilometer scale with special focus on pattern-process interaction under conservation agriculture (chapters 3-5 and 7)

(iv) To utilize models to analyze and understand patterns and processes of lateral water and matter fluxes on the mesoscale to macroscale (chapters 8-10).

(v) To present an extended review regarding the advances made thus far in quantifying the effects of spatio-temporal patterns in land use and management on surface runoff response in agricultural watersheds (chapter 11).

# 1. SPATIAL VARIABILITY OF RAINFALL ON A SUB-KILOMETER SCALE

With minor revisions published:
P. Fiener and K. Auerswald (2009).
Spatial variability of rainfall on a sub-kilometer scale.
Earth Surface Processes and Landforms. 34, 848–859.

***ABSTRACT:*** *The variability of rainfall in space and time is an essential driver of many processes in nature but little is known about its extent on the sub-kilometer scale, despite many agricultural and environmental experiments on this scale. A network of 13 tipping-bucket rain gauges was operated on a 1.4 km$^2$ test site in southern Germany for four years to quantify spatial trends in rainfall depth, intensity, erosivity, and predicted runoff. The random measuring error ranged from 10% to 0.1% in case of 1 mm and 100 mm rainfall, respectively. The wind effects could be well described by the mean slope of the horizon at the stations. Except for one station, which was excluded from further analysis, the relative differences due to wind were in maximum ± 5%. Gradients in rainfall depth representing the 1-km$^2$ scale derived by linear regressions were much larger and ranged from 1.0 to 15.7 mm km$^{-1}$ with a mean of 4.2 mm km$^{-1}$ (median 3.3 mm km$^{-1}$). They mainly developed during short bursts of rain and thus gradients were even larger for rain intensities and caused a variation in rain erosivity of up to 255% for an individual event. The trends did not have a single primary direction and thus level out on the long term, but for short-time periods or for single events the assumption of spatially uniform rainfall is invalid on the sub-kilometer scale. The strength of the spatial trend increased with rain intensity. This has important implications for any hydrological or geomorphologic process sensitive to maximum rain intensities, especially when focusing on large, rare events. These sub-kilometer scale differences are hence highly relevant for environmental processes acting on short-time scales like flooding or erosion. They should be considered during establishing, validating and application of any event-based runoff or erosion model.*

The variability of rainfall in space and time is an essential driver of many processes in nature. This is most obvious for questions such as the analysis and modeling of rainfall–runoff relations (e.g. Bronstert and Bárdossy, 2003; Faurès et al., 1995; Kirkby et al., 2005) or soil erosion processes (e.g. Nearing, 1998; Nyssen et al., 2005), but it is also important for characteristics such as spatial-temporal variability of crop yields, patterns of deposits from atmosphere, soil carbon and nitrogen turnover, etc.

Spatial variability of rainfall on a scale > 100 km$^2$ has been an important topic in hydrology and meteorology research during the last decades. Studies focused on methods to improve the interpolation of rain gauge point measurements (e.g. Borga and Vizzaccaro, 1997; Kruizinga and Yperlaan, 1978; Syed et al., 2003), optimizing rain gauge networks (e.g. Bastin et al., 1984; Papamichail and Metaxa, 1996), or utilizing remote sensing data, especially ground-based radar measurements (e.g. Berne et al., 2004; Borga, 2002; Datta et al., 2003; Quirmbach and Schultz, 2002; Tsanis et al., 2002), to determine the spatial variability of rainfall. On smaller scales (10–100 km$^2$) studies are rarer and test sites are mostly located in areas where strong gradients in rainfall can be expected due to orographic effects in mountainous regions (e.g. Arora et al., 2006; Buytaert et al., 2006) or at coast lines (e.g. Stow and Dirks, 1998), or due to climatic situations with distinct convective storms (e.g. Berne et al., 2004; Desa and Niemczynowicz, 1997; Hernandez et al., 2000).

On a smaller scale (< 10 km$^2$), where many environmental processes are often studied in detail and where rainfall–runoff or erosion models are mostly developed and tested only sparse knowledge exists on the variability of rainfall depth and intensity (e.g. Goodrich et al., 1995; Jensen and Pedersen, 2005; Sivakumar and Hatfield, 1990; Taupin, 1997). Information is needed about the extent and significance of rain variability on this scale, for example to develop and validate erosion and rainfall–runoff models (e.g. Faurès et al., 1995; Johannes, 2001), to understand small-scale variability in soil moisture and hence soil properties, to design urban water management facilities (e.g. Berne et al., 2004), or to validate subscale variability in rain radar data (e.g. Jensen and Pedersen, 2005).

The overall aim of this study was to determine the spatial variability in rainfall depth and maximum intensity, as well as variability of derived parameters within a small test site (1.4 km$^2$) with 13 measuring stations. More specifically the objectives were to:

(i) Determine the importance of spatially variable events during the four-year observation period.

(ii) Analyze the extent of spatial variability for the total rain depth and the maximum intensities on an event basis.

(iii) Analyze the resulting spatial variability of parameters non-linearly related to rainfall, exemplarily shown for rainfall erosivity and predicted daily runoff.

## MATERIAL AND METHODS

### Test site

Precipitation was measured at the Scheyern Experimental Farm (Figure 1), which is located about 40 km north of Munich (48°30’50’’ N, 11°26’30’’ E). The topography, soils and

land use of the area are typical for the Tertiary Hills, an important extensively used agricultural landscape in central Europe. The rolling topography of the test site covered an area of approximately 1.4 km$^2$ of arable land at an altitude of 446 to 500 m above mean sea level (Sinowski and Auerswald, 1999). The mean annual air temperature, measured at the central meteorological station within the experimental farm, was 8.4 °C (for 1994-1998). The measured precipitation was 789 mm yr$^{-1}$ (for 1994-1998) with the highest values occurring from May to August and the lowest occurring in the winter months.

## Measurements

Precipitation was measured between April 1994 and March 1998 at 13 locations within the 1.4 km² research site (Figure 1). To measure precipitation continuously during the winter months eight of the rain gauges were heated. For this study, focusing on rain, we used only measurements from the hydrological summer half-year (May-October) when all stations were

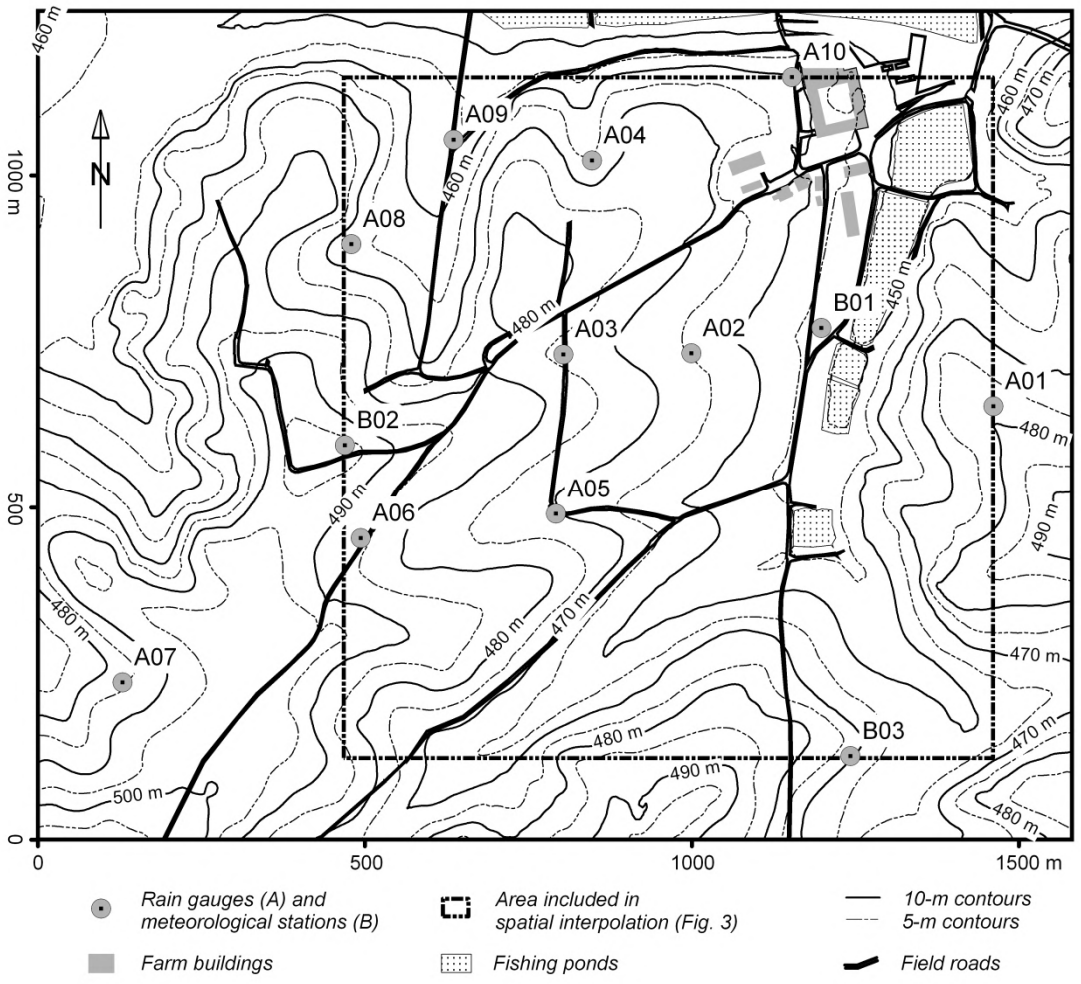


**Figure 1. Topography of the test site in Scheyern (southern Germany) including locations of all rain gauges (A01–A10) and meteorological stations (B01–B03).**

**Table 1. Altitude, mean slope of the horizon and technical data of the measuring stations**

| Station | Altitude a.s.l. [m] | Slope of the horizon† [°] | Measuring resolution [mm] | Collecting area [m²] | Manufacturer |
|---|---|---|---|---|---|
| B01 | 453 | 4.8 | 0.2 | 0.04 | Casella, UK |
| B02 | 496 | 3.0 | 0.2 | 0.04 | Casella, UK |
| B03 | 471 | 10.9 | 0.1 | 0.04 | Casella, UK |
| R01 | 477 | 0.5 | 0.1 | 0.02 | Seba, Germany |
| R02 | 465 | 3.8 | 0.1 | 0.02 | Seba, Germany |
| R03 | 475 | 7.6 | 0.1 | 0.02 | Seba, Germany |
| R05 | 466 | 4.5 | 0.1 | 0.02 | Seba, Germany |
| R06 | 470 | 8.0 | 0.1 | 0.02 | Seba, Germany |
| R07 | 486 | 8.4 | 0.1 | 0.02 | Seba, Germany |
| R08 | 485 | 6.9 | 0.1 | 0.02 | Seba, Germany |
| R09 | 468 | 8.9 | 0.1 | 0.02 | Seba, Germany |
| R10 | 456 | 5.6 | 0.1 | 0.02 | Seba, Germany |
| R11 | 460 | 7.3 | 0.1 | 0.02 | Seba, Germany |

† Calculated assuming harvested fields using an approach developed by Richter (1995) from measurements in 15° segments, which were weighted according to the mean distribution of wind directions.

operational. Measurements were carried out 1.0 m above the ground using automated 0.02-0.04 $m^2$ tipping bucket rain gauges (Table 1). Stations A01-A10 measured precipitation only, while at the stations B01-B03 wind speed, air and soil temperatures at different levels and several other meteorological data were measured as well. The tipping-bucket rainfall data from all stations were aggregated to minute values.

For the analysis of spatial trends of precipitation the characteristics of single events were compared. Therefore, rain events (subsequently referred to as events) were defined as rainfall periods separated from preceding and succeeding rainfall by at least 6 h, during which uncorrected rain larger than 5 mm was measured at Station B01, B02 or 50% of all stations, this is analogous to the definition of an erosive event by Wischmeier and Smith (1978).

To identify erroneous measurements and to prevent persistent failure of single stations, e.g. due to insects, leaves, etc. trapped in the collecting funnel of the tipping buckets, observed rain depths and characteristics were controlled monthly. Moreover, the event durations at the different stations were compared to identify stations with prolonged rain events often indicating a plugged collecting funnel. In the case of any suspicious findings in the data the equipment of the identified station was checked and the measurements were rejected if necessary.

As known from a number of studies the accuracy of tipping bucket rain gauges is sensitive to rain intensity, which was compensated either by correction functions (e.g. Adami and Da Deppo, 1986; La Barbera et al., 2002; Molini et al., 2005) or by improving measuring

techniques (e.g. Overgaard et al., 1998). For this study three of the tipping bucket rain gauges were tested under different rain intensities in the laboratory to derive intensity dependent correction functions. For rain intensities < 30 mm $h^{-1}$, which represents more than 90% of all measured rain events at the test site, no significant relationship between rain intensity and measuring error could be found. However, larger tendencies than those measured in the laboratory experiments can be expected due to a slight fouling of equipment installed for field measurements. The tipping bucket error of the field measurements was determined by collecting the rain water intercepted by the gauges in small tanks buried below ground level near the measuring device. These small tanks were emptied bi-weekly to determine total rain depth which was used to correct the tipping bucket data. Both measurements were closely correlated at all 13 stations ($R^2 > 0.998$), nevertheless a deviation of the tipping bucket measurements between -7% to +8% was found (mean absolute deviation being 3%). The station-dependent relation was used to adjust the tipping bucket data with individual correction factors ranging between 0.927 (A06) and 1.081 (B03).

**Quantifying spatial variability due to wind effects**

Using rain gauges at a height of 1 m above ground causes wind effects which result in differences between measured rain and actual rain reaching the surface. These differences were investigated with additional surface-level rain gauges at the meteorological stations B01 and B02 (Johannes, 2001). For this study dealing with the spatial distribution of rain depth and intensity it is important to focus on differences in wind effects between the 13 rain stations. Such differences can be expected due to different measuring devices and different wind effects mainly caused by different slopes of the horizon at the measuring locations (Table 1). To detect wind effects we firstly categorized all events in: (i) events with spatially random variability in rainfall distribution and (ii) events with spatially systematic variability in rainfall distribution (see next sub-section).

The rainfall of events with spatially random variability was accumulated for each station and a regression analysis was carried out using this accumulated rainfall and the mean slope of the horizon of the individual station. For all A-stations, except A07, and station B03 the difference in rainfall correlated with $R^2 = 0.63$ (probability that R is different from zero, $p = 0.01$) with the difference in topographic sheltering (Figure 2), which is used here as a proxy for wind effects.

The rain depth at the individual A-stations deviated by not more than 2% from the average of all A-stations (excluding A07) if total rain of all random events was accumulated. At A07, however, the rainfall of all random events was 11% smaller on average compared to all other A-stations. This significant difference (two-sided t-test; null hypothesis mean of all A-

stations equal to mean of station A07) was probably caused by higher wind speeds due to the location of A07 in a small depression canalizing wind coming from south and south-west, which are the dominant wind directions of the area (representing 59.2% of all wind directions). At stations B01 and B02 the measured rain decreased less with increasing wind speed than at the A-stations (inclusive B03). In total 5% more rain than the average of all A-stations (except A07, inclusive B03) was measured for all events during the hydrological summer-half year. The major reason probably was the aerodynamically more appropriate design of the B01 and B02 rain gauges with a slightly different slope of the rim of these two stations (Johannes, 2001).

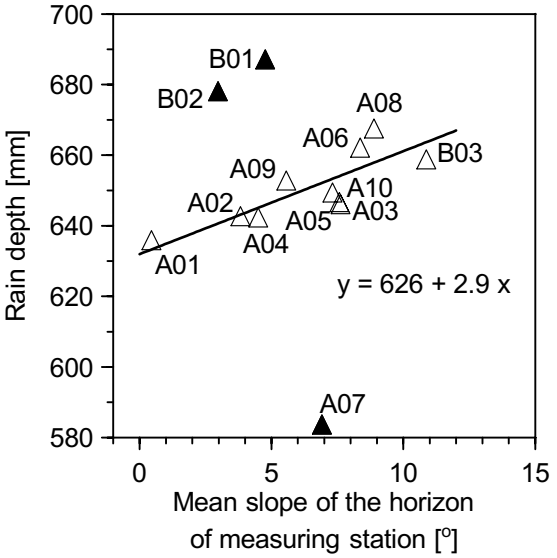


**Figure 2. Mean slope of the horizon of the measuring stations versus rain depth of all random events during the hydrological summer-half years (1994–1997); regression line calculated for all A-stations (except A07) and station B03 represented by unfilled triangles ($R^2 = 0.63$, n = 9).**

When analyzing the wind effects at the stations B01 and B02, where additional surface-level rain gauges were installed, we found a larger measuring error at B02 for accumulated rainfall (1994-1998) of 7% compared to 5% at station B01. This difference can be attributed to higher average wind speeds of 2.3 m $s^{-1}$ at B02 compared to those of 1.3 m $s^{-1}$ at B01. Nevertheless, the analysis of single rain events did not allow a clear relationship to be derived between wind speed and measuring error for each of the stations, because the size of the errors also depended strongly on rain characteristics. In general, the relative error decreased with increasing event size, for example all events < 10 mm had a relative error of 9.0%, while this decreased to 4.2% for all larger events.

The average wind speed during all events with spatially systematic variability [1.7 m $s^{-1}$, standard deviation (SD) = 0.3 m $s^{-1}$] was significantly lower compared to the spatially random events (2.4 m $s^{-1}$, SD = 1.3 m $s^{-1}$) (two-tailed t-test, null hypothesis is equality of means). Hence, as we focus on rainfall events with a spatially systematic variability, no corrections for wind speed were applied due to the total relatively small random error caused by wind effects in the case of these events and the general difficulties to derive clear correction functions. Only measurements from station A07 were excluded from further evaluations due to its specific sensitivity to wind speed. If we use or refer to average rain depths these are calculated according to the Thiessen polygon areas varying between 4.7 and 18.5 ha for the

individual stations (excluding A07) within the rectangle stretched by the measuring locations shown in Figure 1.

**Defining spatially random and spatially systematic variability in rainfall distribution**

To distinguish between events, where the spatial variation of rain was random due to measuring errors and those events with a spatially systematic variability, a multiple regression analysis was performed, applying a linear, an exponential or a polynomial function. For these regression models, using rain depth regressed on X-Y-coordinates of the stations, the null hypothesis that the coefficients of the model (except for intercept) were different from zero was tested applying t-statistics. Events are defined as events with a spatially systematic variability in rainfall distribution (subsequently referred to as gradient events) if one of the model coefficients or the total regression model is highly significant ($p < 0.01$). If the null hypothesis holds not true on this significance level the events were categorized as events with a spatially random variability in rainfall distribution (subsequently referred to as random events). The residuals of the gradient events were then tested for normal distribution and autocorrelation (see later) to examine whether the regression model was appropriate to describe the spatial trend.

To illustrate and discuss the spatial variability of rainfall events within the research area without a predefined spatial model, geostatistical analyses [for theory see Webster and Oliver (2001) and Nielsen and Wendroth (2003)] were carried out for four exemplary gradient events. Semivariograms were constructed with the supplementary package geoR (Diggle and Ribeiro Jr, 2007) of the statistical software GNU R, version 2.6 (R Development Core Team, 2007). For semivariance analysis rain gauge readings of all four gradient events were pooled (Voltz and Webster, 1990) to meet the requirement of at least 30 - 50 data sets ($n = 48$). According to Schuurmans et al. (2007) a pooled semivariogram is almost as good as using event-based semivariograms. Prior to pooling, the data of the individual rains were scaled to a mean of zero and a standard deviation of one to attain second order stationarity among rains. This resulted in an empirical semivariogram, which closely followed a Gaussian model (nugget 0.06, sill 5.09, range 1333 m, Nash-Sutcliffe index 0.9356) where 12 lag classes were weighted according to n/lag when fitting the semivariogram model to give more weight to those lag classes, which contained many data pairs and which were closer to the origin and thus more important for kriging. The small nugget effect and the large sill indicated a strong pattern of the rains compared to the uncertainty. This semivariogram model and the scaled data of the individual rains were then used to construct rain maps by block kriging using $10 \times 10$ m$^2$ blocks with the package gstat (Pebesma, 2004), which were finally rescaled to millimeter units with the mean and standard deviation of the individual rains.

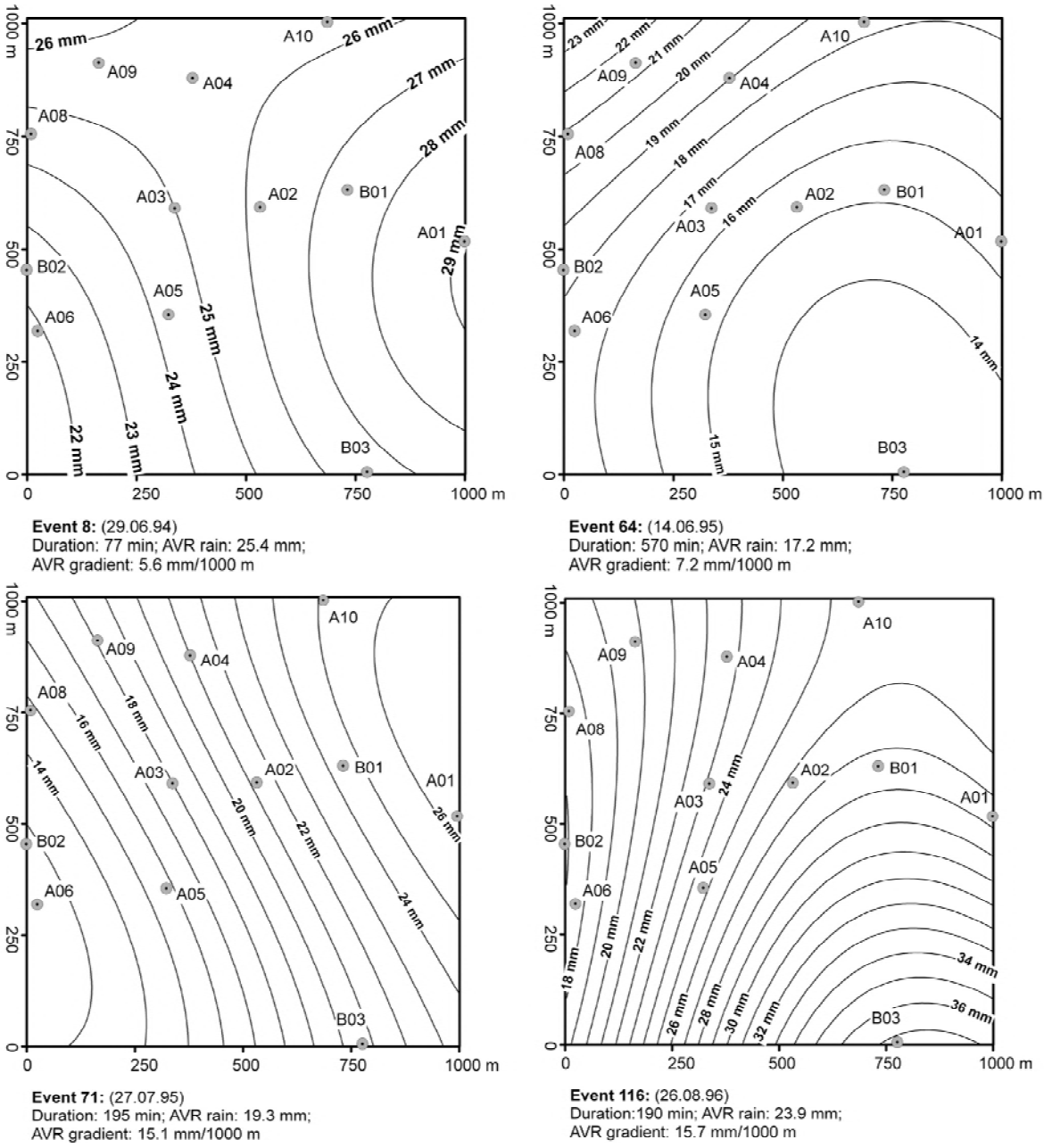


**Figure 3. Interpolation of rain depth (in mm) of four gradient events by block kriging for 10 × 10-m$^2$ blocks; the twelve locations of the measuring stations (A01–A06, A08–A10, B01–B03) are indicated by grey circles; for each four events duration, average rain depth (AVR rain) calculated from the geostatistical interpolation and average gradients in rain depth (AVR gradient) are given. Krige standard deviations averaged over all 10 × 10-m$^2$ blocks are 0.4, 0.5, 0.9 and 1.1 mm for rains 8, 64, 71 and 116, respectively.**

Analysis of the regressions, analysis of the residuals and the exemplarily geostatistically interpolated rain maps (Figure 3), all indicated that the resulting gradient events generally followed a more or less linear trend. Hence, rain depth was then linearly regressed on the

X-Y-coordinates of the stations to determine the mean trend for each gradient event, which later on is used for an easy comparison and further analysis of the resulting trends. Analogously to the spatial interpolation of the four exemplary gradient events a semivariogram was calculated by pooling all gradient events prior and after correcting for the trend by regression analysis to examine to which degree the linear regression equations with predefined spatial behavior adequately quantified and removed the spatial trend and how much autocorrelation was left in the residuals of the regression analysis.

**Parameters derived from rainfall - rain erosivity and runoff prediction**

To elucidate the effects of spatial gradient events on environmental processes at the sub-kilometer scale it is necessary to focus on driving parameters derived from rainfall depth, which may translate rainfall variability sub- or super-proportional to the respective process. As an example for such a parameter the rain erosivity was calculated, which is commonly used to describe the rain potential to detach soil particles and to initiate soil erosion caused by surface runoff. Rain erosivity originally was introduced with the Universal Soil Loss Equation (USLE; Wischmeier and Smith, 1960) and now it is used in many soil erosion models. Rain erosivity $R_{event}$ is calculated according to Equation 1 for all erosive events, defined as events with at least 10 mm of precipitation or a maximum intensity above 10 mm $h^{-1}$ (Schwertmann et al., 1987).

$$R_{event} = Ekin \cdot \mathrm{I}_{\max 30} \quad (1)$$

$$Ekin = \sum_{i=1}^{n} Ekin_i \quad (2)$$

with:

$$Ekin_i = (11.89 + (8.73 \log I_i)) \cdot N_i \cdot 10^{-3} \quad \text{for} \quad 0.05 \le I_i \le 76.2$$

$$Ekin_i = 0 \quad \text{for} \quad I_i < 0.05$$

$$Ekin_i = 28.33 \cdot N_i \cdot 10^{-3} \quad \text{for} \quad I_i > 76.2$$

where $Ekin$ is the total kinetic energy of an event [kJ $m^{-2}$], $I_{\max 30}$ is the maximum 30-min rain intensity of an event [mm $h^{-1}$], $i$ is a time interval during the event with a constant rain intensity, $Ekin_i$, $I_i$, and $N_i$ are kinetic energy, rain intensity and accumulation within time interval $i$, respectively.

In addition daily runoff was calculated for the days with gradient rains applying the Soil Conservation Service (SCS) curve number model (Mockus, 1972). Two contrasting situations on Hydrological Soil Group C were assumed, either small grain favoring infiltration

(curve number 81) or row crops more likely favoring runoff (curve number 85) which both corresponded to the land use on the experimental farm (Fiener and Auerswald, 2007).

## RESULTS

In total 115 events ≥ 5.0 mm were observed in the four hydrological summer-half years (1994-1997). These events were measured at least at eight of the 13 measuring stations (including A07). In case of 52 events all 13 stations were operating. On average between 2.5 (October) and 6.8 events (August) per month occurred during the observation period. These events represent 67% (September) to 90% (July) of the total rain amount in these months. The largest rainfall was 62.2 mm, while the mean and the median of all events in the hydrological summer-half years were 12.6 mm and 9.3 mm, respectively.

When applying the multiple regressions to determine gradient events, the linear, exponential and polynomial models showed similar levels of significance and similar $R^2$ values. The curvilinear regression surfaces were with few exceptions not significantly [tested according to Samiuddin (1970)] better than the linear model. This justified using a linear trend for further analysis in addition to the definition of scale associated with the linear model. Also the geostatistical interpolation examples (Figure 3) justified the use of a linear trend. For 38 events during the hydrological summer-half year the linear regression was at least highly significant ($p < 0.01$). The $R^2$ for the linear regressions ranged between 0.59 and 0.96, with 50% of all $R^2 > 0.81$. Geostatistical analysis of the pooled residuals showed that the linear regressions had eliminated 92% of the pattern as the partial sill dropped from 2.7 to 0.21 with Gaussian models in both cases. The partial sill was less than half as large as the nugget effect for the residuals. The analysis of the model residuals individually for each event, as an example shown for events 8 and 64 (Figure 4), indicated that in case of 34 events (e.g. event 8) the model assumptions (normal distribution and no autocorrelation of residuals) are reasonably met. For four events (including event 64) this was less clear as size of residuals show some spatial clustering and/or residuals are not normal distributed indicating that the trend may be curvilinear but this would not change any conclusion drawn from the simplification of a linear trend within the restricted research area. Hence, we also categorized these events as gradient events. The (almost) linear trends indicate that the precipitation cells causing the trend were larger than the research area and had their minimum and/or maximum outside the research area.

The events were categorized in four sections (0-90°, 90-180°, 180-270° and 270-360°) to determine if the gradients had a preferred direction. The null hypothesis that the number of observed events per section is not significantly different from the equal distribution could not

be rejected on a 5% level applying a Pearson Chi-square test (alternative hypothesis: observations are different from an equal distribution). This corresponds with the notion of precipitation cells of random position relative to the research site.

During the hydrological summer-half year the gradient events only occurred between May and September (Figure 5) with a median rain gradient of 3.3 mm $km^{-1}$ (Table 2). In case of four relatively small events close to our threshold of N > 5.0 mm the gradient was greater than the average rainfall. For 95% of all gradient events the rain gradient was < 7.5 mm $km^{-1}$, while in two cases, which occurred in July and August, a gradient > 10 mm $km^{-1}$

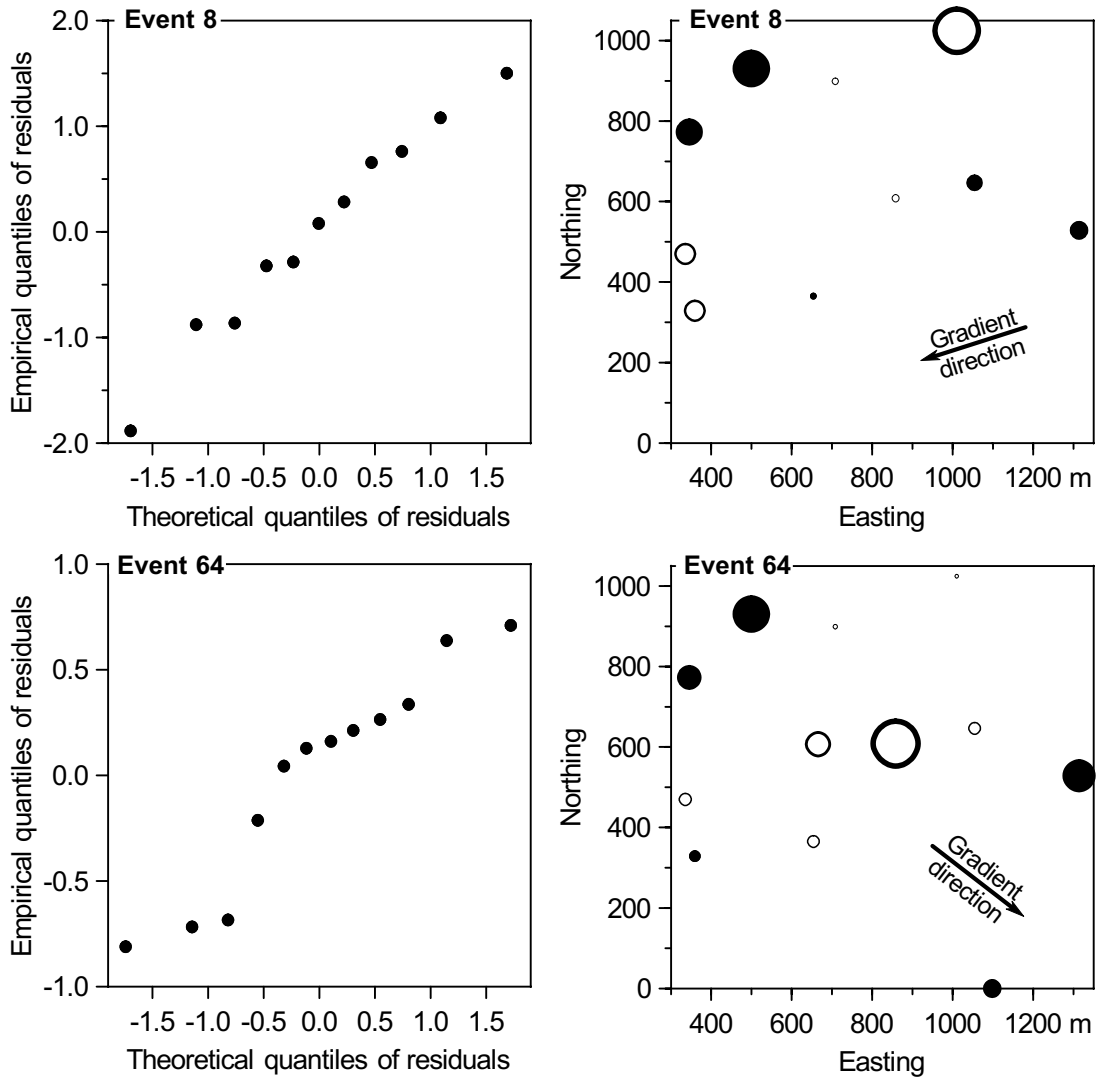


**Figure 4. Analysis of normal distribution (left panels) and spatial distribution (right panels) of residuals derived from linear regression models ($p < 0.001$) for two gradient events ($R^2 = 0.78$ and 0.91 for top and bottom); positive residuals are displayed by black markers, negative residuals by white markers; marker size indicates the value; event 8 exhibited a random distribution of the residuals while event 64 seemed to have a curvilinear trend; the arrows indicate the direction of the gradients, which were 5.6 and 7.2 mm $km^{-1}$ for event 8 and 64, respectively.**

was measured. Except for these two events the frequency of events with high or low rain gradients was similar between June and August (Figure 5).

Sixteen out of 38 gradient events did not meet the definition of erosive rain events. These non-erosive gradient events had a median rain depth of 5.9 mm and a median rain gradient of 2.7 mm km$^{-1}$, thus both were smaller than for the erosive gradient events (median rain depth 15.1 mm, median rain gradient 4.2 mm km$^{-1}$). Within both groups the gradient did not depend on rain depth.

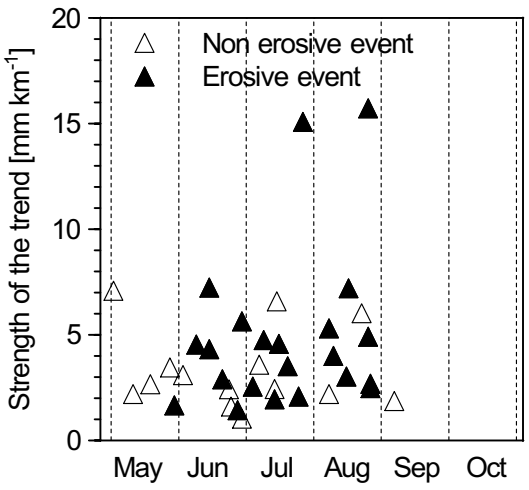


**Figure 5. Date and strength of gradient events in the hydrological summer-half-years from 1994 to 1997.**

Within the hydrological summer-half years (1994-1997) 59 erosive events were identified out of which 22 (37%) were erosive trend events. A trend is hence not unlikely for erosive rains. Most erosive gradient events occurred between June and August (Figure 5). As these months contribute about 70% to annual erosivity in this region (Schwertmann et al., 1987) the erosive events are highly relevant for the simulation of runoff and soil erosion under agricultural land we subsequently focus on the months June to August.

Between June and August 42 erosive events, representing 70% of the total precipitation of 1124 mm, were recorded (1994-1997) (Table 3). The number and the amount of rain of these events were more or less equally distributed within all months. Approximately half of the events had a spatial trend. Hence, on the temporal scale of events the general assumption of a spatially homogeneous rain input used in many small-scale runoff and erosion models is not justified. While the spatially random events produced about 20% more rain than

**Table 2. Statistical data of all 38 rain events with a trend in rain depth observed in the hydrological summer-half-years 1994–1997; rain gradient was calculated with multiple linear regressions using station coordinates (northing and easting); the relative rain gradient was derived from the rain depth at the spatial centre of the test site, which was defined as the average of the station coordinates of B01 and B02; rain depth for the centre point was also calculated with the regression functions.**

| | Rain amount [mm] | Rain gradient [mm km$^{-1}$] | Relative rain gradient [% km$^{-1}$] |
|---|---|---|---|
| Mean | 12.1 | 4.2 | 48 |
| Median | 9.9 | 3.3 | 36 |
| 1st quartile | 6.1 | 2.2 | 20 |
| 3st quartile | 17.2 | 5.1 | 47 |
| Minimum | 2.4 | 1.0 | 9 |
| Maximum | 28.9 | 15.7 | 278 |

**Table 3. Total rain depth, total erosive rain depth and rain erosivity, *R*, for the summer months June, July and August (1994–1997).**

| | | June | July | August | Sum |
|---|---|---|---|---|---|
| Total rain depth | [mm] | 336 | 396 | 391 | 1124 (1130)† |
| Proportion of erosive events | [%] | 66 | 76 | 66 | 70 |
| No. of erosive events | Without trend | 6 | 8 | 7 | 21 |
| | With trend | 6 | 7 | 8 | 21 |
| Rain depth of erosive events [mm] | Without trend | 133 | 189 | 108 | 430 |
| | With trend | 88 | 113 | 151 | 352 |
| $\Sigma R$ [N h$^{-1}$] | Without trend | 12 | 48 | 27 | 87 |
| | With trend | 47 | 23 | 53 | 123 |

† Average rain depth (1961-1990) measured at the German Weather Service (DWD) station in Scheyern located about 1 km east of the test site

gradient events, the cumulative rain erosivity of the gradient events was about 40% larger. Variation in rain erosivity was up to 255% and thus much more pronounced than the variation in total rain depth (maxima < 100% for rains > 6 mm). This super-proportional effect on rain erosivity was caused by differences in rain intensity. While the rain depth differed within the area during a gradient event, the duration of the rain remained greatly unchanged. An increasing rain depth, hence, also increased intensity because rain duration remained unchanged. Thus, in the calculation of the rain erosivity (Equation 1) the maximal 30-min intensity ($I_{max30}$) and the total kinetic energy changed and thus led to the super-proportional effect. The median as well as the 1st and 3rd quartile of $I_{max30}$ for all gradient events was about 1.5 times larger than for all spatially random events. For predicted runoff the effect was even larger, because most of the rainfall would infiltrate under the assumed conditions leading to steep gradients of the excess rainfall. The predicted gradients relative to the spatial average were about two to 20 times larger for runoff than for rain depths (Figure 6).

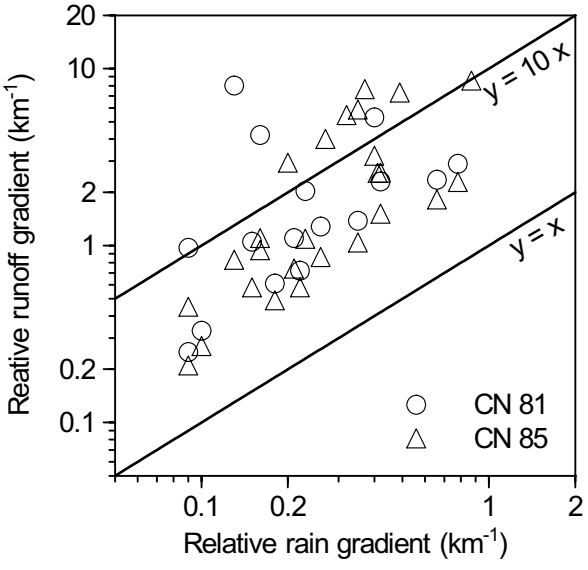


**Figure 6. Gradients in rain and runoff depths (excluding rains, for which no runoff was predicted); gradients given in millimeters per kilometer relative to the mean rain and runoff depth in millimeters.**

For the effects of gradient events, e.g. on erosion, runoff accumulation and peak discharge, the spatio-temporal variability of rainfall also becomes relevant. As an example this was analyzed for the four events with

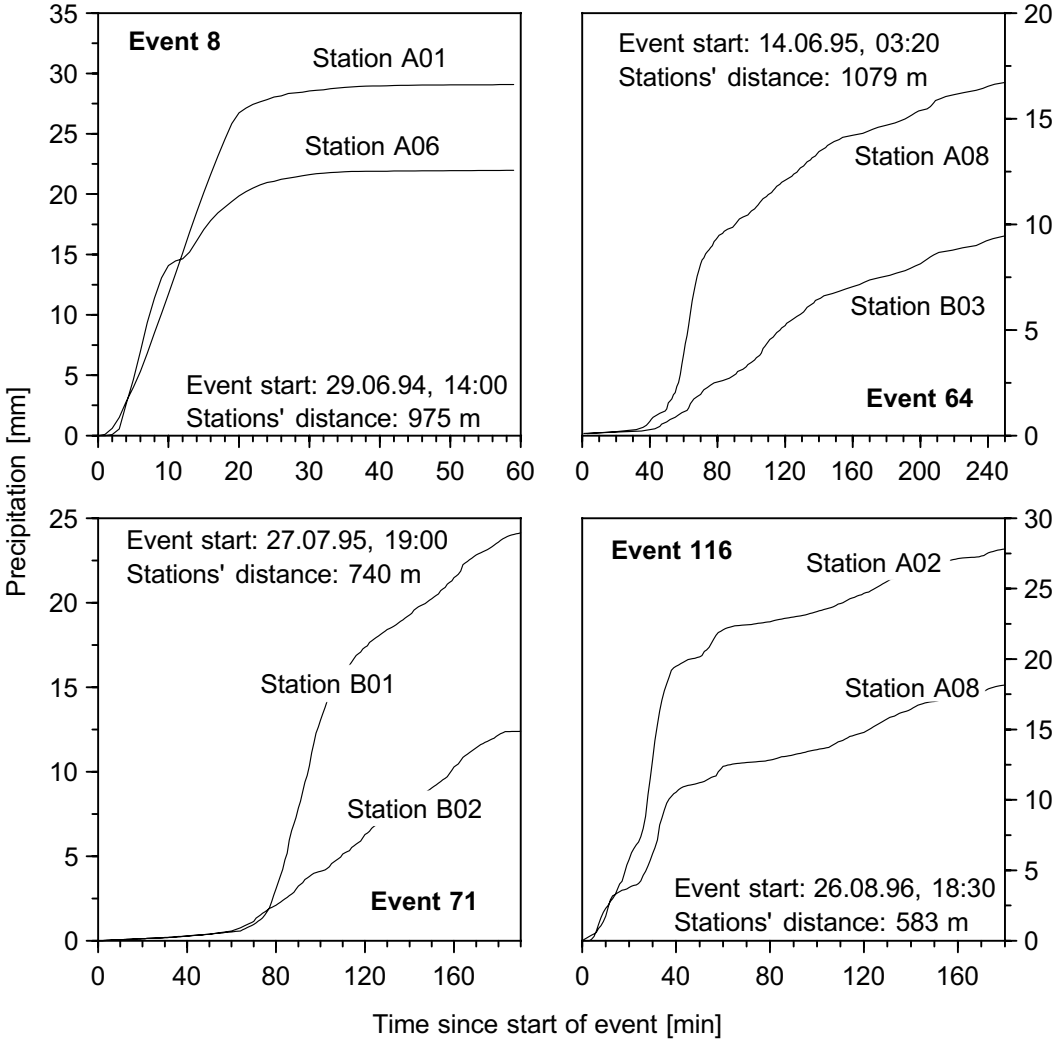


**Figure 7. Cumulative rain of the two measuring stations between which the largest trend of rain depth was determined for the four events shown in Figure 3.**

the largest trends (event numbers 8, 64, 71, and 116) for which the spatial distribution is shown in Figure 3. Within its first 60 min event 8 was the most intense summer storm during the observation period. The difference in precipitation between A06 (22 mm) and A01 (29.1 mm) resulted from only 15 min of different rain intensity (Figure 7). In the eastern part of the test site (A01) rain intensity was nearly constant, while in the western part (A06) intensity decreased during the second half of the event. A similar situation occurred during events 64, 71 and 116 (Figure 7). The differences in total rain depth mainly resulted from short-lasting (< 30 min) differences in rain intensity while the difference in rainfall intensity was negligible during most of the rain. This indicates that the stations operated correctly and that the differences in rainfall depths are not caused by systematic errors in the measuring systems.

In most cases trends were caused by short, high intensity bursts and not by different rain duration. Hence, the importance of trends increases with decreasing length of the considered periods (Table 4). Within the 5 min of highest intensity, the median intensity gradient was 24 mm $h^{-1}$ $km^{-1}$ and the maximum gradient even amounted to 49 mm $h^{-1}$ $km^{-1}$. In contrast, the median gradient in rain depth decreased only from 4.2 to 2.0 mm $km^{-1}$ when the reference period decreased from total rain to 5 min. Hence half of the total gradient evolved during 5 min of rain.

**Table 4. Gradients of maximum rain depth and maximum rain intensity for time intervals between 5 and 60 min and gradients of total rain erosivity [ N $h^{-1}$ $km^{-1}$] for all erosive gradient events (n = 21) in the hydrological summer half-years 1994 to 1997.**

| Rain property | Interval | Median | 1st quartile | 3rd quartile | Minimum | Maximum |
|---|---|---|---|---|---|---|
| Rain depth gradient [mm $km^{-1}$] | 5 min | 2.0 | 1.6 | 3.6 | 0.6 | 4.1 |
| | 10 min | 2.9 | 2.2 | 4.8 | 0.9 | 6.0 |
| | 15 min | 3.3 | 1.8 | 4.7 | 1.0 | 8.1 |
| | 30 min | 3.9 | 1.5 | 5.4 | 0.4 | 13.3 |
| | Total | 4.2 | 2.5 | 5.3 | 1.4 | 15.7 |
| Intensity gradient [mm $h^{-1}$ $km^{-1}$] | 5 min | 24.3 | 19.1 | 42.8 | 7.4 | 48.6 |
| | 10 min | 17.1 | 12.9 | 28.6 | 5.6 | 35.7 |
| | 15 min | 12.9 | 7.0 | 18.7 | 4.0 | 32.2 |
| | 30 min | 7.8 | 3.0 | 10.7 | 0.8 | 26.6 |
| | 60 min | 4.1 | 1.5 | 5.9 | 0.7 | 16.6 |
| Erosivity gradient [N $h^{-1}$ $km^{-1}$] | Total | 2.8 | 1.3 | 4.8 | 0.3 | 31 |

For event 8 (29 June 1994) Figure 8 exhibits large negative and positive differences of intensity in sequence. This behavior characterizes events during which the high-intensity cell moves over the area and hits a large part of the total area but at different times. The gradient in accumulation was thus partly leveled out already during the event. In most cases, however, (three out of four in Figure 8) these high-intensity cells were quite stationary and thus produced a spatial trend, which was still detectable even for the total rain.

## DISCUSSION

### High-intensity cells cause the spatial trend on the sub-kilometer scale

Although there was no synoptic analysis of these events, a connection between convective storms typical for these summer months and gradient events is evident. The findings of (i) a nearly linear trend, (ii) a random orientation of the trend, (iii) the lack of a minimum or maximum within the research area, and (iv) the short periods during which the main portion

of the trend develops indicate that the trend is caused by convective cells, which are larger than the research area (1.4 $km^2$). The steep gradient of the trend, however, makes it unlikely that they are much larger. These trends are hence likely to be underestimated with most methods commonly applied to determine the spatial variation in rainfall.

Our definition of gradient events selected only rains for which the gradient was detectable for the total rain depth. Our definition did not include those gradient events for which a movement of a high-intensity cell cancelled out the effect and those events for which the trend during short periods of rain was too small to override the random error within the measurements. In both cases, the effects on surface hydrology should be small. Hence our conservative definition, although incomplete, should give an appropriate estimate of the hydrological significance of gradient events.

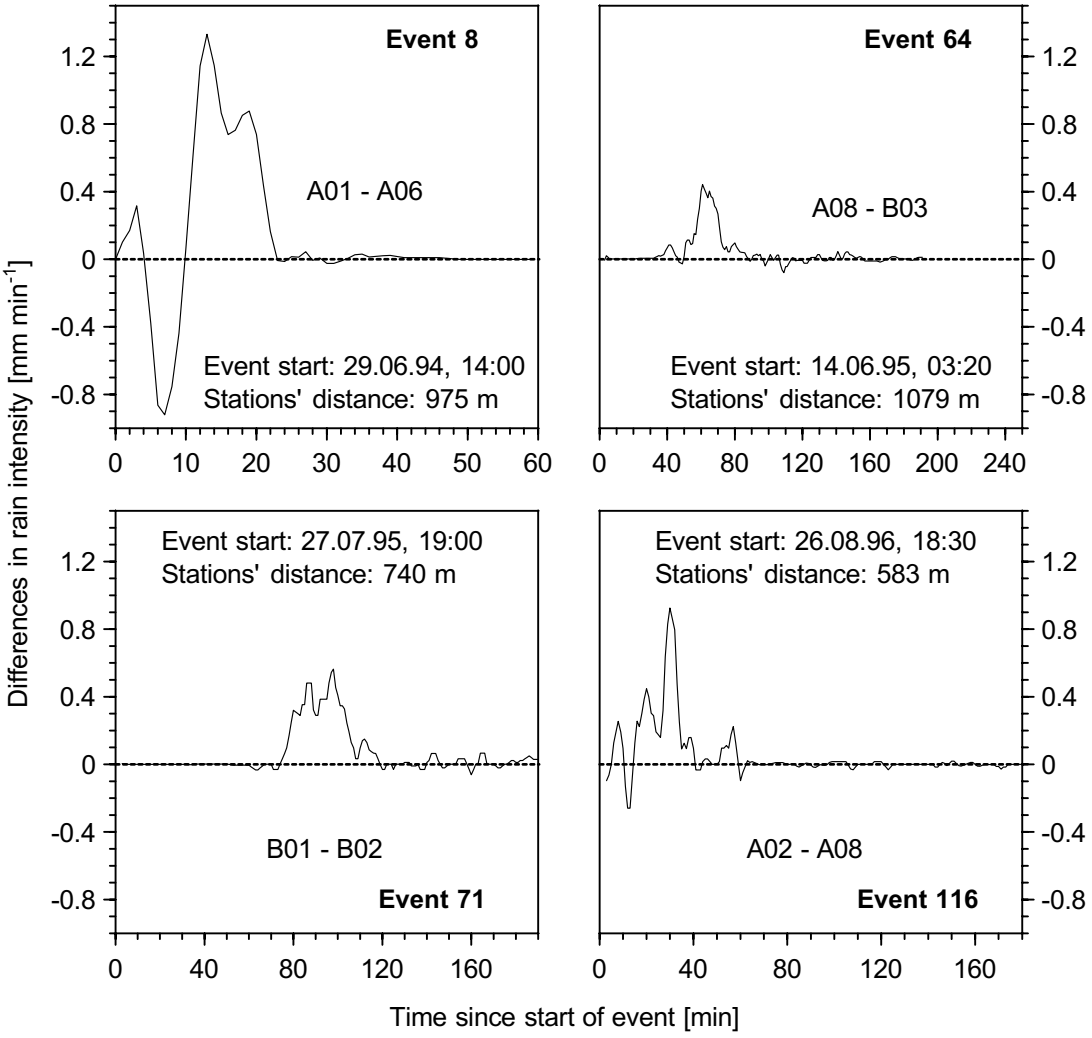


**Figure 8. Differences in rain intensity between station pairs represented in Figure 7 for four events; intensities are smoothed using a moving average of 3 min.**

### Influence of climate on spatial trends on a sub-kilometer scale

There are only a few studies focusing on small-scale (< 10 $km^2$) spatial variability in rainfall depth and intensity (e.g. Goodrich et al., 1995; Hernandez et al., 2000; Jensen and Pedersen, 2005; Niemczynowicz, 1982; Sivakumar and Hatfield, 1990). A study similar to the one presented here was carried out by Goodrich et al. (1995) in a 4.4 ha semi-arid experimental watershed part of the Walnut Gulch experimental site in Arizona. Linear trends in rain depth exhibited gradients between 2.8 and 24.8 mm $km^{-1}$ (mean 12 mm $km^{-1}$) for nine out of 11 events. These gradients were about twice as large as the gradients at the Scheyern test site. Niemczynowicz (1982) evaluated the spatial representativeness of point rain measurements (12 rain gauges, three-year observation) in a 25 $km^2$ urban watershed in Sweden. The structure of the events was not tested but from his data a maximum gradient of 5.5 mm $km^{-1}$ can be derived, which is only one-third of the maximum gradient found at Scheyern (15.7 mm $km^{-1}$). Thus, the gradients seem to increase from the maritime Swedish situation to the sub-continental Scheyern climate and further to the semi-arid, continental climate in Arizona.

### Sub-kilometer scale spatial trends increase with storm size and recurrence interval

Spatial variability of rain depth in a small semi-arid tropical environment was tested by Sivakumar and Hatfield (1990) during two years at 18 rain gauges within a flat 500 ha area. In general, the authors found that spatial variability within the test site increased with storm size. Our study of gradient events shows that also within an event the spatial variability is largest during the high-intensity periods (Table 4). Nevertheless, a trend cannot be generally assumed for any high-intensity period because high intensities were more or less equally distributed between spatial gradient events and random events. For example, $I_{max60}$ > 10 mm was measured four times for gradient events but also four times for random events. Hence, the need to set up a dense network of rain gauges increases (i) with decreasing time interval

**Table 5. Breakdown of average rain trends of all erosive events in the hydrological summer-half year (1994–1997) by the recurrence intervals according to Bartels et al. (1997); where recurrence intervals differed for the 15-, 30- or 60-min maximum intensity of an event, it is assigned to the minimum recurrence interval.**

| | All events | | Gradient events | | |
|---|---|---|---|---|---|
| Recurrence [yr] | Average gradient [mm $km^{-1}$] | Number of events | Average gradient [mm $km^{-1}$] | Number of events | Number of random events |
| 5 – 10 | 10.7 | 2 | 10.7 | 2 | 0 |
| 1 – 5 | 3.9 | 5 | 9.8 | 2 | 3 |
| 0.5 – 1 | 2.7 | 16 | 4.8 | 9 | 7 |
| < 0.5 | 0.6 | 36 | 2.6 | 9 | 27 |
| All | 1.8 | 59 | 4.9 | 22 | 37 |

a respective process is looked at, and (ii) with the influence that single, rare storms have on the respective process because the strength of the gradient increased with increasing size of recurrence interval (Table 5). Hence, if runoff and erosion scenarios for small watersheds are evaluated the potential effects of spatial trends in rainfall become more and more important if rains with increasing recurrence intervals are assumed.

**Process significance of spatial trends on the sub-kilometer scale**

During the four-year observation period spatial gradient events did not occur later than early September. There might be few more gradient events during the winter-half year, which we did not evaluate because of measurement induced variability (snow fall, increasing wind speed error) and failures in measuring stations (snow frozen in funnels, frozen tipping buckets) increase in the winter half-year. Also focusing on events ≥ 5 mm only restricted the total number of gradient events. Therefore, our estimated number of gradient events determined during the observation period is conservative. However, the additional events would have only a small impact on most processes due to their small precipitation depth and flat gradients.

Due to the very short period during which the differences develop, the importance of gradient events increases with decreasing temporal scale of a process. While gradient events are almost unimportant for annual processes like groundwater recharge, they are highly important for rain erosivity or runoff. Their importance is even higher where a certain threshold has to be exceeded for a process to occur. Such a threshold process would be rill initiation (e.g. Fiener et al., 2008; Van Oost et al., 2004). The threshold may be exceeded on one field while the peak intensity remains below the threshold on the neighboring field. Thus, a large difference in the response of the two fields would result despite a relatively small difference in total rain.

Focusing on surface runoff and soil erosion in small agricultural watersheds the hydrological summer half-year and especially the months June to August are important at the research site, as these time periods receive about 90% and 70% of the annual erosivity, respectively (Schwertmann et al., 1987). During the four-year observation period about one-third of all summer events and about half of all events between June and August had a spatial trend. Hence, spatial trends of rain events are significant for small watersheds and should be considered when developing, calibrating, validating and applying event-based runoff and erosion models. Trends in rain intensity and rain erosivity may also contribute to the differences in soil loss observed from replicated plots (e.g. Nearing et al., 1999).

## CONCLUSIONS

A network of 13 rain gauges at a 1.4 $km^2$ test site in southern Germany exhibited a significant spatial trend in rainfall depth for 33% of all events during the summer half-year. The individual trends were essentially linear. Gradients in rainfall depth ranged from 1.0 to 15.7 mm $km^{-1}$ with a mean of 4.2 mm $km^{-1}$ (median 3.3 mm $km^{-1}$) and were clearly not due to errors of the measuring systems or wind effects. While the spatially random events produced about 20% more rain than gradient events, the cumulative rain erosivity of the gradient events was about 40% larger. The gradients in rain lead to much steeper gradients in predicted rain erosivity and predicted runoff. Rain depth of gradient rains on average increased within 1 km distance by 48% of the rain at the central location. In contrast this average increase was more than twice as steep for rain erosivity and runoff.

The trends had no significantly preferred orientation. This suggests that in the longer term there is no difference in rainfall depth within the test site, but in short-time periods or for single events the assumption of spatially uniform rainfall is invalid on the sub-kilometer scale. This seems to apply to many regions where summer rainfall is connected to convective storms and has important implications for any kind of small-scale environmental research depending on appropriate rainfall data.

The strength of the spatial trend was not related to rain depth but increased with rain intensity. The trends thus also increased in strength with recurrence interval. Moreover, the gradients of maximum intensities were more pronounced compared to those of rain depth. This has important implications for any hydrological or geomorphologic process sensitive to maximum rain intensities, especially when focusing on large, rare events. As an example shown for rain erosivity, relative gradients of derived environmental parameters can be much steeper than those of rain depth or intensity. Hence, it will take considerably longer until sub-kilometer scale differences in such parameters level out than the time needed to level out difference in rain depth. These farm-scale differences are highly relevant for environmental processes acting on short-time scales like flooding or erosion. They should be considered during establishing, validating and application of any event-based erosion (or hydrological) model.

# 2. MANAGING EROSION AND WATER QUALITY IN AGRICULTURAL WATERSHEDS BY SMALL DETENTION PONDS

With minor revisions published:
Peter Fiener, Karl Auerswald, and Stephan Weigand 2005.
Managing erosion and water quality in agricultural watersheds by small detention ponds.
Agriculture Ecosystems & Environment. 110:132-142, 2005.

***ABSTRACT.*** *Terrace-contouring systems with on-site water detention cannot be installed in areas of complex topography, small parceling and multi-blade moldboard plow use. However, field borders at the downslope end may be raised at the deepest part where runoff overtops to create detention ponds, which can be drained by subsurface tile outlets and act similar to terrace-contouring systems. Four of such detention ponds were monitored over 8 yrs. Monitored effects included the prevention of linear erosion down slope, the sediment trapping from upslope, the enrichment of major nutrients in the trapped and delivered sediments, the amount of runoff retained temporarily, the amount of runoff reduced by infiltration, the decrease in peak runoff rate and the decrease in peak concentrations of agrochemicals due to the mixing of different volumes of water within the detention ponds. The detention ponds had a volume of 30–260 $m^3$ $ha^{-1}$ and trapped 54–85% of the incoming sediment, which was insignificantly to slightly depleted (5–25%) in organic carbon, phosphorus, nitrogen and clay as compared to the eroding topsoil, while the delivered sediment was strongly enriched (+70–270%) but part of this enrichment already resulted from the enrichment of soil loss. The detention ponds temporarily stored 200–500 $m^3$ of runoff. A failure was never experienced. Due to the siltation of the pond bottom, the short filled time (1–5 days) and the small water covered area, infiltration and evaporation reduced runoff by less than 10% for large events. Peak runoff during heavy rains was lowered by a factor of three. Peak concentrations of agrochemicals (Terbutylazin) were lowered by a factor of two. The detention ponds created by raising the downslope field borders at the point of discharge efficiently reduced adverse erosion effects downslope the eroding site. They are cheap and can easily be created with on-farm machinery. Their efficiency is improved where they are combined with an on-site erosion control like mulch tillage because sediment and runoff input are reduced. Ponds had to be dredged only after the first year when on-site erosion control was not fully effective.*

Storm water detention and retention ponds or basins (referred to as detention ponds in this paper) are common features in storm water management, to retain storm runoff for a certain time and to reduce peak discharge to a level that is bearable for the drainage system (Verstraeten and Poesen, 1999). Besides the reduction of peak runoff rates, there are several additional purposes, like sediment trapping, prevention of downstream linear erosion, or water quality management, which have been addressed in a variety of detention pond sizes, constructions and storage strategies.

In agricultural areas (dry) detention ponds, which typically hold water only during storms, are used to protect infrastructure and private properties from flooding and damages by muddy floods (Boardman et al., 2003; Verstraeten and Poesen, 1999; 2000a). These ponds compensate on-site erosion in the fields, but create high costs for construction, area and maintenance. Especially regular dredging is cost intensive (Boardman et al., 2003). The size of these ponds, for example, in Central Belgium, where they are widely established, reaches volumes of several thousands of $m^3$ (Verstraeten and Poesen, 1999). Besides these flood protection measures, ponds are also constructed to treat agricultural runoff (Rushton and Bahk, 2001). These ponds typically maintain a permanent pool of water between storms to improve water quality by the settling of suspended solids and sediment bound substances.

A similar strategy but with completely different dimensions and layout are terrace-contouring systems with temporary water storage behind the terraces and a controlled, dampened drainage by underground tile outlets (Schwab et al., 1993). This system catches runoff shortly after the source area. Hence, only small volumes of water have to be retained behind each length unit of terrace, which causes little construction costs. A major advantage is that the retention area can still be farmed because water storage will only be shallow and occur during short periods of time, which will not be harmful to the crops as long as sediment input is reduced by additional on-site erosion control measures like mulching. This strategy, however, requires that field layout can be adapted to the landscape morphology. This is only possible in slightly undulated landscapes with large fields. This type of runoff control can hence be widely found in US American and in Australian agriculture, while it cannot be applied in areas where the land is owned by many farmers and with a steep and complex morphology as it is found in Middle Europe and many other areas in the world. In these cases, field borders running perpendicular to the main slope may be reshaped to serve similar purposes as the terrace contouring systems.

This study investigates the performance of such small dry detention ponds (220–490 $m^3$ in size) established at field borders along the drainage ways of hill slopes. The objectives were to evaluate: (i) the on-site effects on linear erosion in the down slope fields; (ii) the trapping efficiency of sediments and sediment bound pollutants; (iii) the reduction of runoff

volumes and peak runoff rates coming from the fields; and (iv) the reduction of peak concentrations of water soluble pollutants by water mixing in the ponds.

## MATERIAL AND METHODS

### Test Site

The test site was part of the Scheyern Experimental Farm of the Munich Research Association for Agricultural Ecosystems (FAM), which is located about 40 km north of Munich. The area is part of the Tertiary hills, an important agricultural landscape in central Europe. The test site covered approximately 22 ha of arable land at an altitude of 461-486 m a.s.1. (48°30'50'' N, 11°26'30'' E). The mean annual air temperature was 8.4° C (for 1993-2001). The average precipitation per year was 834 mm (for 1993-2001) with the highest precipitation occurring from May to July (average maximum 106 mm in July) and the lowest occurring in the autumn and winter months (average minimum 29 mm in October).

The test site consisted of four small adjacent watersheds 1.6-7.8 ha in size (Table 1). The management in the fields followed the principles of integrated farming in combination with an intensive soil conservation system (mulch tillage) (Auerswald et al., 2000). Field sizes ranged from 1.9 to 6.5 ha. The crop rotation consisted of potato (*Solanum tuberosum* L.), winter wheat (*Triticum aestivum* L.), maize (*Zea mays* L.), and winter wheat. This rotation allowed planting of a cover crop (mustard, *Sinapis alba* L.) before each row crop. Maize was planted directly into the winter-killed mustard. Potatoes were planted in ridges formed before sowing the mustard which provided winter-killed cover.

### Detention pond design

The long sides of the fields were mostly oriented perpendicular to the overall slope. Although field size was small, the complex morphology and the restriction to allow for a use of a moldboard plow made it impossible to align the fields exactly along the contour. Runoff hence still would be concentrated in slope depressions within the fields and pass the field border at the bottom of these slope depressions. At these locations, the field borders were raised by earth embank-

**Figure 1. Picture of pond P02 after a runoff event in March 2002; in the centre of the ponded area the perforated riser pipe and the overflow are located; winter wheat was cultivated in the watershed.**

Table 1
Characteristics of the detention ponds and their upslope watersheds

| Watershed characteristics | | | | | | | Detention pond characteristics | | | | |
|---|---|---|---|---|---|---|---|---|---|---|---|
| Watershed no. | Size (ha) | Mean slope (%) | Shape factor $f_h$[a] (–) | Average annual runoff 1994–2001 (1 $m^2$) | Pond no. | Location (–) | Maximum dam height (m) | Dam top width (m) | Maximum volume ($m^3$) | Maximum water level (m) | Diameter orifice plate (m) | Volume per watershed area (1 $m^{-2}$) |
| W01 | 1.60 | 7.40 | 0.31 | 43.4 | P01 | Field | 1.40 | 4.2[c] | 423 | 1.18 | 0.025 | 26.5 |
| W02 | 3.57 | 6.71 | 1.01 | 62.5 | P02 | Field | 1.49 | 1.8 | 486 | 1.25 | 0.040 | 13.6 |
| W05 | 4.05 | 9.27 | 0.84 | 25.4 | P05 | GWW[b] | 1.66 | 4.5[c] | 335 | 1.44 | 0.040 | 8.3 |
| W06 | 7.81 | 9.43 | 0.47 | 6.4 | P06 | GWW | 1.25 | 5.5[c] | 221 | 1.08 | 0.040 | 2.8 |

[a] fh: watershed size/(max watershed length)$^2$.
[b] GWW: grassed waterway.
[c] Embankment top used as farm road.

ments to create small detention ponds. Small earth embankments further extending over the lower field border would additionally prevent runoff from entering the downslope fields and direct runoff into these ponds (Figures 1 and 2). The height of the pond embankments at the point of discharge ranged between 1.25 m (P06) and 1.66 m (P05) with a dam top width from 1.8 m (P02) to 5.5 m (P06), where the top was used as farm road (Table 1). The detention ponds were drained by underground tile outlets. They consisted of 15.6-cm-diameter standpipes, which were perforated to prevent blocking by plant residues (Hickenbottom Inc., Fairfield, IA, USA). Depending on watershed characteristics and pond size orifice plates of either 0.025 or 0.040 m (Table 1) dampened the outflow. At the ponds P02 and P05, which were located downslope from the ponds P01 and P06, respectively, emergency outflow pipes with a diameter of 15.6 cm were also installed (Figure 2). The outflow pipes ended either below the embankment of the ponds in a grassed waterway (P05 and P06) or after 185 and 360 m in the next ditch (P01 and P02).

This pond design should control the runoff during most events without overtopping or using the emergency outflow, and delay runoff and enhance sediment settling time as long as possible without damaging field crops or the waterway grass, which happens approximately after 3–4 days of submergence.

## Measuring Methods

Linear erosion along the thalweg downslope from the ponds was investigated between 1993 and 2001 by frequent field observations. These observations were compared with the damage created by a large thunderstorm in August 1992 just before pond installation and with results from modeling erosion and deposition of the site assuming that no ponds were established. The soil loss from ephemeral gullies and larger rills during the August thunderstorm was evaluated by

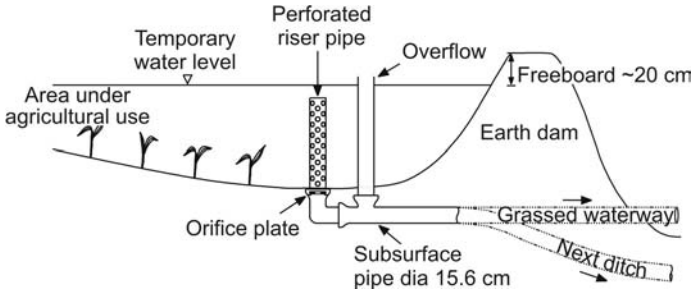


**Figure 2. Schematic diagram of the pond cross-section.**

determining the length of gullies and rills from aerial photos (scale 1:10,000) and measuring their cross-sections in the field in 25 m steps along the gullies and along transects taken perpendicular to the rills. Eroded volume was converted to eroded mass using measured bulk densities. The used GIS-based model (Mitasova et al., 1996) calculates an erosion and deposition index in a 2-m×2-m-grid, based on a high-resolution digital elevation model and a detailed *K* factor (soil erodibility of the Universal Soil Loss Equation, USLE) map of the watershed (Fiener and Auerswald, 2003b).

Outflow volume and rate during runoff events were measured with Coshocton-type wheel runoff samplers, which collected about 0.5% from the total runoff coming from the outflow pipes of the ponds, and lead it to tipping buckets (volume = approximately 85 ml). The number of tips was counted with Delta-T-Loggers (Delta-T Devices Ltd., Cambridge, UK) and runoff samples were taken after defined runoff volumes with an ISCO-Model 3700 portable sampler (Isco, Lincoln, NE, USA). All measuring systems were tested for function at least at the end of each runoff event. A detailed description of the measuring system, including the results of a precision test, can be found in Fiener and Auerswald (2003a). The total sediment delivery of each event was calculated from sediment concentrations determined from subsamples drawn after homogenization and dried at 105° C. The measuring devices were successively installed after landscape redesign in early 1993.

The sediment trapping in the ponds was evaluated by using a grid of erosion pins laid over the pond bottoms in the beginning of 1993. In the first year severe sedimentation in the ponds was measured because after the landscape-redesign in 1992 the fields and the new structures like the embankments were prone to erosion and produced large sediment amounts. Hence, at the beginning of 1994 all ponds were dredged and the erosion pins were installed again. After dredging no further sedimentation was measured because the soil-conservation system of the farm started to work successfully. Hence, the data of sediment trapping efficiencies of the ponds were calculated averaging the sedimentation in 1993 (15 major events had occurred).

To analyze the trapping of sediment bound substances the average concentration of organic carbon ($C_{org}$), calcium–acetate–lactate extractable phosphorus ($P_{cal}$) and potassium ($K_{cal}$), organic nitrogen ($N_{org}$), and clay (< 2 µm) in the pond deposited sediment, the delivered sediment, and the topsoil of the watersheds was determined. A total of 24 sediment samples from the ponds and 50 samples from the largest runoff events in 1993 were taken and compared to data of a soil survey carried out in a 50-m×50-m-grid in all watersheds in 1992 (Auerswald et al., 2001). To account for the variation between the topsoils of the eroding fields and to allow for an application to other sites, the enrichment ratios of nutrients and clay in pond sediment ($ER_P$) and in the delivered sediment ($ER_d$) compared to the topsoil in the watersheds was calculated, exemplarily shown for $ER_d$ in Eq. (1).

$$ER_d = \frac{\sum_{i=1}^{n} C_i m_i \Big/ \sum_{i=1}^{n} m_i}{\sum_{j=1}^{k} C_j / k} \tag{1}$$

$ER_d$ being the average enrichment ratio of nutrients or clay in the delivered sediments, $C_i$ is nutrient or clay content of the $i$-th event and $m_i$, is the respective sediment mass while $C_j$ is nutrient or clay content of the $k$ soil samples in the sampling grid.

The peak discharge reduction was determined from the measured outflow rates and the inflow rates calculated according to Eq. (2):

$$q_{in}(t) = \frac{dV_{pond}}{dt} p_A(t) + q_{out}(t) + i_A(t) + e_A(t) \tag{2}$$

$q_{in}$ being the inflow rate ($m^3\ s^{-1}$), $V_{pond}$ is storage volume in the pond ($m^3$), $p_A$ is precipitation rate on the ponded area ($m^3\ s^{-1}$), $q_{out}$ is outflow rate ($m^3\ s^{-1}$), $i_A$ and $e_A$ are the infiltration and the evaporation rates ($m^3\ s^{-1}$) from the ponded area $A$ ($m^2$), and $t$ is time (s).

$V_{pond}$ and $A$ for time $t$ were calculated from the storage heights, measured every 10 min between 1994 and 1997 with pressure transducers (UMS GmbH, Munich, Germany) connected to Delta-T-Loggers, and data of a detailed geodetic survey carried out in the ponds after dredging in January 1994 (Figure 3). The precipitation rate $p_A$ for time $t$ was calculated from $A(t)$ and the average of two meteorological stations at the research farm located about 500 m east and west from the ponds. Considering the small contribution of evaporation to the water balance of the pond, $e_A$ was estimated from measurements of the German Meteoro-

logical Service (DWD) at the Weihenstephan meteorological station located at a similar situation 25 km southeast of the test site.

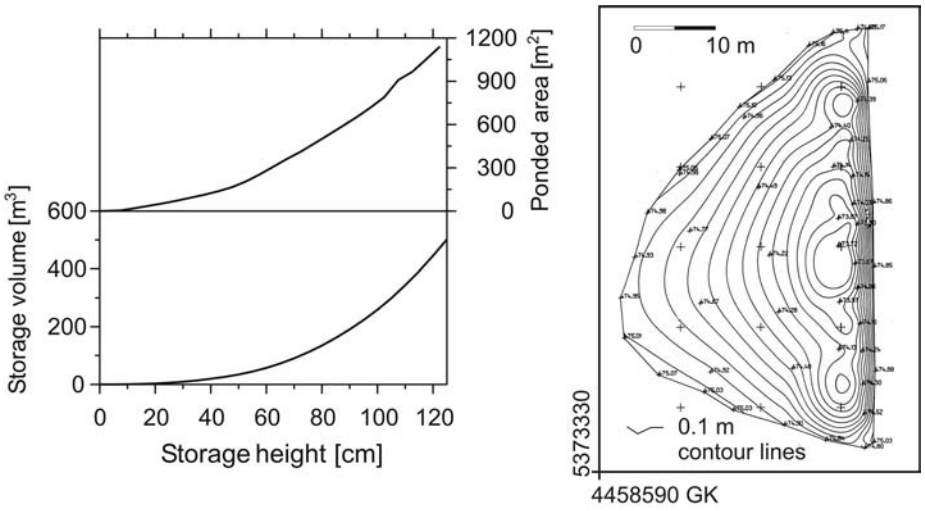


**Figure 3. Storage characteristics and topography of detention pond P02 after dredging at the beginning of 1994; GK: Gauss Krueger coordinates.**

The soil moisture at the start of pond filling and the soil silting at the pond bottom is needed to calculate $i_A$. The ponds were filled in two contrasting situations: (i) after long lasting rains in winter with soils close to field capacity; (ii) in case of heavy thunderstorms in summer, when the soils could be initially dry but when pond filling starts after some rain conditions close to field capacity may be assumed as well, even if this may slightly underestimate infiltration in some cases. The macropores, which then will be filled when pond filling starts, were estimated to contribute 70 L $m^{-2}$ ponded area (Scheinost et al., 1997) to runoff reduction in the ponds. The saturated hydraulic conductivity for the soil at the test site was measured during field surveys (Scheinost et al., 1997), it ranged between $10^{-6}$ and $5.0\times10^{-6}$ $m^3$ $s^{-1}$. Due to the distance of 15–20 m between soil surface and ground water we assume that the effect of storage heights (< 1.66 m) on saturated hydraulic conductivity could be neglected. Soil sealing may occur by the effect of rain prior to pond filling or by siltation afterwards. Adopting measurements of Schröder and Auerswald (2000) at the test site, the saturated hydraulic conductivity was reduced by a factor of about 2.5 to account for sealing, which corresponds to the findings on similar soils by others (e.g. Roth, 1992). Infiltration and evaporation after pond filling then yields the reduction in runoff volume. To separate surface runoff into the components rain and soil water the stable isotope technique was used (Rozanski et al., 2001). This allowed to characterize the individual inflow of a deten-

tion pond and facilitates the interpretation of the measured inflow concentrations of soluble agrochemicals. Isotope signatures determined at the GSF Hydrology Laboratory in Neuherberg (Germany) are given relative to standard mean ocean water in commonly used $\delta$ notation:

$$\delta X = \frac{\left[(R_{\text{sample}} / R_{\text{standard}}) - 1\right]}{10^3} \tag{3}$$

where $X$ being $^2$H or $^{18}$O and $R$ being the respective $^2$H/H or $^{18}$O/$^{16}$O ratio.

While deuterium ($^2$H) and oxygen-18 ($^{18}$O) of rainwater followed the local meteoric water line, water taken by suction cups from the soil deeper than 1.0 m showed little temporal variation ($^2$H = -62.2 ± 2.1 and $^{18}$O = -8.7 ± 0.2). It was close to the average of all isotopic signatures of rain (-72.9 and -10.0, respectively) because recharge occurs mainly in winter months, during which rain is slightly more depleted in heavier isotopes and thus compensates for the enrichment of soil water by evapotranspiration left after the growing period. It also corresponded with the isotopic signature of the ground water. In general, rains from heavy runoff inducing storms often deviate considerably from average soil water signature. In this case the contribution of rainwater and exfiltrating soil water or ground water to surface runoff can easily be computed from the average soil water signature and the signatures measured in rain and surface runoff by mass balance calculations (Eq. (4)).

$$\delta_{\text{runoff}} = \delta_{\text{rain}} F_{\text{rain}} + \delta_{\text{soil}} (1 - F_{\text{rain}}) \tag{4}$$

where $F_{rain}$ is being the fraction of rainwater contributing to runoff, while $\delta$ is the isotopic signature in runoff, rain, and soil water, respectively.

One of the 10 heaviest rain events, out of 1423 events between 1994 and 2001, fell on June 5th 1995 (43.3 mm) on a runoff-prone maize seedbed in W02 and thus produced the tenth largest among 1097 observed runoff events (reoccurrence time of more than 3 yrs).

Seven days before the storm, 1.5 L ha$^{-1}$ of Gardoprim 500® was applied, containing 0.47 kg L$^{-1}$ of the herbicide Terbutylazin. The outflow concentration of Terbutylazin was determined according to standard procedures (Schülein, 1998). Assuming a homogeneous Terbutylazin concentration within the pond (total mixing) and neglecting changes by precipitation, evaporation and infiltration, we calculated the pond inflow concentrations from Eq. (5):

$$C_{\text{in}}(t_{n+1}) = \left\{\left[C_{\text{out}}(t_{n+1})\ \left(V_{\text{pond}}(t_n) + V_{\text{in}}(t_{n+1} - t_n)\right)\right] - C_{\text{out}}(t_n)\ \ V_{\text{pond}}(t_n)\right\}\ /\ V_{\text{in}}(t_{n+1} - t_n) \qquad (5)$$

where $t$ being the time, $C_{in}$ and $C_{out}$ being Terbutylazin inflow and outflow concentration, respectively, $V_{pond}$ pond volume, $V_{in}$ being inflow volume between the two time steps $t_n$ and $t_n$+1;

## RESULTS AND DISCUSSION

The ponds were created with on-farm machinery with almost no costs. Only the inlet raiser and the transmitting pipes had to be purchased. Damage of the crops occurred only during the first year, when heavy siltation was induced (up to more than 0.5 m), because on-site erosion control was still not fully effective. Even in this year the damage was restricted to an area of less than 100 $m^2$ per pond at the deepest part of the pond. A damage of the crops by flooding was never observed, even not for potatoes. Dredging was necessary only after the first year and could also be done with on-farm machinery at low costs. In total, the costs remained below 100 € $ha^{-1}$ $yr^{-1}$ averaged over the entire study period and all ponds. However, the dams had to be inspected regularly to identify problems like weaknesses created by burrowing animals or clogging of the orifice. Moreover, such low maintenance costs are only possible if regularly siltation of the ponds is prevented due to an effective soil-conservation in the watersheds.

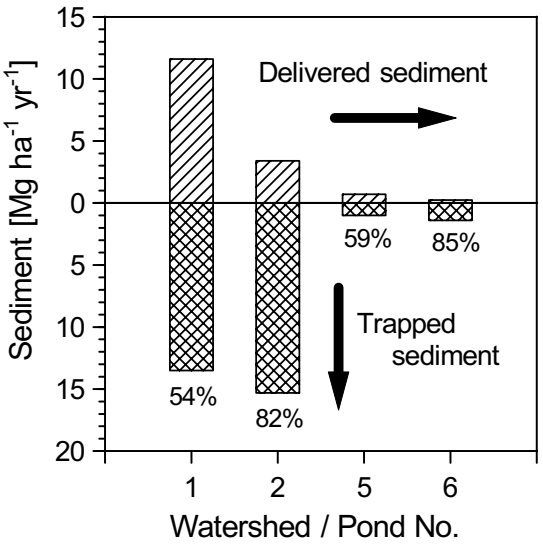


**Figure 4. Sediment trapping of the detention ponds in 1993.**

No linear erosion along the thalwegs downslope the ponds was observed between 1994 and 2001, although those thalwegs were heavily prone to erosion before establishing the ponds. The principal vulnerability of the thalwegs, where runoff from two opposite slopes converges, was shown by modeling (Mitasova et al., 1996) and also impressively demonstrated by the thunderstorm in August 1992. This event, with a rainfall intensity of up to 160 mm $h^{-1}$ and a total rainfall of 60 mm, created ephemeral gullies along the thalwegs were the ponds were installed later, which were up to several meters wide and 80 cm deep. The prevention of linear erosion results not only from the ponds itself, but from their combination with a drainage via a grassed waterway or pipes to the toe slope. In 1993 the four tested ponds trapped between 54 and 85% (Figure 4) and in

total between 1.0 and 15.3 t $ha^{-1}$ $yr^{-1}$. Event-based measuring was possible for 15 major erosion events during that year. Neither relative (54–85%) and total sediment trapping (1.0–15.3 t $ha^{-1}$ $yr^{-1}$), nor sediment trapping and watershed or pond characteristics were related (Table 1, Figure 4). Given the large variation in watershed conditions and storm characteristics of the individual events we concluded that the long-term trapping efficiency was independent from the total sediment input and the characteristics of the tested ponds and ranges between about 50 and 80%. After 1993 erosion control by reduced-tillage techniques in the watersheds became more effective, and hence, the input into the detention ponds decreased to less than 1.0 t $ha^{-1}$ $yr^{-1}$ with only little coarse sediments being transported. The deposited sediment could then not be measured due to the small deposition depth. Even though, similar sediment trapping efficiencies can be assumed given that small erosion events may result in little retention because only clay is transported, or alternatively complete retention if no runoff leaves the pond.

No significant enrichment was found in the pond sediments for the fractions $C_{org}$, $P_{cal}$, $K_{cal}$ and $N_{org}$. Only the clay fraction was depleted with an $ER_P$ of 0.74 (Table 2). In contrast, all measured fractions in the delivered sediment were enriched, most pronounced in case of $K_{cal}$ ($ER_d$ = 2.7), $N_{org}$ ($ER_d$ = 2.4) and clay ($ER_d$ = 2.4). From these measurements two conclusions can be drawn: (i) The sediment in the inflow into the ponds was already enriched compared to the topsoils in the watersheds by a factor of 1.3 as calculated from the total amount of deposited and delivered sediments in 1993 and the enrichment ratios $ER_d$ and $ER_P$; (ii) The ponds increased the enrichment due to a selective sedimentation of the coarse incoming sediments and a preferential loss of the dispersed fines. Residence time within the ponds (roughly 1 d) and water column height (roughly 1/3 of the maxi-

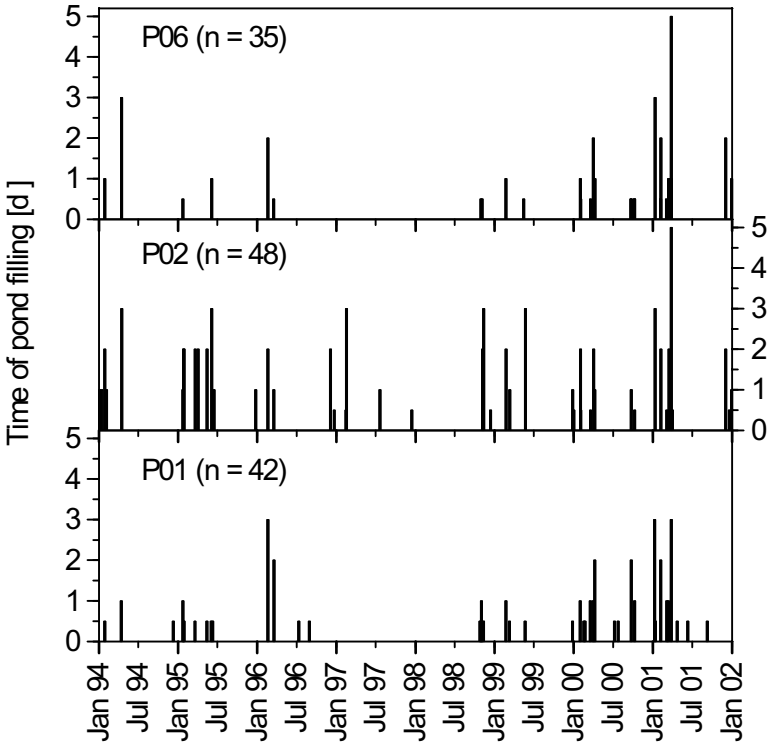


**Figure 5. Pond filling in ponds P01, P02 and P06 between 1994 and 2001. P01 represents the pond with a smaller orifice plate (=2.5 cm) than the others (=4.0 cm); P02 represents the pond with the highest, P06 with the smallest inflow rates.**

mum water level, 0.4 m) allows only for a complete settlement of particles > 2.3 µm if Stokes law is applied under the assumption of negligible turbulences. Hence, due to this enrichment of fine particles in the delivered sediments, the sediment trapping of the ponds was more efficient (54–85%) than nutrient trapping (35–70%).

**Table 2. Average enrichment as compared to the watershed topsoil for pond deposited sediment ($ER_P$) and delivered sediment ($ER_d$) measured in 1993.**

| | $ER_p$ | | $ER_d$ | |
|---|---|---|---|---|
| | Avr | SD | Avr | SD |
| $C_{org}$ | 0.92 | 0.36 a | 1.73 | 0.53 A |
| $P_{cal}$ | 0.96 | 0.33 a | 1.74 | 0.57 A |
| $K_{cal}$ | 1.05 | 0.35 a | 2.66 | 0.99 B |
| N | 0.91 | 0.34 a | 2.39 | 0.76 C |
| Clay | 0.74 | 0.23 b | 2.35 | 0.71 C |

Significantly different groups within each column are marked with different letters (n is 24 for ponded and 50 for delivered sediment). $C_{org}$: organic carbon; $P_{cal}$: calcium–acetate–lactate extractable phosphorus; $N_{org}$: organic nitrogen; $K_{cal}$: calcium–acetate–lactate extractable potassium; Avr: average enrichment; SD: standard deviation.

During the observation period (1994–2001) approximately 36 runoff events occurred per year and each pond was filled for at least 1/2 day on average 5 times a year (Figure 5). Overtopping of dams or draining via the emergency overflow (Figure 1) was not observed. Pond filling reached its highest values and lasted longest (maximum 5 days) at the end of winter and the beginning of spring, when rain and snow melt in combination with partly frozen soils resulted in long-lasting inflow at high rates. In later spring and summer pond filling occurred only after heavy thunderstorms and filling time was in almost all cases < 1 day, hence, crops and grasses were not damaged by ponded water (Figure 5). For single (summer) events the relative filling of the four ponds varied greatly, depending mainly on the type of field crop in the individual watershed and their stage of development. This variation is exemplarily shown for the 43.3 mm storm at the beginning of June 1995 (Figure 6). The relative maximum pond filling (=measured storage height / maximal storage height) ranged from 22% in case of P06 with winter wheat growing in the watershed to 83% in P02, where maize was planted within the watershed. The time of runoff retention varied between 22 h (P06) and 68 h (P02) for this event (Figure 6).

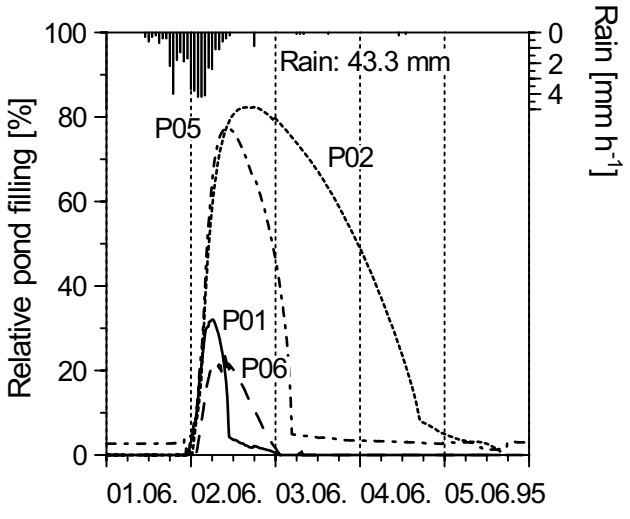


**Figure 6. Relative pond filling (=measured storage height/maximal storage height) of the ponds P01 to P06 for a thunderstorm in early June 1995.**

The runoff inflow rate and runoff volume reduction calculated with Eq. (2) is exemplarily given for pond P02 (Figure 7). Peak runoff rate was reduced from 15.1 to 4.9 L $s^{-1}$, a typical reduction in case of short heavy rains

that initiate a rapid pond filling. The dampening effect was smallest during snowmelt runoff events with a broad runoff peak, where dampening may approach zero. This condition could also be observed for this event due to unique characteristics of the specific watershed with an exfiltration of shallow groundwater following shortly after the surface runoff. The contribution of both sources of runoff to total runoff could be clearly distinguished by the isotope technique (Figure 7). Exfiltration lasted for more than 3 days with a more or less constant exfiltration rate. Under these circumstances of a steady runoff the effect of the pond on the outflow rate becomes small. This is not true, however, for other substances than runoff, which will be treated below.

The total outflow volume of 894 $m^3$ was reduced by 10% calculated by integrating the infiltration and evaporation rates of Eq. (2) after the end of inflow. This is the maximum runoff reduction, which can be expected for all ponds, because the pond P02 had the longest time of runoff retention (Figures. 5 and 6), caused by the prolonged inflow due to extensive exfiltration in the watershed measured with the isotope technique. In general, it can be concluded that runoff reduction by infiltration and evaporation is small in such ponds because of the small ponded area, the short runoff retention (maximum 5 days) and the rain and sedimentation induced sealing of the pond bottoms.

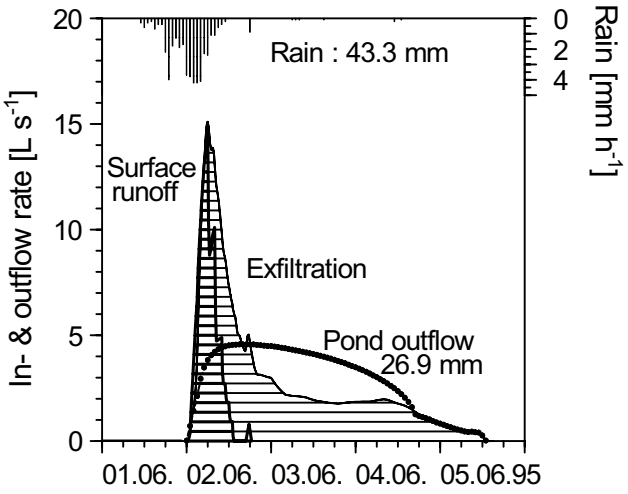


**Figure 7. Rain, inflow and outflow hydrograph of pond P02 for a thunderstorm in early June 1995.**

Due to the small runoff volume reduction by infiltration it can be expected that the amount of dissolved substances will not change too. The decrease in peak concentrations was evaluated for the rain event at the beginning of June 1995, where Terbutylazin was applied in watershed W02 seven days before. The inflow started with a concentration of 25.8 mg $L^{-1}$ and decreased within 3 h to an absolute minimum of 6.1 mg $L^{-1}$ (Figure 8) due to the ongoing depletion of the soil surface, which corresponds with the expectations for a fairly soluble pesticide. The outflow concentration started on the same level as the inflow concentration (negligible ponding at the beginning) and decreased slower to a relative constant level of about 19 mg $L^{-1}$ due to water mixing in the pond. This demonstrates that a large part of the high-concentration runoff was retained by the pond although the very first runoff passed without mixing. The early unmixed outflow will be small due to the fast rising runoff hydrograph in many cases. After about 3 h of runoff the inflow concentration in-

creased again due to the onset of exfiltration runoff identified by the isotope technique (Figure 7) and reached its maximum level of 41.6 mg $L^{-1}$ after about 48 h, while the outflow concentration of the well-filled pond stayed relatively constant (Figure 8). The Terbutylazin peak concentration thus decreased from 41.6 mg $L^{-1}$ in the inflow to 19.8 mg $L^{-1}$ in the outflow. The exfiltration runoff contained even higher concentrations than direct runoff because it contained water from early infiltration stages when the percolating water was still highly charged with the pesticide. Although this behavior is due to the unique constellation of the specific site, it provides prove for our hypothesis of a dampened peak concentration for two different situations. The effect can be clearly seen during early runoff stages (< 3 h), when only surface runoff occurs. This effect should show up in most watersheds. It was also shown, however, for the more complicated situation of exfiltrating groundwater (2 and 3 days) and may hence, be expected for a rather wide range of conditions.

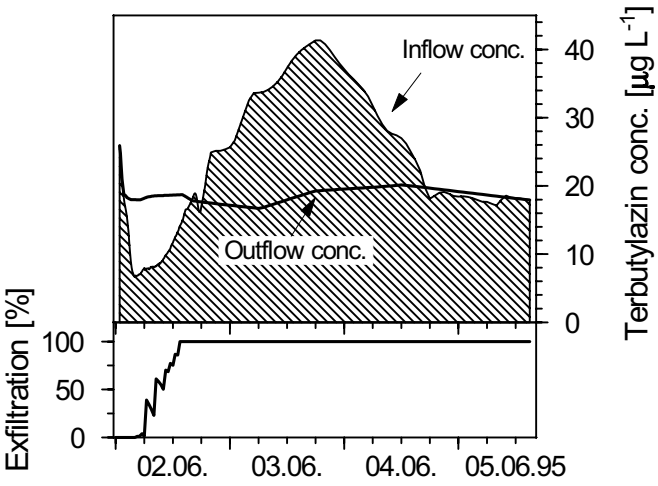


**Figure 8. Pond effects on Terbuthylazin concentrations in the inflow and outflow of pond P02 for a thunderstorm in early June 1995 (upper graph) and proportion of exfiltration to total pond inflow (lower graph).**

Even with soil conservation this type of pond is still useful for sediment and nutrient trapping because some periods of the year may still be vulnerable to erosion, e.g. after potato harvest, while ponds remain throughout the year. Furthermore, during the study period no events with a recurrence time > 5 yrs were observed. It can be expected that without soil conserving crop management ponds would decrease in efficacy for larger events, which are the events for which protection is most necessary. The combination of both measures thus allows to extend flooding protection to a wider range of events at low costs for installation and maintenance.

## CONCLUSIONS

In this study several purposes of small, earth dammed detention ponds, established at field borders, were discussed according to a 9-yr watershed experiment. Prevention of linear erosion in downslope fields, trapping of sediments and sediment bound nutrients, effects on runoff and water-soluble agrochemicals as well as costs were analyzed. The results indicate that: (i) small ponds can prevent linear erosion in downslope fields if outflow is routed to the

toe slope via a grassed waterway or a pipe; (ii) they trap 50–80% of the incoming sediments; (iii) if the ponds are combined with effective soil conservation in the fields, total sediment trapping is small, and hence, costs due to crop damages or necessary dredging operations incurre only in case of severe erosion events; (iv) the ponds can remarkably reduce peak runoff rates. At the test site even for one of the largest runoff events occurring during the study period of 32 watershed years and in case of the pond with the most unfavorable runoff to pond volume ratio, peak runoff rate was reduced to one third; (v) according to the sealing of the pond bottom, the short ponding time and the small ponded area no significant reduction of runoff volume can be expected; and (vi) the ponds can also significantly reduce peak concentrations of agrochemicals, exemplarily shown for the Terbutylazin concentration, which approximately dropped to the half. In general the efficiency of the ponds can be improved by appropriate upslope and downslope measures. An effective erosion control upslope will reduce the loading of the ponds with runoff and sediments and decrease maintenance costs. The combination with a flat-bottomed grassed waterway downslope will make best use of the high infiltration capacity, which can be established on a grassed waterway (Fiener and Auerswald, 2005) fed with runoff over a prolonged time. This type of pond can easily be installed in many complex landscapes and has almost missing restrictions on arable use, if combined with an effective soil conservation system in the fields. Therefore, due to its multiple services it should deserve more attention in conservation planning.

# 3. Effects of Hydrodynamically Rough Grassed Waterways on Dissolved Reactive Phosphorus Loads Coming from Agricultural Watersheds

With minor revisions published:
Peter Fiener and Karl Auerswald (2009)
Effects of hydrodynamically rough grassed waterways on dissolved reactive phosphorus loads coming from agricultural watersheds.
Journal of Environmental Quality, 38, 548-559.

***Abstract.*** *A modified type of grassed waterway (GWW) with large hydrodynamic roughness has proven ability to reduce sediment load and surface runoff under conditions where best management practices on the delivering fields reduce sediment inputs that could otherwise damage the grass cover. It is unknown how such a GWW affects the loading of surface runoff with dissolved reactive phosphorus (DRP). The effect on DRP was tested in a landscape-scale study where DRP concentrations and loads in surface runoff were measured in two watersheds in which GWWs were newly installed and increased in effectiveness over time. Both watersheds were compared with paired watersheds without GWW installation; all watersheds were continuously monitored over 5 yrs (1993–1997). Additionally, DRP concentrations were measured in open field and throughfall precipitation under growing grass and crops in field experiments, and DRP concentrations in surface runoff from straw covered surfaces were determined with laboratory rainfall simulation experiments. Dissolved reactive P in throughfall for the different cover types was highly variable, and the highest concentrations (up to 2.8 mg $L^{-1}$) occurred especially during flowering of the respective crop and after frost events. Dissolved reactive P concentrations in runoff from straw-covered surfaces were slightly higher compared with those from bare soil. On average, there was a small difference in DRP concentrations between throughfall under growing crops and grass and in runoff from bare or straw covered soil surfaces. Hence, the introduction of a relatively small grassed area has little effect on the DRP concentration in surface runoff from the total watershed. This finding was supported by the watershed data, where watersheds with and without GWW showed similar DRP concentrations. No change in DRP concentrations occurred over the 5-yr period. Such GWWs will thus reduce the DRP load analogously to the reduction in total surface runoff.*

Enrichment of surface water bodies with nutrients coming from diffuse sources, especially from agricultural land, has become a major environmental issue in many countries globally because the resulting eutrophication can cause serious ecological and economic damage. As a consequence, substantial effort has been made to reduce nutrient and sediment loads by the implementation of mitigation measures. Reductions of sediment and phosphorus

losses are often considered together because a large proportion of phosphorus is bound to fine-grained sediment (Bechmann et al., 2005; Owens et al., 2007). Mitigation options include improvements in agricultural practices, e.g. no-till, contouring, adapted crop rotations, timely application of fertilizers (Abu-Zreig et al., 2003), and establishment of vegetated filter strips (Dorioz et al., 2006).

Studies to investigate the effects of vegetated filter strips (VFSs) on reducing surface runoff trapping of sediment and nutrients have mainly focused on VFSs located at the downslope end of fields. Experiments have been performed predominantly on field plots subjected to natural or simulated rainfall, as well as various inflow rates and sediment and nutrient inputs (e.g. Borin et al., 2005; Deletic and Fletcher, 2006; Gharabaghi et al., 2006; Uusi-Kämppä et al., 2000). Published studies have tested VFSs of various sizes, different slopes, and different soils and vegetation characteristics. Extremes with very wide filters and very steep slopes have not been widely tested (Dorioz et al., 2006). Moreover, except for a few studies (e.g. Blanco-Canqui et al., 2006; Verstraeten et al., 2006), shallow (not concentrated) inflow has been assumed; hence, in this respect, the optimum performance of the VFSs was often tested. Compared with VFSs, studies focusing on grassed waterways (GWWs), where concentrated flow passes through a long filter located along a thalweg (the deepest continuous line along a valley or watercourse), are relatively rare (e.g. Briggs et al., 1999; Fiener and Auerswald, 2003a; 2005; Hjelmfelt and Wang, 1997).

Studies of phosphorus trapping in VFSs report a wide range of effectiveness. Reduction of total phosphorus load ($P_{tot}$) after passing through the VFSs, which is commonly dominated by trapping of particulate-bound phosphorus ($P_{part}$), ranged between about 90% (e.g. Abu-Zreig et al., 2003; Deletic and Fletcher, 2006; Dillaha et al., 1989) and about 45% (Schmitt et al., 1999; Syversen and Borch, 2005). These studies often do not differentiate between $P_{tot}$, $P_{part}$, and dissolved reactive phosphorus (DRP), which is especially important to eutrophication of surface waters. Regarding DRP, filter efficiency showed a somewhat different picture; it ranged from -83% (Dillaha et al., 1989), indicating an additional DRP load coming from the filter, to 93% (Cole et al., 1997). The efficiency of filters to remove total P from inflow mainly depends on inflow and filter strip characteristics. All studies indicate that sediment and hence $P_{part}$ is trapped within the first few meters of a filter, whereas DRP is more sensitive to filter width because a reduction of DRP load is associated with infiltration processes.

Dissolved reactive P in surface runoff may originate from a variety of sources (Hansen et al., 2002; Kleinman et al., 2004; Sharpley et al., 2002), which may differ in their contribution to total DRP load seasonally and for different land uses. These sources include (Figure 1) (i) DRP in open field precipitation, (ii) DRP from the wash-off and leaching of plant sur-

faces, (iii) DRP leaching from plant residues close to the soil, and (iv) DRP released from the soil by the interaction of runoff with soil or by the exchange of soil water with rain water (shallow return flow). The latter in particular is unlikely to occur in experiments on small plots but may be important on the landscape scale.

Only a few studies have focused on seasonality in VFSs performance to reduce DRP load. Uusi-Kämppä et al. (1997), for example, found that an accumulation of plant residues in the dormant period could lead to a periodic release of DRP. It is also documented that DRP concentrations increase in spring if surface runoff occurs after periods of freezing and thawing of the filter vegetation (Uusi-Kämppä, 2007).

The first objective of this study was to determine the effects on DRP loads of two hydrodynamically rough GWWs. According to earlier studies (Fiener and Auerswald, 2003a; 2005) these GWWs were highly effective (> 90%) in trapping sediments and hence $P_{part}$. The second objective was to identify the sources of DRP loading at the landscape scale to help determine how seasonally variable GWW effectiveness is in surface runoff reduction.

## MATERIAL AND METHODS

### Test site

The effect of hydrodynamically rough GWWs on the surface runoff load of DRP was tested in a landscape-scale study in which DRP concentrations in runoff from two paired watersheds with and without GWWs were continuously measured over 5 yrs (Figure 2). The test site was part of the Scheyern Experimental Farm of the Munich Research Association for Agricultural Ecosystems, which is located about 40 km north of Munich, Germany. The area is part of the Tertiary hills, an important agricultural landscape in Central Europe. It covers an area of approximately 23 ha of arable land at an altitude of 454 to 496 m above sea level (48°30'50'' north, 11°26'30'' east). The mean annual air temperature was 8.4°C (for 1994–2000). The average annual precipitation was 804 mm (for 1994–2000), with the highest values from May to July (average maximum, 116 mm in July) and the lowest values during the winter months (average minimum, 33 mm in January).

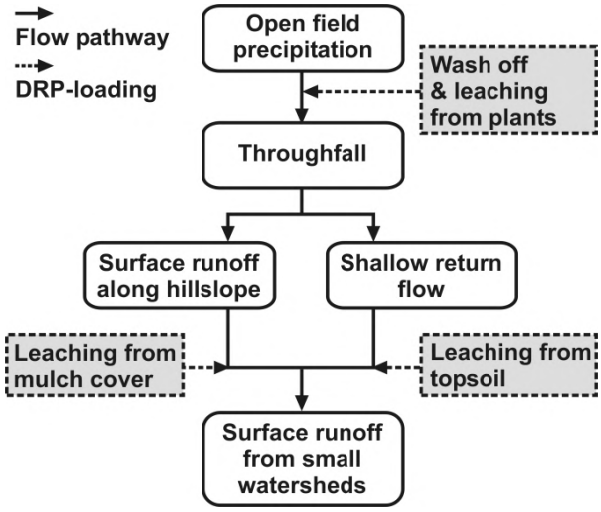


**Figure 1. Schematic diagram of flow pathways and sources of dissolved reactive phosphorus (DRP) loading from open field precipitation to surface runoff from small watersheds.**

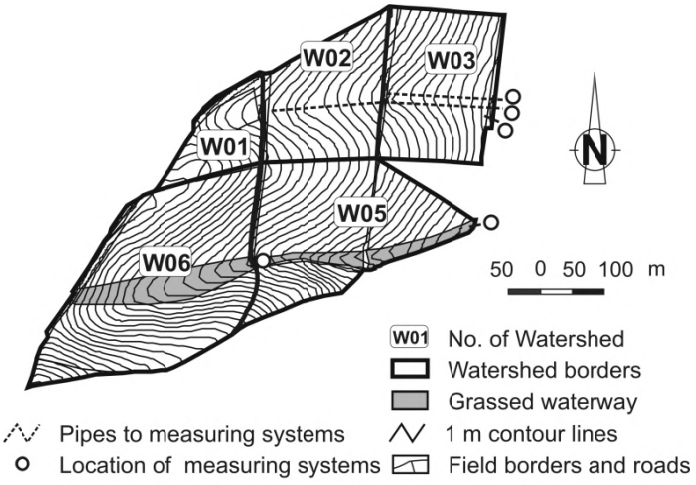


**Figure 2. Topography of the study watersheds with and without grassed waterway including location of monitoring points (flow direction from west to east).**

At the test site, the principles of integrated farming were applied in combination with an intensive soil conservation system in the fields (Auerswald et al., 2000). Due to the high soil phosphorus status in 1993 (Table 1), mineral phosphorus fertilizer was not applied during the experiments. The field sizes ranged from 3.8 to 6.5 ha. The crop rotation consisted of potatoes (*Solanum tuberosum*), winter wheat (*Triticum aestivum*), maize (*Zea mays*), and winter wheat. This rotation allowed for the planting of a cover crop (mostly mustard [*Sinapsis alba*]) before each row crop. Maize was planted directly without any tillage into the winter-killed mustard using a no-till planter. Potatoes were directly planted into ridges, which were formed before sowing the cover crop and were therefore also covered with winter-killed mustard. Reduced tillage allowed the use of the plant residues of maize and winter wheat as mulch cover and avoided soil compaction (Fiener and Auerswald, 2007).

The test site consisted of four small adjacent watersheds - two with a GWW and two without a GWW. The southern part was 13.7 ha in size and had GWWs, and the northern part was 9.4 ha in size and had no GWWs. Each part could be divided into an upper and a lower watershed separated by raised field borders (Figure 2). The GWWs in the southern part were established in 1993. Land use in the contributing fields was changed to a conservation system including mulch tillage (Auerswald et al., 2000). This experimental setup enabled quantification of the effect of GWWs by two independent approaches. First, the paired watersheds with and without GWW could be compared. Second, both GWWs started with common field conditions (see below) and approached their final stage in later years, which allowed a study of their effectiveness over time within each watershed.

The GWW in the western, upper watershed started as a stubble field in 1993 after the harvest of spring barley (*Hordeum vulgare*) in the previous year with straw left on the field. It was established by succession only. The GWW in the eastern, lower watershed was established by sowing grass in 1993, which made it necessary to have a fine seedbed. This seedbed, being located where runoff from the watershed concentrated, was destroyed by runoff events and had to be recreated three times in 1993. Finally, in autumn 1993, a close vegetation cover established and formed the GWW, but a small incision remained along the

drainage line of this GWW. Thus, both GWWs had typical field conditions in the first year (1993) and developed into GWWs in 1994 and later years.

In the GWW of the upper watershed (in the following text referred to as "unmanaged GWW"), succession without any maintenance occurred during the whole 5-yr monitoring period (watershed W06). Consequently, this area could serve more ecological functions (e.g., improving biodiversity or acting as refuge for beneficial organisms; Fiener and Auerswald, 2003b). The vegetation was dominated by fast growing grasses (e.g., *Agropyron repens*, *Dactylis glomerata*, *Arrhenatherum elatius*), tall herbs (e.g., *Epilobium angustifolium*, *Galeopsis tetrahit*, *Galium aparine*), and a few woody plants (e.g., *Salix spec.*, *Rubus spec.*, *Sorbus spec.*). This GWW was 290 m long, with a slope of 5% along its thalweg and an area of 1.06 ha.

The eastern, lower GWW (located in watershed W05) was sown-in during the first year of observation and was annually cut with a mulching mower between July and August (in the following text referred as "cut GWW"). Hence, the vegetation was dominated by fast growing grasses (e.g., *Agropyron repens*, *Dactylis glomerata*, *Arrhenatherum elatius*) and a few herbs (e.g., *Urtica dioica*) but no woody plants. The cut GWW was 370 m long, with a slope of 4% along its thalweg and an area of 0.58 ha.

**Comparability of Paired Watersheds**

To examine the effects of landscape elements, it is necessary to perform landscape scale experiments, like paired-watershed studies in combination with detailed process observations. Paired watershed studies, however, are biased because two watersheds that are identical except for the landscape element to be tested on do not exist. Therefore, differences in precipitation, topography, land use and management, soil, and hydrological properties should be as small as possible between paired watersheds.

The spatial distribution of rainfall at the test site was measured between 1994 and 1997 using 13 rain gauges over an area of 1.4 $km^2$. Spatial trends in precipitation could be found in the case of 33% of all events during the summer half-years, whereas no trends were observed during the winter half-years (Fiener and Auerswald, 2009). However, over the long term, there was no preferred direction in rainfall gradient; hence, homogeneous rainfall over the paired watersheds should be a reasonable assumption.

Land use in both watershed pairs was similar (Table 1), with more than 20% of the area used for set-aside in the upper pairs (W01/02 and W06, respectively) and more dominant agricultural use in the lower pairs (W02/03 and W05, respectively). The crop rotation was identical in all watersheds. Short-term differences in surface runoff and sediment delivery can be expected due to differences in agricultural operations and different positions of the

single fields within the crop rotation. To account for the latter, watersheds W01 and W02 as well as W02 and W03 were combined to get the same proportion of fields with an identical position within the crop rotation as their paired watersheds, W06 and W05, respectively (Fiener and Auerswald, 2003a).

**Table 1. Land use, topography, soil texture, and mean total phosphorus for each watershed, mean annual sediment delivery and runoff measurements (1994–2000), and predicted dissolved reactive phosphorus concentration for paired watersheds with and without grassed waterways (GWW).**

| | Upper watersheds | | Lower watersheds | |
|---|---|---|---|---|
| | W01/02 without GWW | W06 unmanaged GWW | W02/03 without GWW | W05 cut GWW |
| Arable land, % | 75 | 79 | 94 | 85 |
| Set-aside areas, % | 23 | 21 | 4 | 13 |
| Field borders, % | 8 | 3 | 4 | 3 |
| Structures at the divide, % | 14 | 4 | 0 | 0 |
| Structures along the thalwegs (grassed waterway), % | 0 | 13 | 0 | 10 |
| Field roads, % | 2.0 | 0.7 | 1.3 | 2.1 |
| No. of fields | 2 | 2 | 2 | 3 |
| Crop rotation | winter wheat–maize–winter wheat–potatoes | | | |
| Mean slope, % | 7.1 | 9.3 | 7.3 | 9.0 |
| Soil texture | silty loam | | | |
| Mean $P_{CAL}$,[†] g $kg^{-1}$ | 0.089 | 0.073 | 0.094 | 0.053 |
| Sediment delivery, kg $ha^{-1}$ $a^{-1}$ | 312 | 16 (7)[‡] | 303 | 172 (69) |
| Runoff, mm $a^{-1}$ | 34 | 3 | 29 | 26 |
| Predicted DRP[§] | | | | |
| DRP soil solution,[¶] mg $L^{-1}$ | 0.60 | 0.37 | 0.56 | 0.44 |
| DRP-CNS,[#] mg $L^{-1}$ | 1.82 | 1.55 | 1.78 | 1.43 |
| DRP-AGNPS,[††] mg $L^{-1}$ | 0.22 | 0.17 | 0.21 | 0.16 |

[†] Mean $P_{CAL}$ is phosphorus extracted with calcium acetate lactate at pH 4.1 according to Schüller (1969) from a 12.5×12.5 $m^2$ resolution in the watersheds based on a 50-m sampling grid.

[‡] Adjusted according to the ratio of the slope length factors of the differentiating Universal Soil Loss Equation (Fiener and Auerswald, 2003a).

[§] DRP is dissolved reactive phosphorus.

[¶] Mean DRP concentration in the soil solution (1993) predicted with one-point isotherm according to Scheinost and Schwertmann (1995) with a spatial resolution of 12.5×12.5 $m^2$.

[#] Mean DRP concentration in runoff predicted with Cornell Nutrient Simulation (CNS) (Haith et al., 1984).

[††] AGNPS, Agricultural Non-Point Source Pollution Model (Young et al., 1989).

To test if the paired watersheds behave similarly regarding their rainfall excess, this was modeled for different rainfall depths using the USDA Soil Conservation Service curve number model (Mockus, 1972). Because there was almost no difference between the pairs, it was assumed that differences in surface runoff are mainly the result of the GWWs (Fiener and Auerswald, 2003a). Regional ground water was about 20 m below the lowest outlet of one the watersheds. Nevertheless, some shallow return flow was observed, especially during

winter rainfall events, in watershed W02, which may lead to a slight overestimation of GWWs runoff reduction efficiency in winter.

Slight differences between the paired watersheds could be found with respect to topography. To compare particulate phosphorus losses, sediment delivery from the paired watersheds was adjusted using the slope and slope length factor of the differentiating Universal Soil Loss Equation (Flacke et al., 1990), which was extensively tested in the region (Becher et al., 1980; Schwertmann et al., 1987). Details of adjusting the sediment delivery and of pairing the watersheds in general are given in Fiener and Auerswald (2003a).

To prove the similarity of the watersheds regarding their ability to release DRP, relevant soil properties were measured in a 50 × 50 m grid, and the data were geostatistically interpolated, resolving the research area into 12.5 × 12.5 m blocks (Sinowski et al., 1997). The properties measured were soil texture, organic carbon, pH, and bulk density, following standard protocols given in detail by Scheinost and Schwertmann (1995) and Scheinost et al. (1997). Dissolved reactive phosphorus in the soil solution was calculated using a pedotransfer function developed by Scheinost and Schwertmann (1995) for the research area, which uses measured DRP concentrations after equilibrating 0.5 g of soil with 50 mL of a 1.2 mg $L^{-1}$ DRP solution. Additionally, $P_{CAL}$ was measured by extracting phosphorus with calcium acetate lactate at pH 4.1 according to Schüller (1969) (Table 1).

To examine whether the integral response by the interacting factors may cause differences in DRP concentrations coming from the paired watersheds, the expected DRP concentration in surface runoff was modeled. The Cornell Nutrient Simulation (CNS) model (Haith et al., 1984), which uses the P content in soil, clay content, and pH, and the Agricultural Non-Point Source Pollution Model (AGNPS) (Young et al., 1989; 1995), which also considers runoff properties in addition to soil properties, were applied to estimate DRP concentrations in surface runoff of the paired watersheds.

**Dissolved Reactive Phosphorus Measurement**

Dissolved reactive phosphorus load was measured along the flow path from open field precipitation to throughfall precipitation and finally to surface runoff from the small watersheds (Figure 1). Dissolved reactive phosphorus concentration in open field precipitation was measured in bulk rain samples obtained from rain gauges (including dry and wet deposition) and in wet deposition obtained from wet-only samplers. Both samplers were located at the lower end of the watersheds. Rain samples were collected weekly over 1 yr. There were no measurements performed with snowfall.

Dissolved reactive phosphorus concentrations in throughfall precipitation (here defined as the combination of drip-off and open field precipitation reaching the soil surface follow-

ing the use of the term by Van Dam et al. (1987) but excluding stem flow) under growing grass (including some shrubs) and under crops (potato, maize, winter wheat, mustard) were measured over 1 yr (October 1996 to December 1997) with PVC troughs (145 × 8.5 $cm^2$) connected to buried 10-L tanks. The troughs were covered with plastic mesh (mesh size 1 mm) to avoid contamination by particles. Collection tanks were emptied weekly, and tanks and troughs were cleaned with deionized water. Photographs were taken weekly from about 2 m above the vegetation canopy (up to 4 m in the case of full grown maize) covering the troughs. The percentage coverage for the troughs was later determined from the photographs with the line-transect method. Based on these data, the drip-off concentration was calculated according to the following equation:

$$P_{do} = \left[ P_{tf} - P_{ra} \cdot (1 - COVER) \right] / COVER \quad (1)$$

where P is the DRP concentration; the indices *do*, *tf*, and *ra* denote drip-off, throughfall, and bulk rain (dry and wet deposition), respectively; and *COVER* is the relative percentage cover of the trough.

The calculation does not consider water losses by interception and hence underestimates true drip-off concentrations. For example, given 30% interception loss and 80% cover, $P_{do}$ would be 7% higher by considering interception. It can be assumed that the difference in error is small among different crops and grasses and does not change their relative ranking of $P_{do}$, which varied by almost two orders of magnitude.

Straw cover was an important measure to protect the soil between crop growth periods that will also release DRP. Throughfall under straw and release from uncovered soil surfaces cannot be examined in the field under realistic conditions. Hence, a laboratory rainfall simulator (Auerswald et al., 1984) was used to examine DRP release from these surfaces (plot size 0.48 $m^2$). Three types of surfaces were examined: (i) bare soil taken from the plow layer of one field in watershed W02 and W03 and (ii) the same soil material covered with wheat straw ($P_{tot}$ = 0.78 g $kg^{-1}$) or (iii) maize straw ($P_{tot}$ = 1.13 g $kg^{-1}$) from the same field at rates similar to field conditions (2700 kg $ha^{-1}$ and 5400 kg $ha^{-1}$, respectively, with leaves contributing about 0.10 and 0.30 kg $kg^{-1}$, respectively, with the remainder being mainly stalks). Rain (deionized water, intensity 26 mm $h^{-1}$) was applied on nine occasions for 40 min duration, and DRP concentration was measured in runoff samples collected during 10-min periods. Rainfall simulation dates were approximately 2 wk apart. Between the simulations, samples were covered by a wetted textile (without direct contact to the samples) to protect them from dust deposition and to prevent extreme drying. In total, the applied rain amounted

to 156 mm and was applied during approximately 0.5 yr, which corresponds more or less to the winter precipitation at the research site.

For 5 yrs immediately after the establishment of the GWWs, surface runoff (Figure 1) from the watershed experiment was collected at the lowest point in the four watersheds (Figure 2), which were bordered by small dams. Runoff from the dams was transported via underground-tile outlets. The monitoring system was based on a Coshocton-type wheel runoff sampler. The system collected an aliquot of about 0.5% of the total runoff coming from the outflow pipes. For runoff rates between 0.5 and 16 L $s^{-1}$, the measured aliquot differed only slightly-in the range of ±10% from the accurate value of 0.5%. For smaller runoff rates, the system overestimated the runoff volume, but this error was neglected due to the small contribution of these runoff rates to total runoff volume. During the first 2 yrs of the monitoring campaign, the runoff aliquot was collected in tanks. Later, the tanks were replaced by tipping buckets (approximately 85 mL) at the outlets of the sampling wheels, which were connected to ISCO 3700 portable samplers (Isco, Lincoln, NE) that counted the number of tips and automatically collected a runoff sample after a defined runoff volume. The aliquot volume or the number of tips was used to calculate total runoff volumes needed to determine sediment and phosphorus loads. The monitoring details and an accuracy test are given by Fiener and Auerswald (2003a). In the case of sampling with tanks, the runoff aliquot was homogenized by stirring with a submersible pump, and then a sample was collected in an acid-cleaned PE bottle (1 L) the day after a runoff event. The collecting tanks had to be emptied between large events, so additional samples were taken during emptying. The ISCO sampler sampled on a volume proportional basis, and four consecutive 250-mL samples were combined in a 1-L bottle. All samples were immediately transported to the laboratory and filtered (0.45 µm). A few drops of HCl were added, and the filtrates were stored at 2°C. Evaluation of storage and treatment practices (Auerswald and Weigand, 1996) showed only slight and inconsistent influences (the largest was due to filtering). No corrections were applied due to the identical treatment among samples. Within a few days, DRP concentration was measured colorimetrically with a Spectronic 601 (Milton Roy, Ivyland, PA) following the procedure described in John (1970). The same procedure was applied for all other DRP measurements.

**Separation of Direct Runoff and Return Flow in Grassed Waterway Outflow**

The outflow of the GWWs was partitioned using the $\delta^{18}O$ technique (e.g. Rozanski et al., 2001) during two landscape experiments, where concentrated runoff was pumped into the cut and the unmanaged GWW (inflow about 10 L $s^{-1}$), and outflow rate was measured. Details regarding the experimental setup and the results in respect of runoff reduction are given in Fiener and Auerswald (2005). Inflow (taken from ground water), soil water (0.1 and 0.2 m depth), and outflow were sampled, and $^{18}O$ content was determined at the GSF laboratory in

Neuherberg, Germany. Due to the relatively large difference in the $\delta^{18}O$ signature of ground water (average $\delta^{18}O$ = 10.23‰) and soil water (average of both depths = 6.40‰; SD, 0.20‰), the fraction of soil water in outflow ($f_{soil}$), which was sampled in short intervals during both runs, lasting 480 min in the cut GWW (89 samples) and 360 min in the unmanaged GWW (54 samples), could be determined according to Eq. (2):

$$f_{soil} = \frac{\delta^{18}O_{out} - \delta^{18}O_{in}}{\delta^{18}O_{soil} - \delta^{18}O_{in}} \quad (2)$$

where $f_{soil}$ is the fraction of soil water in outflow, and $\delta^{18}O_{out}$, $\delta^{18}O_{in}$, and $\delta^{18}O_{soil}$ are the $\delta^{18}O$ signatures of outflow (runoff), inflow (ground water), and soil water, respectively.

## RESULTS

To evaluate the importance of different runoff components and processes (Figure 1) contributing to DRP loading in the small watersheds, results from laboratory and field measurements of DRP concentrations in these different components are presented first. After this, the integrated response in the small watersheds regarding DRP concentrations and loads are given for the paired-watershed experiments.

### Study of Subprocesses

#### *Open Field Precipitation*

The mean DRP concentration in rain gauge precipitation was 0.06 mg $L^{-1}$ (SD = 0.13; n = 29), and the mean concentration of wet-only sampler precipitation was 0.02 mg $L^{-1}$ (SD = 0.03; n = 20), with summer values about twice as high as winter values. Wet-only precipitation corresponds with the true DRP concentration of rain during runoff events, whereas rain gauge precipitation should be similar to the drip-off from surfaces, which includes dry and wet deposition.

#### *Drip-off and Throughfall Precipitation*

Drip-off concentrations were highly enriched in DRP in comparison to open field precipitation. Peak concentrations (up to 5 mg $L^{-1}$) occurred particularly during flowering of the respective crop and after frost events, indicating that leaching from plants contributes significantly to the DRP load. There was a significant difference ($\alpha < 0.01$) between DRP concentrations in drip-off from grass cover (mean = 1.3 mg $L^{-1}$; SD = 1.3 mg $L^{-1}$; n = 32) and from field cover (mean = 0.7 mg $L^{-1}$; SD = 1.1 mg $L^{-1}$; n = 107). Dissolved reactive phosphorus in

runoff is better characterized, however, by throughfall concentrations (including drip-off and open field rain reaching the soil surface) than by drip-off concentrations alone. Throughfall concentrations for all three cover types were highly variable (Figure 3), but there did not seem to be any general difference between crops and grasses. On average, throughfall under grass was somewhat lower (mean = 0.24 mg $L^{-1}$; 95% confidence interval = 0.09 mg $L^{-1}$) than under crops (mean = 0.38 mg $L^{-1}$; 95% confidence interval = 0.12 mg $L^{-1}$).

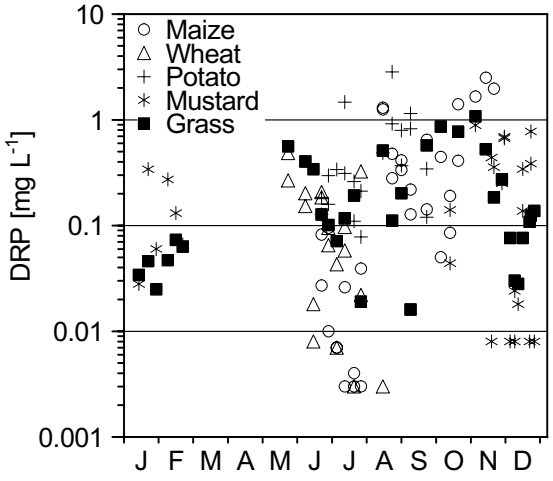


**Figure 3. Seasonal variation of dissolved reactive phosphorus (DRP) concentrations in throughfall under field crops (wheat, n = 31; maize, n = 31; potatoes, n = 20) and cover crops (mustard, n = 37) compared with throughfall under grass and single shrubs (n = 33).**

*Surface Runoff and Shallow Return Flow from Laboratory Experiments*

Runoff generated during laboratory rainfall simulations contained similar DRP concentrations for bare or mulched soil surfaces (Figure 4), spanning a range of concentrations covering one order of magnitude. The average DRP concentration from the bare soil plot (0.52 mg $L^{-1}$; SD = 0.14 mg $L^{-1}$) was similar to the DRP concentration in the soil solution of watershed W02/03 (Table 1), where the soil for the experiment was taken from. This indicates that during the experiments there was a strong interaction between runoff and soil and/or that soil water was probably replaced by rain water. Dissolved reactive phosphorus concentrations from mulched surfaces were about 0.2 mg $L^{-1}$ higher than from bare soil, with slightly higher concentrations from soil covered with wheat straw than from soil covered with maize straw despite the lower $P_{tot}$ and the lower amount of wheat residues covering the soil. Furthermore, the difference was somewhat higher during the first three rainfall events (totaling 52 mm of rain), but there was little variation over the nine rainfall events over half a year. The variation within each rainfall event was also small, except for the first three rainfall experiments. In these early experiments, where straw was only slightly decomposed, the concentration in runoff from mulched surfaces increased during the rainfall event, indicating that leaching from undecomposed straw improves with wetting, which is similar to the behavior that has been reported by Auerswald and Weigand (1996) for woody tree clippings. In general, the results of the rainfall simulations indicate that measured DRP concentrations in runoff coming from the small plots were mainly governed by soil P status and to a smaller extent by their mulch cover.

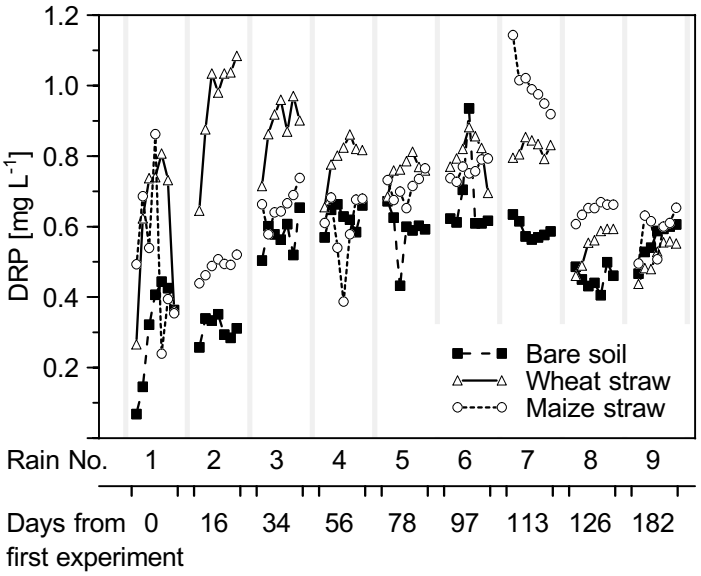


**Figure 4. Dissolved reactive phosphorus (DRP) concentrations during laboratory rainfall simulations on bare soil and soil covered with wheat or maize straw; nine consecutive rainfall events on the same surface covering approximately 0.5 yr (n = 96 for each surface).**

*Runoff and Soil–Vegetation–Residue Interactions within the Grassed Waterway*

During the experiments with concentrated runoff, the fraction of soil water in GWW outflow varied between 1.3 and 19.6%. These results were very close to observations during the first hours of natural rainfall-runoff events in adjoining fields (Fiener et al., 2005), indicating that return flow in the GWWs behaved similarly to that in the adjoining fields. Soil water contributed most to runoff (up to 20%) at the beginning and at the end of GWW outflow (Figure 5). The isotopically enriched leaf water may be leached and lead to a slight overestimation of soil water (Gat, 1996), but this should only have an effect at the beginning. On average, the fraction of soil water during steady-state flow was 9.2 and 4.2% in the unmanaged and cut GWW, respectively. The average fraction of soil water in GWW outflow was also larger in the unmanaged than in the cut GWW (11.4 and 5.2%, respectively). This resulted from the much larger infiltration in the unmanaged GWW (runoff ratio of 0.10 vs. 0.51 in the cut GWW), which may affect the ratio in two ways: (i) it decreases the amount of runoff from inflow, and (ii) it increases the probability of return flow. Calculating the return flow from this fraction and the total runoff shows that during constant runoff, return flow is smaller in the unmanaged GWW (0.2 L $s^{-1}$) than in the cut GWW (0.4 L $s^{-1}$). The higher contribution of soil water to total runoff on the unmanaged GWW thus results only from the first effect (i.e., low direct runoff due to better infiltration). In fact, not only was infiltration improved, but also percolation, which lowered the return flow, was improved. This difference in infiltration between both GWWs mainly resulted from a different cross-sectional area (Fiener and Auerswald, 2005). The initial decrease in the fraction of soil water is caused by the replacement of soil water by rain water in the soil close to the surface. During small rainstorms with little runoff, soil water may contribute 20% to total runoff; this contribution drops below 10% for heavy rains creating large runoff volumes.

In summary, the mean DRP concentration of runoff from bare soil (0.52 mg $L^{-1}$), straw-covered soil (0.70 mg $L^{-1}$), arable crop throughfall (0.38 mg $L^{-1}$), and grass throughfall (0.24 mg $L^{-1}$) were all of a similar order of magnitude (Figure 6). Because surface runoff never contains only runoff from a single component but is the combination of all components, it is unlikely that these small differences have a large impact on the total runoff concentration. Potential differences in soil P status of the GWWs can also have only a small effect, according to the runoff separation with $\delta^{18}O$, which demonstrated that during concentrated runoff within the GWWs, exchange with DRP loaded soil water is less than 20%.

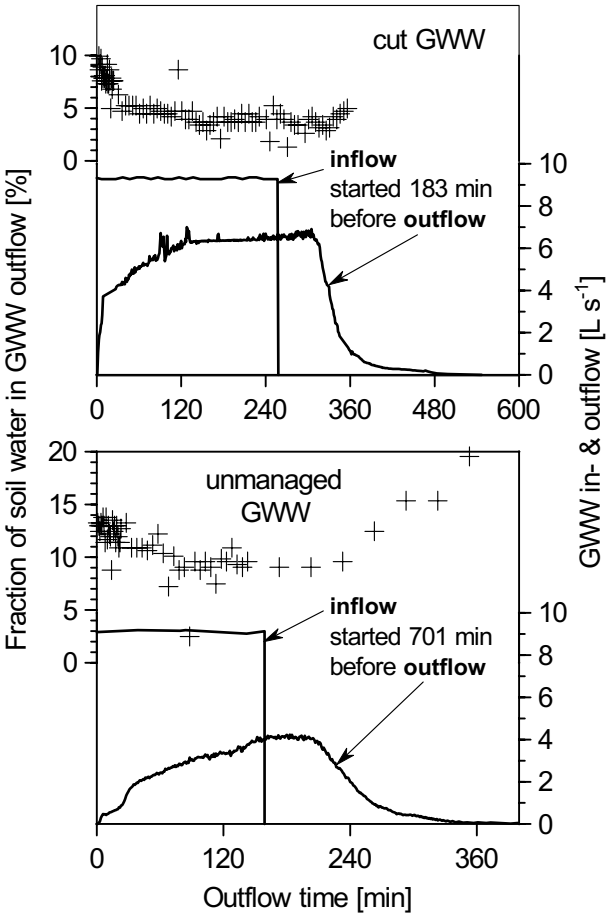


**Figure 5. Fraction of soil water in grassed waterway (GWW) outflow during a landscape experiment (crosses), where the hydrologic effects of concentrated inflow in the cut and the unmanaged GWW were tested (Fiener and Auerswald, 2005); the fraction of soil water in runoff was determined using measured δ18O values of soil water, in- and outflow; GWW in- and outflow rates since the start of outflow are also plotted (lines).**

## Study of Paired Watersheds

Dissolved reactive phosphorus concentrations modeled with the pedotransfer function, with CNS and with AGNPS, predicted slight differences between the watershed pairs. The maximum difference was 0.35 mg $L^{-1}$ in the case of predicting DRP concentration in watersheds W02/03 and W05 using the CNS model, whereas the minimum difference between both pairs was 0.05 mg $L^{-1}$ when AGNPS was applied (Table 1). In general, all predictions indicated slightly smaller DRP concentrations in the case of watersheds with GWWs. On average, predicted DRP concentrations in W06 and W05 were 25 and 22% smaller than in their watershed pairs, respectively, whereas the three predictions differed by up to a factor of nine in absolute values for an individual watershed.

The watersheds with GWW produced considerably less surface runoff and less runoff events than their paired watersheds without GWW. The effect was more pronounced for the

watershed with the unmanaged GWW (90% reduction in runoff volume, 1994–2000) than for the watershed with the cut GWW (10% reduction in runoff volume, 1994–2000). These effects were described and analyzed in detail by Fiener and Auerswald (2003a).

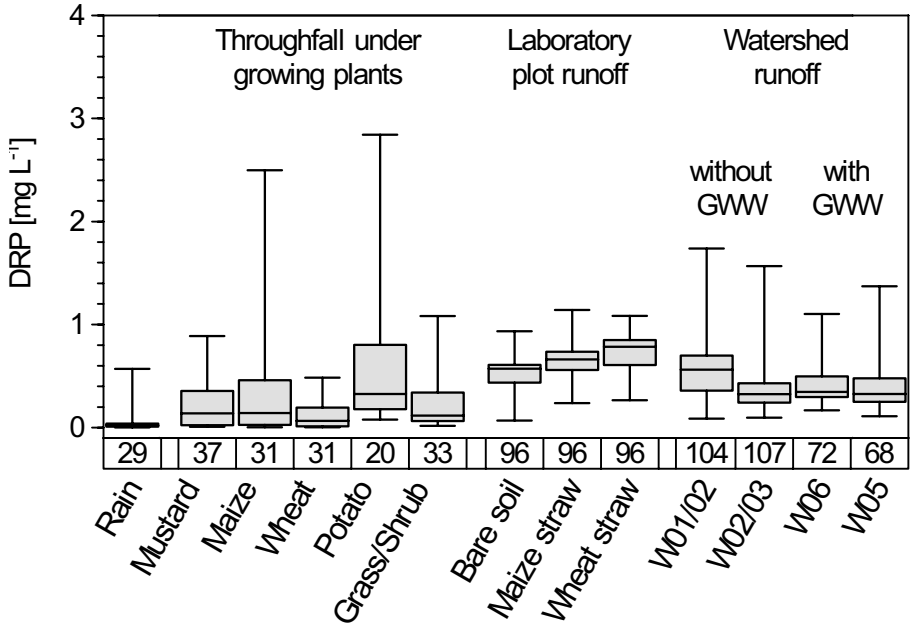


**Figure 6. Dissolved reactive phosphorus (DRP) concentrations in different runoff components and in runoff from all tested watersheds. Boxes represent first and third quartile; line within boxes indicates median, and error bars indicate minimum and maximum; and values below boxes give numbers of samples.**

Dissolved reactive phosphorus concentration in runoff was measured for a total of 351 runoff events. Concentrations were high in both types of watershed with about 40% of all values exceeding 0.5 mg $L^{-1}$ and about 11% exceeding 1.0 mg $L^{-1}$ (Figure 7). In watershed W06 with the unmanaged GWW (mean DRP concentration = 0.43 mg $L^{-1}$; SD = 0.22), a significantly ($\alpha < 0.01$) smaller DRP concentration was measured compared with watershed W01/02 without a GWW (mean DRP concentration = 0.58 mg $L^{-1}$; SD = 0.29). Between watershed W05 with the cut GWW (mean DRP concentration = 0.39 mg $L^{-1}$; SD = 0.22) and W02/03 (mean DRP concentration = 0.36 mg $L^{-1}$; SD = 0.21), no significant difference in mean DRP concentration was found. Mean DRP concentrations in surface runoff from all watersheds were slightly lower compared with bare soil runoff but close to the mean DRP concentration in the soil solution (Table 1), which seems to govern the mean concentration in runoff.

There was an obvious seasonality effect in DRP concentrations from the watersheds with GWW (Figure 8) with two seasonal maxima, one in February and the other in July/August. The maximum in February corresponds to typical thawing phases (often including snow melt) after winter. During this time, the surface runoff reduction by the GWW was also the

least (Fiener and Auerswald, 2006), causing the lowest protection by the GWW. The absolute maximum DRP concentration values were found in July/August, but they were associated with generally smaller runoff events. There was no evidence that the cut grass in late summer, which was left as a mulch cover in W05, increased DRP concentrations compared with the unmanaged GWW.

**Study of Temporal Change**

Focusing on the long-term development of the system, no temporal change in DRP concentration over the 5 yrs between both types of watershed was found (Figure 7), although the effectiveness of best management practices on the fields increased. Runoff and sediment delivery per year in the watersheds without GWW (W01/02 and W02/03) decreased between 1993 and the following years (1994-1997), when the best management practice was fully established, by a factor of 3.6 and 9.4, respectively. In combination with an increasing GWW effectiveness, especially in case of the unmanaged GWW, this led to fewer runoff events in the later years. This increase in effectiveness becomes particularly obvious when comparing runoff events during the first year with those of the last year (Figure 7). The increasing accumulation of plant residues in the unmanaged GWW over time had no adverse effects on DRP concentrations but helped to reduce the number of runoff events reaching the lower watershed boundary. Moreover, the smaller dilution by runoff from the fields deliver-

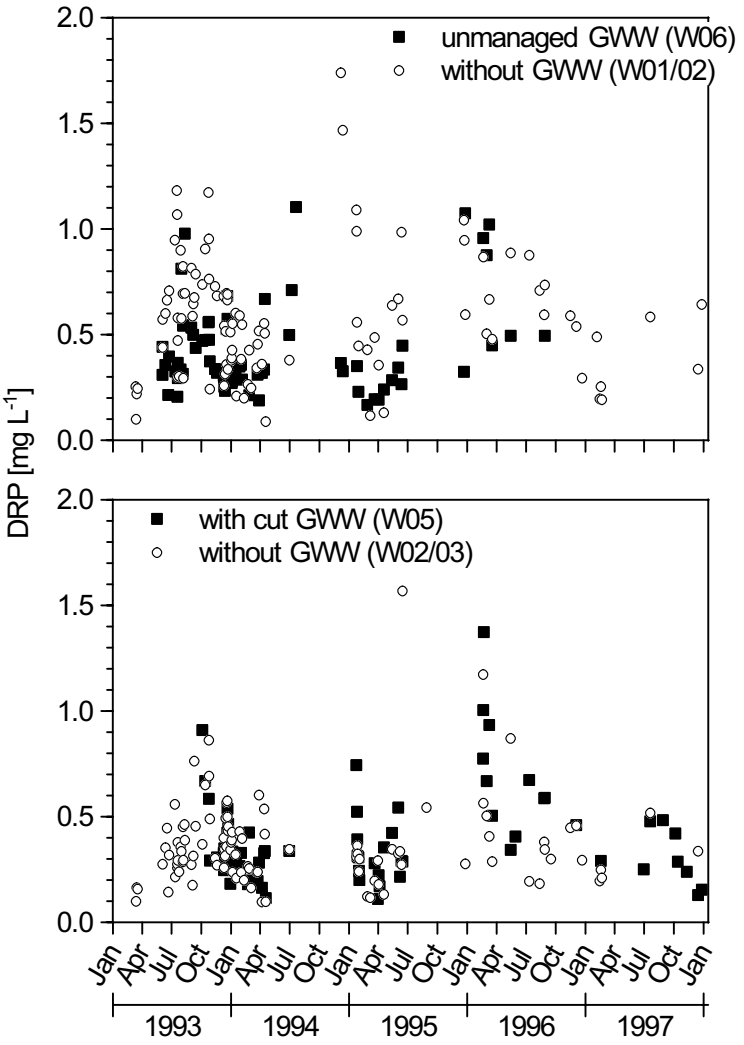


**Figure 7. Dissolved reactive phosphorus (DRP) concentrations in runoff from the paired watersheds (1993–1997) without and with (cut or unmanaged) grassed waterway.**

ing to the GWW had no effect on the DRP concentration at the outlet of the GWW watersheds.

Combining the measured DRP concentrations and the runoff volumes (1993–1998) allowed calculation of total DRP loads exported from the paired watersheds. The differences in average annual DRP concentrations were small, and only one watershed differed significantly (Figure 9). In contrast, DRP loads exported from watersheds with GWW were significantly ($\alpha < 0.01$) smaller than those without GWW by a factor of more than three. Particulate losses were smaller by more than a factor of four (Auerswald, 2002a). Hence, the GWWs reduced total P losses due to the trapping of particulate phosphorus and the infiltration of dissolved phosphorus.

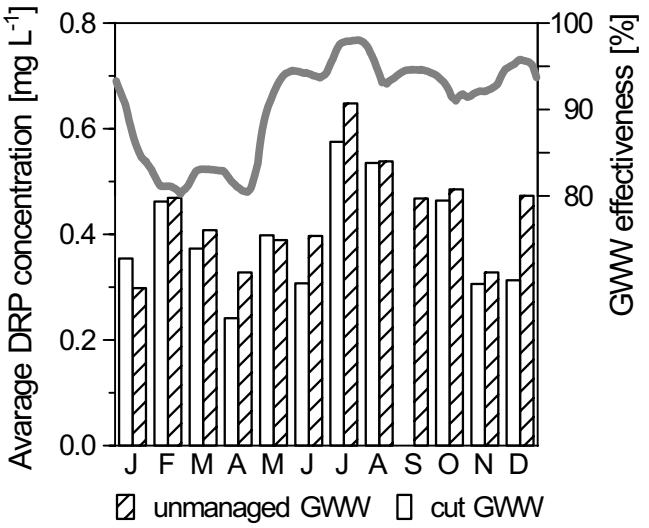


**Figure 8. Seasonal variation in dissolved reactive phosphorus (DRP) concentrations in runoff from watersheds with grassed waterway (GWW); monthly DRP concentrations calculated from 5 yrs measurements (n = 1–5). Line indicates seasonality of runoff reduction by the unmanaged GWW calculated from 8 yrs runoff measurements (1994–2001) in the paired watersheds W01/02 and W06 (average 87%) (Fiener and Auerswald, 2006).**

## DISCUSSION

### Methodological Approach

Sharpley et al. (1995), in summarizing future research needs, noted that more information is needed on the long-term effects of conservation and low-input systems on the transfer of bio-available phosphorus to runoff. Sharpley et al. (1993) also called for long-term field studies, although they are costly, lengthy, and labor intensive. Large landscape elements like GWWs are particularly difficult to evaluate. The effects of GWWs on DRP concentrations and loads can be measured in principle with the following three different approaches: (i) The comparison of paired watersheds, which is the most straight forward approach. Its major advantage is that it integrates all sub-processes acting at the watershed scale. The individual sub-processes and their mutual interactions do not have to be known. It has the disadvantage that the similarity of watersheds is open to debate. Identical watersheds, given their multitude of properties, can never be achieved in nature. (ii) The observation of one watershed in time before and after the establishment of a landscape structure like a GWW. Like paired

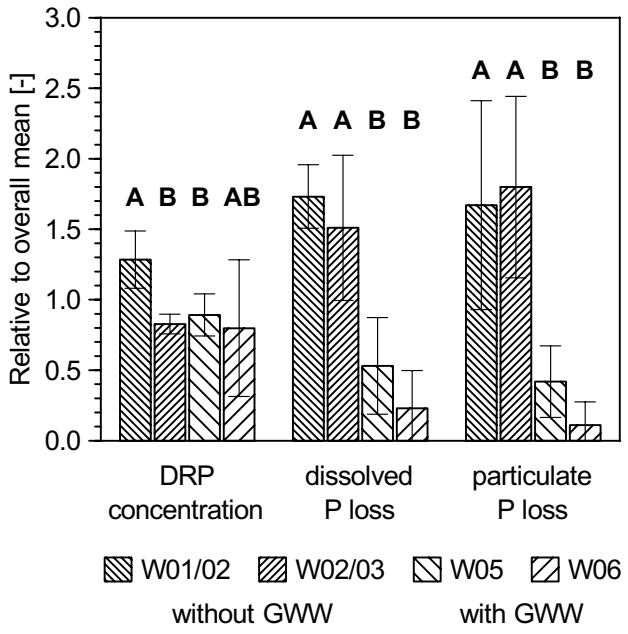


**Figure 9. Dissolved reactive phosphorus (DRP) concentration, dissolved and particulate phosphorus losses of the watersheds without (W01/02, W02/03) and with grassed waterways (W05, W06). Bars display the annual mean relative to the overall mean (0.445 mg $L^{-1}$, 0.015 mg $m^{-2}$ $yr^{-1}$, and 8.15 mg $m^{-2}$ $yr^{-1}$for DRP concentration, dissolved, and particulate phosphorus losses, respectively). Error bars give 95% confidence interval. Different letters denote significantly different watersheds. Mean DRP concentrations were calculated without weighting for runoff volume, while dissolved P losses consider concentration and volume of individual runoff events. Particulate P losses are given for comparison. Taken from Auerswald (2002a).**

watersheds, this approach has the advantage of process integrity but has the added advantage regarding similarity. It is thus a scientifically advantageous approach, but it depends on the precondition that the magnitude of the effect changes with time. Given the high randomness of erosion events and the importance of rare events, this approach calls for long observation periods to quantify the mean or total effect on DRP loss. (iii) The process of DRP loading can be separated in to sub-processes that can be measured separately. This approach is scientifically appealing because it allows insight into the mechanisms. It depends, however, on the precondition that the sub-processes are sufficiently known and can be separated without breaking major feedback or interaction mechanisms. Furthermore, effects on sub-processes alone cannot be expected to directly influence runoff DRP concentrations in complex watersheds due to these feedback mechanisms.

In this study we followed all three approaches to compensate for their individual disadvantages. Sufficient similarity between paired watersheds was achieved by choosing small neighboring watersheds with similar natural and agricultural preconditions (Table 1). It was important that both pairs belonged to one large field before landscape redesign and GWW establishment and that after redesign fields still extended over each watershed pair. This guaranteed that management operations (e.g., harvesting), which are a major source of temporal dissimilarity, were applied more or less simultaneously in the paired watersheds. In addition, to be confident about the similarity regarding potential DRP concentrations in runoff, both pairs were modeled beforehand with three different approaches. All three approaches, although predicting large differences in DRP concentrations, indicated only slight differences between the paired watersheds (Table 1).

Temporal change for the second approach was met in two ways. First, runoff and erosion control measures within the fields became more effective with time. The effect of a GWW on DRP loading should thus increase in strength with time because inflow decreases. Second, both types of GWW became more effective with time, starting with a stubble field in the unmanaged GWW and with seedbed conditions in the cut GWW. Both trends-the decreasing inflow from contributing fields and the increasing efficacy of the GWWs themselves-should act in the same direction regarding DRP loading by the GWW and cause a pronounced temporal change.

**Effects of Grassed Waterways**

All three approaches yielded the same result (i.e., that a hydraulically rough GWW with large amounts of living and dead biomass on the soil surface had little effect on the DRP concentration in surface runoff from the small watersheds). We can therefore be confident about this conclusion. The absence of any effect renders a discussion of the causes of the effect futile; however, it is important to consider why no effect occurred and under which conditions we may expect to observe an effect.

Dissolved reactive phosphorus concentrations in bulk rain were low (0.06 mg $L^{-1}$) but still higher than the reported German average from a review of 10 different studies (Werner et al., 1991). This study had revealed an increase in bulk rain concentrations of about 0.03 mg $L^{-1}$ in the 1960s to 0.05 mg $L^{-1}$ in the late 1980s. Our value, although not significantly different from 0.05 mg $L^{-1}$, agrees well with this trend.

A considerable loading occurred when rainfall passed through the plant canopy, leading to DRP concentrations that are regarded as harmful to water bodies (e.g. Cooper, 1993; Roberson et al., 2007; Sharpley, 1981). Schreiber (1985) determined initial throughfall concentrations from cotton plants of > 0.25 mg $L^{-1}$, which logarithmically decreased with time to about 0.05 mg $L^{-1}$ after about 40 mm of rain. Both concentrations support the range of concentrations measured in this study. The increase in DRP concentration at the outlet of the watersheds after freezing periods and in July/August when wheat (which covered half of the watershed area) was close to harvest agrees with the finding that freezing and thawing and drying of plant tissue promotes leaching (Bechmann et al., 2005; Roberson et al., 2007). According to Schreiber (1985), the large variation in throughfall concentrations is caused by (i) plant growth and nutrient uptake; (ii) leaching properties of living tissue by rainfall as a function of plant age; and (iii) rainfall dynamics, which include intensity, amount, and plant recovery time between events, creating a complex pattern. The large difference between bulk and wet-only rain in our study also indicates that dust deposition contributes to throughfall loading and its variation.

The results from the rainfall experiments with straw-covered surfaces agree well with other studies. Schreiber and McDowell (1985) and Auerswald and Weigand (1996) also reported that DRP concentrations from plant residue leaching increase during rainfall events and then decrease again. In our experiments with low rainfall intensity (26 mm $h^{-1}$), the peak concentration occurred later than in the experiments by Schreiber and McDowell (1985). Experiments conducted on the forest floor (Schreiber et al., 1990) also showed that the peak DRP concentration was higher and occurred later during a rainfall event the lower the rainfall intensity was. During subsequent rainfall events, high DRP concentrations were observed in our study because alternate drying and wetting periods increase the release of DRP by leaching (Cowen and Lee, 1973). The typical hump-shaped time course of the DRP concentration during the first rainfall events disappeared in the case of the last rains, during which the DRP concentration from mulched surfaces behaved similarly to that from bare soil surfaces (Figure 4). This agrees with the findings of Dalal (1979) that decomposing straw at the soil surface increased equilibrium P concentrations of the top soil.

Because the components of DRP loading were similar to other studies, it is not surprising that the concentrations found in watershed runoff were in the same range as reported in many other studies (e.g. Little et al., 2007; Sharpley et al., 1989; 1992; Sharpley, 1993).

The similarity of DRP concentrations resulting from different sources (Figure 6) and the small spatial coverage of the GWW explain why the DRP concentrations at the outflows of the watersheds were not modified by the GWWs. As a consequence, DRP input to water bodies can be reduced most effectively by controlling the amount of runoff. Earlier studies (Fiener and Auerswald, 2005; 2003a) showed that the unmanaged and cut GWW reduced runoff volumes by 90 and 10%, respectively. Field experiments and physically based modeling of concentrated runoff in the GWWs (Fiener and Auerswald, 2005) showed that the small runoff reduction in the cut GWW was mainly caused by its unfavorable cross-sectional area with a (fully vegetated) small incision along the thalweg resulting from storms shortly after sowing-in the grasses. Hence, to obtain the full runoff reduction potential of a GWW, one has to be especially careful during the establishment of such a structure. However, well established hydrodynamically rough GWWs, like the unmanaged GWW in this study, can be an excellent measure to reduce runoff under conditions where total runoff remains low due to the meteorological and land use conditions. In this study, despite frequent runoff events, total runoff without GWW only averaged 16.7 mm $yr^{-1}$ (Auerswald et al., 2000). Under these conditions, GWWs not only reduced DRP losses via runoff but also reduced the number of events with runoff leaving the watershed. This results in less frequent nutrient loading to receiving water bodies, reflected in DRP inputs into neighboring brooks (Honisch et al., 2002). Furthermore, such hydrodynamically rough GWWs have been proven to reduce se-

diment losses to a much larger extent than runoff losses (e.g. Chow et al., 1999; Fiener and Auerswald, 2003a).

There is some debate in the literature about whether over the long term the effectiveness of VFSs may be reduced or even act as a net source of phosphorus in surface runoff because phosphorus saturation may occur in the soil (Dorioz et al., 2006). Loss in effectiveness of such a long structure as a GWW is unlikely as long as sediment input into the GWW does not damage the vegetation. The second long-term effect, an increase in soil phosphorus status in a GWW resulting from long-term infiltration and hence sorption of DRP, is unlikely to occur. If we reasonably assume that (i) the outflow DRP concentration of watershed W01/02 is equal to the inflow concentration in the unmanaged GWW in watershed W06, (ii) the infiltrating DRP becomes fully absorbed within the uppermost 0.3 m of the soil column, and (iii) the measured average annual infiltration (90% of inflow between 1994 and 2000) occurred on only half of the GWW area, total phosphorus in the upper 0.3 m increases by only 6% within 100 yrs. Given the large variation in DRP concentrations between events and the multitude of influences, it is highly unlikely that even this 100 yrs effect will become statistically detectable.

## CONCLUSIONS

The DRP in surface runoff of complex watersheds is composed of plant cover throughfall, runoff from bare surfaces, and runoff from soil surfaces covered with plant residues. Dissolved reactive phosphorus concentrations did not vary largely among these components. Hence, moderate differences in the contribution of the different components to total runoff have little impact on overall DRP concentration. Consequently, hydrodynamically rough GWWs, which provide dense vegetation cover throughout the year but cover only a small area along the path of concentrated flow, exert only a small influence on the DRP concentration at the outflow. This was confirmed in a long-term field-scale study including the comparison of paired watersheds and a change in GWW effectiveness over time. Such GWWs will thus reduce the DRP load analogously to the reduction in total runoff. The extent of runoff reduction and its drivers have been reported in earlier studies (e.g., Fiener and Auerswald, 2003a). In this study, GWWs lowered DRP losses by a factor of 4 to 7 and particulate phosphorus losses by a factor of 4 to 10.

Accumulation of plant residues in the GWWs seemed to have no negative effect on DRP release from the watersheds with GWW. Over the long term, we do not expect an increase in DRP release by the hydrodynamically rough GWWs. In general, GWWs have great potential to reduce dissolved and particulate phosphorus losses from agricultural land.

# 4. ROTATION EFFECTS OF POTATO, MAIZE AND WINTER WHEAT ON SOIL EROSION BY WATER

With minor revisions published:
Peter Fiener and Karl Auerswald (2007)
Rotation effects of potato, maize and winter wheat on soil erosion by water.
Soil Science Society of America Journal. 71: 1919–1925

***ABSTRACT**. The effects of cultivating different crops or applying different management practices on water erosion have been widely evaluated in plot or field experiments. While these experiments have focused on the direct effects of a certain crop, there is comparably little information on how crops influence soil loss during the following years. Our objectives were to evaluate the extent to which water erosion differs between potato (Solanum tuberosum L.) and maize (Zea mays L.), and how these crops influence soil loss of a following winter wheat (Triticum aestivum L.) crop. Soil erosion was measured in four small neighboring watersheds (0.8–4.2 ha in size) during 198 rainfall–runoff events (1994–2001). Each watershed included one field with a crop rotation of winter wheat, potato, winter wheat, and maize. This rotation was shifted by 1 yr for each field, and hence a comparison between the fields as well as a comparison over two crop rotations was possible. Runoff and soil loss from potato and maize differed only slightly because the better protection by cover during maize years was compensated by a better protection by contouring with potato ridges. Both effects were adequately described by the cover management and support practice (C and P) factors of the Revised Universal Soil Loss Equation. A clear difference in soil loss depending on the preceding crop occurred in the succeeding winter wheat fields. Especially in October, November, and February, soil loss after the potato crop was significantly higher. This could be explained by little residue cover, disintegration of large aggregates, and low stability of small aggregates following the potato crop. Carryover effects should be taken into account, optimizing crop rotations with respect to soil conservation. Moreover, they are highly relevant for modeling of water erosion from agricultural areas.*

Soil erosion is regarded as one of the most serious problems in agricultural soil use (Auerswald and Kutilek, 1998; Morgan, 1996). Besides field layout, soil loss can be influenced by the selection of crops and cultivation techniques. Hence, an enormous number of publications exist where different crops and cropping techniques have been compared. For statistical and practical reasons, these experiments are often performed on rather small plots, sometimes only a few square meters in size (Hill and Peart, 1998; Lal, 1998a; Quinton and Catt, 2004; Wischmeier and Smith, 1978). It is questionable whether such results also apply to large areas, like fields or watersheds, where the transport capacity may be considerably

higher than on small plots. Small plots are even more poorly suited to the case of crops grown on ridges perpendicular to the slope because the small amount of runoff rarely exceeds the storage capacity of the furrows between the ridges or causes a breakdown of the ridges, while both may be the case on larger fields. Hence there is a clear demand for experiments on larger fields or small watersheds comparing ridged and unridged crops grown along or across the slope (Foster, 2005).

In most cases, only the year is considered in which a certain crop is grown when comparing the erosion potential of different crops. Row crops like maize, potato, or soybean [*Glycine max* (L.) Merr.] are considered to be crops of high erosion potential unless grown with conservation techniques like reduced tillage, while small grain crops are mostly considered to be less prone to erosion. Carryover effects influencing soil loss during the following year are included in long-term experiments with monocultures, while they are rarely examined in crop rotations. In particular, the amount of crop residues availably for cover in the following year and soil aggregation may vary considerably depending on the preceding crop and will thus be a property that has to be assigned to the preceding crop. Especially preceding crops in no-till systems for small grain cereals have received little attention (Rasmussen, 1999).

We evaluated the hypothesis that soil loss during wheat depends on the preceding crop (maize vs. potato) and we analyzed, at a watershed scale, the direct effects of these crops with special emphasis on the influence of roughness height (flat vs. ridged) and orientation (across and along) on soil loss.

## Study Site and Cropping Practice

The study site was part of the Scheyern Experimental Farm located about 40 km north of Munich in the Tertiary hills, an important agricultural landscape in central Europe. The study site covered four small adjacent agricultural watersheds (W1–W4) with a size of 0.8 to 4.2 ha (Figure 1), situated at an altitude of 458 to 478 m above sea level (48°30′50″ N, 11°26′30″ E). Loamy or silty loamy Inceptisols predominated in all water-

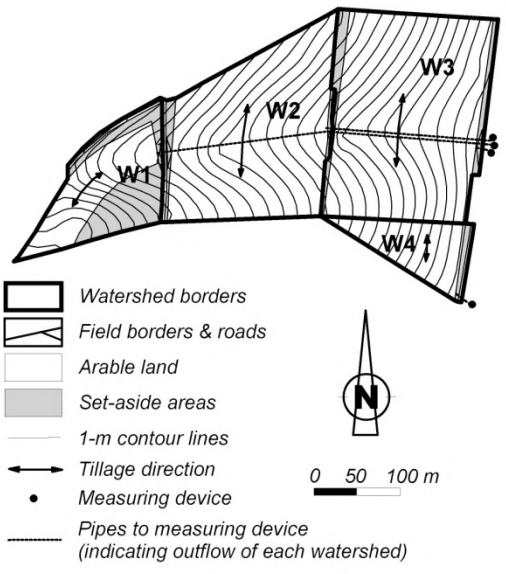


**Figure 1. Watershed topography, field borders, tillage direction and location of measuring devices.**

sheds (Sinowski and Auerswald, 1999). During 1994 to 2001, the mean annual air temperature was 8.4°C and the average annual precipitation was 834 mm.

Each watershed included one field with some set-aside areas (field margins, hedges) and farm roads (Table 1). All fields were cropped with a rotation consisting of potato, winter wheat, maize, and winter wheat. The crop rotation was implemented in autumn 1992 after 1 yr (1992) of spring barley (*Hordeum vulgare* L.) and 1 yr of winter wheat (1991) on all fields to create similar starting conditions. Before that, all fields were part of one large field and were mainly farmed with small grain crops without additional soil conservation measures. The measuring period started 2 yrs after the implementation of the rotation and extended from January 1994 to December 2001, covering 8 yrs and two full rotations.

**Table 1. Morphology, land use, slope, soil texture and soil erodibility represented by the *K* factor of the USLE for the tested watersheds.**

| | Watershed No. | | | |
|---|---|---|---|---|
| | W1 | W2 | W3 | W4 |
| Morphology | | | | |
| Size, ha | 1.6 | 3.6 | 4.2 | 0.8 |
| Mean slope, % | 7.4 | 6.9 | 7.3 | 7.5 |
| Land use | | | | |
| Arable land, % | 53.1 | 94.9 | 92.9 | 90.3 |
| Set-aside areas, % | 44.6 | 3.4 | 6.6 | 5.6 |
| Field roads, % | 2.4 | 1.7 | 0.6 | 4.1 |
| Soil texture | | | | |
| Clay, kg/kg | 0.17 | 0.22 | 0.21 | 0.19 |
| Silt, kg/kg | 0.38 | 0.47 | 0.58 | 0.56 |
| Sand, kg/kg | 0.45 | 0.31 | 0.21 | 0.25 |
| Soil erodibility (*K* factor) | 0.32 | 0.43 | 0.49 | 0.49 |

The crop rotation was shifted by 1 yr for each field to have every crop in every year (Table 2). Hence, a comparison between the fields and a comparison between crops was possible. On average, winter wheat was planted at the end of October and harvested in mid-August. After winter wheat harvest, a cover crop (mustard, *Sinapis alba* L.) was cultivated before each row crop. Potato ridges were already formed before mustard seeding and potato and maize were planted directly into the winter-frost-killed mustard, maintaining some mustard cover also after planting potato. Potato was planted at the end of April and harvested in early October, while maize was planted about 1 wk later and harvested 2 wk later than potato. Wide, low-pressure tires were used on all machinery to reduce soil compaction and to avoid the development of wheel-track depressions, which usually encourage runoff (Auerswald et al., 2000; Fiener and Auerswald, 2003b).

In general, the tillage direction was perpendicular to the main slope, except for Watershed W1, which had an unsuitable layout (Figure 1). Large deviations from the contour can be found within each field, however, due to the undulating terrain and the rectangular field shape necessary for effective field management.

**Table 2. Crop rotation in the tested watersheds and climatic properties during the experimental period; precipitation, *R* factor and temperature were derived from data of two meteorological stations at the research farm; the potential evapotranspiration of grass was taken from measurements at a German Weather Service Station about 30 km North-East of the test site.**

| Year | Crop in Watershed No. | | | | Climate | | | |
|---|---|---|---|---|---|---|---|---|
| | W1 | W2 | W3 | W4 | Precipitation mm yr$^{-1}$ | *R* factor N h$^{-1}$ yr$^{-1}$ | Annual mean air temperature °C | $ET_{pot}$‡ mm yr$^{-1}$ |
| 1994 | Maize | WW | Potato | Potato | 838 | 144 | 10.3 | 653 |
| 1995 | WW† | Maize | WW | WW | 791 | 66 | 8.6 | 579 |
| 1996 | Potato | WW | Maize | Maize | 671 | 95 | 6.5 | 524 |
| 1997 | WW | Potato | WW | WW | 659 | 57 | 8.0 | 646 |
| 1998 | Maize | WW | Potato | Potato | 901 | 85 | 8.4 | 669 |
| 1999 | WW | Maize | WW | WW | 899 | 77 | 8.4 | 613 |
| 2000 | Potato | WW | Maize | Maize | 940 | 110 | 9.0 | 699 |
| 2001 | WW | Potato | WW | WW | 976 | 78 | 8.2 | 683 |

†winter wheat; ‡ potential evapotranspiration of grass

## MATERIALS AND METHODS

### Measuring Runoff and Sediment Delivery

Runoff was collected at the lowest points of the watersheds where field borders were built to form small dams. From the dams, runoff was transmitted via underground tile outlets to the measuring systems. The measuring systems were based on a Coshocton-type wheel runoff sampler collecting an aliquot of about 0.5% from the total runoff coming from the outflow pipes. The aliquot volume was measured and at least one sample was taken during or after each event, which was later dried at 105°C to determine the sediment concentration.

During the first 2 yrs of the measuring campaign, the runoff aliquot was collected in 1-m$^3$ tanks, in which a 10-L bucket was hanging to collect small events (< 2 m$^3$ runoff) and the coarse sediment of large events. The coarse sediment was dried completely, while the fine sediment was agitated by a submersible pump (maximum flow 200 L min$^{-1}$) for some minutes and then an aliquot was taken from the outflow of the pump. In later years, tipping buckets (volume ~85 mL) were installed at the outlets of the sampling wheels, which were connected to ISCO 3700 portable samplers (Teledyne ISCO, Lincoln, NE) that counted the number of tips and, after a defined runoff volume, automatically collected a sample from the undisturbed runoff before it flowed over the Coshocton-type wheel. Both methods avoided errors in sediment concentration introduced by collection tanks, which are difficult to homogenize before aliquot sampling (Ciesiolka et al., 2006). All measuring systems were tested

for function at the end of each runoff event. A more detailed description of the measuring systems and the results of a precision test can be found in Fiener and Auerswald (2003a).

**Evaluating Soil Characteristics, Soil Cover, and Management Effects**

To evaluate the reasons for differences in soil loss and to determine the effects of potato and maize on the following winter wheat crop, we monitored (i) soil characteristics, namely aggregate size and aggregate stability, (ii) soil cover, (iii) surface roughness, and (iv) management effects. Less variability relative to soil erosion events can be expected for these parameters because only a little interaction with rainfall occurs. Therefore, the variability of these parameters was determined with a high temporal and spatial resolution for a shorter period than the erosion measurements, which reflected the full 8 yrs.

During and after the cultivation of potato and maize, the different aggregate properties were measured up to 10 times at five different locations within the watersheds between 1993 and 1995. The top 3 cm of soil was carefully sampled to avoid aggregate stress and disintegration. The soil was air dried and sieved into fractions 8 to 5, 5 to 2, 2 to 1, and < 1 mm, and the median diameter was calculated from these fractions. Aggregate density was measured with 10 replications for the 8- to 5-mm aggregates according to Becher et al. (1990). Water drop penetration time (Bisdom et al., 1993) was measured for 0.03-g drops of deionized water imbibed by 8- to 5-mm aggregates. Aggregate density, size distribution, and water drop penetration were measured for only a subset of samples. Aggregate stability was determined for 1- to 2-mm aggregates with the percolation test (Auerswald, 1995), which measures the flow of deionized water through a column of 10 g of initially dry aggregates for 10 min. Water flow is sensible to aggregate breakdown during fast wetting. To account for differences in soil texture of sampling locations, the percolation rates were corrected for differences in sand content using the equation of Mbagwu and Auerswald (1999).

Soil roughness under winter wheat after potato and maize was evaluated in two typical fields located in Watersheds W1 and W3 between October 1994 and May 1995. The chain method (Saleh, 1993) was used, where a 1-m-long chain with 5-mm links was placed on the soil surface, and the distance between the two ends of the chain was measured. Due to the measuring direction perpendicular to the tillage direction, the measurements represent random and tillage roughness for the winter wheat fields, which were cultivated using identical procedures after both preceding crops. In total, 14 measuring campaigns (total n = 74) after potato and eight campaigns after maize (total n = 41) were performed. From these measurements, the roughness index (*RFR*) of EUROSEM (Morgan et al., 1998) was calculated, defined by the shortest distance between two points on the ground (*X*) and the total distance

measured along the soil surface ($Y$), which can easily be converted into random roughness (Jester and Klik, 2005):

$$RFR = \frac{Y - X}{Y} \cdot 100 \quad (1)$$

Plant and residue cover were measured biweekly during the vegetation period, every four weeks in autumn and spring, and before and after each soil management operation. The measurements were performed at three locations in each field between January 1993 and April 1997. Residue cover was measured along a pocket rule, while plant cover was determined from photographs taken from a height of up to 4 m (in the case of full-grown maize) using picture analysis and plant height measured with a pocket rule in the field.

For a direct comparison of the soil loss from potato and maize in the four watersheds, the combined effect of soil cover and management, especially the direction of tillage and hence of potato ridges, were taken into account by applying the *CP* factor of the Revised Universal Soil Loss Equation (RUSLE, Renard et al., 1996), which is the most appropriate model to be used with long-term averages. The RUSLE is based on the Universal Soil Loss Equation (USLE, Wischmeier and Smith, 1960), which has been extensively validated in this landscape (e.g., Schwertmann et al., 1987). The *C* factor was calculated from the seasonal variation in three subfactors quantifying prior land use, mulch cover, and crop cover and the seasonal variation in rain erosivity. The crop cover subfactor (including tall weeds) was calculated from plant height and plant cover according to Wischmeier and Smith (1978), which is identical to the method for the RUSLE equation (Yoder et al., 1997). The mulch cover (including stones and small weeds growing close to the surface) was considered according to the equation by Kainz (1989), which was developed from rainfall simulator experiments performed in a neighboring region and under similar cropping conditions. The prior land use subfactor was set to 0.8 following the recommendations of Wischmeier (1975). This value agreed well with many results from rainfall simulator experiments under seedbed conditions on the research farm (Schröder and Auerswald, 2000) and the surrounding landscape (summarized in Schwertmann et al., 1987). The seasonal variation of rain erosivity is called the erosion index (Wischmeier, 1959) and is the ratio between the erosivity within a certain period and the annual erosivity. We report a daily erosion index expressed as a percentage per day. A constant value of 0.27% $d^{-1}$ would denote a lack of any seasonality. To smooth the large fluctuations between individual days, a linearly weighted moving average (t ± 30 d) was calculated. The same procedure was used to smooth the average seasonal distribution of precipitation.

The *P* factor depends on the crops' specific roughness, the tillage orientation relative to the local slope, the slope gradient, and the upslope drainage area. The parameters of orientation, gradient, and drainage area were derived from a detailed geodetic survey (Warren et al., 2004). It was resolved in a cascading triangular irregular network (Flacke et al., 1990) of 3424 triangles with a mean size of 31.4 $m^2$ and the *P* factor was then calculated for each triangle according to its individual topographic parameters (Kagerer and Auerswald, 1997) and, finally, the area-weighted *P* factors of all triangles within a watershed were combined to yield the overall *P* factor.

## RESULTS AND DISCUSSION

### Direct Effects

During the observation period (1994–2001), on average, 198 rainfall–runoff events were measured per watershed. Focusing on the vegetation period (May–August), 1.48 events per month occurred, on average, during the 16 watershed years with winter wheat cultivation, while 2.09 and 1.69 events per month occurred during the eight watershed years of potato

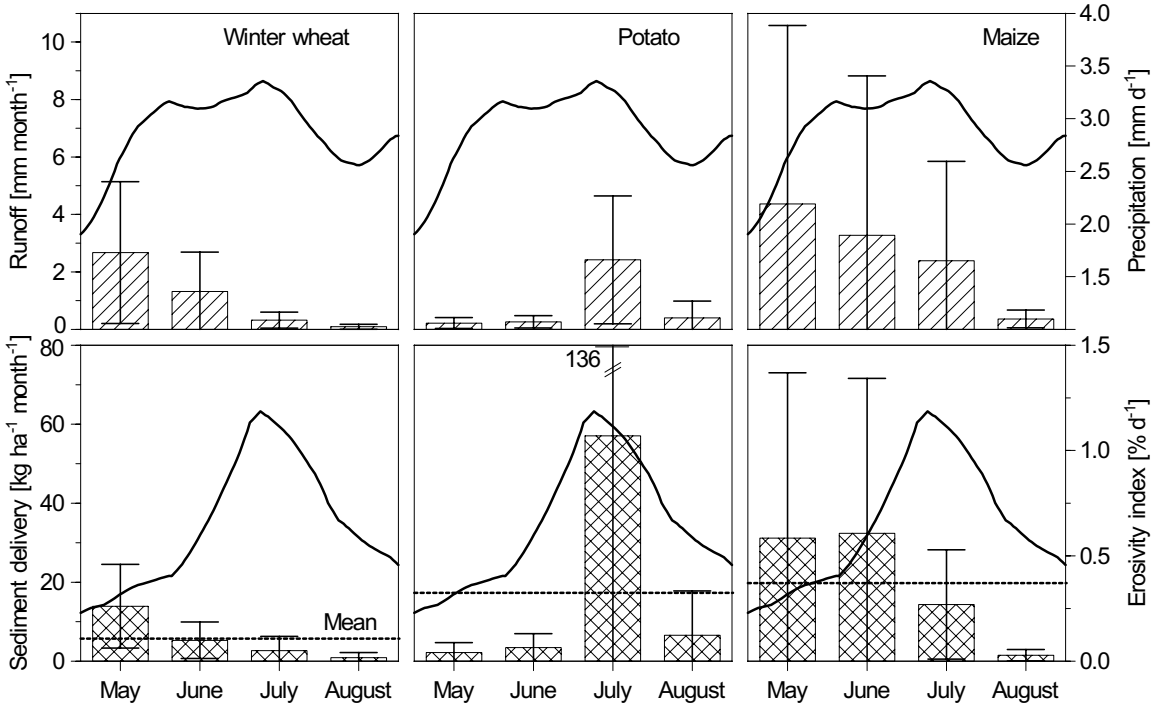


**Figure 2. Bars: runoff (top) and sediment delivery (bottom) during the vegetation period from watersheds where winter wheat, potato and maize were cultivated. Results are arithmetic means to allow a comparison with results from other studies although 95% confidence intervals (error lines) below zero indicate that the measurements were not normally distributed. Lines: precipitation (top) and erosivity index (bottom). All data were averaged over 1994-2001 with 16 watershed years for winter wheat and 8 watershed years for maize and potato and two meteorological stations for precipitation properties.**

and maize cultivation, respectively. The monthly average runoff during the vegetation period for winter wheat, potato, and maize was 1.10, 0.82, and 2.60 mm, respectively (Figure 2). In the case of winter wheat and maize, the runoff per month decreased from May to August, whereas the monthly rain amount increased from May to July. For potato, the highest runoff volumes were observed in July, while runoff was always < 0.4 mm $mo^{-1}$ for all other months. The large confidence intervals, especially in the case of maize, indicate that runoff from the small watersheds was highly variable among years because of a year-to-year variability in plant growth and storm size distribution, and possibly due to interactions with watershed characteristics.

Remarkably, the highest sediment delivery (57 kg $ha^{-1}$ $mo^{-1}$) matched with the month of the highest erosivity index only for potato because potato reached 80% soil cover only for a short period of time in contrast to the two other crops (Figure 3). The monthly average sediment delivery during the vegetation period for winter wheat, potato, and maize was 5.7, 17.3, and 19.8 kg $ha^{-1}$, respectively (Figure 2). Comparing winter wheat and potato, a similar runoff amount led to a more than threefold higher sediment delivery in the case of potato. Nevertheless, except for Watershed W1, maize produced slightly more sediment delivery than potato. This agreed with different *CP* factors for the four watersheds. While the *P* factor in potato was lower due to the effect of the ridges, the *C* factor was higher because the residues of the preceding cover crop were partly destroyed when planting and ridging potato and because the potato crop established slowly (Figure 4). This resulted in a similar combined *CP* factor for maize and potato as long as potato was grown along the contour. The protection by ridges was not effective in Watershed W1 due to the field layout. The predicted combined *CP* factor for this watershed, therefore, is about

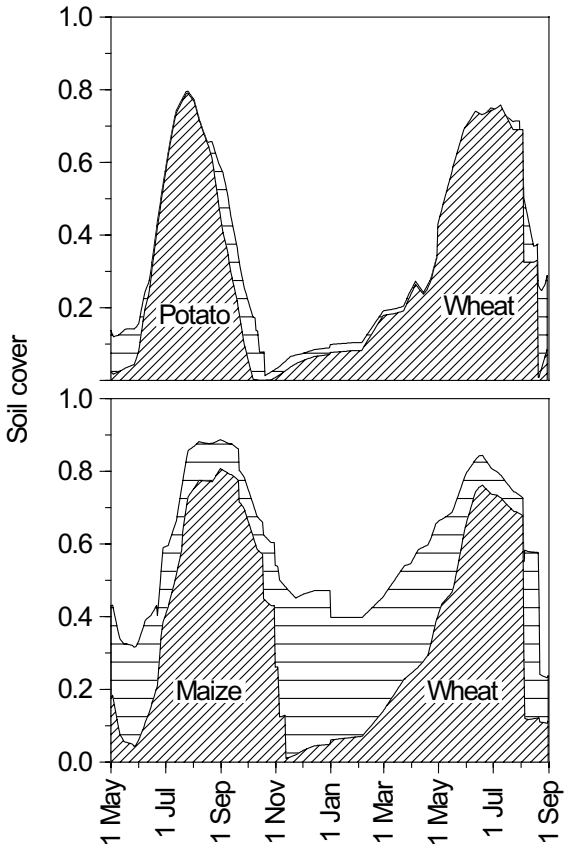


**Figure 3. Total soil cover measured at nine fixed positions distributed over the tested watersheds during 4 yrs for the potato-wheat and the maize-wheat sequence. Diagonal hatched area denote plant cover, horizontally hatched area denotes the amount of residue cover contributing to total soil cover.**

five times higher for potato than for maize (Figure 4). This also agreed well with the measured soil deliveries from this watershed, which were about four times higher for potato (224 kg $ha^{-1}$ $yr^{-1}$) than for maize (56 kg $ha^{-1}$ $yr^{-1}$), although both values are based on only 2 yrs. We may conclude that the direct effects exerted by the crops due to differences in cover and surface roughness are well predicted by the *C* and *P* factors. The direct effects of both crops mainly acted via soil cover and ridge roughness.

**Carryover Effects**

While during the vegetation period the differences between potato and maize were small even when all watersheds were combined (17.3 vs. 19.8 kg $ha^{-1}$ $mo^{-1}$; Figure 2), the picture changed when the following wheat crop was also considered (Figure 5). The soil loss of the potato–winter wheat sequence (41.4 kg $ha^{-1}$ $mo^{-1}$) was more than twice that of the maize–winter wheat sequence (19.0 kg $ha^{-1}$ $mo^{-1}$). The difference was especially large during the first months after the preceding crop, when the protection by the wheat crop itself was missing or small (ratio between potato–winter wheat and maize–winter wheat sequence of 3.9 for the average sediment delivery of November and December) but it was still detectable under full-grown wheat (ratio of 2.1 for the average between May and August). Especially in years with a large erosive event shortly after potato harvest and wheat sowing, large soil losses were measured.

Three main reasons for the differences in soil loss between winter wheat after potato and after maize were identified: (i) soil protection from rain impact by plant and plant residue cover, (ii) hydraulic roughness influenced by aggregate and residue roughness, and (iii) aggregate stability.

The potato harvest decreased the residue cover, on average, to about 2% (1993–1996). In contrast, about 45% of cover was left, on average, after maize harvest (Figure 3). Therefore, the soil was less protected from raindrop impact and, moreover, hydraulic roughness caused by residues was reduced and hence it must be assumed that the surface runoff veloci-

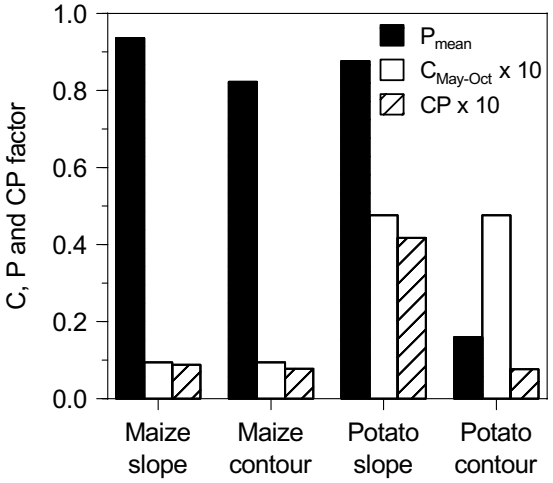


**Figure 4. Average surface-crop and cover factor *C* and management protection factor *P* of the RUSLE (Renard et al., 1996). The *P* and *CP* factors were calculated separately for watershed W1, where ridges followed the slope (maize slope/potato slope), and watersheds W2 – W4, where ridges followed contours (maize contour /potato contour).**

ty was larger (e.g., Gilley et al., 1986) after potato, increasing detachment and transport capacity.

Additionally, sieving the soil for the potato harvest caused a mechanical disintegration of large aggregates and a weakening of small aggregates. The median aggregate diameter was considerably smaller after the potato harvest than before harvest or compared with the maize field (Figure 6), although in both cases field operations after the row crop harvest were identical (chisel plowing, sowing of winter wheat). Thus, the roughness caused by soil aggregates was decreased and the aggregate transportability was increased due to the potato harvest.

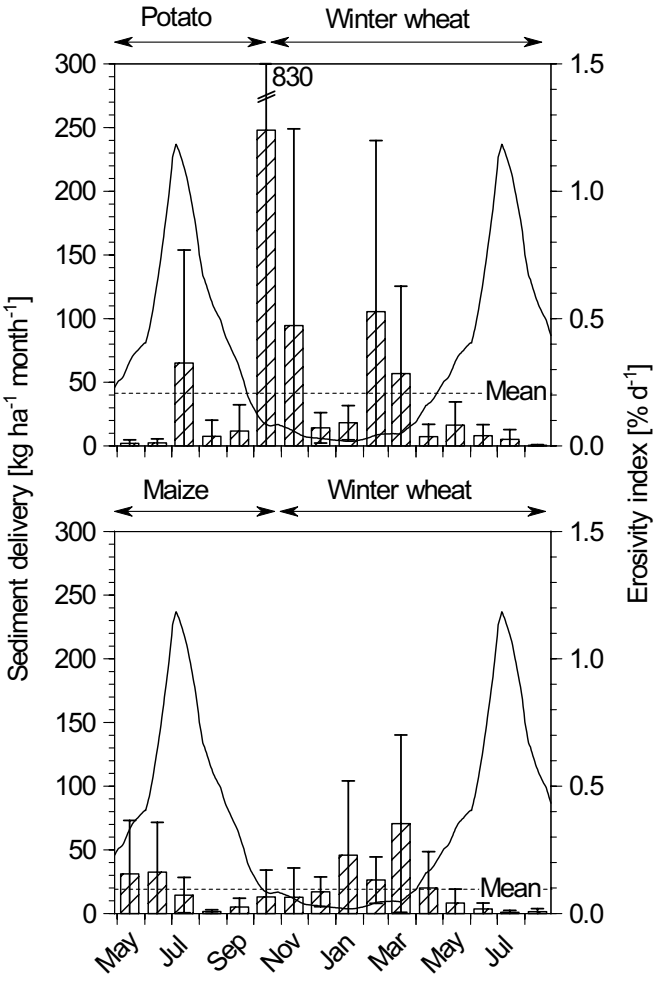


**Figure 5. Bars: Monthly average sediment delivery between 1994 and 2001 for the potato-winter wheat (n=7) and the maize-winter wheat rotation (n=8), respectively; error lines indicate the 95-% confidence intervals (see comment Figure 2); Lines: erosivity index.**

The difference in soil roughness, indicated by the different amount of residue and different aggregate size, was also evident from the roughness measurements. The average *RFR* under winter wheat after potato (*RFR* = 18.6, SD = 3.8, n = 74) was significantly ($P < 0.01$) smaller then the *RFR* measured under winter wheat after maize (*RFR* = 21.8, SD = 4.2, n = 41). In both cases, no trend in *RFR* development between October 1994 and May 1995 could be found.

The weakening of the aggregates due to the mechanical strain during potato cultivation becomes obvious from the percolation stability test (Figure 7). This strain already occurs during potato growth due to planting, ridging, and the raindrop impact on a surface, which is less protected by cover than under maize. The percolation stability was lower by a factor of four under potato compared with maize. The trafficking of the furrows with narrow tires reduced the percolation stability further compared with ridges (0.41 and 0.60 mL $min^{-1}$, respectively; with n = 6 each and $P < 0.05$). Under wheat, the difference in aggregate stability

between maize and potato was inherited, although a slight increase in stability following the row crop occurred in both cases.

In contrast to percolation stability, density of the 8- to 5-mm aggregates remained unchanged. It varied between 1.52 and 1.93 g $cm^{-3}$ and was 0.4 to 0.6 g $cm^{-3}$ higher than the bulk density. Variation within a sample was larger than between samples. Also, the water drop penetration time was similar for all samples.

In general, the suspected reasons for a carryover effect of potato to the following winter wheat crop were proven by measurements of soil properties and plant residue cover. This strengthens the notion that the measured difference in soil loss is not accidental due to the stochastic nature of erosion events but is the consequence of systematic differences in soil state after different crops. The carryover effect of potato to following small grain crops should be taken into account for soil conservation planning and the effects on soil properties should be taken into account for erosion modeling.

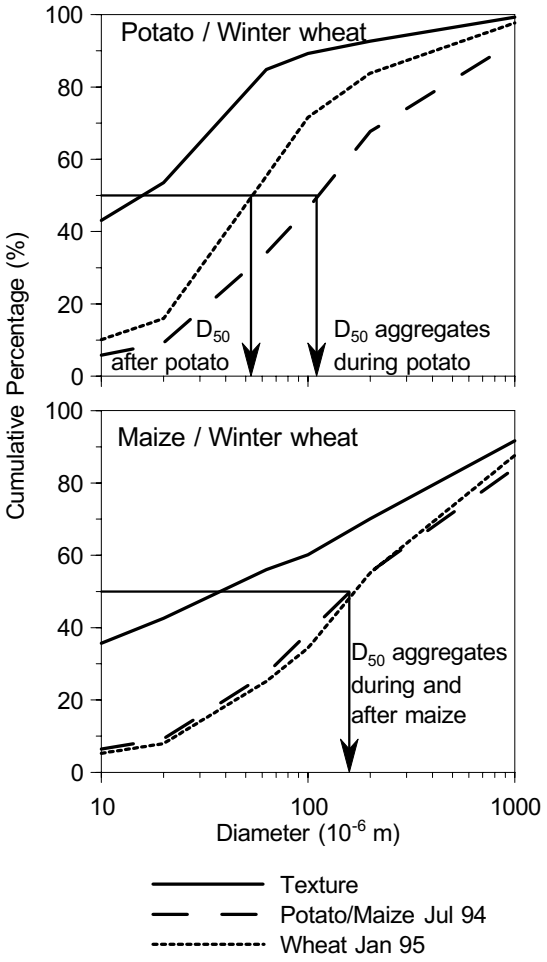


**Figure 6. Aggregate size of the topsoil (0-3 cm) sampled at two locations in July 1994 (during the row crop) and January 1995 (after row crop harvest and winter wheat establishment) for the maize–winter wheat (close to Watershed W1) and the potato–winter wheat sequences (in Watershed W3); $D_{50}$ is the median aggregate diameter.**

Even with the ridges oriented mainly perpendicular to the slope and with a mulched cropping system, potato remained an erosive crop because of its negative carryover effect on the following wheat crop, which did not profit from the ridge roughness or the mulch. In addition to its effect in promoting water erosion, potato also enhances tillage erosion (Kachanoski and Carter, 1999) and soil losses with harvested tubers (Auerswald et al., 2006; Ruysschaert et al., 2006) and thus must be regarded as one of the most erosive crops.

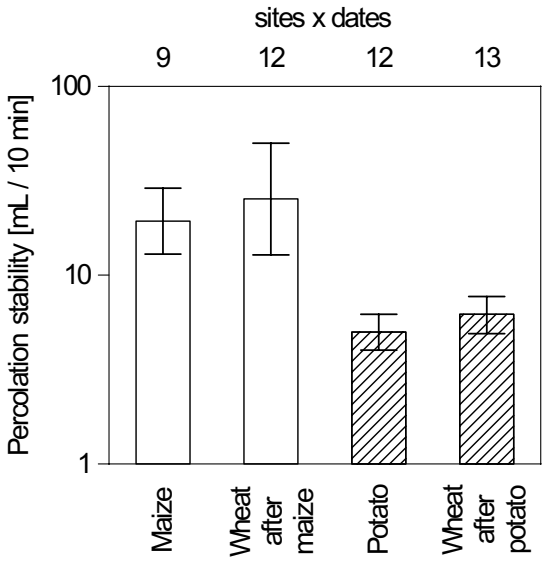


**Figure 7. Percolation stability measured at five different locations within the watersheds between 1993 and 1995. Error bars indicate the 95% confidence interval for the mean percolation stability.**

## CONCLUSIONS

A mulch-planting potato system protects the surface less than mulched maize. When potato was planted along the contour, the reduced cover was compensated by the effect of the potato ridges due to runoff retention and deceleration, compared with more cover and less roughness under maize. Therefore, about the same soil loss was measured for maize and potato. The effects of cover and roughness on the soil loss could be well quantified by the *C* and *P* factors of the RUSLE.

Large differences in soil loss, however, occurred under the wheat crop following these row crops. Soil loss under wheat was about two times greater after potato than after maize. Less residue cover after potato, disintegration of large aggregates during the potato harvest, and a lower aggregate stability were detected and can explain this. Potato thus increases erosion more than maize but this is mainly caused by the adverse carryover effects and not directly during the year of potato cultivation.

This carryover effect should be taken into account when optimizing crop rotations with respect to soil conservation; for example, a crop with slow development of plant cover such as spring-sown crops should not follow a crop like potato. Moreover, it is highly relevant for the modeling of water erosion from agricultural areas.

# 5. LAYER-SPECIFIC ANALYSIS AND SPATIAL PREDICTION OF SOIL ORGANIC CARBON USING TERRAIN ATTRIBUTES AND RESULTS FROM SOIL REDISTRIBUTION MODELING

Submitted (09/09):
V. Dlugoß, P. Fiener and K. Schneider.
Layer-specific analysis and spatial prediction of soil organic carbon
using terrain attributes and results from soil redistribution modeling.
Soil Science Society of America Journal.

***ABSTRACT.*** *High-resolution soil organic carbon (SOC) maps are a major prerequisite for many environmental studies dealing with carbon stocks and fluxes. Especially in hilly terrain, where SOC variability is most pronounced, high quality data are rare and costly to obtain. In this study factors and processes influencing the spatial distribution of SOC in three soil layers (< 0.25, 0.25-0.5, and 0.5-0.9 m) in a sloped agricultural catchment (4.2 ha) were statistically analyzed, utilizing terrain parameters and results from water and tillage erosion modeling (with WaTEM/SEDEM). Significantly correlated parameters were used as covariables in regression kriging (RK) to improve SOC mapping for different input data densities (6-37.9 soil cores per hectare) compared to ordinary kriging (OK). In general, patterns of more complex parameters representing soil moisture and soil redistribution correlated highest with measured SOC patterns, and correlation coefficients increased with soil depth. Analogously, the relative improvement of SOC maps produced by RK increased with soil depth. Moreover, a relative improvement of RK was achieved with decreasing input data density. Hence, an expectable decline in interpolation quality with decreasing data density could be reduced especially for the subsoil layers incorporating soil redistribution and wetness index patterns in RK. The optimal covariable differed between the soil layers indicating that bulk SOC mapping deduced from topsoil SOC measurements might not be appropriate in sloped agricultural landscapes. However, generally more complex covariables, especially patterns of soil redistribution, exhibit a great potential in improving subsoil SOC mapping.*

Soils play a major role in the global carbon cycle. Approximately 1500 Pg C are stored in the topmost meter of soils worldwide corresponding to twice the amount of atmospheric C and triple the amount of C stored in the biosphere (Schlesinger, 2005). Nevertheless, the role of this reservoir as $CO_2$ sink or source in global climate and environmental issues is not clearly understood. To analyze the possibilities of soils of sequestering atmos-

pheric $CO_2$ as well as for other environmental issues (e.g. analysis of soil quality and adaptation of management practices) detailed and precise maps of the distribution of soil organic carbon (SOC) are an essential prerequisite. Especially in agricultural regions the complex arrangement and combination of topography, soil and management practices and thereby controlled biological processes lead to a high spatial variability of SOC. Under rolling topography the spatial heterogeneity of SOC in agricultural fields is also affected by soil redistribution processes. Most studies dealing with soil and SOC redistribution indicate an increase of SOC in depositional areas as compared to regions of erosion, where SOC is depleted (e.g. Mabit et al., 2008; Ritchie et al., 2007). However, there are also opposite findings published in literature. For example, Arriaga and Lowery (2005) found that the introduction of clayey subsoil material into the plow layer due to erosion of the topsoil stabilized and hence increased SOC content in the topsoil. Below the plow layer the expected decrease in SOC occurred in areas of erosion, while more or less constant SOC contents were found throughout the soil profile in regions of soil deposition (Arriaga and Lowery, 2005).

To produce accurate SOC maps, in general, different kinds of interpolation schemes are applied based on point measurements. As field measurements are costly and time-consuming, the improvement of interpolation methods while using secondary information was extensively tested (e.g. Odeh et al., 1994; Takata et al., 2007). Therefore, terrain parameters of various complexities were used as proxies for relief driven processes of pedogenesis. In most studies primary terrain parameters, which can nowadays easily be derived from digital elevation models (DEMs), such as (relative) elevation (Mueller and Pierce, 2003; Ping and Dobermann, 2006; Sumfleth and Duttmann, 2008), slope (Mueller and Pierce, 2003; Ping and Dobermann, 2006; Sumfleth and Duttmann, 2008; Takata et al., 2007), aspect (Odeh et al., 1994; 1995), and curvature (Takata et al., 2007; Terra et al., 2004) were used as secondary information. These primary terrain parameters can also be combined to more complex secondary terrain parameters or indices comprising landscape processes more explicitly. Often the wetness (or topographic) index (Beven and Kirkby, 1979) is tested for its capability to improve the interpolation of soil organic carbon and other soil properties (e.g. Herbst et al., 2008; Sumfleth and Duttmann, 2008; Takata et al., 2007). Besides these terrain parameters also other parameters are used as covariables for interpolation schemes in literature. Takata et al. (2007), for example, use the enhanced vegetation index, whereas Chen et al. (2000) use soil color to successfully predict the spatial distribution of SOC. Both parameters are derived from remote sensing data. Another covariable utilized effectively to improve the interpolation of SOC is the electrical conductivity of the topsoil layer (Ping and Dobermann, 2006; Simbahan et al., 2006; Terra et al., 2004).

A variety of statistical and geostatistical methods for interpolating point data with and without consideration of secondary information exist (Isaaks and Srivastava, 1989; Webster

and Oliver, 2001). While more simple statistical approaches, like a (multiple) linear regression performed well under certain circumstances to interpolate SOC (e.g. Mueller and Pierce, 2003), often geostatistical kriging approaches accounting for the spatial structure of SOC as well as of that of covariables performed better. Whereas ordinary kriging utilizes the spatial autocorrelation of the target variable alone, there are several geostatistical techniques that allow for the incorporation of a spatial trend caused by spatial patterns of secondary parameters in the kriging approach. Most often regression kriging (RK) or kriging with external drift (KED) are applied. In contrast to KED, which is a one-algorithm system, RK is a stepwise approach combining a regression between target and covariable with simple or ordinary kriging of the regression residuals. Whereas the target and the covariable have to be linearly related in KED, RK also allows for the integration of more complex regression models (i.e. multiple linear or non-linear functions). KED and linear RK only differ in the computational steps used, but the resulting predictions are the same given the same input data (target and covariable) and the same regression fitting method (Hengl et al., 2007).

Odeh et al. (1995; 1994) defined three types of regression kriging, of which regression kriging model C, where the trend function is calculated using ordinary least squares, and the residuals are interpolated using ordinary kriging, was successfully used in improving the interpolation of soil organic carbon as well as that of other soil properties in many studies (e.g. Herbst et al., 2008; Sumfleth and Duttmann, 2008; Takata et al., 2007; Terra et al., 2004).

A geostatistically more sophisticated approach, which overcomes some statistical deficiencies of KED and RK in incorporating secondary parameters, is REML-EBLUP (Lark et al., 2006). In this method the trend model is estimated using residual maximum likelihood (REML), and subsequently the estimated parameters are used for the empirical best linear unbiased prediction (EBLUP). However, Minasny and McBratney (2007a; 2007b) who compared RK model C with REML-EBLUP for interpolating four different soil properties concluded that, although statistically somewhat inappropriate, RK used in many SOC studies (e.g. Sumfleth and Duttmann, 2008; Takata et al., 2007; Terra et al., 2004) has proven to be a robust technique for practical applications. In concordance to these findings (Chai et al., 2008), who analyzed the effect of different covariables on the spatial interpolation of soil organic matter, concluded that REML-EBLUP performed more stable in their study, but that the improvement was not significant compared with RK.

To our knowledge all studies explicitly dealing with the interpolation of SOC and its possible improvement by incorporating covariables in the interpolation process are focused on the topsoil layer (< 0.3 m, e.g. Mueller and Pierce, 2003; Ping and Dobermann, 2006; Simbahan et al., 2006; Sumfleth and Duttmann, 2008; Takata et al., 2007; Terra et al., 2004).

However, the spatial patterns of SOC in agricultural catchments might differ substantially in different soil depths, an aspect which should be taken into account for soil carbon balancing studies as well as for simulations of soil carbon dynamics.

The objectives of this study are: (i) To evaluate the soil layer specific spatial patterns of SOC in a small agricultural catchment and to analyze their relation to spatial patterns of terrain parameters and results from soil redistribution modeling, and (ii) to evaluate if these (easily available) parameters can serve as improving covariables in a layer-specific interpolation of SOC data by regression kriging, and hence potentially allow for a reduction of SOC sampling density without loss of mapping quality.

## MATERIALS AND METHODS

### Test site

The test site is part of the Pleiser Hügelland; a hilly landscape located about 30 km in the southeast of Cologne in North Rhine-Westphalia, Germany. It covers a small catchment of approximately 4.2 ha at an altitude of 125-154 m a.s.l. (Figure 1) which is part of a large agricultural field (50°43'N, 7°12'E). Slopes range from 1° in the western up to 9° in the eastern part with a relatively flat thalweg area heading to the outlet.

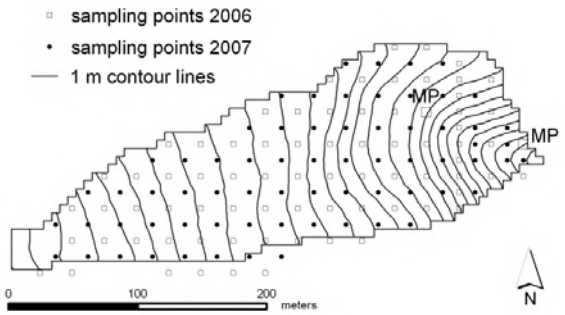


**Figure 1: Test site with location of soil sampling points; each of the two micro-plots (MP) consists of nine sample points arranged in a 1×1 m grid; flow direction is from east to west.**

The mean annual air temperature was 10.0 °C and the average precipitation per year was 765 mm (1990-2006) with the highest rainfall intensities occurring from May to October (data from the German Weather Service station Bonn-Roleber, situated about 1 km to the west of the test site, 159 m a.s.l.).

Due to its fertile, loess containing silty and silty-loamy soils classified as Alfisols (USDA, 1999) and its proximity to the agglomeration of Cologne-Bonn the test site is intensively used for arable agriculture. The present crop rotation consists of sugar beet (*Beta vulgaris* L.), winter wheat (*Triticum aestivum* L.), and winter barley (*Hordeum vulgare* L.). Since 1980 a no-till system was established with mustard (*Sinapis arvensis* L.) cultivated as cover crop after winter barley.

**Soil sampling and SOC measurement**

In order to investigate the vertical and horizontal distribution of SOC in the test site a first set of soil samples was taken in April 2006. It consisted of 92 soil cores of which 71 cores were situated in a regular 25×25 m raster. To account for a possible small scale spatial variability of SOC, additionally a north south transect in the eastern part of the test site with point distances of 12.5 m and two micro-plots consisting of nine sample points each in a 1×1 m raster were augered. In each of the micro-plots the central sample point belongs to the regular 25×25 m raster. Micro-plots were located in order to cover different slope positions. To densify this first sampling grid, in March 2007 a second set of soil cores (n = 65) was taken in a 25×25 m raster which was offset by 12.5 m to the north and west in relation to the 2006 raster. Additionally, three samples were taken near the outlet of the test site to account for a small colluvial area. Thus, soil samples exist on a regular 17.7×17.7 m raster with a density of 37.9 samples per ha (Figure 1), with additional samples along a transect and in two micro-plots. Within each sampling campaign soil cores were extracted with a Pyrckhauer soil auger (approximately 2 cm diameter) and soil samples were taken in three depths (I: 0-0.25 m, II: 0.25-0.5 m, and III: 0.5-0.9 m). All sampling points were surveyed with a dGPS (differential Global Positioning System) with a horizontal accuracy between 0.5 and 2 m.

After oven drying at 105°C for 24 hours the samples were ground and coarse particles were separated by 2 mm-sieving. Recognizable not decomposed organic matter particles were removed. Total C content was determined by dry combustion using a CNS elementar analyzer (vario EL, Elementar, Germany). Although loess soils in the area are in most cases deeply decalcified all soil samples were checked for lime ($CaCO_3$) with hydrochloric acid (10%). If any inorganic C content was recognized, its amount was determined according to the Scheibler method (Deutsches Institut für Normung, 1996). Combining both methods if necessary, soil organic carbon (SOC) was calculated from total minus inorganic carbon.

**Calculation of terrain parameters and spatial patterns of soil redistribution**

Three types of parameters possibly affecting the spatial distribution of SOC were calculated: (i) primary terrain attributes, (ii) secondary indices combining different primary terrain attributes and representing landscape processes more explicitly, and (iii) parameters representing soil redistribution patterns based on water and tillage erosion modeling. The derivation of these parameters was based on a digital elevation model (DEM) with a 6.25×6.25 m grid. The DEM was derived from laser scanner data (2–3 m point distance) provided by the Landesvermessungsamt North Rhine-Westphalia using ordinary kriging within the Geostatistical Analyst of the Geographical Information System ArcGis 9.2 (ESRI

Inc., USA). The grid size of 6.25×6.25 m was chosen to assure that each sampling point is located in the centre of a grid cell.

The following primary terrain attributes were calculated using ArcGis 9.2: The relative elevation (RE), which is the vertical distance of every grid cell to the outlet of the catchment, the slope S, the aspect A, and the curvature. The curvature is the second derivative of the surface and is separated into profile curvature (C-prof; curvature in the direction of maximum slope) and plan curvature (C-plan; curvature perpendicular to the direction of maximum slope). Another primary terrain attribute used in this study is the catchment area CA calculated for each grid cell using the extension HydroTools 1.0 for ArcView 3.x (Schäuble, 2004) applying the multiple flow algorithm of Quinn et al. (1991). The catchment area takes into consideration the amount of surface water that is distributed towards each grid cell. The parameter thus is related to soil moisture and infiltration as well as erosion and deposition. The two combined indices, wetness index (WI) and stream power index (SPI), differentiate between these two process groups more explicitly through the incorporation of the local slope gradient. The wetness index (WI) characterizes the distribution of zones of surface saturation and soil water content in landscapes (Beven and Kirkby, 1979) and is calculated as:

$$\mathrm{WI} = \ln \frac{SCA}{\tan \mathrm{S}} \tag{1}$$

where *SCA* is the specific catchment or contributing area ($m^2\ m^{-1}$) orthogonal to the flow direction and is calculated as the catchment area CA divided by the grid size (6.25 m) and S is the slope (°).

The stream power index (SPI) is the product of the specific catchment area *SCA* ($m^2\ m^{-1}$) and slope S (°) (Moore et al., 1993). It is directly proportional to stream power and can thus be interpreted as the erosion disposition of overland flow.

$$\mathrm{SPI} = SCA \cdot \tan \mathrm{S} \tag{2}$$

One deficit of the SPI is that deposition is not represented. In order to more precisely consider soil redistribution processes, namely water ($E_{wat}$), tillage ($E_{til}$) and total ($E_{tot}$) erosion and deposition, corresponding patterns were calculated applying the long-term soil erosion and sediment delivery model WaTEM/SEDEM version 2.1.0 (Van Oost et al., 2000; Van Rompaey et al., 2001; Verstraeten et al., 2002).

WaTEM/SEDEM is a spatially distributed model combining WaTEM (Water and Tillage Erosion Model) (Van Oost et al., 2000) and SEDEM (Sediment Delivery Model) (Van Rompaey et al., 2001). WaTEM consists of a water and a tillage erosion component that can be runed separately. The water erosion component uses an adapted version of the Revised Universal Soil Loss Equation (RUSLE, Renard et al., 1996). Adaptations consist of the substitution of slope length with the unit contributing area calculated following Desmet and Govers (1996) and the integration of sedimentation following an approach of Govers et al. (1993). Tillage erosion is caused by variations in tillage translocations over a landscape and always results in a net soil displacement in the downslope direction. The net downslope flux $Q_{til}$ (kg $m^{-1}$ $yr^{-1}$) due to tillage implementations on a hillslope of infinitesimal length and unit width is calculated with a diffusion-type equation adopted from Govers et al. (1994) and is proportional to the local slope gradient:

$$Q_{til} = k_{til} \cdot \mathrm{S} = -k_{til} \frac{dh}{dx} \tag{3}$$

where $k_{til}$ is the tillage transport coefficient (kg $m^{-1}$ $yr^{-1}$), S is the local slope gradient (%), $h$ is the height at a given point of the hillslope (m) and $x$ the distance in horizontal direction (m). The local erosion or deposition rate $E_{til}$ (kg $m^{-2}$ $yr^{-1}$) is then calculated as:

$$\mathrm{E_{til}} = -\frac{dQ_{til}}{dx} = \frac{d^2h}{d^2x} \tag{4}$$

As tillage erosion is controlled by the change of the slope gradient and not by the slope gradient itself, erosion takes place on convexities and soil is accumulated in concavities. The intensity of the process is determined by the constant $k_{til}$ that ranges between 500 and 1000 kg $m^{-1}$ $yr^{-1}$ in Western Europe (Van Oost et al., 2000).

A second module of WaTEM/SEDEM is the calculation of sediment transport and sedimentation. The sediment flow pattern is calculated with a multiple flow algorithm. The sediment is routed along this flow pattern towards the river taking into account its possible deposition. Deposition is controlled by transport capacity computed for each grid cell. The transport capacity is the maximal amount of sediment that can pass through a grid cell and is assumed to be proportional to the potential rill (and ephemeral gully) erosion volume (Van Rompaey et al., 2001). If the local transport capacity is lower than the sediment flux, deposition is modeled.

WaTEM/SEDEM requires the input of several GIS maps as well as various constants and was implemented as follows: The 6.25×6.25 m DEM served as the basis for the calculations. Additionally, a land use map containing field boundaries and a map containing the tillage direction of the test site were derived from digital aerial photographs delivered by the Landesvermessungsamt North Rhine-Westphalia. The *K* factor of the RUSLE was also given as a map with values of 0.058 and 0.061 kg h $m^{-2}$ $N^{-1}$ in the test site. This map was deduced from a digital soil map (scaled 1:50000) provided by the Geological Survey of North Rhine-Westphalia. Accounting for the crop rotation and the implemented soil conservation practice in the test site the *C* factor was set to 0.05 (Deutsches Institut für Normung, 2005). The *R* factor of the USLE was calculated with a regression equation between *R* factor and mean daily summer precipitation developed for North Rhine-Westphalia (Deutsches Institut für Normung, 2005). Therefore precipitation data (1990-2006) of the German Weather Service station Bonn-Roleber were used, resulting in an *R* factor of 67 N $h^{-1}$ $yr^{-1}$. Since no sediment yield data for model calibration were available, modeling was first performed on a 20×20 m grid, which equals the grid size in earlier, calibrated simulations under similar environmental conditions in the Belgium Loess Belt (Verstraeten et al., 2006). The results of this first simulation were used to recalibrate the transport capacity coefficients to run the model on a 6.25×6.25 m grid. All other constants necessary for running WaTEM/SEDEM were set to default, since no absolute but only relative erosion and deposition values were needed.

**Statistical and geostatistical analysis**

*Statistical analysis*

For statistical and geostatistical analysis three SOC input grids with different sampling densities were created. To achieve a dense 17.7×17.7 m sample raster ($R_{17}$) SOC data of the 2006 and 2007 sampling campaign were combined in each soil layer. For the topsoil layer it was assumed that inter-annual differences of sampling date and thus of planted crops, soil management, and climate could lead to differences of SOC concentrations gained from the two sampling campaigns. Thus, after an estimation of normal distribution by skewness coefficients, a Student's T-test (although not optimal when used with spatially autocorrelated data) was applied to estimate the equality of means of the SOC data of the two sampling years. In the two deeper soil layers these influences were considered negligible. Here the SOC contents of the two sampling dates were simply combined to one data set. The 2006 sampling points (n = 92) arranged in a 25 m raster ($R_{25}$) served as input data set with a medium density of 16.9 samples/ha for each soil layer. To produce a low density 50 m input raster ($R_{50}$; n = 44) every second data point of $R_{25}$ was eliminated resulting in a density of

approximately 6 samples/ha. Each raster contained the transect and the two micro-plots to incorporate the short distances in geostatistics.

To test the relation between the spatial patterns of SOC and the spatial patterns of potential covariables, Pearson correlation coefficients were calculated between all parameters and the SOC data for each soil layer and each raster width, respectively. For this correlation analysis the eight additional points of the micro-plots were excluded, since all nine sampling points of a micro-plot are located in one grid cell with one value for the relevant parameter. Parameters significantly ($p < 0.05$) related to SOC in a soil layer were tested for their potential to improve interpolation results when used as a linear trend in regression kriging.

*Geostatistical analysis*

Geostatistical methods are based on the theory of regionalized variables (Matheron, 1963). For further information concerning the theoretical background of geostatistics we refer to Isaaks and Srivastava (1989) or Webster and Oliver (2001). The basic assumption is that sample points close to each other are more similar than sample points that are far away from each other. This spatial autocorrelation is quantified in the empirical semivariogram of the sampled data, where the semivariance is plotted as a function of lag distance. For a data set $z(x_i)$, $i = 1,2,...$, the semivariance $\gamma$ of a certain lag distance $l$ is calculated as

$$\gamma(l) = \frac{1}{2n(l)} \cdot \sum_{i=1}^{n(l)} (z(x_i) - z(x_i + l))^2 \tag{5}$$

with $n(l)$ being the number of pairs of data points separated by $l$. To apply this semivariogram in the following interpolation process, known as kriging in geostatistics, a theoretical model has to be fit to the sample variogram.

Ordinary kriging (OK) that only uses the spatial autocorrelation of the target variable can be considered as the basic geostatistical interpolation method. It is a kind of weighted spatial mean, where sample point values $x_j$ are weighted according to the semivariance as a function of distance to the prediction location $x_0$. The weights $\lambda_i$ are chosen by solving the ordinary kriging system in order to minimize the kriging variance:

$$\begin{aligned} &\sum_{i=1}^{n} \lambda_i \gamma(x_i, x_j) + \varphi = \gamma(x_i, x_0) \\ &\sum_{i=1}^{n} \lambda_i = 1 \end{aligned} \tag{6}$$

where $\gamma(x_i, x_y)$ is the semivariance between the sampling points $x_i$ and $x_j$ and $\gamma(x_i, x_0)$ is the semivariance between the sampling point $x_i$ and the target point $x_0$ and $\varphi$ is a Lagrange-multiplier necessary for the minimization process (Ahmed and De-Marsily, 1987).

The regression kriging used in this study follows regression kriging model C described in Odeh et al. (1995) and accounts for a possible trend in the data combining linear regression with ordinary kriging of the residuals. In a first step a linear regression function of the target variable with the covariables is used to create a spatial prediction of the target variable at the new locations. In a second step ordinary kriging is applied to the residuals of the regression resulting in a spatial prediction of the residuals. Finally, the spatially distributed regression results and the kriged residuals are added to calculate the target variable at all new locations.

As a prerequisite of geostatistics, SOC data in each soil layer and in each raster width should be normally distributed. Following Kerry and Oliver (2007a) this prerequisite can be met in geostatistical analysis if the absolute skewness coefficient (SC) is < 1. Moreover, data with an asymmetry caused by aggregated outliers need not to be transformed if the absolute SC is < 2 (Kerry and Oliver, 2007b). If this was true, SOC data were not transformed. For use in regression kriging the residuals resulting from linear regression with the significantly correlated parameters in each soil layer and in each raster width should also be normally distributed. Skewness coefficients as well as normal Q-Q plots of residuals were analyzed. In case residuals showed strong deviations from normal distribution, the corresponding parameters were transformed to logarithms and linear regression was performed again (subsequently these transformed covariables are indicated by the subscript tr).

For each raster width and for each of the three soil layers SOC was interpolated using OK and RK with the selected parameters as covariables to target points spanning a 6.25×6.25 m raster within the test site. For the construction of omnidirectional empirical semivariograms of the original SOC data as well as of the residuals the maximum distance up to which point pairs are included was set to 200 m which is half of the maximum extent of the test site in east-west-direction. Lag increments were set to 10 m. In each approach two theoretical variogram models (exponential and spherical) and three methods for fitting the variogram model to the empirical variogram including ordinary least squares (i.e. equal weights to all semivariances) and two weighted least square methods (weighting by $n_p$ = number of pairs and weighting by $n_p l^{-2}$ with $l$ = lag distance) were applied. To evaluate the various theoretical variograms against the original data and to choose the best model a cross-validation procedure was implemented. In cross-validating each of the original data points is left out one after another and the value at that location is estimated by kriging (OK and RK) with the selected variogram model and the remaining data.

As a measure of spatial dependence the ratio of nugget to sill (%) was calculated reflecting the influence of the random component to the spatial variability. Following Cambardella et al. (1994) nugget-to-sill ratios between 0 and 25% show that data are highly spatially structured with low nugget variances, whereas ratios between 25 and 75% indicate moderate spatial dependence. Data with ratios > 75% are weakly spatially structured with a high proportion of unexplained variability.

**Validation**

To validate the kriging results and to compare the different geostatistical approaches made with high-density $R_{17}$ as input grid, cross validation was used, since no independent validation data set for this raster width was available. No sample points should be left out for the creation of a validation data set in order to avoid a loss of information in the input data. When using the reduced sampling grids $R_{25}$ or $R_{50}$ as input data, the 2007 sampling points ($n$ = 67) were used for validation and for comparing the different kriging approaches within each raster width.

To evaluate the goodness-of-fit of the various kriging results a set of indices was used. To account for the bias and the precision of the prediction the mean error *ME* and the root mean square error *RMSE* were calculated:

$$ME = \frac{1}{n}\sum_{i=1}^{n}(O_i - M_i) \tag{7}$$

$$RMSE = \sqrt{\frac{1}{n}\sum_{i=1}^{n}(O_i - M_i)^2} \tag{8}$$

where $n$ constitutes the number of points in the validation sample or the number of points used for cross-validation, and $O_i$ are the observed and $M_i$ the predicted values. The *ME* should be close to zero for unbiased predictions, and the *RMSE* should be as small as possible. Additionally, the model-efficiency coefficient (*MEF*) by Nash and Sutcliffe (1970) was calculated.

$$MEF_i = 1 - \frac{\sum_{i=1}^{n}(O_i - M_i)^2}{\sum_{i=1}^{n}(O_i - \overline{O})^2} \tag{9}$$

The *MEF* is a measure of the mean squared error to the observed variance and ranges between $-\infty$ and 1. If the value of *MEF* = 1, the model or interpolation represents a perfect fit. If the error is the same magnitude as the observed variance (*MEF* = 0), the arithmetic mean $\overline{O}$ of the observed values can represent the data as good as the interpolation.

The relative improvement *RI* (%) of prediction precision of RK with the selected covariables compared to OK was derived as:

$$RI = \frac{RMSE_{\mathrm{OK}} - RMSE_{\mathrm{RK}}}{RMSE_{\mathrm{OK}}} \cdot 100 \qquad (10)$$

where $RMSE_{\mathrm{RK}}$ and $RMSE_{\mathrm{OK}}$ are root mean square errors for a certain regression kriging approach and for ordinary kriging, respectively.

The statistical and geostatistical analysis was carried out with GNU R version 2.6 (R Development Core Team, 2007) and the supplementary geostatistical package gstat (Pebesma, 2004).

## RESULTS AND DISCUSSION

### Measured horizontal and vertical SOC distribution

Since Student´s T test clearly showed that the SOC contents of the two sampling dates in soil layer I belong to the same population, SOC contents in each soil layer were combined to one data set. After merging the data sets SOC values in soil layer I range from 0.68 to 1.67 % kg kg$^{-1}$, in soil layer II from 0.13 to 1.19 % kg kg$^{-1}$ and in soil layer III from 0.04 to 1.18 % kg kg$^{-1}$ (Table 1). Maximum values in all soil layers can be found in the flat area near the outlet of the test site (Figure 2) indicating accumulation of SOC by depositional processes. Another small area of relatively high SOC concentrations most pronounced in the two upper layers is located in the upper part near the southern boundary of the test site. We assume that this was caused by a former

**Table 1. Statistics of SOC content [% kg kg$^{-1}$] for the 2006, 2007 and the merged (merg.) dataset in three soil depths (I: 0-0.25 m; II: 0.25-0.5 m; III: 0.5-0.9 m).**

| Soil layer | Data | n† | Mean | Median | SD‡ | CV§ | Min¶ | Max# | SC†† |
|---|---|---|---|---|---|---|---|---|---|
| I | 2006 | 92 | 1.16 | 1.14 | 0.18 | 15.13 | 0.68 | 1.68 | 0.75 |
| II | 2006 | 92 | 0.67 | 0.67 | 0.22 | 32.62 | 0.13 | 1.19 | 0.24 |
| III | 2006 | 92 | 0.32 | 0.24 | 0.18 | 62.13 | 0.05 | 0.90 | 1.51 |
| I | 2007 | 67 | 1.11 | 1.08 | 0.16 | 12.23 | 0.85 | 1.43 | 0.30 |
| II | 2007 | 68 | 0.75 | 0.77 | 0.23 | 30.44 | 0.18 | 1.18 | -0.32 |
| III | 2007 | 68 | 0.36 | 0.33 | 0.22 | 62.55 | 0.04 | 1.18 | 1.57 |
| I | merg. | 159 | 1.14 | 1.12 | 0.17 | 14.91 | 0.68 | 1.68 | 0.74 |
| II | merg. | 160 | 0.71 | 0.71 | 0.22 | 30.99 | 0.13 | 1.19 | 0.01 |
| III | merg | 160 | 0.34 | 0.27 | 0.21 | 62.61 | 0.04 | 1.18 | 1.50 |

† n: number of sample points; ‡ SD: standard deviation; § CV: coefficient of variation; Min: Minimum; # Max: Maximum, †† SC: skewness coefficient

area of dung storage, but no detailed data to verify or falsify this assumption regarding its location exist. Remarkably, the SOC distribution of the mid soil layer shows more small scale variability than that of the other two soil layers.

In general, a decrease of SOC content and an increase of spatial variability expressed by the coefficient of variation (CV) with increasing soil depth can be observed (Table 1). The low spatial variability in soil layer I can be deduced to homogenization caused by management practices as well as to high turnover rates of soil organic matter. Skewness coefficients indicate that only the third soil layer was not normally distributed. This non-normality is caused by outliers aggregated in the depositional area near the outlet of the test site (Figure 2) and was therefore not corrected for further geostatistical analysis.

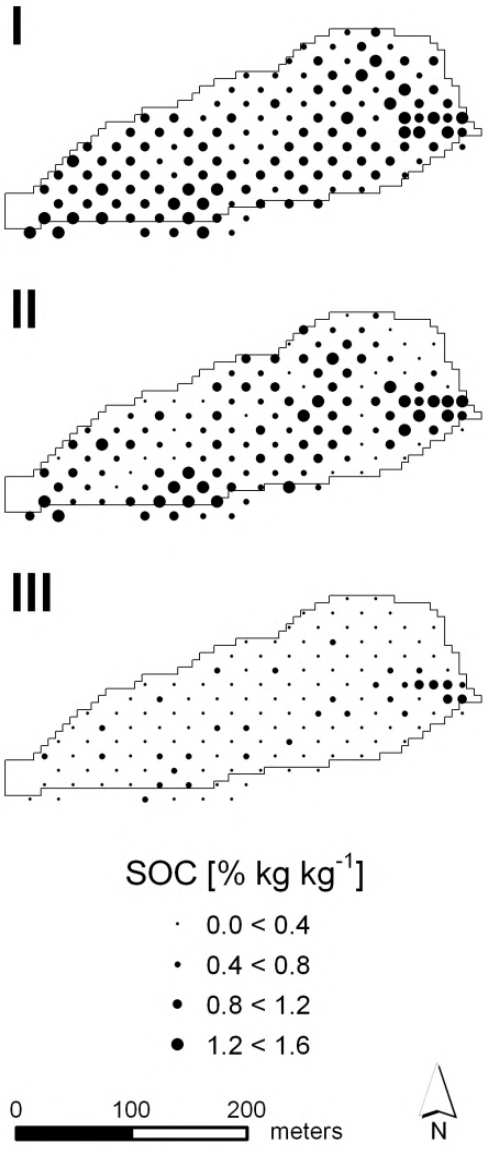


**Figure 2. Measured SOC contents [% kg kg$^{-1}$] at the 17.7×17.7 m raster sampling points for soil layers I (0-0.25 m), II (0.25-0.5 m), and III (0.5-0.9 m).**

## Terrain parameters and patterns of soil redistribution

The spatial patterns of the calculated terrain and soil redistribution parameters are shown in Figure 3 while statistics are given in Table 2. All parameters show a considerable spatial variability within the test site, indicating their appropriateness for use in RK. The relative elevation RE has a clear tendency from west to east with a maximum value of 27.4 m at the western boundary of the test site and a minimum of 0 m at the outlet. The slope S shows a more complex pattern: almost two third of the test site (mid to western part) are relatively flat with slopes ranging between 1 and 2°. Steep slopes (up to approximately 9.5°) exist in the eastern part. Incorporated into this easterly part is a very small thalweg area with still higher slopes (3-5°) than the flat westerly part. The spatial distribution of the aspect A indicates the differentiation between a south facing (values > 135°) and a north facing slope (values < 45°) in the east. The flat wes-

terly part is orientated to the east with aspects ranging from approximately 60 to 120°. Profile and plan curvature show a diffuse behavior in the flat west, whereas the pattern of convexities and concavities in the east corresponds well to the derived slope pattern. The catchment area CA and the two indices WI and SPI are distributed in similar patterns with a con-

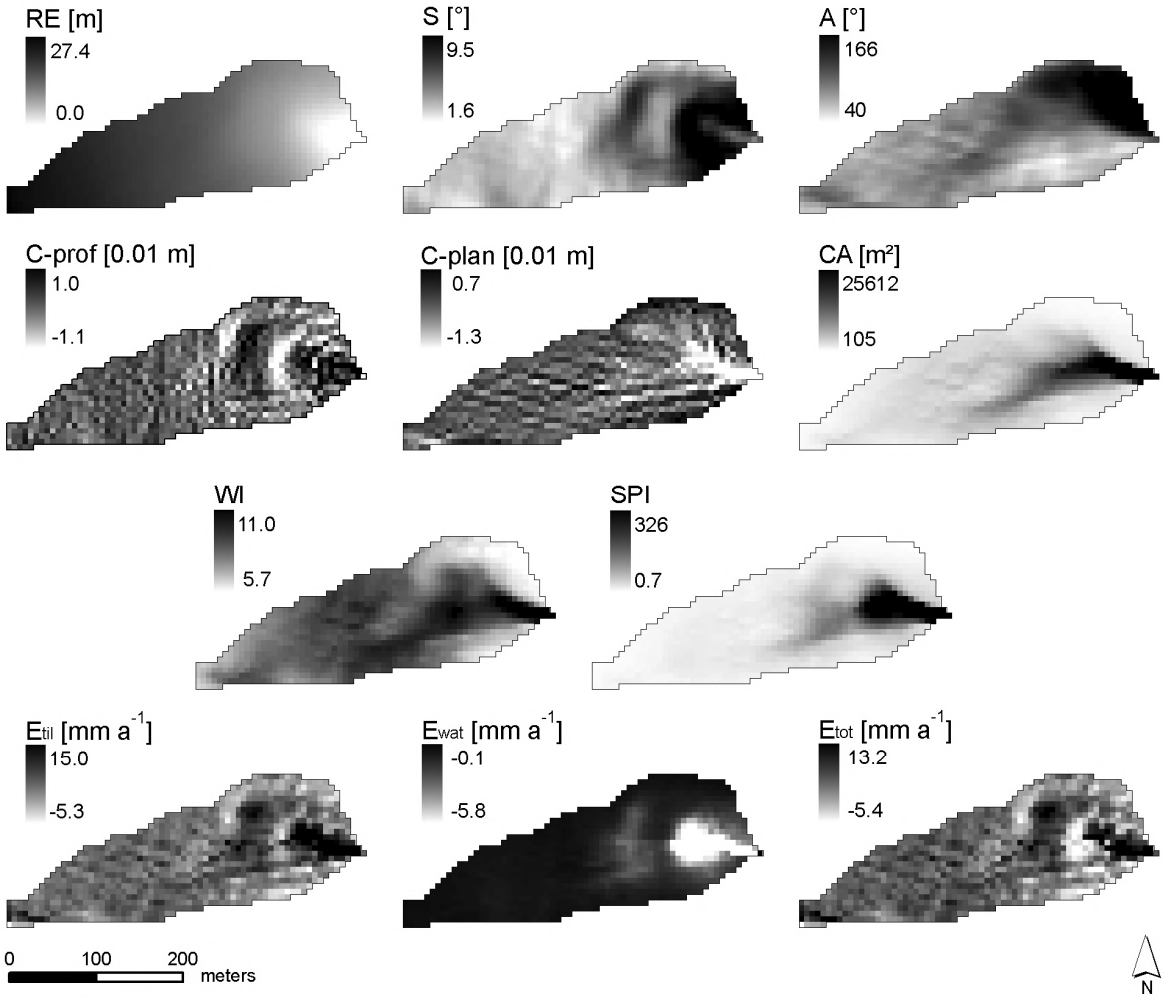


**Figure 3: Maps of terrain attributes and patterns of soil redistribution derived from WaTEM/SEDEM; for abbreviations of parameters refer to Table 2; a positive curvature (C-prof and C-plan) indicates that the surface is upwardly convex, and a negative value indicates that the surface is upwardly concave; regarding the erosion patterns ($E_{til}$, $E_{wat}$, and $E_{tot}$) negative values represent erosion, while positive ones represent deposition.**

centrated area of high values near the outlet of the test site. Compared to SPI this area is smaller in north-south-direction and more elongated in east-west-direction in the patterns of CA and WI.

**Table 2: Statistics of terrain attributes and soil redistribution parameters within the test site ($n$ = 1030); considered are: relative elevation RE, slope S, aspect A, profile and plan curvature (C-prof and C-plan), catchment area CA, wetness index WI, stream power index SPI, and patterns of tillage ($E_{til}$), water ($E_{wat}$) and total ($E_{tot}$) erosion.**

| Parameter | Mean | Median | SD† | CV‡ | Min§ | Max¶ | SC†† |
|---|---|---|---|---|---|---|---|
| RE [m] | 15.82 | 16.44 | 5.97 | --- | 0.00 | 27.42 | -0.31 |
| S [°] | 3.93 | 3.21 | 1.87 | 47.58 | 1.56 | 9.46 | 1.05 |
| A [°] | 87.33 | 78.82 | 28.17 | 32.26 | 40.37 | 166.38 | 1.23 |
| C-prof [0.01 m] | -0.03 | -0.02 | 0.20 | --- | -1.08 | 0.95 | -0.10 |
| C-plan [0.01 m] | -0.04 | -0.01 | 0.26 | --- | -1.27 | 0.72 | -1.05 |
| CA [m²] | 1568.91 | 868.15 | 2634.86 | 167.94 | 105.17 | 25612.13 | 5.45 |
| WI | 7.79 | 7.90 | 0.90 | --- | 5.73 | 11.00 | -0.03 |
| SPI | 20.67 | 7.15 | 41.19 | 199.27 | 0.68 | 325.99 | 4.28 |
| $E_{til}$ [mm $yr^{-1}$] | 0.02 | -0.16 | 1.49 | --- | -5.28 | 15.00 | 2.96 |
| $E_{wat}$ [mm $yr^{-1}$] | -0.50 | -0.23 | 0.66 | --- | -5.81 | -0.02 | -3.58 |
| $E_{tot}$ [mm $yr^{-1}$] | -0.47 | -0.44 | 1.30 | --- | -5.39 | 13.19 | 1.82 |

† SD: standard deviation; ‡ CV: coefficient of variation., which cannot be calculated for variables containing negative values or possessing a negative skewness coefficient (Isaaks and Srivastava, 1989);
§ Min: Minimum; ¶ Max: Maximum; †† SC: skewness coefficient.

Comparing the distributions of tillage and water erosion ($E_{til}$ and $E_{wat}$) derived from WaTEM/SEDEM clearly shows different spatial patterns of erosion and deposition resulting from these two processes, which agrees well with other studies (Govers et al., 1994; Van Oost et al., 2000). Areas with the steepest slopes have the highest water induced erosion rates resulting in an aggregated area of high erosion rates with values between -1.5 and -5.8 mm $yr^{-1}$ in the test site. This aggregated area corresponds well to the areas of high values of SPI indicating that these parameters represent similar processes. The rest of the test site is dominated by only slight water induced erosion rates with values between -1 and 0 mm $yr^{-1}$. No water induced deposition is calculated inside the test site, since WaTEM/SEDEM is not capable to model the backwater effect induced by landuse change at the outlet of the test site. Tillage induced erosion generally occurs on convexities and on the downslope side of field boundaries, whereas deposition occurs on concavities and on the upslope side of field boundaries (Govers et al., 1994; Van Oost et al., 2000). High tillage induced deposition rates with values ranging from 2 up to 15 mm $yr^{-1}$ occur in the thalweg area near the outlet of the test site, whereas highest erosion rates (-0.5 to -3.0 mm $yr^{-1}$) occur on the shoulders of the north-south-facing slope in the easterly part. The most pronounced difference between water and tillage erosion patterns can be found along the thalweg: here deposition by tillage counteracts with water induced erosion. The pattern of total erosion

($E_{tot}$) combines the two soil redistribution patterns. Most grid cells experiencing tillage induced deposition along the thalweg area are still depositing sites in the total erosion pattern.

**Relation between SOC and secondary parameters**

Among the primary terrain attributes, C-prof, C-plan and CA show significant linear relationships to SOC in all soil layers and in all input raster (Table 3). Correlation coefficients with C-prof and CA are always positive, whereas correlations with C-plan are always negative. Additionally, RE shows negative correlations with SOC in soil layer III for all raster widths. The SPI and the soil redistribution patterns based on water and tillage erosion modeling all significantly correlate with SOC in all soil layers and in all raster widths, whereas the WI is only significantly correlated with SOC in the two subsoil layers. Correlations between SOC and $E_{til}$ and $E_{tot}$, respectively, are positive in each soil layer and in each raster width indicating an accumulation of SOC in depositional sites and a loss of SOC on eroding sites. In contrast and unexpectedly, the water induced erosion pattern expressed by $E_{wat}$ and SPI results in a different picture: Here high modeled erosion rates by water correspond to high

**Table 3: Quality of correlation between SOC content [% kg kg$^{-1}$] and all calculated parameters in the three soil layers (I: 0-0.25 m; II: 0.25-0.5 m; III: 0.5-0.9 m) expressed as Pearson correlation coefficients; results are given for the three different raster widths ($R_{17}$, $R_{25}$, $R_{50}$) used as input for geostatistics; for abbreviations of parameters refer to Table 2.**

| | SOC $R_{17}$ ($n_I$ = 143 , $n_{II,III}$ = 144) | | | SOC $R_{25}$ (n = 76) | | | SOC $R_{50}$ (n = 28) | | |
|---|---|---|---|---|---|---|---|---|---|
| | I | II | III | I | II | III | I | II | III |
| RE [m] | -0.04 | -0.03 | -0.28$^{**}$ | -0.16 | -0.15 | -0.31$^{**}$ | -0.37 | -0.23 | -0.45$^{*}$ |
| S [°] | 0.13 | 0.03 | 0.14 | 0.22 | 0.15 | 0.28$^{*}$ | 0.26 | 0.15 | 0.37 |
| A [°] | 0.12 | -0.01 | 0.08 | 0.28$^{*}$ | 0.05 | 0.10 | 0.37 | -0.12 | 0.04 |
| C-prof [0.01 m] | 0.37$^{**}$ | 0.44$^{**}$ | 0.39$^{**}$ | 0.49$^{**}$ | 0.47$^{**}$ | 0.44$^{**}$ | 0.53$^{**}$ | 0.70$^{**}$ | 0.55$^{**}$ |
| C-plan [0.01 m] | -0.28$^{**}$ | -0.36$^{**}$ | -0.56$^{**}$ | -0.38$^{**}$ | -0.34$^{**}$ | -0.44$^{**}$ | -0.46$^{*}$ | -0.45$^{*}$ | -0.52$^{**}$ |
| CA [m²] | 0.19$^{*}$ | 0.27$^{**}$ | 0.67$^{**}$ | 0.36$^{**}$ | 0.46$^{**}$ | 0.66$^{**}$ | 0.48$^{**}$ | 0.51$^{**}$ | 0.65$^{**}$ |
| WI | 0.14 | 0.35$^{**}$ | 0.53$^{**}$ | 0.08 | 0.37$^{**}$ | 0.41$^{**}$ | 0.24 | 0.48$^{**}$ | 0.46$^{*}$ |
| SPI | 0.25$^{**}$ | 0.29$^{**}$ | 0.67$^{**}$ | 0.38$^{**}$ | 0.43$^{**}$ | 0.67$^{**}$ | 0.53$^{**}$ | 0.52$^{**}$ | 0.71$^{**}$ |
| $E_{til}$ [mm yr$^{-1}$] | 0.36$^{**}$ | 0.45$^{**}$ | 0.67$^{**}$ | 0.48$^{**}$ | 0.51$^{**}$ | 0.57$^{**}$ | 0.59$^{**}$ | 0.59$^{**}$ | 0.61$^{**}$ |
| $E_{wat}$ [mm yr$^{-1}$] | -0.22$^{**}$ | -0.25$^{**}$ | -0.53$^{**}$ | -0.25$^{*}$ | -0.32$^{**}$ | -0.50$^{**}$ | -0.51$^{**}$ | -0.45$^{**}$ | -0.68$^{**}$ |
| $E_{tot}$ [mm yr$^{-1}$] | 0.33$^{**}$ | 0.42$^{**}$ | 0.55$^{**}$ | 0.41$^{**}$ | 0.41$^{**}$ | 0.35$^{**}$ | 0.47$^{**}$ | 0.50$^{**}$ | 0.40$^{**}$ |

$^{*}$ significant at 95%, $^{**}$ significant at 99%.

SOC concentrations in each soil layer. This resulted from the counterbalancing effect of water and tillage erosion which in most cases lead to a net deposition considering both processes, while water erosion alone would lead to net erosion. Hence, it is misleading to use water erosion alone as covariable for any SOC interpolation scheme in agriculturally used landscapes.

In general, the linear relationship between SOC and the two indices as well as between SOC and the erosion/deposition patterns increases with increasing soil depth within each raster width. The same is true for the relationship between SOC and CA. This indicates (i) that relief driven processes play a less significant role in the topsoil layer where periodic management operations homogenize soil properties in agricultural areas and (ii) that more process-related terrain attributes such as CA, the two indices WI and SPI, and the patterns of soil redistribution play a more important role in the spatial distribution of soil organic carbon in the deeper soil layers. The correlation between SOC and water erosion (SPI and $E_{wat}$) as well as between SOC and tillage erosion ($E_{til}$) indicates the importance of erosion and deposition in the deeper soil layers. The increasing correlations of SOC with CA and WI with increasing soil depth indicate that also processes affecting soil moisture and infiltration influence the SOC patterns in these soil layers. The WI represents areas where water accumulates, and zones with higher WI values tend to have higher biomass production, lower SOC mineralization, and higher sediment deposition compared to zones of low WI (Terra et al., 2004).

In some respect our results disagree with other results where correlations between SOC and various primary terrain attributes could be found. Mueller and Pierce (2003) for example derived the highest correlation coefficients between SOC and elevation in three different raster widths for the topsoil layer. Other authors (e.g. Takata et al., 2007; Terra et al., 2004) also showed significant positive correlations with slope and/or CA and WI (e.g. Sumfleth and Duttmann, 2008; Terra et al., 2004).

## SOC kriging results

### *High density SOC input data*

In the three soil layers different combinations of theoretical variogram models and weighting methods performed best for the original SOC data. Theoretical variogram parameters (Table 4) show that the original SOC data of $R_{17}$ are moderately to highly spatially structured for all three soil layers with low nugget-to-sill ratios. Ranges are much larger than the raster width with a maximum value of 216 m for the SOC data in soil layer I, indicating that the sampling scheme used here accounts for most of the spatial variation of SOC in the three soil layers. The nugget variances comprising small scale variability as well as measurement errors are close to zero in all soil layers. Mean errors calculated from cross-validation for OK in each soil layer are close to zero indicating unbiased predictions (Table 4).

**Table 4: Theoretical semivariogram parameters of original SOC data and residuals resulting from linear regression with different covariables as well as cross-validation results from ordinary (OK) and regression kriging (RK) of SOC content [% kg kg$^{-1}$] in three soil layers (I: 0-0.25 m; II: 0.25-0.5 m; III: 0.5-0.9 m) using the 17.7 m raster data set ($R_{17}$) ($n_I$ = 159; $n_{II,III}$ = 160); RK results are included only when improving the prediction compared to OK; no covariable indicates OK; for exponential models the practical range is given; goodness-of-fit was tested using mean error (*ME*), root mean square error (*RMSE*), model efficiency (*MEF*), and relative improvement (*RI*). The subscript tr indicates that covariables were transformed to logarithms so that linear regression residuals meet normal distribution.**

| Soil layer | Covariable† | Theoretical semivariogram parameters | | | | | | Kriging results | | | |
|---|---|---|---|---|---|---|---|---|---|---|---|
| | | Model | Weights‡ | Nugget | Sill | Range [m] | Nugget/ Sill [%] | *ME* | *RMSE* | *MEF* | *RI* [%] |
| I | --- | exponential | equal | 0.013 | 0.034 | 216 | 40 | -0.001 | 0.123 | 0.45 | --- |
| | C-prof | exponential | equal | 0.008 | 0.023 | 113 | 33 | -0.002 | 0.115 | 0.53 | 6.50 |
| II | --- | exponential | $n_p l^{-2}$ | 0.000 | 0.054 | 40 | 0 | -0.002 | 0.196 | 0.23 | --- |
| | C-prof | exponential | $n_p l^{-2}$ | 0.000 | 0.038 | 28 | 0 | -0.001 | 0.192 | 0.26 | 2.04 |
| | C-plan | exponential | $n_p l^{-2}$ | 0.000 | 0.047 | 35 | 0 | -0.001 | 0.192 | 0.25 | 2.04 |
| | CA | exponential | $n_p l^{-2}$ | 0.000 | 0.051 | 35 | 0 | -0.002 | 0.194 | 0.24 | 1.02 |
| | WI | exponential | $n_p l^{-2}$ | 0.000 | 0.050 | 36 | 0 | -0.002 | 0.190 | 0.28 | 3.06 |
| | $E_{til}$ | exponential | $n_p l^{-2}$ | 0.000 | 0.039 | 28 | 0 | -0.002 | 0.187 | 0.29 | 4.59 |
| | $E_{wat}$ | exponential | $n_p l^{-2}$ | 0.000 | 0.050 | 37 | 0 | -0.002 | 0.195 | 0.24 | 0.51 |
| | $E_{tot}$ | exponential | $n_p l^{-2}$ | 0.000 | 0.040 | 29 | 0 | -0.002 | 0.187 | 0.29 | 4.59 |
| III | --- | spherical | $n_p$ | 0.013 | 0.044 | 64 | 30 | -0.002 | 0.145 | 0.53 | --- |
| | C-plan | spherical | $n_p$ | 0.011 | 0.030 | 64 | 37 | -0.001 | 0.139 | 0.57 | 4.14 |
| | $CA_{tr}$ | spherical | $n_p$ | 0.008 | 0.037 | 79 | 23 | -0.001 | 0.131 | 0.62 | 9.66 |
| | $WI_{tr}$ | spherical | $n_p$ | 0.010 | 0.041 | 87 | 24 | -0.002 | 0.130 | 0.62 | 10.35 |
| | $SPI_{tr}$ | spherical | $n_p$ | 0.009 | 0.037 | 73 | 25 | -0.000 | 0.136 | 0.59 | 6.21 |
| | $E_{til}$ | exponential | equal | 0.000 | 0.024 | 22 | 0 | -0.003 | 0.134 | 0.60 | 7.59 |
| | $E_{tot}$ | spherical | $n_p$ | 0.012 | 0.030 | 53 | 40 | -0.002 | 0.134 | 0.60 | 7.59 |

† For abbreviations of covariables refer to Table 2; ‡ Weighting of the semivariogram model is done by ordinary least squares (i.e. equal weights to all semivariances) and two weighted least square methods (weighting by $n_p$ = number of pairs and weighting by $n_p l^{-2}$ with $l$ = lag distance [m]).

Root mean square errors resulting from OK are 0.12, 0.20 and 0.15 % kg kg$^{-1}$ SOC for soil layers I, II, and III, respectively, corresponding to approximately 10, 28 and 44% of the mean SOC values in the different soil layers (Table 1). This indicates a loss of precision with increasing soil depth. In contrast, model efficiency (*MEF*) is highest in soil layer III (*MEF* = 0.53) and lowest in soil layer II (*MEF* = 0.23). The SOC maps derived from OK (Figure 4) represent well the spatial distributions of SOC in each soil layer which were already visible in the patterns of the measured SOC values at the sampling points (Figure 2).

Regarding the theoretical variogram parameters of the residuals resulting from linear regression with the different significantly related covariables in the three soil layers (Table 4), the same conclusions as for the original SOC data in each soil layer can be drawn. The residuals are moderately or even highly spatially structured, and ranges are larger than the raster widht.

The sill of the different residual variograms is reduced compared to the sill of the raw data in all soil layers reflecting the success of regression fitting (Hengl et al., 2004; Terra et al., 2004). Nugget variances are all close to zero.

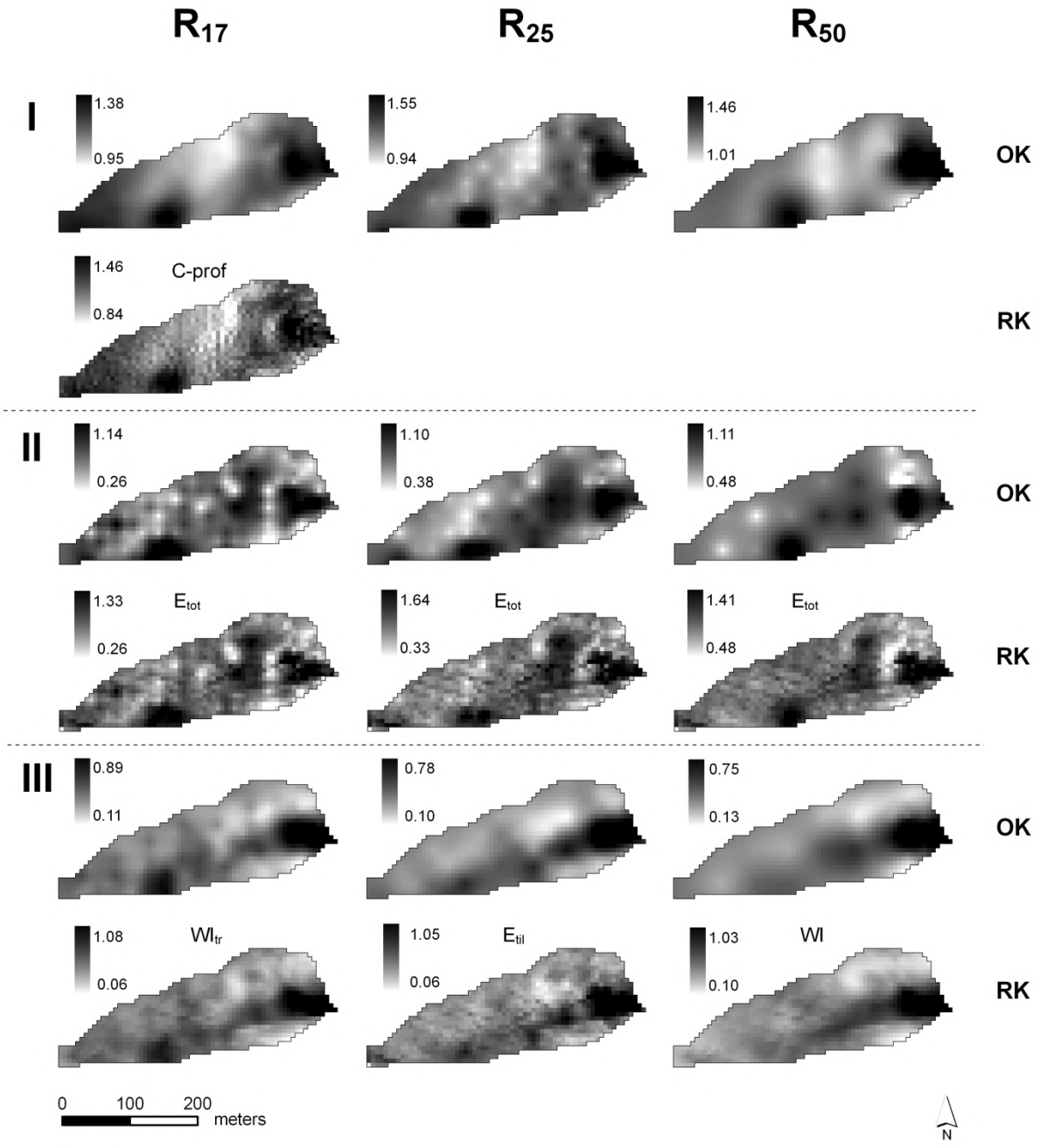


**Figure 4: Maps of SOC content [% kg kg$^{-1}$] for three soil layers (I: 0-0.25 m; II: 0.25-0.5 m; III: 0.5-0.9 m) resulting from ordinary (OK) and the best regression kriging (RK) approach using three different raster widths $R_{17}$ (17.7×17.7 m), $R_{25}$ (25×25 m) and $R_{50}$ (50×50 m) as input; covariables of the RK approaches are given above each map; for abbreviations of covariables refer to Table 2. The subscript tr indicates that covariables were transformed to logarithms so that linear regression residuals meet normal distribution**

In all three soil layers the geostatistical interpolation of SOC could be improved incorporating covariables in RK (Table 4). For soil layer I this was only one covariable, namely C-prof. For soil layer II C-prof, C-plan, CA, WI, and the three soil redistribution patterns derived from modeling were able to ameliorate interpolation results, and in soil layer III improvements were achieved by using C-plan, $CA_{tr}$, $SPI_{tr}$, $WI_{tr}$, $E_{til}$ and $E_{tot}$ as covariables in RK. Mean errors were still close to zero for all kriging approaches in all soil layers indicating unbiased predictions. Due to the high spatial density of the original SOC data relative improvements of the described RK approaches compared to OK were only low to moderate in all three soil layers. In soil layer II and III the integration of the more complex covariables outperformed that of the primary terrain parameters (Table 4). In general, spatial distributions resulting from the best RK approach in each soil layer (Figure 4) are similar to those derived from OK but show more small scale variability.

*Medium to low density SOC input data*

Although a minimum number of at least 50 better 100-150 sampling points is recommended for geostatistical analysis (Webster and Oliver, 2001), the theoretical semivariogram parameters of the SOC data and the values describing the goodness-of-fit for OK of the two reduced input raster widths $R_{25}$ (n = 92) and $R_{50}$ (n = 44) still show reasonable results in each soil layer (Table 5 and Table 6). As for the high density sampling grid ($R_{17}$) different combinations of theoretical variogram models and weighting methods performed best for the original SOC data. Nugget-to-sill ratios show that the primary SOC data in the two subsoil layers are highly spatially structured in case of both raster widths, and SOC data in the topsoil are moderately spatially dependent. This indicates that the low density sampling schemes are still suitable to resolve the spatial continuity of the original SOC data. For $R_{25}$ the ranges are larger than the raster width, only in soil layer II in $R_{50}$ this is not the case. But since the short distances formed by the transect and the two micro-plots were kept in each input raster, we assume that the results of the $R_{50}$ interpolation are still reasonable. Nugget and sill variances of the original SOC data tend to be in the same order of magnitude than in $R_{17}$ for each soil layer. Mean errors resulting from OK are still relatively low indicating unbiasedness, and relations of the root mean square errors to the mean values of the original SOC data also remain similar compared with the relations in $R_{17}$ for each soil layer. Model efficiency through OK is 0.23 ($R_{25}$) and 0.14 ($R_{50}$) in soil layer I and 0.01 ($R_{25}$) and 0.15 ($R_{50}$) in soil layer II. Higher values for OK are again reached in the deepest soil layer where a *MEF* of 0.34 ($R_{25}$) and 0.39 ($R_{50}$) can be found.

The interpolated SOC distributions resulting from OK with the medium and low input data sets (Figure 4) are smoothed compared to those using the high density input data set in each soil layer. But even with coarse sampling ($R_{50}$), there is still a pronounced area with high

**Table 5: Theoretical semivariogram parameters of original SOC data and residuals resulting from linear regression with different covariables as well as results from ordinary (OK) and regression kriging (RK) with SOC content [% kg $kg^{-1}$] in three soil layers (I: 0-0.25 m; II: 0.25-0.5 m; III: 0.5-0.9 m) using the 25 m raster data set ($R_{25}$) ($n$ = 92); the values describing the goodness-of-fit result from the comparison with a validation data set ($n$ = 67); RK results are included only when improving the prediction compared to OK; no covariable indicates OK; for exponential models the practical range is given; goodness-of-fit was tested using mean error (*ME*), root mean square error (*RMSE*), model efficiency (*MEF*), and relative improvement (*RI*). The subscript tr indicates that covariables were transformed to logarithms so that linear regression residuals meet normal distribution.**

| | | Theoretical semivariogram parameters | | | | | | Kriging results | | | |
|---|---|---|---|---|---|---|---|---|---|---|---|
| Soil layer | Covariable† | Model | Weights‡ | Nugget | Sill | Range [m] | Nugget/ Sill [%] | *ME* | *RMSE* | *MEF* | *RI* [%] |
| I | --- | exponential | Equal | 0.003 | 0.035 | 41 | 9 | -0.033 | 0.118 | 0.23 | --- |
| II | --- | exponential | $n_p l^{-2}$ | 0.000 | 0.052 | 40 | 0 | 0.058 | 0.226 | 0.01 | --- |
| | WI | exponential | $n_p l^{-2}$ | 0.000 | 0.050 | 37 | 0 | 0.049 | 0.217 | 0.09 | 3.98 |
| | $E_{til}$ | spherical | $n_p$ | 0.006 | 0.029 | 34 | 20 | 0.055 | 0.221 | 0.06 | 2.21 |
| | $E_{wat}$ | exponential | $n_p l^{-2}$ | 0.000 | 0.047 | 31 | 0 | 0.058 | 0.223 | 0.04 | 1.33 |
| | $E_{tot}$ | exponential | $n_p l^{-2}$ | 0.000 | 0.031 | 25 | 0 | 0.053 | 0.207 | 0.17 | 8.40 |
| III | --- | spherical | equal | 0.010 | 0.044 | 56 | 23 | 0.053 | 0.181 | 0.34 | --- |
| | C-plan | spherical | $n_p l^{-2}$ | 0.001 | 0.032 | 57 | 3 | 0.053 | 0.171 | 0.41 | 5.55 |
| | $CA_{tr}$ | spherical | equal | 0.006 | 0.040 | 65 | 16 | 0.048 | 0.159 | 0.50 | 12.15 |
| | $WI_{tr}$ | spherical | equal | 0.016 | 0.044 | 67 | 26 | 0.047 | 0.159 | 0.48 | 12.15 |
| | $SPI_{tr}$ | spherical | equal | 0.006 | 0.037 | 57 | 17 | 0.051 | 0.167 | 0.43 | 7.73 |
| | $E_{til}$ | exponential | $n_p l^{-2}$ | 0.000 | 0.027 | 53 | 0 | 0.054 | 0.158 | 0.50 | 12.71 |
| | $E_{wat}$ | spherical | equal | 0.013 | 0.037 | 66 | 35 | 0.053 | 0.172 | 0.40 | 4.97 |
| | $E_{tot}$ | spherical | equal | 0.015 | 0.034 | 70 | 44 | 0.050 | 0.159 | 0.49 | 12.15 |

† For abbreviations of covariables refer to Table 2; ‡ Weighting of the semivariogram model is done by ordinary least squares (i.e. equal weights to all semivariances) and two weighted least square methods (weighting by $n_p$ = number of pairs and weighting by $n_p l^{-2}$ with $l$ = lag distance [m]).

SOC concentrations in the east in all soil layers. The second region with high SOC values (southern edge and centre), however, is no longer detectable in the $R_{50}$-interpolation results for the deepest soil layer.

As was the case in $R_{17}$, nugget-to-sill ratios and the ranges of the various residuals for the different soil layers show a moderate to high spatial structure. Sills are also lower than for the original SOC data, and nuggets are close to zero.

In contrast to the use of the high resolution sampling grid $R_{17}$ as input data no improvements compared to OK were achieved in soil layer I by RK when using $R_{25}$ and $R_{50}$ (Table 5 and Table 6). In soil layer II RK including total erosion improved predictions best with $R_{25}$ and $R_{50}$ (*RI* = 8.4 and 6.2%, respectively). Relative improvements in soil layer III were even higher in the medium and low density raster than for soil layer II. In $R_{25}$ the spatial pattern of tillage erosion and in $R_{50}$ the wetness index WI performed best in improving RK results (Table 5 and 6).

In general, relative improvements in soil layer II and III referring to RK vs. OK were more pronounced in case of medium and low density compared to the high density input data. Moreover, SOC maps produced by RK in soil layer II and III with $R_{25}$ and $R_{50}$ (Figure 4) show considerably more detail and compare more favorably to the spatial patterns produced with $R_{17}$ input data. Although a direct comparison of the interpolation results with the different input raster widths is not possible due to a missing independent data set, it has to be recognized that a reduction of input data density seems to slightly decrease *MEF* and increase *RMSE* with decreasing data density.

Except for the high density input data, our results for the topsoil layer are in correspondence with Terra et al. (2004) who found that OK predicted SOC best compared to cokriging, regression kriging and multiple regression for the uppermost 30 cm and for three different densities of input data (8, 32 and 64 samples/ha). In contrast, other authors (Mueller and Pierce, 2003; Simbahan et al., 2006; Sumfleth and Duttmann, 2008) could improve the prediction of SOC in the topsoil layer by using (relative) elevation and electrical conductivity,

**Table 6: Theoretical semivariogram parameters of original SOC data and residuals resulting from linear regression with different covariables as well as results from ordinary (OK) and regression kriging (RK) of SOC content [% kg kg$^{-1}$] in three soil layers (I: 0-0.25 m; II: 0.25-0.5 m; III: 0.5-0.9 m) using the 50 m raster data set ($R_{50}$) ($n$ = 44); the values describing the goodness-of-fit result from the comparison with a validation data set ($n$ = 67); RK results are included only when improving the prediction compared to OK; no covariable indicates OK; for exponential models the practical range is given; goodness-of-fit was tested using mean error (*ME*), root mean square error (*RMSE*), model efficiency (*MEF*), and relative improvement (*RI*). The subscript tr indicates that covariables were transformed to logarithms so that linear regression residuals meet normal distribution.**

| | | Theoretical semivariogram parameters | | | | | | Kriging results | | | |
|---|---|---|---|---|---|---|---|---|---|---|---|
| Soil layer | Covariable† | Model | Weights‡ | Nugget | Sill | Range [m] | Nugget/ Sill [%] | *ME* | *RMSE* | *MEF* | *RI* [%] |
| I | --- | spherical | $n_p$ | 0.014 | 0.047 | 75 | 30 | -0.055 | 0.139 | 0.14 | --- |
| II | --- | exponential | $n_p l^{-2}$ | 0.000 | 0.060 | 48 | 0 | 0.015 | 0.210 | 0.15 | --- |
| | C-prof | exponential | $n_p l^{-22}$ | 0.000 | 0.019 | 15 | 0 | 0.015 | 0.206 | 0.18 | 1.90 |
| | $E_{til}$ | spherical | $n_p$ | 0.011 | 0.029 | 48 | 41 | 0.019 | 0.202 | 0.20 | 3.81 |
| | $E_{tot}$ | spherical | $n_p$ | 0.012 | 0.029 | 50 | 40 | 0.015 | 0.197 | 0.25 | 6.19 |
| III | --- | spherical | $n_p$ | 0.007 | 0.071 | 79 | 10 | 0.046 | 0.174 | 0.39 | --- |
| | WI | spherical | $n_p$ | 0.010 | 0.070 | 75 | 14 | 0.028 | 0.149 | 0.55 | 14.37 |
| | $E_{til}$ | spherical | $n_p$ | 0.012 | 0.045 | 76 | 27 | 0.041 | 0.158 | 0.49 | 9.20 |
| | $E_{tot}$ | spherical | equal | 0.018 | 0.050 | 84 | 36 | 0.040 | 0.162 | 0.47 | 6.90 |

† For abbreviations of covariables refer to Table 2; ‡ Weighting of the semivariogram model is done by ordinary least squares (i.e. equal weights to all semivariances) and two weighted least square methods (weighting by $n_p$ = number of pairs and weighting by $n_p l^{-2}$ with $l$ = lag distance [m]).

respectively, as covariables in regression kriging and/or kriging with external drift. Their studies show that the sampling density plays an important role for improving the performance of geostatistics when incorporating covariables. E.g. Mueller and Pierce (2003) also used three different input raster widths in their test site. For their high resolution input raster with a density of 10.7 samples/ha they also found only modest differences between the applied interpolation techniques, but for their two reduced raster widths (2.7 and 1 sample/ha) different interpolation methods incorporating covariables could outperform OK. This was also true for the three test sites of Simbahan et al. (2006) with sampling densities of 2.5 to 4.2 samples/ha. Our result of no or only slight improvements in the first soil layer might be caused by (i) our high sampling densities (37.9, 16.9, and 6 samples/ha), (ii) homogenization effects of management, and (iii) the area of high SOC concentrations at the southern boundary of the test site which is most pronounced in the topsoil. This area cannot be deduced to relief driven processes, and in combination with homogenization is thus leading to relatively low correlations between SOC and the various parameters in the topsoil layer.

In contrast, considerable improvements of RK over OK in our study were achieved in the two subsoil layers. In soil layer II this improvement was highest when using the patterns of tillage or total erosion as covariable in RK. This indicates that especially tillage induced erosion and deposition processes affect the SOC distribution in this layer. This makes it necessary to not only consider water induced soil redistribution processes, which are already represented in other primary and secondary terrain attributes (CA and SPI) used here and in other studies. Relative patterns of tillage erosion and deposition can easily be derived with well tested and relatively simple erosion and sediment delivery models like the WaTEM/SEDEM model. To implement the tillage erosion component only a DEM and an estimation of the tillage transport coefficient are required (Van Oost et al., 2000).

Although the tillage and total erosion pattern could also significantly improve SOC prediction in the deepest soil layer in all three raster widths, comparable and in some instances even better results were produced by RK with CA and WI. This indicates that not only soil redistribution processes affect the spatial distribution of SOC in the deepest soil layer but also processes concerning the spatial distribution of infiltration and soil moisture. Both processes may increase SOC contents in the thalweg area due to (i) infiltration and absorption of dissolved organic carbon (DOC) and (ii) limited mineralization of SOC in case of high soil moisture contents.

In contrast to the topsoil layer in the two subsoil layers improved SOC interpolations can actually be obtained when using a high density of input data for RK. This is possibly caused by higher spatial variations of SOC in these soil layers, expressed as coefficient of variation (Table 1).

Our results indicate that SOC patterns in different soil layers can be linked to different processes. Whereas the topsoil pattern is homogenized by tillage operations, the patterns of the subsoil layers are more pronounced and driven by soil redistribution and moisture / infiltration differences. Patterns of topsoil SOC distribution might be dissimilar to subsoil layers particularly in hilly agriculturally used areas. Thus, estimating total SOC pools from topsoil SOC, for instance by applying remote sensing techniques (e.g. Stevens et al., 2008), is not be appropriate.

## CONCLUSIONS

Factors and processes affecting the spatial distribution of soil layer specific SOC in a hilly agricultural catchment were analyzed, while correlating measured SOC data with primary terrain parameters, combined indices as well as spatial patterns of soil redistribution derived from modeling. In general, Pearson correlation coefficients showed that the linear relationship between SOC and the more process-related indices and erosion/deposition patterns was higher than between SOC and relatively simple terrain parameters. Correlation coefficients increased with increasing soil depth indicating that relief driven processes in the small catchment play a less significant role in the topsoil layer, where periodic agricultural management practices homogenize soil properties.

To produce detailed and precise maps of the SOC distribution in the three soil layers, the performance of OK and RK with the significantly correlating parameters was tested using three input raster widths with decreasing sampling density. Results showed that especially in the subsoil layers the geostatistical interpolation of SOC could be improved, when covariables were incorporated. In the mid soil layer (0.25-0.5 m) the best result was produced by RK with the patterns of tillage and total erosion, indicating the importance of soil redistribution (especially the inclusion of tillage erosion) for the spatial distribution of SOC in agricultural areas. In the third soil layer (0.5-0.9 m) tillage and total erosion as well as the wetness index and partly the catchment area performed best. This indicates that besides soil redistribution also processes concerning the distribution of soil moisture affect the spatial pattern of SOC in the deepest soil layer. In general, relative improvements of RK vs. OK increased with increasing soil depth and with reduced sampling density. Hence, the expectable decline in interpolation quality with decreasing data density can be reduced for the subsoil layers integrating results from soil redistribution modeling and spatial patterns of soil moisture indices as covariables in RK.

In general, it could be shown that (especially) an integration of patterns in soil redistribution in kriging approaches, can substantially improve SOC interpolation of subsoil data in hilly arable landscapes. This is an important finding insofar as high resolution subsoil SOC

data are rare and most promising data improvements due to new remote sensing techniques are limited to topsoil SOC.

# 6. THE EFFECT OF SOIL REDISTRIBUTION ON SOIL ORGANIC CARBON: AN EXPERIMENTAL STUDY

In review for Biogeosciences
H. Van Hemelryck, P. Fiener, K. Van Oost, and G. Govers. 2009.
The effect of soil redistribution on soil organic carbon: an experimental study.
Biogeosciences Discussions 6: 5031-5071.

***ABSTRACT.*** *Soil erosion, transport and deposition by water drastically affect the distribution of soil organic carbon (SOC) within a landscape. Furthermore, soil redistribution is assumed to have a large impact on the exchange of carbon (C) between the pedosphere and the atmosphere. There is, however, significant scientific disagreement concerning the relative importance of the key-mechanisms at play. One of the major uncertainties concerns the fraction of SOC that is mineralized when soil is eroded by water, from the moment when detachment takes place until the moment when the SOC becomes protected by burial. In this study, the changes in C-exchange between soil and atmosphere as affected by soil redistribution processes were experimentally quantified. During a laboratory experiment, three types of erosional events were simulated, each of which was designed to produce a different amount of eroded soil material with a different degree of aggregation. During a 98-day period, $CO_2$-efflux was measured in-situ and under field conditions on undisturbed soils with a layer of deposited soil material. Depending on the initial conditions of the soil and the intensity of the erosion process, a significant fraction of eroded SOC was mineralized after deposition (between 14 and 22%). However, results also suggest that deposition produces a dense stratified layer of sediment that caps the soil surface, leading to a decrease in SOC decomposition in deeper soil layers. As a result, the net effect of erosion on SOC can be smaller, depending on the functioning of the whole soil system. In this study, soil redistribution processes contributed an additional emission of 2 to 12% of total C contained in eroded sediment.*

Soil erosion, transport and deposition by water and tillage drastically affect the distribution of soil organic carbon (SOC) within a landscape (Ritchie and McCarty, 2003; Zhang et al., 2006). Furthermore, soil redistribution is assumed to have a large impact on the exchange of carbon (C) between the pedosphere and the atmosphere, through its influence on both input rates of C to the soil and changes in decomposition of SOC (Gregorich et al., 1998; Harden et al., 1999; Lal, 2003; Liu et al., 2003; Smith et al., 2005; Stallard, 1998; Van Oost et al., 2007; Yoo et al., 2005). Three key mechanisms could be identified, which can alter the flux of C between the soil and the atmosphere: (i) Dynamic replacement: at eroding sites, the depleted SOC pool can, at least partially, be replaced by newly assimilated C (Harden et al., 1999). Continued C input and a decrease in SOC available to decomposition can

lead to a net gain of C at these sites. (ii) Burial of topsoil SOC and reduced decomposition: as suggested by Stallard et al. (1998), the rate of decomposition of SOC in depositional settings can be reduced due to a combination of physical and chemical processes, such as increased soil wetness, limited aeration, compaction and physical protection of the deposited soil material within newly formed aggregates (De Gryze et al., 2007; Gregorich et al., 1998), leading to a preservation of buried C. (iii) Transport and increased decomposition: the disruptive energy of forces applied to the soil by water erosion (raindrop impact, the shearing force of flowing water and collision with other aggregates), may cause the breakdown of aggregates (Lal, 2003). This process of disaggregation exposes previously protected SOC to microbial decomposition and combined with a relatively greater proportion of labile SOC within larger soil aggregates (Six et al., 2000) could lead to rapid mineralization of this easily decomposable C following water erosion.

It must also be noted that part of the eroded SOC is transported to distal environments and fluvial systems. It's fate, however, is still largely unclear though recent research suggests that even old SOC may become mineralized when transported in water (Cole and Caraco, 2001).

Concerning the relative importance of the above-mentioned key mechanisms there is, however, significant scientific disagreement. Together with a lack of process knowledge, opposing assumptions hamper an accurate estimation of the impact of soil redistribution on the terrestrial carbon balance (Berhe et al., 2007). Notwithstanding this ongoing debate, it is generally agreed that the soil system potentially plays a major role in controlling atmospheric carbon dioxide concentrations (Amundson, 2001). Globally, the soil reservoir stores approximately 2344 Pg C in the top 3 meters (1502 Pg C in the first meter) (Jobbagy and Jackson, 2000). Even a small additional relative flux to/from this system as a result of increased storage/respiration of SOC through soil erosion, could substantially affect soil carbon storage and atmospheric $CO_2$ concentrations. Attempts to globally assess this effect by linking carbon dynamics to soil erosion and deposition patterns resulted in the assertion of a net sink of up to 1.5 Pg C $yr^{-1}$ (Smith et al., 2005; Stallard, 1998) as well as a net source of 1.1 Pg C $yr^{-1}$ (Lal, 2003). More recently, and based on an integrated study of the different, simultaneously occurring processes and their interactions, an erosion-induced sink of 0.12 Pg C $yr^{-1}$ on global agricultural land was proposed (Van Oost et al., 2007).

One of the major uncertainties concerns the fraction of SOC that is mineralized when soil is eroded by water, from the moment when detachment takes place until the moment when the SOC becomes protected due to burial (Lal, 2003), and this is the major focus of this study.

Published estimates of this fraction are often indirectly obtained and vary widely. Based on the distribution of soil organic matter components along an eroded soil catena, Beyer et al. (1993) estimated 70% of the non-humin fraction of soil C in colluvial material to be decomposed during translocation or shortly after deposition. Jacinthe et al. (2001) compared SOC inventories and quality of SOC on cropland and adjacent depositional zones. The pools of labile C in the deposits (on average 9% of total SOC) were 20 to 46% lower than expected. The latter could be interpreted as the result of mineralization of labile C pools during transport and deposition. When combining inventories of SOC and erosion tracers from a wide range of agricultural soils to derive evidence for erosion-induced carbon dynamics, Van Oost et al. (2007) concluded that losses of C associated with transport are relatively minor and that most deposited C is effectively preserved.

The few experimental studies, in which estimates of eroded C mineralization are supported by direct quantitative data, neither succeed to provide a unique answer. Jacinthe et al. (2002) measured the $CO_2$-efflux from incubated samples of runoff, generated during simulated rainfall events on different small soil blocks. Despite large differences in sediment delivery rate and initial soil C content, a consistent 31 to 37% of total eroded C was found to be potentially mineralizable. Polyakov et al. (2004) subjected five soil plots, positioned at different slopes and connected in a cascade fashion, to simulated rainfall. Subsequently, $CO_2$-efflux from undisturbed soil samples taken on erosion and deposition plots was measured during an incubation experiment. On the soil samples with deposition, 15% of the deposited C mineralized during the experiment, resulting in a 26% higher emission of $CO_2$, compared to the control sites. There was no significant difference in mineralization of C between the eroded soil samples and the control soil samples. Jacinthe et al. (2004) incubated runoff samples collected during a one-year period at the outlet of small watersheds under cultivation. Mineralizability of eroded C, proved to be dependent on the rainstorm type, generating the runoff and varied from 30-40% for low-energy rainstorms, to only 13% during high-intensity storms.

Thus, relatively few data are available with respect to the mineralization of SOC as affected by erosion, transport and subsequent deposition. Moreover the estimates thus far show considerable variation. Various factors explain the ambiguities: first of all, the mineralizable fraction of eroded SOC often is estimated as the potentially mineralizable C, measured during an incubation of soil samples. An alternative would be to measure effective in-situ mineralization under field conditions. Furthermore, different things are measured: while in some studies, measurements were done on disturbed runoff samples, intact soil samples are used in others. Experimental and field conditions also vary widely and the effects of variations in initial soil conditions and/or erosion intensity are not well understood. It may be hypothe-

sized that the degree of aggregate disruption during erosion and transport plays an important role in subsequent SOC mineralization (Jacinthe et al., 2004).

The main objective of this study is therefore to experimentally quantify the changes in C exchange between soil and atmosphere as affected by erosion in case of different initial soil conditions and erosion rates used to simulate typical agricultural erosion events.

## MATERIALS AND METHODS

### Experimental Design

Three types of simulation experiments were conducted, each of which was designed to produce a different amount of eroded soil material and different levels of aggregation. For each type of simulation experiment, 2 replicates were performed. An overview of the experimental set-up is presented in Figure 1. The eroded sediment was deposited in a depositional area. These depositional areas consisted of 2.25 m long, 0.61 m wide and 0.25 m deep soil trays set at zero slope. The trays were filled with 0.22 m of soil taken from the top 0.15 m soil layer of an arable field close to Leuven, Belgium. The soil is a typical silt loam of the Belgium Loess Belt with average sand, silt and clay content of respectively 20%, 73% and 7% and an average SOC content of 1.52%. To fill the trays as homogeneously as possible, the used soil was air-dried and sieved at 0.02 m before filling. To reach a bulk density comparable to that of arable land, the depositional trays were filled in layers of ca. 0.03 m. Each layer was similarly moistened and compacted to obtain an average dry bulk density of $1.39\times10^{6}$ g $m^{-3}$. The bottom of the tray was perforated, to allow drainage, and covered with a water permeable textile to avoid clogging of the percolation holes with soil material. In total, six depositional areas were prepared for the experimental runs and two as additional control soil beds.

In general, sediment input into the depositional areas was produced with two set-ups. On the one hand, a clear water flow was applied over an erosion flume (2.32 m long x 0.60 m wide x 0.24 m deep, set at 15º slope), connected at its lower edge to the depositional tray and filled with 0.18 m of soil, analogously to the depositional areas. The surface runoff water was supplied from a small overflow basin at the upslope end of the flume equipped with a flow control device to ensure a fixed inflow discharge (Figure 1a). On the other hand, a homogeneous mixture of soil and water was pumped directly onto the depositional area (Figure 1b).

In detail, the following three experimental procedures were used:

(i) One set of two replicate runs was carried out after filling the erosion flume with moistened soil material over which a clear water flow was applied (wet soil runs, abbreviated

WSR). Using a relatively high inflow discharge, rill flow conditions, optimal for unselective erosion of aggregated sediment, were simulated (Beuselinck et al., 2000). The high initial moisture content of the soil greatly enhanced the erosion resistance of the loamy soil, likely resulting in a decreased sediment production on the erosion flume (Govers et al., 1990).

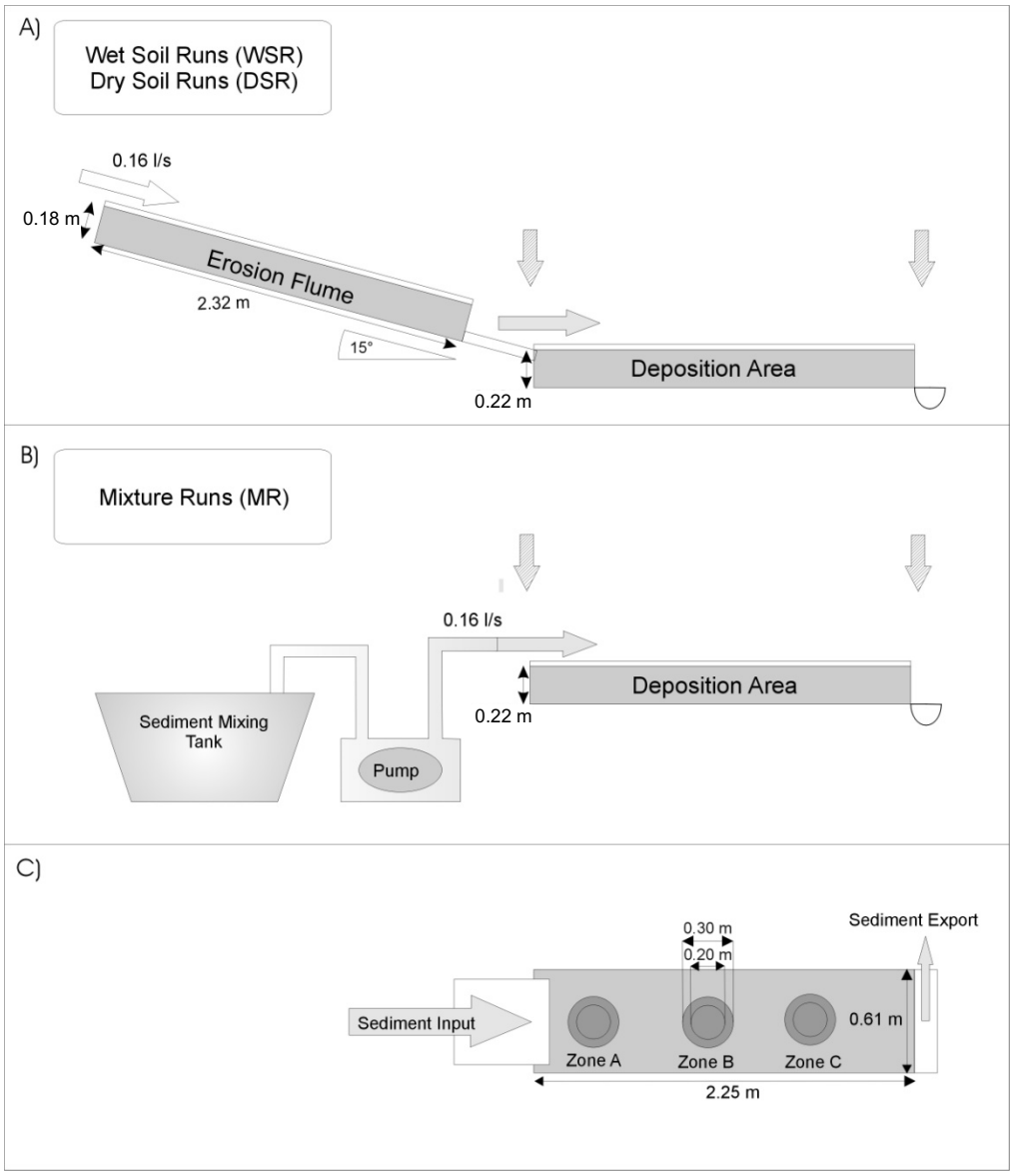


**Figure 1: Schematic side-view diagram of experimental set-up for the three types of simulation experiments: a) wet soil runs (WSR), dry soil runs (DSR) and b) mixture runs (MR). c) Top view diagram of the depositional area with deposition zones A, B and C and location of inner and outer PVC rings, extracted for $CO_2$-efflux measurements. Vertical arrows in a) and b) indicate runoff sampling locations.**

(ii) In a second set of two runs, the same procedure as for the WSR was used with the exception that the center section of the erosion flume (2.32 m long, 0.15 m wide and 0.08 m deep) was filled with air-dried soil rather than moistened soil (dry soil runs, abbreviated DSR). Upon rapid wetting, slaking of some dry soil aggregates, i.e. breakdown due to com-

pression of air entrapped within the aggregates, is assumed to occur (Kemper et al., 1985; Le Bissonnais, 1996). Subsequently the resultant soil material is more easily entrained by the water flow leading to higher erosion rates in the erosion flume and consequently higher deposition rates in the depositional area (Govers, 1991).

(iii) During the last pair of runs, a homogeneous mixture of soil and water, with a sediment concentration of 150 kg $m^{-3}$ was prepared in a 0.8 $m^3$ mixing tank and pumped directly into the depositional area (mixture runs, abbreviated MR). Continuous mixing of the water and sediment using a centrifugal pump ensured that aggregates were largely destroyed prior to the experiment. As such, this set-up simulated interrill flow, transporting detached primary soil particles after aggregate breakdown by raindrop impact or dispersion in water (Di Stefano and Ferro, 2002). For practical reasons, the MR was conducted 50 days after the WSR and DSR.

All experimental runs lasted 15 min., except for the WSR, which lasted 30 min. in order to create a sufficient amount of deposition, despite the low erosion rates. During all runs, an inflow discharge of about $1.6\times10^{-4}$ $m^3$ $s^{-1}$ was used.

The set-ups of the experiments as described above, closely resembled different agricultural erosion events, typical for the region of Belgium (Steegen, 2001).While the DSR simulated a typical summer erosion event after a period of drought, the MR reproduced a winter event after prolonged rainfall broke down soil aggregates to a great extent. The WSR were intermediate between DSR and MR, representing an erosion event in case of a moist and well-structured soil.

**Measuring sediment and SOC delivery and sampling of deposition**

In order to calculate the fluxes of sediment and SOC through the system, 200-800 ml runoff samples were collected at the in- and outlet of the depositional area at regular time intervals (every 4 min. during WSR, every 2 min. during DSR and MR).

After each experimental run, the depositional area was divided into three zones (A, B, C) along the direction of the water flow with zones A and C closest to the inlet and the outlet of the depositional area, respectively (Figure 1c). In each zone and in the control soils, a cylindrical sample of the topsoil (0.05 m depth, 100 $cm^3$) was taken to determine the soil dry bulk density.

Next, an inner and an outer PVC ring were inserted into the deposited sediments and the original soil bed of all depositional zones (A, B and C), thereby carefully avoiding disruption of the soil structure. The outer ring (Ø 0.3 m) was inserted to the bottom of the deposition tray and created a buffer zone around the inner ring (Ø 0.2 m), which was introduced to a

depth of 0.1 m. Next, the rings and the undisturbed soil cores within, were carefully excavated and transferred to a sand box with an adjustable water table, to allow the soil cores to drain and equilibrate to constant soil moisture content (Figure 2a). Using a similar procedure, three undisturbed soil cores were sampled from the control soil beds without deposition.

The inner rings were later on used to measure $CO_2$-efflux during a consecutive 98-day period. After the $CO_2$-efflux measurement period, the soil cores were sliced up longitudinally so that the thickness of the sediment deposit could be determined (Figure 2b). Next the deposited soil was sampled carefully, in order not to include any soil material from the original soil bed.

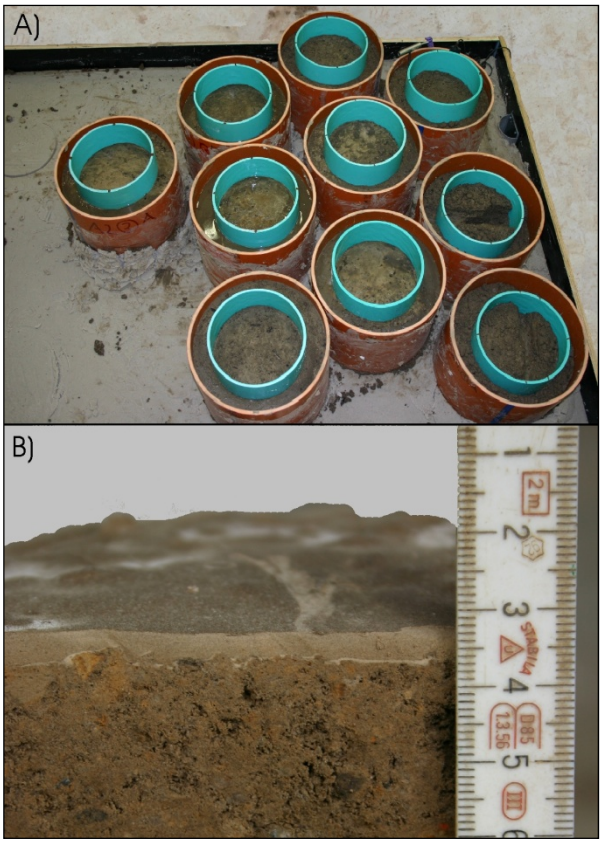


**Figure 2: a) Sand box with undisturbed soil cores from deposition zones. b) Cross-section of soil core, sampled after the mixture runs with a 0.5 cm deposition layer clearly visible on top of the original soil bed.**

### Sediment and SOC laboratory analyses

All soil samples (from parent soil, deposited sediment and collected runoff) were oven-dried at 45º C for three days. The runoff samples were weighed to determine the sediment concentration. Dried samples were ground with a mortar and pestle. The grain-size distribution of the deposited sediment was determined using a Coulter Counter LS 13 320 laser diffraction particle size analyzer (Beckman Coulter, USA). To determine SOC concentration an ANCA 20-20 GSL mass spectrometer (Sercon Ltd, UK) was used.

### Calculation of sediment and SOC mass balances

The amount of deposited sediment and SOC can be calculated in two distinct ways. In a first method (M1), a sediment mass balance is computed as the difference between the in- and output of sediment in the depositional area. The input (output) of sediment in/from the depositional area was calculated as the area under the curve of sediment discharge at the inlet (outlet) of the depositional area (further abbreviated as sediment inflow and sediment

outflow, respectively) during an experimental run. The mass of SOC, deposited in the depositional area, was similarly calculated as the difference between the time-integrated product of sediment discharge and SOC concentration at the inlet and outlet of the depositional area.

In a second method (M2), the amount of deposited sediment and SOC can in principle be calculated by extrapolating the mass of deposited sediment and SOC, contained within the extracted PVC rings, to the whole depositional area. As this method was based on the results of measurements on soil samples, taken at the end of the $CO_2$-efflux measurements (98 days), the thus estimated amount of SOC in the deposited sediment has to be considered the SOC, remaining after 98 days of $CO_2$-efflux measurements. Concerning the estimated amount of sediment, it can be assumed that no sediment moved from the depositional area during the $CO_2$-efflux measurements. Using M2, we however need to account for the fact that the distribution of deposited sediment as well as SOC was spatially non-uniform. The volume of the deposited sediment layer on an undisturbed soil core, excavated from zone A, B or C in the depositional area, was estimated based on five measurements of the deposition layer thickness. In the depositional area, the eroded sediment was deposited in a wedge-shaped layer, as runoff was constrained within the sidewalls of the deposition tray. Therefore the estimated volume of deposited sediment per unit area for one soil core could be assumed to approximate the average volume of deposited sediment per unit area in the rectangular zone (A, B or C) centered around this soil core. The total mass of deposited sediment in the depositional area was then calculated as:

$$M = \sum_{i=A,B,C} \frac{sedVol_{ring,i}}{A_{ring}} \times A_i \times BD_i \qquad (1)$$

where $M$ is the total mass of sediment deposited in the depositional area [g], $sedVol_{ring,i}$ is the estimated volume of the deposited sediment within a PVC ring, sampled from zone A, B or C, $A_{ring}$ is the area of the upper surface of a PVC ring, $BD_i$ is the soil dry bulk density in zone A, B or C and $A_i$ is the surface area of the rectangular zone A, B or C.

Based on the sample location of the undisturbed soil cores, the lengths of the rectangular zones A, B and C were 0.57, 0.57 and 1.11 m respectively. The width of all rectangular zones was equal to the width of the depositional tray (0.61 m).

Next the mass of deposited sediment calculated using M2, was compared with the mass of deposited sediment calculated using M1. If the mass of deposited sediment, as calculated by both methods, differed by more than 5%, the surface area of zones A, B and C was slightly altered until the recalculated mass of deposited sediment in M2 matched the mass of

deposited sediment according to M1. Total deposited SOC, still present after the $CO_2$-efflux measurements, was then calculated as the product of the mass of deposited sediment in zones A, B and C and the SOC concentration in the layer of deposited sediment within the corresponding soil rings. This calculation methodology furthermore allows for an estimation of the distribution of deposited sediment and SOC (after $CO_2$-efflux) along the flow direction in the depositional area. The two independent estimates of SOC in the deposited sediment before and after 98 days of $CO_2$-efflux measurements can be evaluated in function of the measured cumulative $CO_2$-efflux.

**Measuring $CO_2$-efflux, soil temperature and moisture**

$CO_2$-efflux, soil temperature and soil moisture were measured on the undisturbed soil cores, sampled in the zones of the depositional area of each replicated experimental run, after they were placed on a sand box for drainage. Additionally, measurements were carried out on three, identical undisturbed soil cores sampled from a reference soil without deposited sediment. These undisturbed soil cores were used as controls to determine the effects of sediment deposition on $CO_2$-efflux. Measurements on WSR, DSR and control soil cores were carried out for 98 days, while for technical reasons the MR were shifted by 50 days and hence measurements on MR soil cores only lasted 48 days.

The sand box with the soil cores was initially placed inside the laboratory, where diurnal air temperature variations were limited. 77 days after conducting the wet and dry soil runs (or 27 days after conducting the mixture runs), the sand box was placed outside, under a shed, for 21 more days. Exposed to wind and varying outside temperature conditions, the soil cores were allowed to dry out.

During the measurement period, $CO_2$-efflux, temperature and moisture were measured at increasing time intervals (from two times daily to twice a week). Measurements were always performed in the late afternoon. $CO_2$-efflux from the inner soil core was monitored using a LI-COR 8100-103 survey chamber (Ø 0.2 m) and a LI-COR LI-8100 infrared gas analyzer (LI-COR, USA). Temperature and volumetric moisture content of the soil cores were measured, with a TESTO 110 soil thermometer (TESTO, Belgium) and a 0.16 m, two-rod time domain reflectometry, TRIME-EZ probe, connected to a TRIME-HD display device (Imko GmbH, Germany), respectively.

The cumulative $CO_2$-efflux on all soil cores was approximated as an area under the curve (AUC) over the measurement period. For comparison reasons, the cumulative $CO_2$-efflux, evolved from MR-soil cores over the course of the 27-day measurement period inside the laboratory, was linearly extrapolated over a 77-day period, as this was the measurement period for WSR, DSR and control soil cores. Inside the laboratory, diurnal temperature varia-

tion was limited and hence measured $CO_2$-effluxes should well represent the daily average $CO_2$-efflux. For the 21 days of measurements in open air, however, the afternoon measurements of $CO_2$-efflux most likely represent an overestimate of the daily average $CO_2$-effluxes.

### Statistical analysis of $CO_2$-efflux, soil temperature and moisture

The effect that the amount of deposited sediment and its degree of aggregation has on variations in $CO_2$-efflux, soil temperature and soil moisture, was examined using a repeated measures ANOVA with PROC MIXED in SAS 9.1 software (SAS Institute Inc., USA). Each simulation experiment (WSR, DSR and MR) and each zone in the depositional area (A, B and C) was considered a different 'treatment' of a reference soil by adding a layer of deposited sediment of certain thickness and varying degree of aggregation. The measurements on the undisturbed soil cores, sampled on similar locations in the depositional area after the two experimental runs, were considered as replicates. The repeated measures ANOVA allows for the comparison of 'treatments' averaged over time as well as for the detection of any time trends. In addition to a univariate ANOVA, repeated measures analysis accounts for the correlation over time between measurements on one soil core (Hedeker and Gibbons, 2006; Littell et al., 1998). As such it was possible to detect any statistically significant difference in the measured $CO_2$-efflux, soil temperature and soil moisture between undisturbed soil core samples from the three different simulation experiments and/or zones of the depositional area.

The analyses were conducted separately on the measurements inside and outside the laboratory as measurements are influenced differently by varying environmental conditions between both periods. Statistical comparison of the measurements on the MR soil cores versus measurements on the DSR and WSR soil cores was done, assuming that all experimental runs were conducted on the same day. However, for clarity reasons, in all graphs of measurements versus time, results were plotted relative to the day on which WSR and DSR were conducted (defined as day 0). For all statistical tests, statistical significance was accepted at $p \leq 0.05$. All values in this paper are reported as mean ± SE, unless otherwise stated.

## RESULTS

### Runoff of sediment and SOC

Runoff from the erosion flume (only during WSR and DSR) began on average two minutes after initiation of the water flow at the upslope end of the flume. Two minutes after runoff generation, the sediment-laden water reached the end of the depositional area.

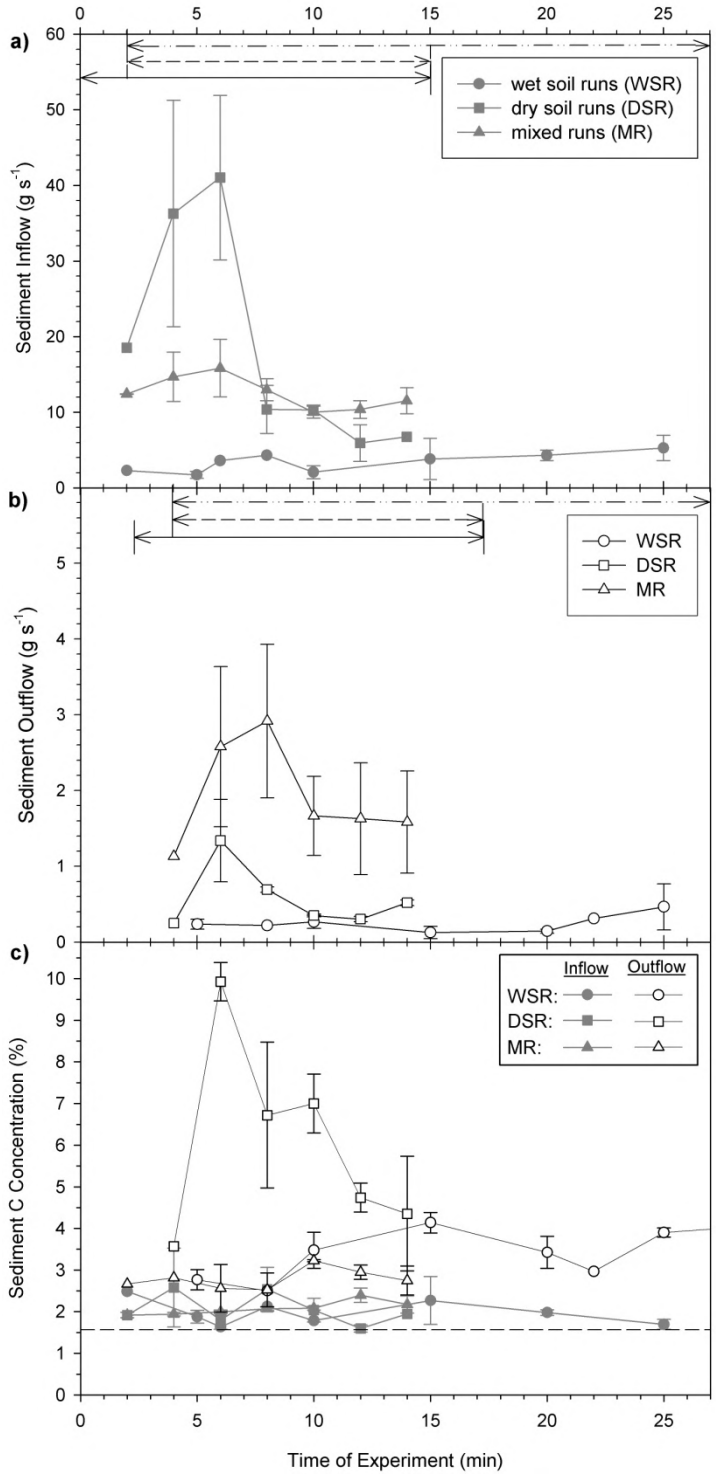


**Figure 3: a) Sediment inflow (g $s^{-1}$), defined as sediment discharge measured at the inlet of the depositional area for the three simulation experiments (average of replicate runs). b) Sediment outflow (g $s^{-1}$), defined as sediment discharge measured at the outlet of the depositional area for the three simulation experiments (average of replicate runs). c) Sediment carbon concentration (%) in runoff at the inlet (gray) and outlet (white) of the depositional area for the three simulation experiments (average of replicate runs). The dashed line marks the average carbon concentration in the original soil. The arrows in a) and b) mark the duration of runoff for each experiment: WSR (dot-dashed), DSR (dashed), MR (full line). Error bars indicate the standard error of the mean.**

The controlled inflow discharge remained fairly constant ($1.60 \pm 0.02 \times 10^{-4}$ $m^3$ $s^{-1}$) throughout all experimental runs. The steady-state outflow discharge averaged over all experimental runs amounted to $1.20 \pm 0.20 \times 10^{-4}$ $m^3$ $s^{-1}$, with the higher variability between experimental runs probably resulting from differences in soil moisture content of the depositional soil beds before the simulation experiment. The average runoff ratio for the depositional areas in these experiments was therefore $0.70 \pm 0.07$.

Sediment inflow and sediment outflow varied distinctly within and between experimental runs (Figure 3a). During the WSR experiments, sediment loss from the erosion flume was low and relatively constant throughout the duration of the experimental runs (average sediment inflow of 4.2 g $s^{-1}$). A small rill incised in the erosion flume soil bed and gradually extended upslope, mainly by back-cutting from the outlet of the erosion flume. In contrast to this gradual erosion process, the measured sediment inflow was high during the first 7 minutes of the DSR experiments (average sediment inflow of 34.6 g $s^{-1}$) but decreased for the remainder of the dry soil experimental runs to an average sediment inflow of 8.3 g $s^{-1}$. These measurements are consistent with the observation of the rapid washing out of the air-dried soil from the centre section of the erosion flume in the beginning of these experiments. During the MR experiments, a homogeneous mixture of dispersed soil and water was pumped directly into the deposition area with a controlled inflow discharge. This resulted in a relatively constant initial sediment inflow (average sediment inflow of 13.8 g $s^{-1}$ during the first 7 minutes of the experiments). The slight decrease in sediment inflow for the second half of the experimental runs (average sediment inflow of 10.6 g $s^{-1}$), most probably was due to the settling of the largest sediment particles in the mixing tank.

Sediment outflow (Figure 3b) during the WSR (average 0.22 g $s^{-1}$) and DSR (average 0.59 g $s^{-1}$) was 20- to 30-fold lower than the sediment inflow. This implied that the bulk of the eroded soil material was deposited on the depositional soil bed. In case of the MR, sediment settling in the depositional area was less effective due to the dispersed nature of the sediment. This resulted in an average sediment outflow of 1.93 g $s^{-1}$, only 6-fold lower than the sediment inflow.

Throughout all experimental runs, eroded sediment, entering and leaving the depositional area, was enriched in organic carbon, relative to the source soil (Figure 3c). This enrichment is expressed by the SOC enrichment ratio ($ER_{SOC}$), defined as the ratio of C content of the eroded soil to that of the source soil. The average $ER_{SOC}$ of sediments entering the depositional area was fairly constant ($1.32 \pm 0.05$). Sediments leaving the depositional area were even more enriched in SOC, with enrichment ratios of $2.30 \pm 0.10$, $4.74 \pm 0.53$ and $1.72 \pm 0.28$ for WSR, DSR and MR respectively.

**Mass of deposited sediment and SOC**

The results of the mass calculations are summarized in Table 1 and Table 2. The amount of sediment, deposited in the depositional area, was lowest during the WSR ($5.66\times10^3$ g), resulting from both low sediment in- and outflow (Figure 3). Roughly 2.5 times more sediment was deposited ($1.47\times10^4$ g) during the DSR, as high sediment inflow and concurrent low sediment outflow resulted in the deposition of the bulk of a large amount of eroded sediment. During the MR, despite the high sediment inflow, only an intermediate amount of sediment was deposited ($9.32\times10^3$ g). During the WSR and DSR, the bulk of the eroded sediment was deposited upon entering the depositional area and the amount of deposition decreased rapidly towards the depositional area outlet. During the MR, the mass of deposited sediment also decreased along the direction of the flow, although much less pronounced as during the WSR and DSR. The above-mentioned patterns of erosion, deposition and export were reflected in the sediment delivery ratio (SDR). While most of the eroded sediment was retained in the depositional area during the WSR and DSR (SDRs of 7.6% and 3.0% respectively), sediment settling in the depositional area was distinctly less effective during the MR (SDR of 17.2%).

**Table 1: Sediment mass balance of the depositional area for the three simulation experiments.**

| SEDIMENT MASS BALANCE | Wet Soil Runs (WSR) | | Dry Soil Runs (DSR) | | Mixed Runs (MR) | |
|---|---|---|---|---|---|---|
| Total Deposition – M1 [g] | 5662 | (± 446) | 14692 | (± 1319) | 9317 | (± 457) |
| Deposition per Unit Length – M2 [g $cm^{-1}$] | | | | | | |
| Zone A | 78.9 | (± 1.4) | 230.0 | (± 39.9) | 89.6 | (± 3.7) |
| Zone B | 11.6 | (± 2.2) | 40.8 | (± 10.9) | 38.6 | (± 0.4) |
| Zone C | 4.7 | (± 0.8) | 13.3 | (± 7.3) | 28.5 | (± 0.3) |
| Sediment Delivery Ratio – M1 [%] | 7.6 | (± 1.8) | 3.0 | (± 0.4) | 17.2 | (± 0.1) |

The average SOC concentration in the deposited sediment, calculated from the balance between SOC in- and outflow, amounted to a steady 1.86 ± 0.08%. Consequently, for all experimental runs, the mass of deposited SOC was proportional to the mass of deposited sediment (Table 2). For the WSR and DSR, no apparent enrichment or depletion in SOC could be observed between the zones of the depositional area. After the MR, however, sediment deposited at the inlet of the depositional area was clearly depleted in SOC, while the sediment at the area outlet was enriched in SOC. The SOC delivery ratios for the WSR and DSR were two (14.0%) and three (10.7%) times as high as their respective sediment delivery ratios, while with a SOC delivery ratio of 21.9%, the SOC enrichment of the outflow during the MR was less pronounced. After 98 days of $CO_2$-efflux measurements, the mass of SOC

in the deposited sediment, as calculated by M2, had decreased by 20% and 14% for WSR and DSR respectively. For the MR, a decrease of 22% was observed after only 48 days of $CO_2$-efflux.

**Table 2: SOC mass balance of the depositional area for the three simulation experiments.**

| SOC MASS BALANCE | Wet Soil Runs (WSR) | | Dry Soil Runs (DSR) | | Mixed Runs (MR) | |
|---|---|---|---|---|---|---|
| Total Deposition M1 [g] | 103 | (± 16) | 267 | (± 14) | 181 | (± 18) |
| Total Deposition M2 [g] | 66 | (± 22) | 229 | (± 22) | 140 | (± 11) |
| Deposition per Unit Length – M2 [g $cm^{-1}$] | | | | | | |
| Zone A | 1.17 | (± 0.02) | 4.00 | (± 1.49) | 0.38 | (± 0.10) |
| Zone B | 0.15 | (± 0.01) | 0.62 | (± 0.15) | 0.79 | (± 0.10) |
| Zone C | 0.07 | (± 0.01) | 0.20 | (± 0.09) | 0.69 | (± 0.03) |
| SOC Delivery Ratio – M1 [%] | 14.0 | (± 4.4) | 10.7 | (± 1.2) | 21.9 | (± 3.5) |

The dispersed grain-size distribution of the deposited sediment complements the above analysis of soil redistribution. The sediment deposited in zone A during the WSR and DSR was texturally similar to the original soil material, although slightly coarser (4% more sand). Further along the flow path (zone B and zone C), the deposited sediment was entirely enriched in silt (+12%) and depleted in sand (-12%). The dispersed grain-size distribution of the sediment deposited during the MR, was identical in all zones with a substantial enrichment in fine particles (13% depletion in sand and 12% more silt).

### Effects of soil temperature and moisture on $CO_2$-efflux

Soil temperature and soil moisture are frequently identified as dominant factors, controlling the $CO_2$-efflux (Davidson et al., 1998; Smith et al., 2003). Therefore a prior analysis of these environmental variables was mandatory to dissociate their influence from any erosional effect on $CO_2$-efflux.

During the first 56 days after conducting the WSR and DSR, the soil temperature remained rather constant on all soil cores (15.11 ± 0.04 ˚C, 15.15 ± 0.05 ˚C and 15.42 ± 0.07 ˚C respectively for soil cores from WSR, DSR and control soils without deposition). Next, a sudden substantial increase in solar insolation and outside air temperature (+10 ˚C), led to a warming of all soil cores by ca. 2.8 ˚C. This warmer period coincided with the start of measurements on soil cores from the MR experiments. This, consequently, limited the distinction between the effect of warmer soil temperatures and any erosional effect for the

MR. Therefore, a first analysis included only measurements on WSR, DSR and control soil cores during the first 56 days of the measurement period.

A repeated measures ANOVA of soil temperatures for this period revealed a significant interaction effect ($p = 0.021$) between experiment (WSR, DSR and control soil cores) and time (56 days of measurements inside the laboratory) (Table 3). Soil temperatures increased by 1.6 °C on average during the first 15 days after conducting the experiment and remained almost constant thereafter. Comparison at individual time points, however, revealed a more pronounced temperature increase on control soil cores, resulting in an overall significant temperature difference of 0.3 °C between WSR and DSR soil cores on the one hand and control soil cores on the other hand.

**Table 3: Repeated measures ANOVA of soil temperature for the initial period inside the laboratory (left: analysis of WSR, DSR and control soil cores during 56 days of measurements) and outside the laboratory (right: analysis of WSR, DSR, MR and control soil cores during 21 days of measurements). (Num DF: Numerator degrees of freedom; Den DF: denominator degrees of freedom).**

| Source of Variation | Soil Temperature (inside) | | | | Soil Temperature (outside) | | | |
|---|---|---|---|---|---|---|---|---|
| | Num DF | Den DF | F | P-value | Num DF | Den DF | F | P-value |
| Experiment | 2 | 26.1 | 10.25 | 0.0005 | 3 | 24 | 5.58 | 0.0047 |
| Time | 23 | 196 | 258.76 | <0.0001 | 4 | 69.4 | 144.02 | <0.0001 |
| Time x Experiment | 46 | 196 | 1.55 | 0.0211 | 12 | 69.4 | 2.83 | 0.0033 |

When the soil cores were moved to the open air after 77 days, the depositional layers quickly started to dry out while cracks formed on the surface. Repeated measures ANOVA for the outside period, revealed a significant interaction effect ($p = 0.003$) for soil temperature between experiment and time (Table 3). In the open air, the soil temperatures varied with air temperature (Figure 4) and were on average higher than inside the laboratory (16.90 ± 0.20 °C, 16.30 ± 0.42 °C, 16.78 ± 0.43 °C and 17.30 ± 0.48 °C for WSR, DSR, MR and control soil cores, respectively). Soil cores from DSR were somewhat colder (between 0.5 °C and 1.0 °C) than other soil cores, although the difference was only statistically significant for warmer days.

The, initially high, volumetric moisture contents (average 39.0 ± 0.6%) decreased considerably during the week following the experimental runs and equilibrated at 31.9 ± 0.3% for the remainder of the measurement period inside the laboratory (Figure 4). For soil moisture, no interaction ($p = 0.23$), nor experiment effect ($p = 0.22$) was found for the measurements taken in the laboratory after WSR and DSR experiments (Table 4).

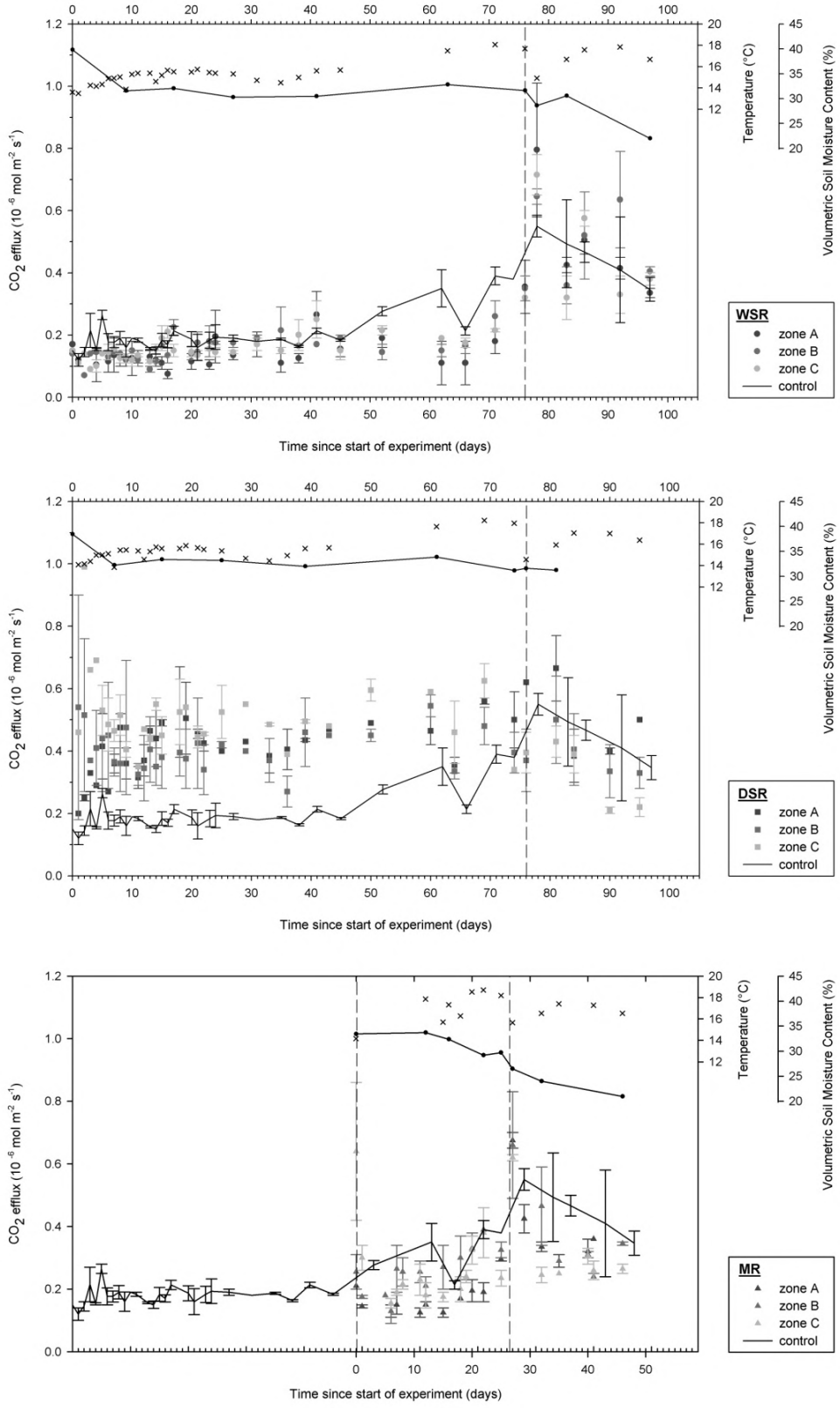


**Figure 4: $CO_2$-efflux per experiment and per zone of the depositional area (zone A, B and C). The black line connects measurements of $CO_2$-efflux on control soil cores. Soil temperature (°C, crosses) and volumetric soil moisture content (%) per experiment. The rightmost dashed vertical line marks the time at which soil cores were relocated to the outside of the laboratory.**

**Table 4: Repeated measures ANOVA of soil moisture for the period inside the laboratory (left: analysis of WSR, DSR and control soil cores during 56 days of measurements) and outside the laboratory (right: analysis of WSR, DSR, MR and control soil cores during 21 days of measurements). (Num DF: Numerator degrees of freedom; Den DF: denominator degrees of freedom).**

| Source of Variation | Soil Moisture (inside) | | | | Soil Moisture (outside) | | | |
|---|---|---|---|---|---|---|---|---|
| | Num DF | Den DF | F | P-value | Num DF | Den DF | F | P-value |
| Experiment | 2 | 48 | 1.58 | 0.2158 | 3 | 51 | 14.77 | <0.0001 |
| Time | 3 | 48 | 14.05 | <0.0001 | 2 | 51 | 6.53 | 0.003 |
| Time x Experiment | 6 | 48 | 1.41 | 0.2301 | 6 | 51 | 4.03 | 0.002 |

Upon exposing the soil cores to wind and outside air temperatures, the soil started to dry, although at different rates depending on experiment. A significant time by experiment interaction effect was found (Table 4, $p = 0.002$). After 7 days in the open air, the average moisture content amounted to 30.6 ± 1.0%, 31.2 ± 0.7% and 32.2 ± 1.4% for WSR, DSR and control soil cores respectively but only 24.0 ± 0.4% for MR soil cores.

Thus, during the first 56 days of measurements inside the laboratory, volumetric soil moisture content was similar for all soil cores and was rather constant in time. Soil temperature differences, although significant, were small and not likely to conceal any erosional effects. During the 21 measurement days in open air, soil temperature and moisture were variable in time, depending on weather conditions. Again, no clear significant differences among soil cores were observed, except for the MR soil cores, which dried quickly in open air. Given that conditions were completely different inside and outside the laboratory, further analyses of $CO_2$-efflux were performed separately for both periods.

### $CO_2$-efflux

During the initial measurement period (the first 56 days after conducting the experimental runs), the average $CO_2$-efflux amounted to 0.15 ± 0.01, 0.43 ± 0.02 and 0.18 ± 0.01× $10^{-6}$ mol $CO_2$-C $m^{-2}$ $s^{-1}$ for WSR, DSR and control soil cores respectively (Figure 4). A repeated measures ANOVA of $CO_2$-efflux measurements (Table 5) revealed a significant effect of experiment ($p = 0.0001$). A post-hoc Tukey test for pair wise comparison indicated that, overall, $CO_2$-efflux was significantly higher on soil cores, taken after the DSR experiments, compared to $CO_2$-efflux from WSR and control soil cores ($p < 0.0001$). Despite a significant effect of time, average $CO_2$-fluxes were mostly steady, with larger variability only during the initial measurements on DSR soil cores. No significant difference could be

observed between soil cores, sampled in different zones of the depositional area and thus characterized by various amounts of deposition.

**Table 5: Repeated measures ANOVA of $CO_2$-efflux for the period inside the laboratory (left: analysis of WSR, DSR and control soil cores during 56 days of measurements) and outside the laboratory (right: analysis of WSR, DSR, MR and control soil cores during 21 days of measurements). (Num DF: Numerator degrees of freedom; Den DF: denominator degrees of freedom).**

| Source of Variation | $CO_2$-efflux (inside) | | | | $CO_2$-efflux (outside) | | | |
|---|---|---|---|---|---|---|---|---|
| | Num DF | Den DF | F | P-value | Num DF | Den DF | F | P-value |
| Experiment | 6 | 8.49 | 20.02 | 0.0001 | 9 | 47 | 1.85 | 0.0847 |
| Time | 20 | 89.7 | 3.77 | <0.0001 | 4 | 47 | 4.85 | 0.0023 |
| Time x Experiment | 120 | 91.7 | 1.29 | 0.1006 | 36 | 47 | 6.86 | <0.0001 |

As mentioned previously, the soil temperature of all soil cores increased by an average of 2.8 ˚C, after 56 days of measurements. $CO_2$-efflux increased in subsequent days, with the largest increase measured on control soil cores (+ $0.12\times10^{-6}$ mol $CO_2$-C $m^{-2}$ $s^{-1}$ on average) compared to WSR and DSR (+ 0.03 and + $0.07\times10^{-6}$ mol $CO_2$-C $m^{-2}$ $s^{-1}$ on average, respectively). This period with higher soil temperatures also coincided with the beginning of measurements on MR soil cores. The initial $CO_2$-efflux on MR soil cores ($0.22 \pm 0.01\times10^{-6}$ mol $CO_2$-C $m^{-2}$ $s^{-1}$) was intermediate between the initial $CO_2$-efflux on WSR and DSR soil cores. However, there is a large probability that the $CO_2$-efflux was biased by the higher soil temperatures. Noteworthy is the lower than average $CO_2$-efflux on MR soil cores sampled in zone A, close to the inlet of the depositional area ($0.15 \pm 0.01\times10^{-6}$ mol $CO_2$-C $m^{-2}$ $s^{-1}$) as compared to an average value of $0.25 \pm 0.02\times10^{-6}$ mol $CO_2$-C $m^{-2}$ $s^{-1}$ on zone B and C soil cores.

Upon relocating the soil cores out of the laboratory, a pulse of high $CO_2$-efflux was observed on most of the soil cores with deposited sediment. In the subsequent days, $CO_2$-efflux was quite variable and presumably controlled by the interplay between changing soil temperatures and decreasing soil moisture content. A repeated measures ANOVA (Table 5) revealed an interaction effect ($p < 0.0001$) between experiment and time. Overall, no significant differences between soil cores from different experiments and/or zones could be detected. Average fluxes were highest on WSR and control soil cores ($0.44 \pm 0.03$ and $0.44 \pm 0.05\times10^{-6}$ mol $CO_2$-C $m^{-2}$ $s^{-1}$, respectively) compared to DSR soil cores $CO_2$-efflux ($0.39 \pm 0.03\times10^{-6}$ mol $CO_2$-C $m^{-2}$ $s^{-1}$) and MR soil cores $CO_2$-efflux ($0.31 \pm 0.02\times10^{-6}$ mol $CO_2$-C $m^{-2}$ $s^{-1}$). The latter lower fluxes resulted from $CO_2$-efflux on zone C soil cores, being smaller

than those on zone A and B soil cores, though not statistically significant at all individual time points.

After standardizing the $CO_2$-efflux of the MR experiment to the total time period of 77 days, when measurements were done inside the laboratory, an estimated amount of 12, 35, 15 and 12 g $CO_2$-C $m^{-2}$ was respired respectively from the WSR, DSR and MR depositional area and a control soil of equal surface area. For the whole of the measurement period (inside and outside the laboratory), these estimates amounted to 24, 45, 24 and 21 g $CO_2$-C $m^{-2}$ respectively. Thus, for the 98-day measurement period of this experiment, deposition contributed to an additional emission, relative to the control soil cores, of 4, 12 and 2% of total C, contained in the deposited sediment, for WSR, DSR and MR respectively. These values are considerably lower than the estimated decrease of SOC in the deposited sediment, calculated as the difference in mass of deposited SOC before and after the experiment. This implies that high losses of SOC from the deposited sediment are compensated for by lower mineralization rates in the underlying original soil.

## DISCUSSION

### Characterization of the erosion and deposition patterns

The experimental set-up was designed to obtain different patterns of deposition with different characteristics of the deposited sediment, in terms of aggregate distribution, SOC content and its availability to decomposition. As such, the experiments simulated the seasonal variability of erosion and deposition events, typical for the Belgian Loess belt. The characteristics of the deposited sediment are the result of the interplay between the processes of erosion and deposition. During the former, selective entrainment of fine and less dense soil particles is controlled by the transport capacity of the overland flow (Beuselinck et al., 2000; Schiettecatte et al., 2008) while conversely, heavy and coarse soil particles are likely to be deposited early. The soil can also be eroded, transported and deposited in aggregated form (Beuselinck et al., 2000; Meyer et al., 1992; Schiettecatte et al., 2008) while these soil aggregates can possibly disintegrate progressively along their pathway (Le Bissonnais, 1996). Soil organic carbon is redistributed according to the redistribution of soil particles and depending on its availability: as loose soil organic matter, adhered to sediment particles or encapsulated within soil aggregates. As such the eroded soil becomes enriched or, conversely, depleted in SOC in the course of the erosion and deposition processes, resulting in a distinct redistribution pattern of sediment and SOC (Di Stefano and Ferro, 2002).

The differences in the amount of measured sediment and SOC deposition between the experiments (Table 1 and Table 2) are in agreement with the objectives of the different experimental set-ups, used to create variations in erosion rate. The high initial moisture content of

the soil in the erosion flume during the WSR, impeded the entrainment of large amounts of soil particles, while conversely, during the DSR, slaking of the dry soil aggregates in the erosion flume resulted in soil particles susceptible to water erosion and consequently high erosion rates. As larger soil aggregates are found to contain a relatively larger portion of more labile soil organic matter (Six et al., 2000), it could be hypothesized that this break-down of soil aggregates during the DSR, resulted in the prompt exposure of previously encapsulated SOC, which there upon became available to decomposition.

From the resemblance of the dispersed grain-size distribution of sediment in the WSR and DSR to the texture of the original soil, it can be assumed that, during above-named experiments, the bulk of the eroded and transported soil was deposited in aggregated form upon entering the depositional area. The residual smaller aggregates, enriched in silt, and loose soil particles were deposited towards the outlet of the depositional area. Still, Beuselinck et al. (2000) argued that it is plausible that a significant portion of fine soil particles can be trapped between larger soil aggregates and contra-intuitively could be deposited in zone A as well. From the grain-size distribution of the dispersed sediment deposited during the MR, it could be hypothesized that, despite pump-mixing, larger sand grains settled to the bottom of the mixing tank before deposition. Upon entering the depositional area a slight sorting effect could be observed with gradual enrichment of sediment deposits in clay-sized particles and particularly SOC, towards the outlet of the depositional area. Nonetheless, during all experiments, the C enrichment ratios, measured at the inlet of the depositional area, were higher than 1 and hint at a slight preferential transport of finer soil particles, which are primarily bound to SOM.

The degree of aggregation of the eroded sediment can also explain for the observed difference in sediment and SOC delivery ratios between the experiments (Table 1 and Table 2). During the WSR and DSR, the bulk of the eroded soil in aggregated form could not be transported to the outlet. Only a small fraction of probably very fine soil particles, highly enriched in SOC, was exported from the depositional area. However, when the sediment was more dispersed during the MR, the rather large SDR and SOC delivery ratio evidenced the export of a significant portion of fine-sized soil particles and OC. Low SDRs, well below 20%, are not unlikely in a field situation (Steegen et al., 2001). The latter also implies that it is very important to study SOC dynamics in depositional areas.

**$CO_2$-efflux as influenced by erosion and deposition**

The range of measured $CO_2$-effluxes in this study ($0.04 - 1.34\times10^{-6}$ mol $CO_2$-C $m^{-2}$ $s^{-1}$) is comparable to measured soil respiration rates of mineral, agricultural soils, reported in the

**Table 6: Comparison of this study with three other experimental studies**

| | Jacinthe et al. (2002) | Jacinthe et al (2004) | Polyakov et al. (2004) | This Study | | |
|---|---|---|---|---|---|---|
| **Description of study set-up** | Measurements of mineralizable C in incubated runoff samples, collected during rainfall simulation (60 min, 30 mm $hr^{-1}$) experiments on small soil blocks (0.45 m x 0.30 m x 0.03 m). Soil blocks were taken on three fields with different tillage treatments (no-till, chisel-till and moldboard plow). | Measurement of mineralizable C in incubated runoff samples, collected from May 2001 to May 2002 at the outlet of five small (0.79 - 1.1 ha) watersheds under different management practices (no-till, chisel-till, disk-till, pasture, forest). Measurements of mineralizable C were compared across energy classes of the rainfall causing the runoff. | Laboratory rainfall experiment (90 min, 80 mm $hr^{-1}$), simulating erosion and deposition on five small soil plots (1.00 m x 0.30 m x 0.03 m) with different slopes, connected in cascade fashion as an imitation of a hillslope profile. Measurement of mineralization of C from undisturbed soil cores taken on erosional, depositional and control sites. | **WSR** | **DSR** | **MR** |
| C content source soil [%] | 0.94 | 1.76 | 1.79 | | 1.52 | |
| SOC enrichment ratio of eroded soil | 1.98 | 1.26 | 1.38 | | 1.32 | |
| Basal soil respiration [g $CO_2$-C $kg^{-1}$ soil] | 0.03 – 0.19 | 0.36 | 0.34 | | 0.11 | |
| Mineralization of eroded SOC | | | | | | |
| [% of eroded SOC] | 40 | 16 – 42 | / | / | / | / |
| [% of eroded SOC, additionally mineralized, relative to a control soil] | / | / | 17 | 4 | 12 | 4 |

literature (see Raich et al. (1995) for a global dataset and e.g. Lohila et al. (2003), Bajracharya et al. (2000) and Tufekcioglu et al. (2001) for specific case studies). In addition, the results of this study were compared with those of three other experimental studies (Jacinthe et al., 2002; 2004; Polyakov and Lal, 2004), specifically addressing the impact of erosion and deposition processes on SOC decomposition (Table 6). It can be seen that the basal soil respiration, expressed as 100-day $CO_2$-efflux of an undisturbed soil (in g $CO_2$-C $kg^{-1}$ soil), was also, only slightly different between the various studies. Thus, our laboratory measurements yield realistic values of $CO_2$-efflux and we may therefore have some confidence that our results are applicable to field conditions.

In Figure 5, the amount of SOC, initially deposited in the depositional area (M1), is compared to the sum of the cumulative $CO_2$-C efflux and the mass of SOC in the deposited sediment at the end of the $CO_2$-efflux measurements (M2). It was found that these SOC mass balances before and after the experiment were very similar for all experiments, i.e. the sum of the SOC still present in the deposited sediments after the experiments and the respired $CO_2$-C were very similar to the amount of SOC that was initially deposited. The latter suggests that the measured $CO_2$-C originated to a large extent from the decomposition of SOC in the deposited sediment.

In general, no differences in $CO_2$-efflux were observed between the different zones in the depositional area within the same experiment (except for zone A during the MR). As the amount of deposited sediment differed distinctly between the different zones in the depositional area, the above suggests that the $CO_2$-efflux does not strongly depend on the amount of deposited sediment and that SOC decomposition, contributing to the measured $CO_2$-efflux, mainly takes place in the uppermost layer of the deposited sediments.

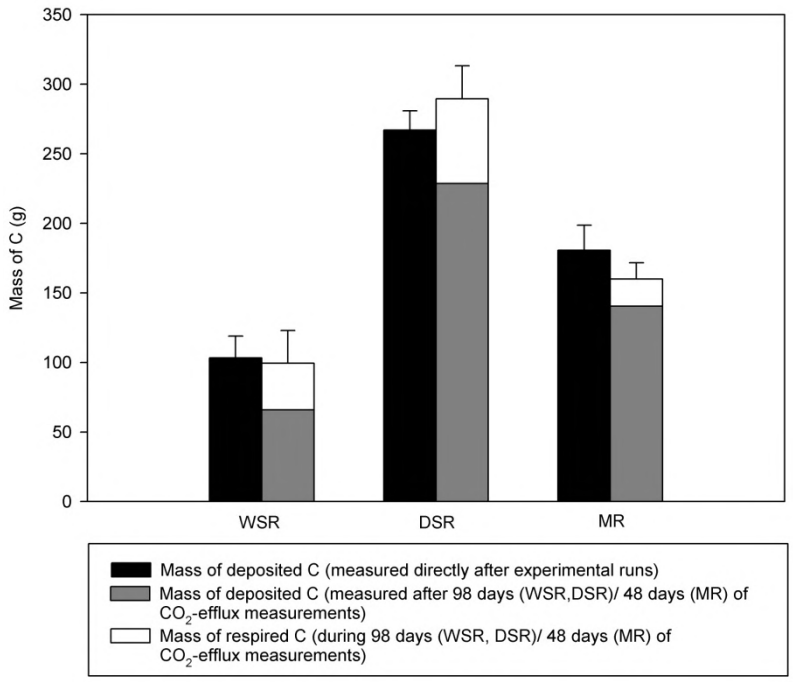


**Figure 5: Comparison between the mass of deposited C, directly after the experimental runs (M1) and the sum of the mass of respired $CO_2$.**

Other studies on well-structured soil profiles have shown that significant SOC mineralization can take place at greater depths (Fierer et al., 2003; Tang et al., 2003). However, observations suggest that deposition produces a dense stratified layer of sediment that caps the soil surface (Fox et al., 1998). This will limit gas (and oxygen) diffusion in the soil profile and ultimately result in a decrease of SOC decomposition at greater depths (Schjonning et al., 2003). The above hypothesis however, is not supported by abundant empirical evidence and thus requires further study.

Our analysis shows that the deposition of eroded sediment indeed led to a significant additional $CO_2$-efflux towards the atmosphere during the DSR experiments. This can be attributed to the strong mechanical disruption of dry soil aggregates by slaking upon wetting, leading to the exposure of previously protected SOC and the deposition of significant amount of soil material. However, it should be pointed out that slaking did not lead to a complete disruption of aggregate structure: from grain-size distribution and SDR, it could be argued that the soil is mainly transported and deposited as micro-aggregates, a phenomenon earlier described by Beuselinck et al. (2000). During the WSR experiments, we did not observe a significant increase of $CO_2$-efflux: during these experiments, soil disruption was much less intense. Aggregates were transported and deposited in more or less intact form. Hence, no major effect on $CO_2$-efflux should be expected. During the MR, the additional $CO_2$-efflux was also comparatively small. At first sight this is unexpected, given the fact that mechanically dispersed soil material was used: a possible explanation for this minor effect is that a large fraction of the potentially mineralizable SOC was exported from the depositional area, leaving a more stable SOC fraction at the soil surface in the deposited sediments. Our data thus confirm the findings of Jacinthe et al. (2004): the effect of erosion on SOC mineralization may depend considerably on the type of erosion event and the soil conditions at the moment when erosion occurs.

The fraction of eroded SOC that was rapidly mineralized after deposition (< 100 days) varied between 14 and 22%. These amounts are comparable to those reported in other studies, often with a completely different design (Table 6). At first sight, these findings imply that erosion and deposition may indeed lead to a significant release of SOC to the atmosphere, thereby contradicting the findings of Van Oost et al. (2007).

However, expressed as the additional $CO_2$-efflux relative to a control soil, the net effect of erosion on SOC is much smaller (between 2 and 12%). The most likely explanation for this finding is that the presence of a thick depositional layer hampers mineralization below the top layer, which is compensated for by an increased $CO_2$-efflux from the deposition layers and this to a different extent, depending on the conditions in the experiment. This finding shows that, when the overall effect of erosion is to be assessed, one cannot solely focus on

the properties of the deposited sediments. The presence of the latter appear to affect the functioning of the whole soil system, so part of the mineralization of SOC within the deposited layer is offset by a decrease in mineralization deeper within the soil profile. Our results should therefore be compared to those reported by Polyakov and Lal (2004), who incubated intact soil cores with layers of deposited sediment and estimated 16% of eroded and redeposited C to be additionally susceptible to mineralization.

**Implications for field-scale C-fluxes**

The implications of the results of this study for field-scale C-fluxes are difficult to determine because of the simplification of the experimental system compared to a real world situation where variations in temperature, moisture as well as additional effects of plant growth, field management, etc. can be expected. Nevertheless, as experimental conditions (SOC enrichment, amount of deposition and measured SDR) were representative for field conditions, a tentative extrapolation of the results of this study can be indicative for effects of erosion and deposition on SOC in a field situation. Hence, Figure 6 presents a simple SOC budget of our system with C losses as a result of export from the system and possible C losses or gains due to changing C-efflux in the area of deposition. In general, small erosional events on a moist and well-aggregated soil (represented by WSR) have only a minor effect on C-loss, which is mainly resulting from sediment delivery. Erosion of a dry soil could lead to a distinct C-loss by additional respiration from SOC, previously occluded in broken-down soil aggregates. If the eroded soil is highly dispersed, the main loss of SOC occurs by export from the system. It can, however, be hypothesized that an additional amount of SOC is lost by respiration during the dispersion process or after export.

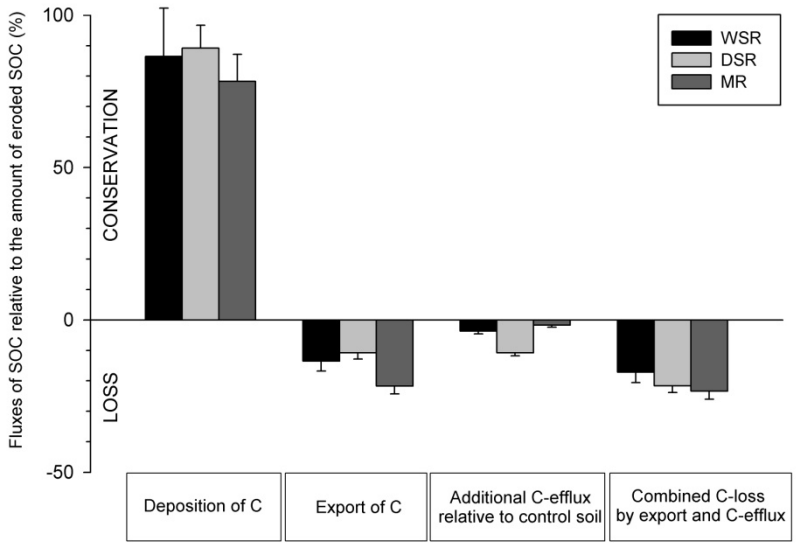


**Figure 6: Fate of eroded SOC (%) in the three simulation experiments, expressed relative to the total amount of eroded SOC.**

Although this study contributed in estimating potential mineralization of eroded SOC after deposition and SOC delivery in function of the erosional event, additional research is required to obtain information on the unknown fluxes of $CO_2$-C at erosional sites and in distant depositional basins and fluvial systems. To integrate these results into a C-balance on longer timescales, account should be taken of the spatial patterns of soil redistribution, spatial variation of SOC input and depth-dependent decomposition of organic matter in soils.

## CONCLUSION

In this study, the effect of erosion, transport and subsequent deposition on the mineralization of SOC was experimentally quantified. During a laboratory experiment, three types of erosional events were simulated, each of which was designed to produce a different amount of eroded soil material with a different degree of aggregation. During a 98-day period, in-situ measurements of $CO_2$-efflux on undisturbed soils with a layer of deposited soil material, and this under field conditions, allowed us to quantify more accurately how erosion affects C-exchange between the soil and the atmosphere.

Depending on the initial conditions of the soil and the intensity of the erosion process, a significant fraction of eroded SOC was mineralized after deposition (between 14 and 22% of eroded SOC). Slaking of initially dry soil aggregates during the process of erosion, lead to the exposure of previously encapsulated SOC and subsequent mineralization of this SOC after deposition. On the contrary, when the initial soil was moist and well-structured, soil was eroded and transported in aggregated form and no major effect on $CO_2$-efflux was observed. When the soil was completely dispersed, prior to the experiments, a large fraction of sediment and potentially mineralizable SOC was exported, resulting in a minor effect on $CO_2$-efflux in the depositional area.

However, results also suggest that deposition produces a dense stratified layer of sediment that caps the soil surface and leads to a decrease in SOC decomposition in deeper soil layers. The latter implies that in order to assess the net effect of erosion on SOC, the functioning of the whole soil system needs to be taken into account. As such, soil redistribution processes contributed to an additional emission of only 2 to 12% of total C contained in the deposited sediment.

Further research is required to determine the effect of erosion on SOC at erosional sites and assess the fate of eroded SOC, exported to fluvial systems and distant depositional basins.

# 7. EVALUATION OF A DYNAMIC MULTI-CLASS SEDIMENT TRANSPORT MODEL IN A CATCHMENT UNDER SOIL-CONSERVATION AGRICULTURE

With minor revisions published:
P. Fiener, G. Govers, and K. Van Oost. 2008. Evaluation of a dynamic multi-class sediment transport model in a catchment under soil-conservation agriculture. Earth Surface Processes and Landforms 33: 1639-1660.

***ABSTRACT.*** *Soil erosion models are essential tools for the successful implementation of effective and adapted soil conservation measures on agricultural land. Therefore, models are needed which predict sediment delivery and quality, give a good spatial representation of erosion and deposition, and allow to account for various soil conservation measures.*

*Here, we evaluate how well a modified version of the spatially distributed multi-class sediment transport model (MCST) simulates the effectiveness of control measures for different event sizes. We use 8-yr runoff and sediment delivery data from two small agricultural watersheds (0.7 and 3.7 ha) under optimized soil conservation. The modified MCST model successfully simulates surface runoff and sediment delivery from both watersheds; one of which was dominated by sheet and the other was partly affected by rill erosion. Moreover, first results of modeling enrichment of clay in sediment delivery are promising showing the potential of MCST to model sediment enrichment and nutrient transport.*

*In general, our results and those of an earlier modeling exercise in the Belgian Loess Belt indicate the potential of the MCST model to evaluate soil erosion and deposition under different agricultural land use. As the model explicitly takes into account the dominant effects of soil-conservation agriculture it should be successfully applicable for soil-conservation planning/evaluation in other environments.*

Soil erosion has been recognized for a long time as one of the most serious environmental problems associated with agricultural land use (Morgan, 1996). It has severe on-site as well as off-site impacts. On-site problems cover the loss of topsoil and fertilizer, the decrease in crop yield (where plants are eroded, covered by sediments or in case of gullying) in the short term and a decrease in soil fertility in the long-term (Lal, 2001). The off-site problems, which are nowadays more in the public and political focus, are the pollution of surface waterbodies with suspended sediments and colloids (Bilotta et al., 2007; e.g. Haygarth et al., 2006) and other substances attached to the sediment particles

(e.g., phosphorus and pesticides), the silting of riverbeds, reservoirs and ponds, as well as the damage of infrastructure and private properties by local muddy floods (Boardman et al., 2003; Verstraeten and Poesen, 1999).

Soil erosion and deposition models are essential tools for the implementation of effective and site-specific soil conservation measures on agricultural land. During the last decades several models have been developed. All of these models have different strengths and limitations because each was developed against the background of a particular philosophy, for different objectives, and for specific site conditions (Grunwald and Frede, 1999).

Still very common is the empirical, spatially and temporally lumped Universal Soil Loss Equation (USLE, Wischmeier and Smith, 1978) and its derivates like the Revised USLE (RUSLE, Renard et al., 1991), or the Erosion-Productivity Impact Calculator (EPIC, Williams, 1985). These models assume in principle a spatially uniform slope, although they have been applied to complex terrain coupling with GIS, e.g. in the differentiated USLE (dUSLE, Flacke et al., 1990).

In order to improve the reliability, generality, and accuracy of erosion prediction, more physical process-based erosion models have been developed within the last decades. The more recent ones are: the Water Erosion Prediction Project (WEPP, Flanagan and Nearing, 1995), the European Soil Erosion Model (EUROSEM, Morgan et al., 1998), the Kinematic Runoff and Erosion Model (KINEROS2, Smith et al., 1995), and the Limburg Soil Erosion Model (1996b; LISEM, De Roo et al., 1996a). Due to the complexity and the spatial and temporal variation of erosion processes a large number of parameters have been integrated in these models. Hence, much attention was paid to the acquisition of input data (Jetten et al., 1996). Nevertheless, these models do not necessarily perform better then the lumped, empirical based models, mainly because input errors increase with model complexity (Jetten et al., 2003) and because of uncertainties in model structure and process representation (Parsons et al., 2004).

In this context, reduced complexity modeling has received increasing attention during the past few years. This tendency can be found generally in the environmental sciences and is basically due to the fact that it is now realized that better predictions might be obtained using simpler model structures with a reduced parameter space rather than very complex model systems for which the necessary parameter values and input data are impossible to obtain (2000; e.g. Brazier et al., 2001). Examples for such models are: the Sealing Transfer Runoff Erosion Agricultural Modification model (STREAM, Cerdan et al., 2001), and the Water and Tillage Erosion Model (WaTEM, Van Oost et al., 2000) .

However, there exists a trade-off between reduced model complexity and the predictive power of a soil erosion model. This is especially relevant when evaluating the on- and off-site effects of different land management strategies. For this purpose, a model should (i) predict the amount as well as the size distribution of sediments delivered from an agricultural watershed, which is a major prerequisite for a reasonable prediction of the erosion and export of sediment bound substances such as particulate organic matter and nutrients, (ii) give a good spatial representation of where erosion and deposition is actually occurring at different scales, (iii) account for effects of different erosion control measures, namely changes in tillage techniques and field layout as well as the implementation of grass filter strips etc., and (iv) provide explicit information about the quality of the model predictions and the uncertainty associated with the model.

This study focuses on the dynamic Multi-Class Sediment Transport model (MCST) developed by Van Oost et al (2004). Although this model uses a limited set of parameters, it is dynamic and accounts for size-selectivity during sedimentation, within a two-dimensional context on an event basis. Erosion patterns, sediment delivery and sediment quality can therefore be modeled. Thus far the model has only been tested for rainfall-runoff events in a small conventionally managed watershed (3.0 ha) in the loam belt of Belgium, where measured erosion and deposition patterns after a series of winter storms were used for model validation (Van Oost et al., 2004). To use the model under different environmental conditions, especially to account for soil conservation techniques, more rigorous model testing and possibly model modifications are necessary.

Our objectives were (i) to validate the MCST model using a unique 8-yr monitoring data set from two small watersheds (0.7 and 3.7 ha) managed using optimized soil conservation techniques, located in Southern Germany, (ii) to modify the model in terms of process representation in order to simulate adequately soil erosion processes under soil conservation and (iii) to carry out first tests of the modified model's ability to predict grain size distribution in delivered sediments, a prerequisite to simulate the transport of sediment bound substances.

## MATERIALS AND METHODS

### Study site

The study site is part of the Scheyern Experimental Farm located about 40 km north of Munich in the Tertiary hills, an important agricultural landscape in Central Europe. The study site covered two small adjacent agricultural watersheds 3.7 ha and 0.7 ha in size (Figure 1), situated at an altitude of 454 to 469 m above sea level (48°30'50'' North,

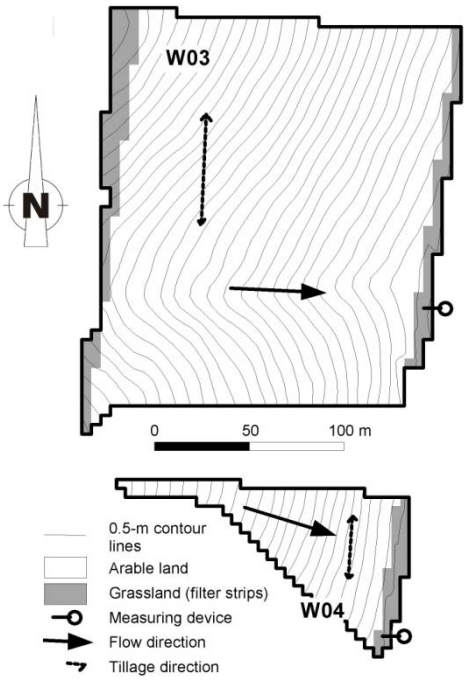


**Figure 1. Topography, field borders, tillage direction and location of measuring devices in watershed W03 and W04.**

11°26'30'' East). Loamy and silty loamy Inceptisols dominate throughout the watershed (Sinowski and Auerswald, 1999), with a median grain size diameter between 12.5 and 16 µm. Between 1994 and 2001 the mean annual air temperature was 8.4°C, and the mean annual soil temperature at a depth of 0.05 m under grass was 10.2°C. Ground frost was observed approximately 21 days per year occurring between December and the beginning of March. The average annual precipitation (1994 to 2001) was 834 mm.

Both watersheds drained a single large field with a crop rotation consisting of potato (*Solanum tuberosum* L.), winter wheat (*Triticum aestivum* L.), maize (*Zea mays* L.), and winter wheat. Before each row crop a cover crop (mustard, *Sinapis alba* L.) was cultivated after wheat harvest in August. Potato ridges were already formed prior to mustard seeding and potatoes and maize were planted directly into the winter-frost killed mustard, maintaining some mustard cover after planting the potatoes. Wide low-pressure tires were used on all machinery to reduce soil compaction and to avoid the development of wheel-track depressions, which usually encourage runoff (Auerswald et al., 2000; Fiener and Auerswald, 2003b). At the downslope end of the field in both watersheds a 5-10 m wide vegetated filter strip (VFS) was established, wherein the runoff is routed along a slightly elevated field road to the watershed outlet (Figure 1).

## Data collection

Runoff was continuously collected between 1994 and 2001 at the outlet of the watersheds. The measuring systems were based on a Coshocton-type wheel runoff sampler collecting an aliquot of 0.52-0.55% (watershed W03 and W04, respectively) from the total runoff coming from the outflow pipe. The aliquot volume was measured and at least one sample was taken during or after each event, which was later dried at 105°C to determine the sediment concentration. The measuring system was tested for function at the end of each runoff event. A more detailed description of the measuring system and the results of a precision test can be found in Fiener and Auerswald (2003a).

Two meteorological stations were located about 500 m and 100 m from the watersheds at 453 and 480 m above sea level, respectively. At these stations triggered rainfall data (0.2 mm per trigger) were collected. For modeling the measurements were aggregated to minute values and the data of the farther station were only used in case of equipment failure of the nearer station. Precipitation events were differentiated when no rainfall was measured for at least 6 h.

Plant and residue cover was measured bi-weekly during the vegetation period, four-weekly in autumn and spring, and before and after each soil management operation. The measurements were carried out at three locations in the field of the tested watersheds and in three neighboring fields with identical crop rotation between January 1993 and April 1997. Residue cover was measured manually using a pocket rule. Plant height was determined in the field and plant cover was derived from photographs taken around noon from a height up to 4 m (in case of full-grown maize) using image analysis. Therefore, photographs were digitized and the percentage of plant cover was calculated after interactively determining all areas with and without plant cover. Between January 1994 and April 1997 the cover measurements made in the watershed were directly used for modeling. From May 1997 to December 2001 an average cover of each specific crop was derived from all measurements (including measurements in neighboring fields) covering 16-yrs of winter wheat and 8-yrs of maize and potato, respectively. This average cover information was adjusted to account for field operations, which were all monitored during the total measuring campaign (1994-2001).

Soil samples were taken in a 50×50 m grid in both watersheds to derive soil properties, like grain size distribution, carbon and nutrient content etc. For model parameterization we used the grain size distribution in the topsoil (0-0.2 m) homogenized by field operations. To determine grain size distribution the topsoil samples were dispersed, decalcified and analyzed with the sieve-pipette method.

**Modeling Structure**

A detailed description of the MCST model was given by Van Oost et al. (2004). Here, we give an overview of the most important components and focus on the modifications made in this study. MCST is a grid based model and has three major components: (i) a runoff generation module using a modified SCS curve number (*CN*) technique, (ii) a runoff routing algorithm that redistributes runoff via flow paths to the outlet of a watershed taking into account flow direction effects due to tillage roughness, and (iii) an erosion, transport and deposition module calculating the spatial distribution of soil erosion and deposition.

*Runoff generation*

The runoff generation routine in the original MCST was only tested for wet winter conditions under conventional agriculture Van Oost et al. (2004). To apply the model for different seasons under conservation agriculture, the originally used SCS curve number technique was fundamentally modified to account for variations of antecedent soil moisture, effects of cover management, soil crusting, run-on and infiltration after the end of rain event (afterflow infiltration) in areas of high infiltration capacities.

In the original SCS *CN* model the antecedent soil moisture content (AMC) is taken into account for three different soil moisture conditions (dry, average and wet) represented by different equations to calculate the *CN*s (e.g. Chow et al., 1988). The incorporation in terms of three AMC levels causes unreasonable and sudden jumps in the *CN*-variation. To prevent these and to objectify the simulation, an approach developed by Mishra et al. (2004) was adopted. In this approach, which was tested for about 63,000 storm events from 234 watersheds in the USA varying in size from 0.1 ha to 30,350 ha, runoff generation is calculated taking the five days antecedent precipitation $AP_5$ into account (Eq. 1).

$$R_{CN} = \frac{\left(P - I_a\right) \cdot \left(P - I_a + AM\right)}{P - I_a + AM + MR} \tag{1}$$

$$I_a = \lambda \cdot MR \tag{2}$$

$$AM = 0.5 \cdot \left[ -\left(1+\lambda\right) \cdot MR + \sqrt{\left(1-\lambda\right)^2 \cdot MR^2 + 4 \cdot AP_5 \cdot MR} \right] \tag{3}$$

where $R_{CN}$ is the estimated direct surface runoff (mm), $MR$ is the potential maximum retention (mm), $I_a$ is the initial abstraction (mm), $P$ is the total precipitation of an event (mm), $AM$ is the antecedent soil moisture (mm) and $AP_5$ is the antecedent 5-day precipitation amount (mm).

In the original curve number technique, time is not represented and hence the technique does not allow accounting for variations in rainfall intensity and duration. Van Oost (2003) found that using Eq. 4 to account for rainfall intensity significantly improved the prediction of direct runoff from a small agricultural watershed in the Belgium loam belt, so this was also implemented.

$$R = R_{CN} \cdot (I_{\max 10} / 10)^{\alpha} \tag{4}$$

where $I_{\max 10}$ is the maximum 10-minute rainfall intensity and $\alpha$ is a calibration parameter.

Furthermore, to use the curve number technique in small agricultural watersheds under different cropping practices the selection of *CN*s used to calculate *MR* should follow objective rules accounting for surface conditions, namely soil cover and crusting stage. To represent the effect of soil cover on *CN*s an approach presented by Auerswald and Haider (1996) was adopted. These authors found in plot experiments (plot size 7-187 m², 1-h rain of 60-74 mm, SCS-*CN* hydrological soil group C) carried out at the Scheyern test site and in the surrounding landscape that there is a more distinct difference between *CN*s for different field conditions than represented by the original approach (e.g. USDA-SCS, 1986). In general the experiments demonstrated a strong relationship between soil cover by plants and plant residues and *CN*. For small grains this is described by Eq. 5 (Auerswald and Haider, 1996), while for row crops Eq. 6 can be used (Auerswald, 2002a).

$$CN_{SG} = 87 - 47 \cdot COVER \qquad (n = 51, R = -0.91) \tag{5}$$

$$CN_{RC} = 80 - 40 \cdot COVER \qquad (n = 23, R = -0.77) \tag{6}$$

where *COVER* represents relative soil cover (plants and plant residues), $CN_{SG}$ and $CN_{RC}$ are *CN*s for small grains and row crops, respectively, standard error for the Pearson Correlation Coefficient *R* is 0.06 and 0.13 for Eq. 5 and 6, respectively, for both equations *R* is significantly different from 0 ($P < 0.001$).

The plot experiments were carried out under uncrusted conditions (personal communication K. Auerswald) and, hence, crusting was introduced following Eq. 7 (Van Oost, 2003).

$$CN = CN_{SG/RC} + \frac{1}{5} \cdot CR \cdot c \tag{7}$$

where *CR* is the crusting stage (Govers, 1986), $CN_{SG/RC}$ are *CN*s derived from Eq. 5 and 6, and *c* is a crusting coefficient.

The crusting stages vary between 0 and 5 representing the full range of crusting stages, from a non sealed, initial fragmentary structure with all fragments clearly distinguishable to a continuous state with depositional crusts (Govers, 1986). The value of $c$ is set so that the $CN$ for crusting stage 5 equals the $CN$ of 0% soil cover according to Eq. 5 and 6 (for small grains $c$ = 87 - $CN_{SG}$, for row crops $c$ = 80 - $CN_{RC}$). The introduction of crusting stages into the $CN$ calculations was successfully applied for a small agricultural watershed in the Belgium Loam Belt, where crusting stages were monitored over three years (Van Oost, 2003).

To ensure the applicability of the model, where such measurements are not available, we introduced and modified a soil crusting approach developed by Schröder and Auerswald (Schröder, 2000; Schröder and Auerswald, 2000). The principal ideas of this approach are: (i) Following Morin and Benyamini (1977) the decrease in infiltration rate caused by soil crusting can be described by a negative exponential equation taking into account start and minimum (end) infiltration rate, rainfall energy and a parameter representing soil susceptibility to crusting. (ii) If the soil is protected by a plant or a residue cover the effective rainfall energy is reduced and hence the soil is less vulnerable to crusting. (iii) The initial infiltration rate for an event following a crusting event is equal to the end infiltration rate of the preceding event. (iv) During a period without rain there is a decay of the existing crust caused by earthworm activity and soil crack formation. Due to the complex interaction of soil properties (texture, organic carbon content, pH etc.), earthworm activity as well as soil temperature and moisture the authors did not find any adequate physically basis to calculate the time of recovery. Therefore a simple estimate is used applying a crust half-life time of 30 days approximated from field experience.

For our approach we modified the original exponential equation introducing crusting stages instead of start and minimum infiltration rates (Eq. 8).

$$CR(t_1) = CR_{\max} - (CR_{\max} - CR(t_0)) \cdot e^{-C_B \cdot Ekin_{eff}(t_1)} \tag{8}$$

where $CR(t_1)$ is the crusting stage after time $t_1$, $CR(t_0)$ is crusting at the beginning of the event, $CR_{\max}$ equals crusting stage 5, and $Ekin_{eff}$ is the effective kinetic rain energy.

$$Ekin_{eff} = \int_{t_0}^{t_1} Ekin(t) \cdot (1 - COVER) \cdot dt \tag{9}$$

where *Ekin* is the energy of a rainfall for time *t*, and $t_0$ is the start time of a rain event.

Kinetic rainfall energy *Ekin* is calculated following the standard USLE procedure (Wischmeier and Smith, 1958) also applied under German conditions (Schwertmann et al., 1987). For 53 rainfall experiments at the Scheyern research farm carried out on plots under seedbed conditions with a wide range of soil textures (plots of 8 m², 1-h rain of 60-63 mm, slope 1-14%, clay content 12-31%, silt content 15-67%) Schröder and Auerswald (2000) found that a kinetic rainfall energy of about 400-500 J $m^{-2}$ produced a fully crusted soil, a result that is in line with other experiments on loamy and clay soils (e.g. Lado et al., 2004). Further rainfall experiments with different soil cover (n=39, cover 10-25%) allowed to confirm that the relationship between crusting and rainfall kinetic energy can also be used for surfaces covered with vegetation residue provided that the effective kinetic rain energy reaching the soil surface, $Ekin_{eff,}$ is used.

The soil crusting parameter $C_B$ was determined based on the 53 rainfall experiments under seedbed conditions, where the start and minimum infiltration rate (crusting stage 0 and 5, respectively) were measured and rainfall kinetic energy was calculated from measured rain intensities, $C_B$ was most strongly related to soil texture: For soils of texture class 1, i.e. soils with a clay content between 15 and 22% the average $C_B$ is 0.015 (SD 0.007, $n$ = 19). For soils of texture class 2, characterized by a silt content < 50% the average $C_B$ was 0.0075 (SD = 0.005, $n$ = 34).

To approximate the recovery of crusting stages (or infiltration rates) Eq. 10 was used. Moreover, crusting stage was set to zero in case of any tillage operation.

$$CR(t_0,n) = CR(t_{end},n-1) - CR(t_{end},n-1)\cdot(1-e^{fr\cdot\Delta t}) \tag{10}$$

where $CR(t_0,n)$ is the crusting stage at the beginning of a new event, $CR(t_{end}, n\text{-}1)$ is the crusting stage at the end of the previous event, *fr* is a recovery parameter, and $\Delta t$ is the time of crust recovery. Due to a lack of clear information on the factors controlling crust recovery, a simple time dependency is used, where *fr* was set to -0.02 to reach a half life time of crusts of 30 days.

*Runoff routing*

In the MCST model a numerical solution of the kinematic wave approximation is used to estimate discharge and water depth at every location in the grid at all time steps. MCST uses different hydrological models for sheet flow and concentrated (rill) flow. Sheet flow is modeled according to the Manning's equation and it is assumed that the

flow width equals the grid cell size. For self-forming rills, flow velocities and cross-sectional areas are predicted from discharge alone (Govers, 1992b). Moreover, the model uses a multiple-flow algorithm for sheet flow, while a single flow algorithm is used for rills.

The model assumes sheet flow until a critical shear stress of 0.9 Pa is exceeded which is sufficient to initiate rill formation on an erodible loamy soil (Govers, 1985). In this study, shear stress was calculated as:

$$\tau = \rho \cdot g \cdot D \cdot S \cdot \left( \frac{n_g}{n} \right)^{3/2} \tag{11}$$

where $\tau$ is shear stress (Pa), $\rho$ is water density (kg $m^{-3}$), $g$ is the gravity (m $s^{-2}$), $D$ is the flow depth (m), $S$ is the local slope, $n_g$ is the Manning's roughness coefficient for bare soil, and $n$ is the Manning's roughness coefficient depending on plant and plant residue cover.

Compared to the original MCST the term $(n_g/n)^{3/2}$ in Eq. 11 was added to the general shear stress calculation to account for the reduced shear stress affecting the soil surface, if the soil is protected by plant residues (Govers, 1992a). This situation can typically be found under soil conservation agriculture or if soil is covered by dense grass due to the installation of vegetated filter strips (VFS). The Manning's roughness coefficients for surfaces covered with plant residues are calculated following Gilley et al. (1991). From flume experiments (flow rates $5.24\times10^{-4}$ – $1.01\times10^{-1}$ $m^3$ $s^{-1}$) these authors derived empirical relationships between different types of plant residues (cover 15-99%) and Manning's $n$. For Reynolds numbers < 20,000 Eq. 12 can be used for different residues types:

$$n = 1.89\ 10^{-2} \cdot (COVER_R)^{0.712} \ / \ \mathrm{Re}^{0.142} \tag{12}$$

where $COVER_R$ is surface cover by plant residues, and Re is Reynolds number.

For the calculation of Manning's $n$ in the model a Reynolds number of 2000 was used. For watershed W03 typical values calculated for Re range between 250 and 2000. Hence, the Re number used to calculate $n$ leads in most cases to a conservative estimate of the hydraulic roughness effect of soil cover introduced by soil conservation. Clearly, this correction procedure could be improved if more information on runoff hydraulics on vegetation covered surfaces would be available.

To decide whether runoff will follow the topographical or the tillage direction the

TCRP model of Takken et al. (2001b) is used. They found that runoff patterns on agricultural land are strongly affected by tillage direction. Incorporation of these effects in runoff routing significantly improved prediction of erosion and deposition patterns.

To allow for run-on and afterflow infiltration, which both can be prominent in the case of soil conservation measures like grassed waterways, simple estimates of these infiltration rates derived from the *CN* methodology are used in the modified MCST. If runoff is routed into a grid cell, where no rain excess occurred till time *t*, re-infiltration $I_{RE}$ (mm $s^{-1}$) is calculated and the initial abstraction of this cell is reduced by the re-infiltrated volume:

$$I_{RE}(t) = \frac{(I_a - P) \cdot D_d}{D_s} \tag{13}$$

where $P$ is the cumulative precipitation (mm) till time $t$, $D_d$ is the event duration in days (-) used to scale $I_a$ and $P$, and $D_s$ is the event duration (s).

Afterflow infiltration is assumed if runoff is routed through a grid cell that previously produced infiltration excess. This is especially important for areas along the thalwegs of a watershed, where runoff lasts longest after the end of a precipitation event, and where conservation measures can effectively reduce runoff velocity due to an increased hydraulic roughness. This afterflow infiltration $I_{AF}$ (mm $s^{-1}$) is estimated using Eq. 14:

$$I_{AF}(t) = I_{cum} / D_s \tag{14}$$

where $I_{cum}$ is the cumulative infiltration (mm) during an event according to the SCS-*CN* methodology ($I_{cum}=MR\ (P-I_a)\ /\ (P-I_a+MR)$).

Based on the dynamic simulation of rainfall, infiltration and runoff generation, the MCST model calculates an effective steady-state flow and effective runoff duration.

*Erosion, transport and deposition*

The erosion, transport and deposition component of the MCST model uses a concept of three different erosion/deposition domains, representing areas dominated by different erosion/deposition processes as proposed by (Beuselinck et al., 1999a, Figure 2). Below a critical threshold, no entrainment of particles occurs and sediment deposition is governed by simple settling as a function of fall velocity (domain 1). Above this threshold, two other domains were identified where entrainment of original soil, deposition, and re-entrainment of the deposited particles all occur simultaneously. In domain 3 entrainment

and re-entrainment are dominant resulting in net erosion while in domain 2 deposition is dominant but significant sediment re-entrainment occurs.

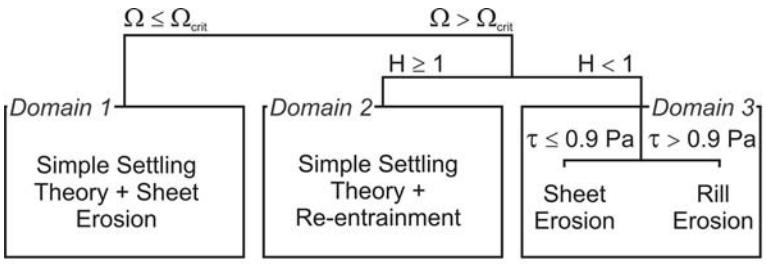


**Figure 2. General implementation scheme of modified dynamic Multi-Class Sediment Transport model (MCST).**

The concept was implemented in the MCST model of Van Oost et al. (2004) and was successful in predicting the erosion/deposition pattern in a small agricultural watershed (3 ha) in the Belgium loam belt after a wet winter (1992-1993). Under these conditions (conventional cultivation of winter wheat with a cover < 10%, erosion prone silty loam) erosion/deposition is dominated by rill erosion in areas where $\Omega > \Omega_{cr}$ and deposition of the rill-eroded sediment at the foot slope: it was therefore not necessary to explicitly account for sediment transport by interrill runoff. To predict soil erosion during the vegetation period under soil conservation agriculture, sheet erosion, driven by a combination of rain drop impact and flow transport, must be explicitly taken into account. Therefore, we modified the process description for Domain 1 (Figure 2).

It is generally accepted that soil detachment by splash far exceeds the transporting capacity of interrill flow, so that interrill erosion is basically a transport-limited process (Foster and Meyer, 1975). Interrill transporting capacity was modeled using the interrill transporting capacity relationships developed by Everaert (1991). Based on a series of flume experiments with typical interrill flow discharges (unit discharge: 0.002 – 0.025 $m^2\ m^{-1}\ s^{-1}$), Everaert developed transporting capacity relationships. On slopes ranging from 1.7 to 17.4%, without and with rain on the surface (intensity of 60 mm $h^{-1}$) the solid discharge in case of a median sediment diameter between 33 and 122 μm can be expressed as,

$$q_s = 1.74 \cdot 10^{-6} \cdot \Omega_{eff}^{1.07} \cdot D_{50}^{0.47} \qquad (R^2 = 0.89;\ n = 394) \qquad (15)$$

and the effective stream power is calculated as (Foster and Meyer, 1972; Govers, 1990):

$$\Omega_{eff} = \Omega^{3/2} \cdot D^{-2/3} \qquad (16)$$

where Ω is stream power (g $s^{-3}$), $D$ is the flow depth (cm).

Eq. 15 is used to model interrill sediment transport in Domain 1. If the sediment input into a raster cell is larger than its specific potential to transport solid discharge, size-selective deposition is assumed. Therefore, ten equally distributed sediment classes represented by specific settling velocity classes are used and continuous mixing of water and sediment is assumed (Beuselinck et al., 1999a). Sediment concentration $c_i$ for each settling velocity class is given by (Beuselinck et al., 1999b; Hairsine et al., 2002):

$$c_i(x) = c_{i0} \cdot e^{\frac{-v_i x_i}{q}} \quad , \quad i = 1, 2, \ldots I - 1 \tag{17}$$

where $c_{i0}$ is the initial concentration of velocity class $c_i$, $v_i$ is settling velocity of class $i$, and $x_i$ is the evaluation distance.

In contrast to the approach used to model sediment re-entrainment (domain 2 and 3) changes in grain size distribution due to selective deposition are not taken into account to calculate interrill sediment transport in Domain 1.

Erosion and deposition in Domain 2 and 3 are calculated according to the original MCST model (Van Oost et al., 2004). If the local stream power exceeds $\Omega_{cr}$, the shielding factor $H$, from the Hairsine and Rose model (Hairsine and Rose, 1992a; 1992b), is calculated to decide whether net deposition (Domain 2) or net erosion (Domain 3) occurs:

$$H = \frac{(\sigma - \rho) \cdot g \cdot \sum v_i \cdot c_i}{\sigma \cdot F \cdot (\Omega - \Omega_{cr})} \tag{18}$$

where $\sigma$ is sediment density (kg m$^{-3}$), $\rho$ water density (kg m$^{-3}$), and $F$ is the fraction of stream power used for re-entrainment. As $H$ is a shielding factor, its maximum value is set to $H = 1$.

If $H = 1$ (Domain 2), simultaneous re-entrainment and deposition of sediment occurs. The variation of sediment concentration with distance downslope can then be described as follows for steady state flow (Sander et al., 2002):

$$\frac{dc_r}{dx} = \left[ \frac{\gamma^*}{\sum_{i=1}^{I} v_i c_i} - 1 \right] \cdot \frac{v_i c_i}{q} \quad , \qquad i = 1, 2, \ldots . I \tag{19}$$

where

$$\gamma^* = \gamma \cdot q^{1-1/m} \cdot \left[1 - \frac{\Omega_{cr}}{\Omega}\right], \tag{20}$$

$$\gamma = \frac{F \cdot \sigma \cdot \rho \cdot S \cdot K^{1/m}}{\sigma - \rho} \tag{21}$$

and the flow depth $D$ is given by the generalized depth discharge equation

$$D = \left(\frac{q}{K}\right)^{1/m} \tag{22}$$

where $q$ is the unit discharge ($m^2\ s^{-1}$), and $K$ is a coefficient related to surface slope and hydraulic roughness ($K = S^{1/2} / n$), and $m$ is a flow constant of 5/3 for turbulent flow (Beuselinck et al., 2002).

From these equations the spatial pattern of sediment deposition and sorting of all sediment size classes can be calculated if values for $c_i$, $v_i$, $q$, $S$, $D$ and $\sigma$ are known at the entry and the exit of each grid cell.

If $H < 1$, net erosion occurs (Domain 3). As long as the flow shear stress (Eq. 11) is below the critical value for rill initiation of 0.9 Pa, interrill erosion is modeled according to Eq. 15. If $\tau$ exceeds the critical value, rill detachment is calculated as a function of slope and discharge following Eq. 23:

$$Dr = a_{rill} \cdot S^{ser} \cdot Q_{rill}^{de} \tag{23}$$

where $Dr$ is the detachment rate ($kg\ m^{-1}\ s^{-1}$), $a_{rill}$ is a rill erodibility factor, $S$ is the local slope gradient and $Q_{rill}$ is the rill discharge and *ser* and *de* are topographical exponents, which are based on rill erosion experiments conducted by Gimenez and Govers (2002), and are set to fixed values of: *ser* = 0.9 and *de* = 0.73 (Govers et al., 2007).

**Model implementation**

To simulate runoff formation and routing in the runoff module a precalibration procedure, using nine runoff events (> 0.5 mm) in watershed W03, was applied to determine the parameters $\lambda$ and $\alpha$, accounting for antecedent soil moisture (Eq. 3) and rain intensity (Eq. 4), as well as $a_{rill}$ to consider the site-specific rill erodibility (Eq. 23). The optimal parameter

set was determined using the highest model efficiency coefficient (*MEF*) as proposed by Nash and Sutcliffe (1970).

$$MEF_i = 1 - \frac{\sum_{i=1}^{n}(O_i - M_i)^2}{\sum_{i=1}^{n}(O_i - \overline{O})^2} \tag{24}$$

where $O_i$ is observed and $M_i$ is modeled variable of parameter set *i*.

The main input data required for the model, except for the calibration parameters given in the results section, are summarized in Table 1. Moreover, ten equally distributed sediment size classes for each watershed were calculated from the soil sampling at the test site. The time step used for modeling was 60 s.

**Table 1. Main input data, parameters and variables of the Multi-Class Sediment Transport model (MCST).**

| Description | Symbol | Unit | Range/Value |
|---|---|---|---|
| Digital terrain model | | m | 5×5 |
| Land use map | | | |
| Soil cover for each field and land use | | % | 0-100 |
| Tillage roughness (and direction) for each field | $R_o$ | m | 0-0.25 |
| Hydraulic roughness fields | $n$ | s $m^{-1/3}$ | 0.016-0.300 |
| Hydraulic roughness vegetated filter strip | $n_{VFS}$ | s $m^{-1/3}$ | 0.20 |
| Water density | $\rho$ | kg $m^{-3}$ | 1000 |
| Sediment density | $\sigma$ | kg $m^{-3}$ | 1800-2600 |
| Vertical mixing coefficient | | / | 1 |
| Characteristic settling velocity for class i | $v_i$ | m $s^{-1}$ | 1.6 $10^{-7}$ – 3.4 $10^{-2}$ |
| Threshold of re-entrainment | $\tau_{cr}$ | Pa | 0.6 |
| Threshold of rill erosion | | Pa | 0.9 |
| Re-entrainment parameter | $F$ | / | 0.1 |
| Curve Number | $CN$ | / | 65 |

The output of the model consists of the following maps: discharge of every time step, effective discharge, stream power, location of sheet and rill erosion, net erosion/deposition, and deposition of each sediment size class. Moreover, a hydrograph, total runoff, total sediment output, and sediment size distribution at the outlet are also calculated.

## RESULTS AND DISCUSSION

### Measurements

During the observation period (1994-2001) 1413 rainfall events have resulted in 218 and 154 runoff and sediment delivery events in watershed W03 and W04, respectively. On average a runoff of 38.5 mm $yr^{-1}$ (runoff coefficient: 0.05) and a sediment delivery of 437 kg $ha^{-1}$ $yr^{-1}$ were measured in W03 during the 8-yr observation, while in W04 measured average annual runoff was 9.6 mm $yr^{-1}$ (runoff coefficient 0.01) and sediment delivery was 40 kg $ha^{-1}$ $yr^{-1}$ (Figure 3). The difference in runoff coefficient by a factor 5 was probably caused by a different area ratio between field and vegetated filter strip (VFS -field area ratio equals 1/28 and 1/8 in W03 and W04, respectively). The area and topography also play an important role in sediment production and delivery: W03 has a much higher total sediment yield because this watershed has longer and partly steeper slopes and a clearly defined thalweg which is more prone to rill erosion. The formation of rills was observed in W03 after a few larger events, while nearly no rills developed in W04.

The relatively low rates of soil erosion and runoff are attributed to the soil conservation techniques established in the watersheds which result in a high soil cover by plants and plant residues throughout the year (Figure 4) (Auerswald et al., 2000; Auerswald and Haider, 1996; Fiener and Auerswald, 2001). Hence, during the vegetation period (April – November), when the highest rain intensities can be expected (e.g. Bartels *et al.*, 1997), only few storms produce significant runoff volumes (> 0.5 mm). Nevertheless, these storms dominate the erosion (72% of the total annual sediment delivery) within this period, two large erosion events contributed substantially to the total sediment delivery in watershed W03. These events, occurring within two weeks after potato harvest in October 1998 (Figure 3), produced a sediment delivery of 1715 and 467 kg $ha^{-1}$, respectively, representing 61.5% of total sediment delivery measured within the 8-yr observation period. In contrast, relatively low sediment delivery rates were observed in W04, which drains the same large field as W03: here only 55 and 4 kg $ha^{-1}$ was measured for the same events, which again can be attributed to a shorter slope length and hence absence of intensive rill formation and a wider vegetated filter strip at the down-slope end of the watershed.

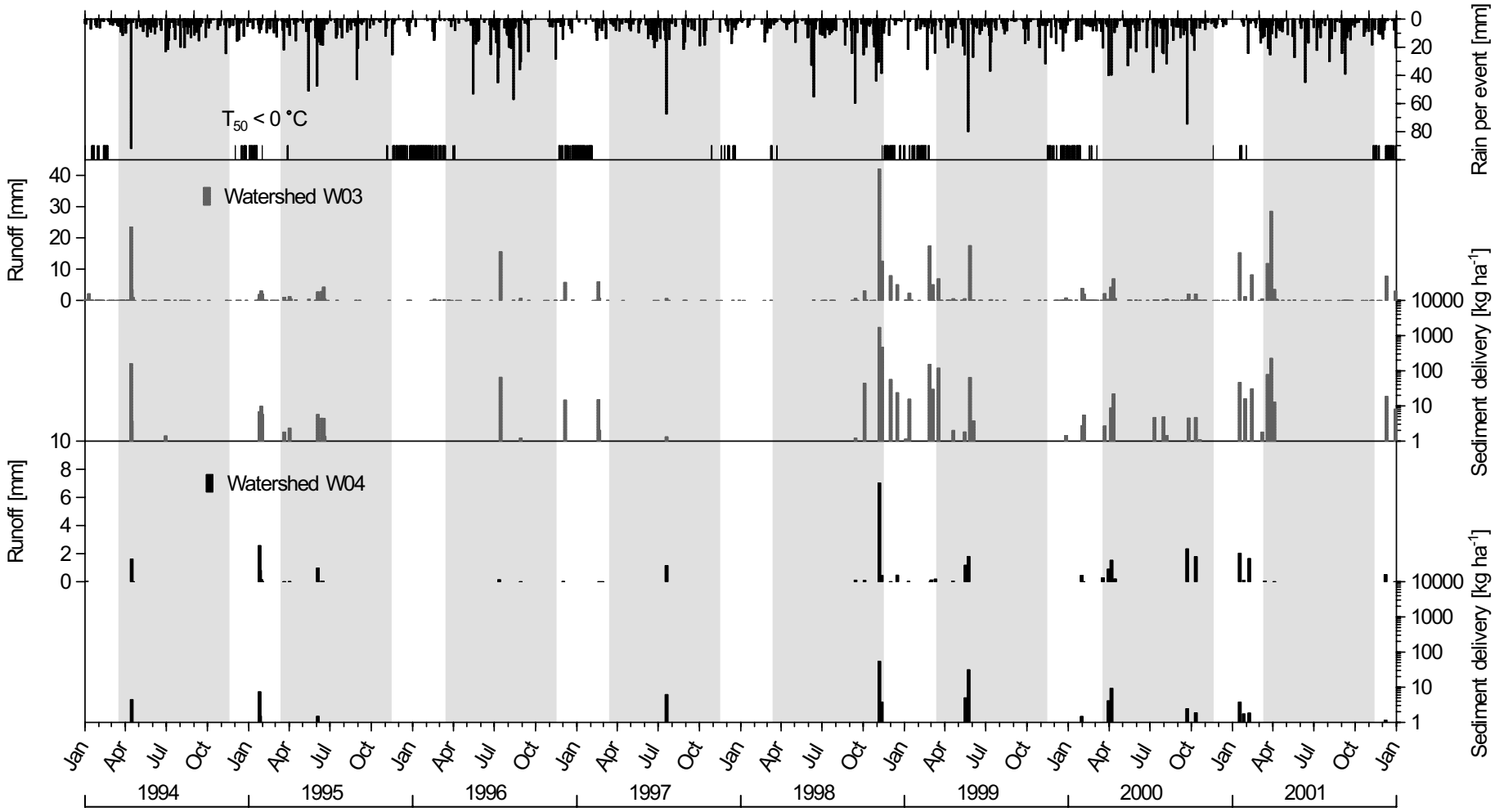


**Figure 3. Measured rainfall, runoff, sediment delivery and air temperature below 0°C (1994-2001) at the tested watersheds in Scheyern; only those events are shown where runoff from watershed W03 ≥ 0.5 mm; grey bars indicate time periods (April to November) used for modeling as long as the air temperature was above 0°C.**

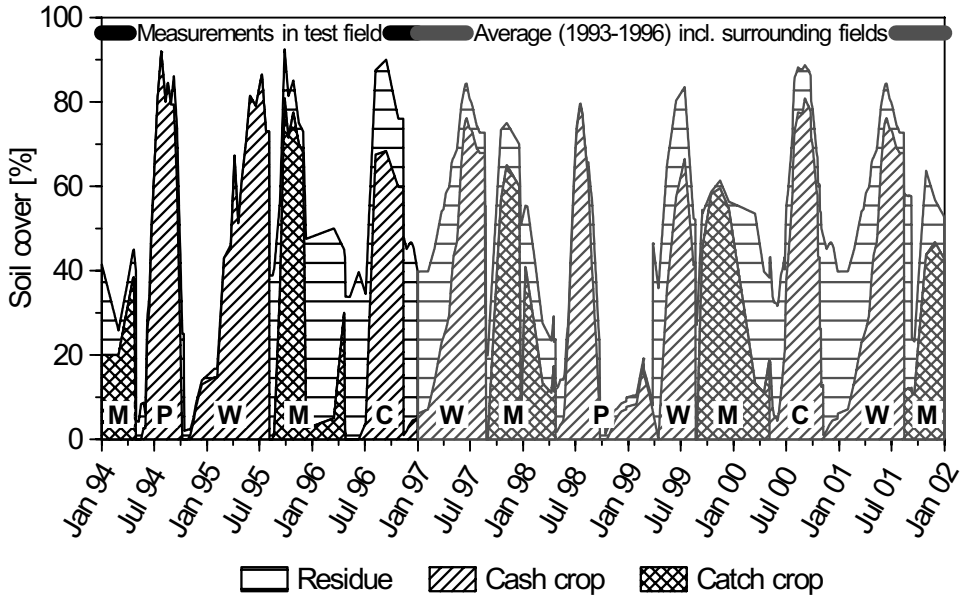


**Figure 4. Averaged field soil cover derived from measurements within the field drained by watershed W03 and W04 and from three surrounding fields, with an identical crop rotation and similar soils; Between 1994 and 1996 the measurements within the test field were used; From 1997 to 2001 the soil cover was derived from the average cover measurements (1994-1996) in the test field and in the three neighboring fields, taking into account the individual field operations within the test field occurring 1997 to 2001; (W = wheat, C = maize, P = potato, M = mustard).**

## Modeling

The MCST model is not able to represent snow melt and ground frost and events where these processes played an important role were excluded from our analysis. For the test site snow and ground frost free conditions are met for the period from April to November (Figure 3). During the 8-yr observation 108 and 92 events occurred between April and November in W03 and W04, respectively, representing 86 and 84% of the total measured sediment delivery.

For practical reasons and due to the fact that only the largest events dominate the erosion processes, only those events with a runoff in watershed W03 ≥ 0.5 mm were modeled. The selected events represent 95.5% of runoff and 98.7% of sediment delivery measured in W03 between April and November (1994-2001). For watershed W04 the same events were modeled to evaluate if the model has the ability to handle more rill erosion driven events in W03 as well as interrill dominated events in W04. An overview of all modeled events and the associated event and watershed characteristics is given in Table 2.

**Table 2. Precipitation and field characteristics, measured and modeled runoff and sediment delivery, for all runoff events in watershed W03 ≥ 0.5 mm; $P_{tot}$ is the total precipitation of an event; $I_{max10}$ is the maximum 10-minute rain intensity, AR5 is the 5-days antecedent rain; $Q_{obs/mod}$ is the observed and modeled runoff; $SD_{obs/mod}$ is the observed and modeled sediment delivery; *CN* and *n* field is the curve number and the Manning's *n* within the field located in both watersheds.**

| Date | No. Event | Precipitation characteristics | | | | Watershed W03 | | | | | Watershed W04 | | | | | Field conditions in W03 and W04 | | |
|---|---|---|---|---|---|---|---|---|---|---|---|---|---|---|---|---|---|---|
| | | $P_{tot}$ [mm] | $I_{max10}$ [mm/h] | Duration [h] | AR5 [mm] | $Q_{obs}$ [mm] | $Q_{mod}$ [mm] | $SD_{obs}$ [kg/ha] | $SD_{mod}$ [kg/ha] | Calibration data = 0; validation data = 1 | $Q_{obs}$ [mm] | $Q_{mod}$ [mm] | $SD_{obs}$ [kg/ha] | $SD_{mod}$ [kg/ha] | Calibration data = 0; validation data = 1 | Tillage rough-ness [cm] | *CN* Field | *n* Field |
| 04/12/1994 | 100 | 86.8 | 8.4 | 38.8 | 9.4 | 27.0 | 32.0 | 161.9 | 134.5 | 0 | -[+] | - | - | - | - | 25 | 82 | 0.024 |
| 04/16/1994 | 101 | 2.4 | 1.2 | 9.5 | 88 | 0.9 | 0.0 | 0.2 | 0.0 | 0 | 0.00 | 0.00 | 0.00 | 0.00 | 1 | 25 | 85 | 0.024 |
| 03/21/1995 | 137 | 23.2 | 3.6 | 49.0 | 12 | 1.0 | 0.0 | 1.8 | 0.0 | 1 | 0.04 | 0.00 | 0.18 | 0.00 | 1 | 2 | 78 | 0.016 |
| 04/02/1995 | 141 | 11.8 | 2.4 | 33.0 | 11.2 | 1.6 | 0.0 | 3.3 | 0.0 | 1 | 0.01 | 0.00 | 0.06 | 0.00 | 1 | 2 | 81 | 0.016 |
| 06/02/1995 | 147 | 49.0 | 7.2 | 24.7 | 18.2 | 2.7 | 5.8 | 5.8 | 42.4 | 1 | 0.98 | 3.13 | 1.49 | 7.70 | 1 | 2 | 72 | 0.016 |
| 06/13/1995 | 149 | 18.2 | 6 | 23.5 | 17.4 | 2.9 | 0.2 | 4.5 | 10.7 | 1 | 0.04 | 0.00 | 0.18 | 0.00 | 1 | 2 | 83 | 0.016 |
| 06/15/1995 | 150 | 20.4 | 16.8 | 11.2 | 21.2 | 4.3 | 1.4 | 4.4 | 36.9 | 0 | 0.04 | 0.00 | 0.16 | 0.00 | 1 | 2 | 86 | 0.016 |
| 06/19/1995 | 151 | 8.4 | 4.8 | 25.8 | 24 | 0.5 | 0.0 | 1.4 | 0.0 | 1 | 0.01 | 0.00 | 0.03 | 0.00 | 1 | 2 | 81 | 0.016 |
| 07/05/1996 | 175 | 73.6 | 9.6 | 67.1 | 11.8 | 15.5 | 9.5 | 65.4 | 71.1 | 0 | 0.14 | 3.27 | 0.64 | 14.03 | 1 | 5 | 79 | 0.071 |
| 08/28/1996 | 178 | 30.4 | 9.6 | 16.3 | 59.2 | 0.7 | 1.9 | 1.2 | 15.7 | 0 | 0.00 | 0.00 | 0.00 | 0.00 | 1 | 5 | 76 | 0.056 |
| 09/11/1998 | 222 | 60.6 | 7.2 | 43.2 | 8.6 | 0.7 | 3.2 | 1.2 | 23.3 | 0 | 0.12 | 0.00 | 0.20 | 0.00 | 1 | 25 | 72 | 0.021 |
| 09/29/1998 | 224 | 42.6 | 9.6 | 125.5 | 10.6 | 3.1 | 3.1 | 44.4 | 31.3 | 0 | 0.09 | 0.00 | 0.26 | 0.00 | 1 | 0 | 88 | 0.016 |
| 10/29/1998 | 228 | 107.4 | 13.2 | 156.1 | 45.6 | 42.1 | 34.5 | 1714.9 | 761.4 | 1 | 7.03 | 5.56 | 54.92 | 58.66 | 1 | 0 | 87 | 0.016 |
| 11/09/1998 | 229 | 38.6 | 4.8 | 155.6 | 16.2 | 12.6 | 5.8 | 467.4 | 58.2 | 1 | 0.46 | 0.00 | 3.79 | 0.00 | 1 | 0 | 87 | 0.016 |
| 04/19/1999 | 247 | 26.4 | 4.8 | 88.6 | 9.2 | 0.5 | 0.0 | 2.0 | 0.0 | 1 | 0.05 | 0.00 | 0.53 | 0.00 | 1 | 2 | 84 | 0.092 |
| 05/14/1999 | 252 | 25.6 | 31.2 | 27.0 | 27.2 | 0.5 | 0.0 | 1.8 | 0.0 | 0 | 1.18 | 0.00 | 4.98 | 0.00 | 1 | 2 | 68 | 0.051 |
| 05/21/1999 | 253 | 80.6 | 8.4 | 62.8 | 0.2 | 17.5 | 13.9 | 64.5 | 74.4 | 0 | 1.79 | 10.69 | 31.08 | 18.27 | 1 | 2 | 69 | 0.046 |
| 09/22/2000 | 309 | 74.8 | 12 | 39.2 | 12.4 | 2.0 | 12.3 | 4.5 | 67.1 | 1 | 2.33 | 10.31 | 2.46 | 16.21 | 1 | 5 | 66 | 0.029 |
| 10/07/2000 | 311 | 30.8 | 4.8 | 47.1 | 22.6 | 2.1 | 0.0 | 4.7 | 0.0 | 1 | 1.79 | 0.00 | 1.88 | 0.00 | 1 | 5 | 70 | 0.029 |

[+] no measurements due to equipment failure

*Hydrology*

The precalibration procedure of the hydrology module to determine the optimal parameter set for $\lambda$ and $\alpha$, accounting for antecedent soil moisture and rain intensity, showed that the model is highly sensitive to changes in $\lambda$, while changes in $\alpha$ have only a minor effect as long as $\lambda$ is close to the optimal value (Figure 5). An optimal model performance for the nine calibration events (Table 2) indicated by a *MEF* of 0.88 and a *RMSE* of 3.2 mm could be obtained using a $\lambda$ of 0.2 and an $\alpha$ of 0.7. The calibration results in exactly the standard $\lambda$ value used in the original SCS-*CN* approach. From Figure 5 it is obvious that the calibrated value of $\alpha$ gives a very similar model efficiency as the one which could be reached using an $\alpha$ of 0.9 obtained by Van Oost (2003) through a similar calibration procedure for a Belgian watershed.

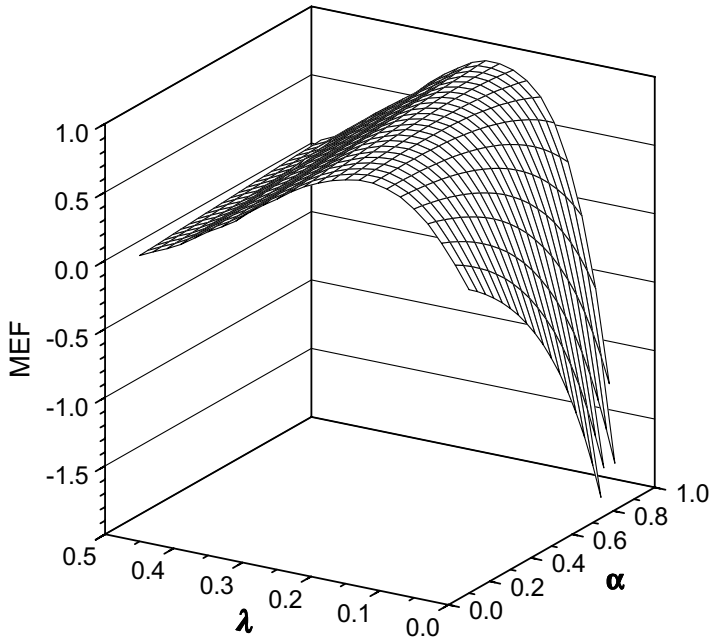


**Figure 5. Model efficiency (*MEF*) calculated according to Nash and Sutcliffe (1970) for the hydrological module of MCST varying the calibration parameters $\lambda$ and $\alpha$, accounting for antecedent soil moisture (Eq. 3) and rain intensity (Eq. 4).**

Based on the standard model parameterization (Table 1) and the calibrated values of $\lambda$ and $\alpha$, the comparison of measured and predicted runoff volumes for all 19 events in watershed W03 larger than 0.5 mm, shows a reasonable model performance (*MEF* = 0.86, *RMSE* = 4.1 mm). This is especially true for the larger events dominating the overall erosion during the observation period (Table 2, Figure 6). For smaller events (measured runoff < 3 mm), the modified MCST model partly overestimated runoff and for some events no runoff was simulated while a runoff between 0.5 to 2.1 mm (average = 1.0 mm) was observed. This indicates that for small storms it is problematic to use a static value of λ to determine the initial abstraction or rainfall amount which must be reached before rain excess occurs. This problem was already reported by Hawkins et al. (1985): they concluded that the standard *CN*

method should only be used for storm depths of at least 0.46 times the maximum retention depth for average moisture conditions. Comparing measured and predicted runoff volumes for all 18 events in watershed W04, in general a much weaker model performance (*MEF* = -2.3, *RMSE* = 3.0 mm) was determined. This might have three main reasons: (i) The runoff module was calibrated for W03, (ii) in W04 the observed runoff volumes (maximum 7.0 mm, Table 2) were generally smaller and therefore higher errors can be expected due to the increasing event variance with decreasing event size (e.g. Nearing, 2006); (iii) As the observed runoff volumes in W04 vary only between 0 and 47 $m^3$, while in W03 volumes from 20 to 1550 $m^3$ were measured, the relative runoff reduction effect of the downslope VFS in both watersheds is more pronounced in the smaller watershed W04. Hence, the model results are in general much more sensitive to parameterization and size of the VFS. This is shown for event 253 (Figure 7, Table 2). The simulation of the effects of such small structures is difficult due to a lack of data on their temporally variable properties (e.g. Fiener and Auerswald, 2006), the unknown degree of concentration of runoff within these structures, and a potentially too coarse spatial resolution, which does not account for the exact size and geometry of the VFS. Due to these problems the analysis of erosion and deposition modeling is focused on the larger runoff events dominating the overall erosion in both watersheds. For these larger events the overall performance of the runoff module, indicated by an overall *MEF* in both watersheds of 0.82 and a *RMSE* of 3.6, is assumed to be sufficient.

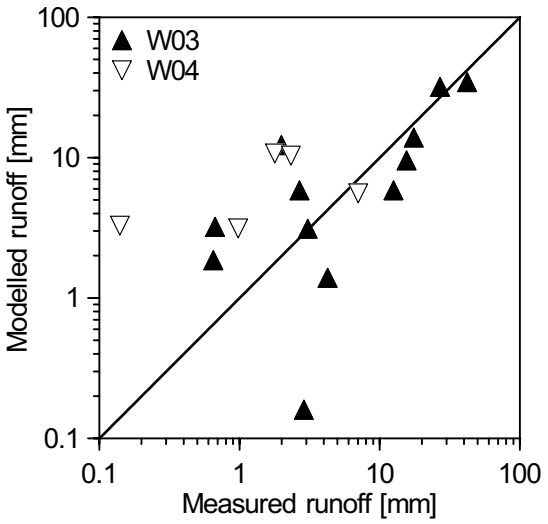


**Figure 6. Measured vs. modeled runoff in watershed W03 and W04 for measured runoff events in watershed W03 ≥ 0.5 mm.**

*Erosion and Deposition*

As more important erosion events occurred in watershed W03, the data from this watershed are mainly used to evaluate the erosion-deposition component of the model. Nevertheless, the erosion and deposition modeling is also tested against data from W04 to evaluate if the model predicts the occurrence of rills correctly. Based on effective discharge and effective event duration the patterns of erosion and deposition as well as sediment delivery from the watersheds were modeled.

As there are no data from rill erosion experiments using soils from the research farm in Scheyern, the erosion module has to be calibrated to determine the rill erodibility coefficient $a_{rill}$. Best results for the nine calibration events were reached for a rill erodibility coefficient of 46 (*MEF* = 0.88, *RMSE* = 17.7 kg ha$^{-1}$).

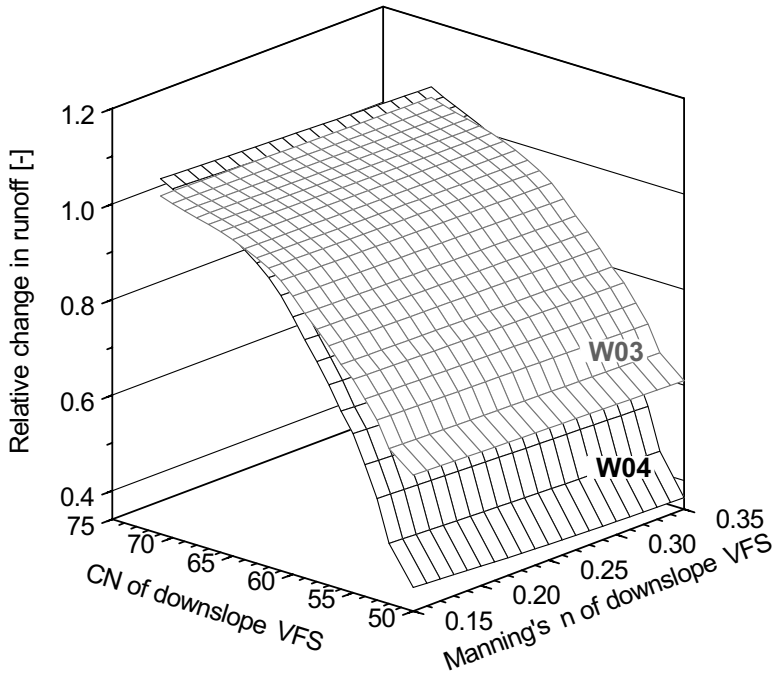


**Figure 7. Relative change in modeled runoff volume for event 253, comparing the results of the standard parameterization of the vegetated filter strips (VFSs) located at the down-slope end of watershed W03 and W04 with results from varying Manning's *n* and Curve Number (*CN*) for the VFSs; standard parameterization for the VFSs is $n_{VFS}$ = 0.2 and $CN_{VFS}$ = 65 (Table 1).**

Based on the calibration a comparison between measured and modeled sediment delivery for a validation data set is shown in Figure 8. The generally smaller sediment delivery per watershed area in watershed W04 compared to W03 is well represented by the model. Nevertheless, sediment delivery from W04 is overestimated for all events < 2.5 kg ha$^{-1}$, again indicating problems with runoff prediction for these small events. This represents a general problem in model accuracy in case of watersheds under soil-conservation. As event size decreases due to conservation measures the variance in sediment delivery of single events increases, which was shown by Nearing et al. (1999) for more than 2000 natural rainfall events on erosion plots distributed all over the United States.

For the largest event (No. 228, Table 2) the modeled effective discharge in W03 was about 7-times larger than in W04 (Table 3), while the modeled sediment delivery differs by a factor of about 13. While in watershed W04 nearly no linear erosion in rills was predicted (Figures 9 and 10) and no rills were documented by a qualitative observation, the erosion in the larger watershed W03 was dominated by rill erosion, which was modeled (Figures 9 and 10) and also qualitatively observed after the event. Nevertheless, in W03 the sediment delivery for this largest event, representing 67% of total sediment delivery, was significantly underestimated. In case of event 228 a heavy rain (P = 107 mm; $I_{max10}$ = 13.2 mm h$^{-1}$) fall on

an erosion prone field shortly after potato harvest. Due to field operations during harvest the soil had nearly no cover (< 2%) and the soil was in a very erodible condition as it was sieved by the potato harvester thereby decreasing the stable aggregate diameter (e.g. a $D_{50}$ of 120 and 55 µm was measured before and after harvest, in 1995) (Fiener and Auerswald, 2007). Moreover, the VFS at the downslope end of the watershed was partly damaged due to repeated crossing with the potato harvester.

Under these specific conditions the model underestimates the sediment delivery by a factor of 2.3 which is probably caused by the static parameterization of soil and VFS properties. The difficulties to predict erosion and deposition accurately in case of event 228 is a major reason for the relatively low *MEF* of 0.62 and high *RMSE* of 238 kg ha$^{-1}$ for the erosion model validation, because both measures of goodness-of-fit are highly sensitive to the largest values of a comparison. The situation in case of event 228, especially the partly failure of the VFS, also points out a general problem in the parameterization of erosion models under very specific conditions, which are not properly monitored even at a research farm. This

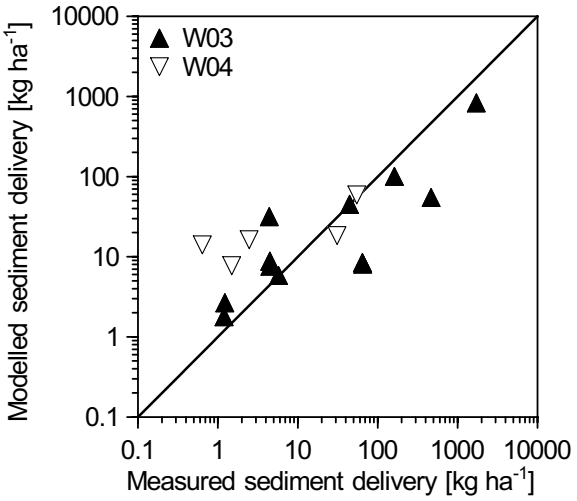


**Figure 8. Measured vs. modeled sediment delivery in watershed W03 and W04 for measured runoff events in watershed W03 ≥ 0.5 mm.**

**Table 3. Range of results for modeled effective discharge ($Q_{eff}$), sediment delivery, spatial proportion of erosion/deposition Domains, as well as total sediment delivery ratio ($SDR_{tot}$) for watersheds W03 and W04.**

| | Watershed W03 | | | Watershed W04 | | |
|---|---|---|---|---|---|---|
| | Max | Min | Average | Max | Min | Average |
| $Q_{eff}$ outlet (m$^3$ s$^{-1}$) | 0.0243 | 0.00 | 0.0088 | 0.0035 | 0.00 | 0.0016 |
| Sediment delivery (kg ha$^{-1}$) | 761.4 | 0.0 | 69.8 | 58.7 | 0.0 | 6.4 |
| Area of watershed in†: | | | | | | |
| Domain 1 (%) | 100.0 | 82.1 | 98.4 | 100.0 | 93.7 | 99.1 |
| Domain 2 (%) | 0.5 | 0.0 | 0.1 | 0.0 | 0.0 | 0.0 |
| Domain 3 (%) | 17.3 | 0.0 | 1.5 | 6.3 | 0.0 | 0.8 |
| Proportion of deposition in†: | | | | | | |
| Domain 1 (%) | 100.0 | 38.5 | 77.0 | 100.0 | 100.0 | 100.0 |
| Domain 2 (%) | 61.5 | 0.0 | 23.0 | 0.0 | 0.0 | 0.0 |
| $SDR_{total}$† | 0.52 | 0.15 | 0.34 | 0.29 | 0.15 | 0.22 |

† Results given for all events were a runoff > 0.0 was modeled

is even more problematic for optimized soil conservation systems, where larger events are rarer compared to conventional agriculture, and where these events more often occur in case of a partly failure of the conservation system, which is difficult to parameterize.

Considering the fact that soil erosion is an inherently variable phenomenon (e.g. Nearing, 1998), we may conclude that the MCST model yields promising results for conservation tillage. Nevertheless, further analysis of model uncertainties and further tests under different land management conditions must be carried out for an ongoing improvement of the model.

Rill erosion was qualitatively observed by regular field visits during the observation period (1994-2001), therefore the modeled rill erosion after large events along the thalweg of W03 and the near absence of rills in W04 could be confirmed. Moreover, as expected, modeled sedimentation in the VFS at the downslope end of the watersheds was indeed found in the field after the larger events.

Focusing on the model representation of the processes in the different domains (Figure 2, Table 3), most areas in both watersheds belong to Domain 1, representing sheet erosion and simple settling (average area in W03 and W04, 98.4 and 99.1% respectively). This indicates that in both watersheds sheet erosion is the dominant process during most events. Only for the larger events in W03 Domain 2 and 3 are more prominent (maximum: 17.3 and 0.5%, respectively). Despite the small area of the field experiencing re-entrainment (domain 2), domain 2 can dominate total deposition in W03 in case of large events (Table 3) and its explicit consideration may therefore improve modeling of sediment size-selective erosion and deposition in a watershed experiencing significant erosion. Re-entrainment in Domain 2 was not modeled for any of the 18 events in W04.

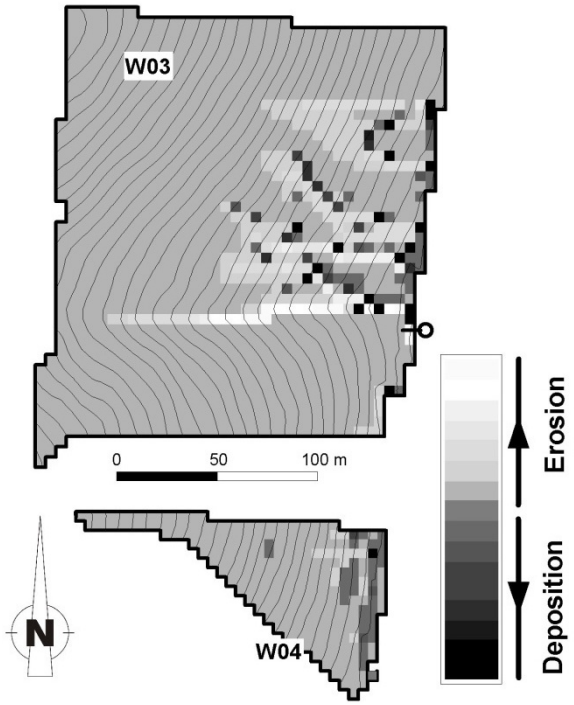


**Figure 9. Spatially distributed modeling of erosion and deposition in the watersheds W03 and W04 for event No. 228 occurred at the beginning of October 1998.**

Due to the fact that no detailed field surveys of changes in topsoil texture after erosion events were made, which would have been more or less impossible because of the small erosion and deposition amounts under the soil conservation system, it is not possi-

ble to compare measured and modeled patterns of clay, silt or sand enrichment within the watersheds. However, the enrichment of clay and organic matter in sediments leaving the watersheds was measured in all 16 watersheds (including the test-watersheds) of the Scheyern research farm in 1993 and 1994. From these data Auerswald and Weigand (1999) derived a relationship between enrichment of fines, total sediment delivery of an event and median texture in a watershed (Eq. 25).

$$\log(ER) = -0.27 + 0.45\ \log(D_{50}) - 0.05\ \log(SD) \qquad (R^2 = 0.51,\ n = 195) \qquad (25)$$

where $ER$ is the enrichment of clay and organic matter (-), $D_{50}$ is the median grain size (µm) of a watershed, and $SD$ is the sediment delivery (t ha$^{-1}$).

As Eq. 25 was derived from the tested watersheds and 14 others of similar scale (0.5 – 16 ha) we assume that it is reasonable to compare the results from Eq. 25 with the clay enrichment modeled by MCST (Figure 11). For total clay delivery the modeled clay enrichment fits very well with the results of the Auerswald and Weigand (1999) approach. This is a first indication that MCST is capable to predict clay enrichment in delivered sediments. As the enrichment of sediment bound nutrients and organic matter is often closely related to the enrichment of clay in delivered sediments (e.g. Auerswald and Weigand, 1999; Steegen et al., 2001) MCST also has, therefore, the potential to predict nutrient or organic matter delivery.

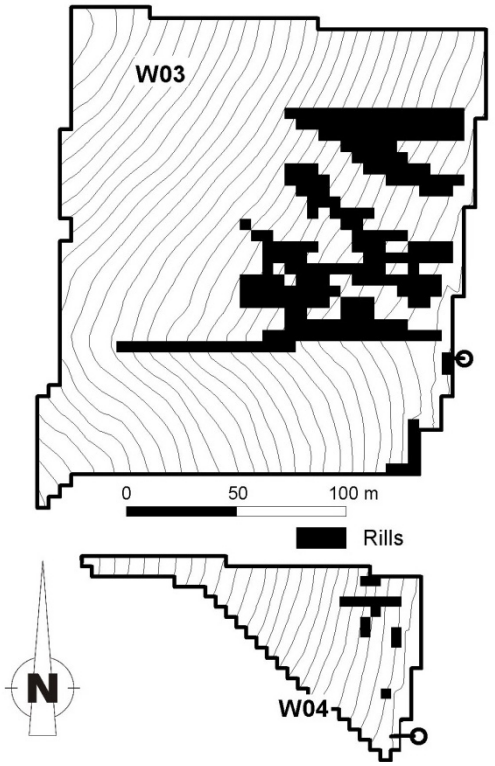


**Figure 10. Modeled rill pattern in the watersheds W03 and W04 for event No. 228 occurred at the beginning of October 1998.**

*Representation of soil conservation agriculture*

One of the main goals of this study was to test if the MCST model can adequately represent soil erosion and deposition under conservation agriculture. Therefore, the main aspects of soil conservation in fields, namely permanent soil cover, adapted crop rotation and minimum mechanical soil disturbance, as well as structural measures like reducing field sizes, VFS or grassed waterways were taken into account.

The aspects of cover management and adopted crop rotation are considered in MCST, as soil cover is one of the dominant parameters in the model. It affects (i) runoff formation, which was intensively tested in rainfall experiments (Auerswald and Haider, 1996; Schröder and Auerswald, 2000) used to modify the traditional *CN*-technique, (ii) runoff velocity, because of its dependence on hydraulic roughness and the decision between interrill and rill flow, (iii) peak discharge, which is reduced when runoff velocity decreases, and (iv) afterflow infiltration, which increases with decreasing runoff velocity. All these aspects have a strong impact on modeled runoff volume and peak discharge, this is illustrated for a range of surface covers in case of event 100 occurring in April 1994 (Table 4). For example, if the surface residue cover increases from 0 to 50% a decrease in runoff volume of 46% and in peak discharge of 57% is modeled.

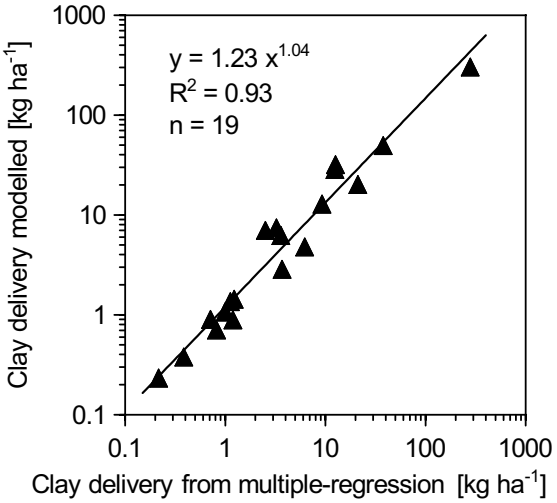


**Figure 11. Comparison between clay delivery calculated with a multiple-regression approach (Auerswald and Weigand, 1999) using modeled total sediment delivery and median sediment size in watershed W03 and W04 (Eq. 25) and the clay delivery due to the sediment size-selective modeling presented in this study.**

While modeled peak discharge is more or less linearly related to plant and plant residue cover, modeled sediment delivery is not (Figure 12). For example, if residue cover in case of event 100 increases from 0 to 5% (10% plant cover) the total sediment delivery decreases by 24% (134 kg) because no rills are modeled at the downslope end of the thalweg of W03. Hence, sediments are deposited instead of being delivered to the outlet. This indicates that the model is sensitive to slight changes in cover management, which can reduce total

**Table 4. Modeled effect of soil residue cover on Curve Number and hydraulic roughness (Manning's *n*), and hence on runoff volume, peak discharge and volume of afterflow infiltration shown for a 86.8 mm rain occurred on 12.-14/04/94 in watershed W03; for the calculations a constant plant cover of 20% is assumed.**

| Residue cover | Curve number | Manning's *n* | Runoff volume | | Peak discharge | | Afterflow infiltration | |
|---|---|---|---|---|---|---|---|---|
| [%] | | | [m³] | [%] | [m³ s⁻¹] | [%] | [m³] | [%] |
| 0 | 85 | 0.016 | 1350 | 100 | 0.063 | 100 | 73 | 5 |
| 10 | 84 | 0.031 | 1282 | 95 | 0.056 | 89 | 90 | 7 |
| 20 | 82 | 0.045 | 1166 | 86 | 0.049 | 78 | 101 | 9 |
| 30 | 80 | 0.057 | 1061 | 79 | 0.043 | 69 | 106 | 10 |
| 40 | 77 | 0.068 | 913 | 68 | 0.036 | 57 | 106 | 12 |
| 50 | 73 | 0.079 | 727 | 54 | 0.027 | 43 | 103 | 14 |

sediment delivery significantly. This was indeed the case for W03 where, in an 8-yr observation period, rills were most likely to occur in case of total cover failure (e.g. event No. 228) and nearly no rills have been observed as long as a small surface cover could be maintained.

In addition to the representation of soil cover, the MCST model also allows simulation of soil conservation measures like VFS or grassed waterways. By taking into account their high hydraulic roughness and infiltration capacity, the calculation of runoff velocity, run-on, afterflow infiltration, transport capacity and erodibility is modified. Minimum mechanical disturbance is only indirectly represented in the model by taking residues cover into account and by using a site-specific rill erodibility factor. The static parameterizations of site-specific soil properties inhibit the representation of seasonal or inter annual variations and long-term changes in soil structure. This can be problematic in case of rare specific soil conditions, e.g. the case of the largest erosion event during the 8-yr observation period (event No. 228, Figure 8), where the soil was strongly disturbed and disaggregated after potato harvest.

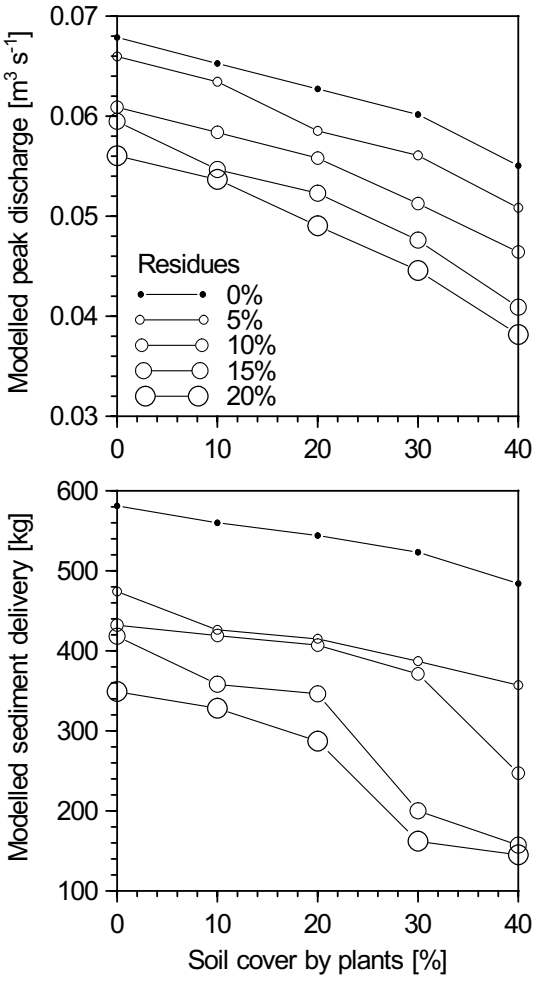


**Figure 12. Effects of changes in soil cover by plants and plant residues on modeled peak discharge and sediment delivery, exemplarily shown for event No. 100, which occurred in April 1994 (Table 2).**

The importance of low frequency, high magnitude events becomes relatively more important under conservation agriculture than under conventional agriculture as they occur only in the relatively short periods when the soil is unprotected, e.g. after potato harvest and damage of the VFS in watershed W03. Moreover, these rare events are often the result of site-specific conditions, which are extremely difficult to represent, e.g. the partial failure of the VFS in W03 in case of event No. 228.

One of the incentives to develop and test MCST was that erosion models often need a large number of parameters for which data are often not available. While MCST also still

needs a considerable number of parameter values: model behavior is still transparent as the role of the various parameters can be easily understood. An advantage of the model is also that many of its modules are based on existing model structures so that an estimate of most parameter values can be obtained from available literature, at least for silty loam soils. Its dynamic, 2D nature nevertheless implies that MCST is primarily aimed at applications in a research environment.

## CONCLUSIONS

The monitoring of runoff, sediment delivery and watershed characteristics clearly show that optimized soil conservation minimizes soil loss. Nevertheless, even under optimal soil conservation practices, soil protection is insufficient during short periods, e.g. shortly after potatoes harvest in case of the largest measured event, and large erosion and deposition events may occur. As these events are rarer compared to conventional agriculture, data sets covering longer periods of time are required to evaluate the erosion potential of a soil conservation system and to test the performance of models. The 8-yr data record used in this study provided a comprehensive basis for model testing and modification.

In this study a modified version of the MCST model was used. To consider soil conservation measures in the watersheds, effects of soil cover on runoff formation, runoff routing, run-on and afterflow infiltration as well as rill erosion were taken into account. Moreover, algorithms for interrill erosion, more prominent under soil-conservation, where rills can be widely prevented, were implemented.

Application of this modified MCST model indicated that in case of runoff events > 3 mm the model simulated runoff accurately, while for small events results are biased by the threshold behavior of the modified SCS-Curve Number technique and probably also by the dominant effects of runoff conservation structures like VFS, which are difficult to parameterize. As the larger events dominate the erosion and deposition within the watersheds the overall results of the runoff module are promising. Moreover, the relative simple model structure and the calibration results for $\lambda$ and $\alpha$ (Figure 5), which indicate that the modeled runoff is only slightly sensitive to $\alpha$ and the value of $\lambda$ can set to the SCS-*CN* standard value, warrant a wider applicability.

The model also showed reasonable results for sediment delivery (*MEF*=0.62; *n*=37), and for larger events, modeled interrill, rill and sedimentation patterns were confirmed by qualitative field observations. In most cases, soil conservation measurements were adequately represented in the model by taking into account the effects on soil plant and plant residue cover. In principle, the model is easy to use in other watersheds under soil conservation, where soil cover data can be estimated. However, better data on rill erodibility may be ne-

cessary as well as a better approach to predict the effect of vegetation cover on runoff hydraulics as it was recently shown that the approach developed by Gilley et al. (1991) may not always be applicable (Giménez and Govers, 2008).

The application also demonstrated some fundamental limitations to the modeling of single events: single events may play a very important role but characterization of the causative rare and site-specific soil conditions leading to high erosion rates can be extremely difficult.

The sediment size-specific modeling of deposition successfully reproduced the clay enrichment at the watershed outlet as proposed by a regression model developed at the research farm (Auerswald and Weigand, 1999). As such, the model is one of the first 2-D models to have the potential to dynamically model the delivery of sediment bound substances to water courses. The fact that space can be represented correctly in the model is essential: tillage direction as well as the presence of soil conservation structures cannot be accounted for when a 1-D hillslope profile approach is used.

# 8. INFLUENCE OF SCALE AND LAND USE PATTERN ON THE EFFICACY OF GRASSED WATERWAYS TO CONTROL RUNOFF

With minor revisions published:
Peter Fiener and Karl Auerswald (2006)
Rotation effects of potato, maize and winter wheat on soil erosion by water.
Ecological Engineering. 27: 208–218

***ABSTRACT**. Grassed waterways (GWWs) are established where runoff from arable land concentrates. They provide travel distances of some hundreds meters over hydraulically rough, flat-bottomed surfaces. Studies in small watersheds (< 100 ha) have demonstrated a large reduction in runoff volume and peak discharge but it is unknown to which extent large watersheds (> 1000 ha) also benefit from these effects, when other land uses than arable land also contribute and when travel time increases due to the increasing flow path length. We analyzed this by a modeling approach because controlled experiments can hardly be applied for large watersheds. Two summer, one prior and one after small grain harvest, and one winter condition and recurrence times of 2, 10, 20 and 50 yrs were taken into account. Land use was assumed to be either dominated by arable land (80%) or varying between sub-watersheds with arable land contributing only 45% on average. Under predominantly arable land use 2.3% of the total land was found suitable to be converted to GWWs, while for a diversified land use only 0.8% of the total land called for a GWW. For all conditions the efficacy of GWWs to reduce runoff volume and peak discharge decreased only slightly with increasing watershed size. Under arable land use and summer conditions runoff volume was reduced by about 30% and peak discharge by about 40% with somewhat higher values for more frequent storms and lower values for rare storms. The efficacy was considerably lower under winter conditions and for a diversified land use where only a small proportion of GWWs was assumed. Runoff reduction was affected more and may drop below 5% under unfavorable conditions (low GWW percentage, winter, large events) while still a reduction in peak discharge of at least 15% was observed even under most of the unfavorable conditions despite a loss of land of only 0.8%. GWWs hence contribute considerably to flood control even in watersheds larger than 1000 ha and especially when summer floods are the main problem.*

Flooding of private properties and public infrastructure is a common problem in agricultural watersheds (Bielders et al., 2003). Several studies have been undertaken in the last decades pertaining to the occurrence of (muddy-) flooding and related damages in specific agricultural regions throughout Europe, i.e. South Downs in the UK (Boardman et al., 1994),

the Pay the Caux in France (Papy and Douyer, 1991) and central Belgium (Bielders et al., 2003; Verstraeten et al., 2003).

To treat these problems grass has been widely used to control runoff and sediment delivery. Plot and field studies have been carried out to quantify sediment trapping and runoff control in vegetative filter strips (VFSs) (Barfield et al., 1998; Chaubey et al., 1994; 1995; Le Bissonnais et al., 2004; Schmitt et al., 1999; Syversen, 2005; Syversen and Borch, 2005). Depending on experimental setups the runoff reduction of the VFSs varied between 6% (Chaubey et al., 1994) and 89% (Schmitt et al., 1999). In most cases only low-volume sheet flow in the VFSs was tested and hence the results can hardly be extrapolated to VFS located along streams, where storm runoff enters as concentrated flow and leaves the grassed area again after some 10 m. Studies evaluating the effects of VFS on a watershed scale are rare and show a decrease in VFS efficiency with increasing scale, due to runoff concentration and bypassing of VFS (Verstraeten et al., 2006).

In contrast to VFS, grassed waterways (GWWs) are established only where runoff concentrates and provide travel distances of some hundred meters. The efficiency of GWWs in reducing runoff has been investigated only in a few studies (Briggs et al., 1999; Chow et al., 1999; Fiener and Auerswald, 2003b; 2003a; 2006). Briggs et al. (1999), for example, found a runoff reduction of 47% by a GWW in a laboratory experiment, but their experimental setup was similar to that of many VFS experiments. In a landscape experiment where potato production with commonly up-and-down slope cultivation was compared to combined terraces-GWW systems, the average runoff was reduced by 86% after establishing the terraces-GWW systems (Chow et al., 1999). Fiener and Auerswald (2003a) found a runoff reduction of 8% and 91% for two GWWs tested in an 8-yr landscape experiment. Moreover, there were some physically based modeling approaches dealing with runoff over grassed surfaces (Deletic, 2001; Fiener and Auerswald, 2005; Munoz-Carpena et al., 1999), whereby Fiener and Auerswald (2005) focused explicitly on the concentrated flow in GWWs. These authors found that the main GWW characteristics governing its runoff control efficiency were its length, a flat-bottomed cross-section, and the hydraulic roughness of the vegetation in dependency of flow depth.

The high efficacy found in these studies may be misleading, because in larger watersheds only some parts are suitable for the establishment of a GWW, thus decreasing the overall effect of the GWW. Furthermore, runoff travel time generally increases with increasing watershed size. A given increase in travel time caused by a GWW will thus lose relative importance with increasing watershed size. Despite the convincing results on the effects of GWWs on small (< 100 ha) watersheds, large caveats exist regarding their effect on large (> 1000 ha) watersheds. This would call for a long-term examination of their effect in large water-

sheds. That kind of controlled experiment (e.g., Loftis et al., 2001) is not always practical in larger watersheds due to high costs and the problem of finding a pair of similar watersheds which can be calibrated during a pretreatment period. Therefore, modeling is the first choice. The difficulty arises that the modeling has to be able to handle a large, heterogeneous watershed, which calls for simplicity in the modeling approach, but on the other hand it has to be detailed enough to consider small landscape elements like GWWs and their determinants.

Here we use such a modeling approach to test the hypothesis that the efficacy of establishing GWWs changes with scale and with land use pattern.

## MATERIALS AND METHODS

### Test site

The Lauterbach watershed is located in North Rhine-Westphalia, Germany, about 10 km East of Bonn. The hilly area is part of the foothills of the Rheinisches Schiefergebirge (Rhenian Slate Mountains) and is draining into the river Sieg. The watershed covers an area of approximately 16.7 $km^2$ at an altitude of 69–321 m a.s.l. (50°44' N, 7°12' E). The mean annual air temperature, measured at a meteorological station about 15 km northeast of the watershed at 195m a.s.l., was 10.2 °C (for 1993–2003). The average precipitation per year was 1027 mm (for 1993–2003) with the highest precipitation intensities per day occurring from May to October (maximum 52.4 mm $d^{-1}$ occurring in June 1998).

Due to its fertile, loess–containing silty and silty loamy soils and its proximity to the agglomeration of Cologne-Bonn, most of the area is intensively used for arable agriculture competing with expanding residential areas in the villages. On the steeper slopes mainly located in the Southern

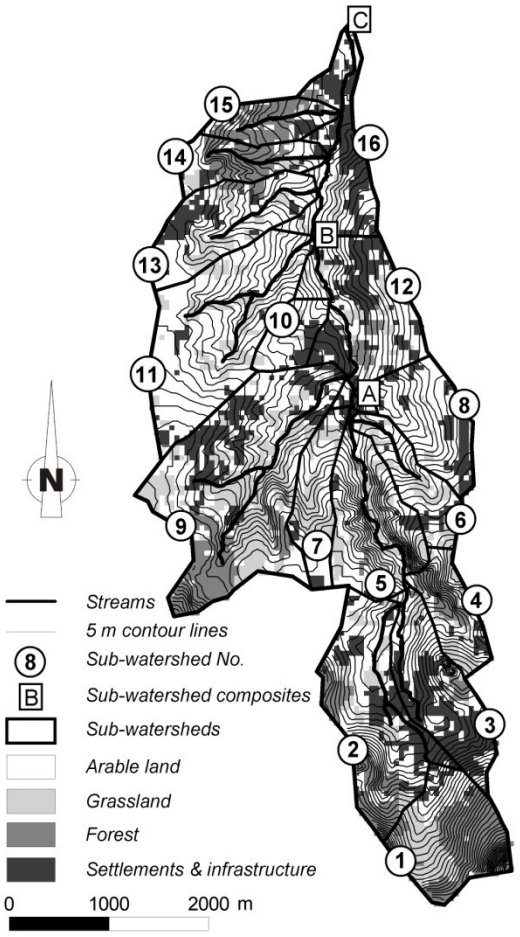


**Figure 1: Topography and land use of the Lauterbach watershed; land use determined from Landsat TM scenes of April and July 2003; numbers indicate the different sub-watersheds, while letters (A-C) indicate points along the Lauterbach used to calculate runoff from a combination of the upstream sub-watershed.**

**Table 1. Land use in the Lauterbach watershed and the Dissenbach sub-watershed determined from Landsat TM scenes of April and July 2003.**

| Arable land | | Grass land | Forests | Settlements and infrastructure |
|---|---|---|---|---|
| Small grains | Row crops | | | |
| Lauterbach watershed (= diversified land use) | | | | |
| 31% | 14% | 21% | 14% | 20% |
| Dissenbach sub-watershed (= predominantly arable land use) | | | | |
| 59% | 21% | 16% | 0% | 4% |

part of the watershed grassland, forests as well as settlements can be found (Figure 1, Table 1). Small grains were cultivated on 69% of the arable land, dominated by wheat (*Triticum aestivum* L.) and barley (*Hordeum vulgare* L.). On the remaining 31%, row crops were planted, mainly sugar beets (*Beta vulgaris* L.) and maize (*Zea mays* L.), as well as some potatoes (*Solanum tuberosum* L.).

## Modeling

Runoff volume and peak discharge were modeled in 16 subwatersheds (37–272 ha in size) according to a modified SCS curve number (*CN*) technique in combination with a runoff travel time estimation and the graphical discharge method (USDA-SCS, 1986). To simulate the runoff at three locations along the Lauterbach (Figure 1, points A–C), describing composite watersheds of about 700–1700 ha, the runoff from the subwatersheds was routed in the Lauterbach using Manning's equation. In more complex and sophisticated grid-based models, flow depth and flow velocity depends on the grid cell size used for modeling the watershed. In our case this approach is not satisfying, because the effect of GWWs must take into account the cross-section and roughness along the drainage line. Our approach, which is simpler in concept, allows focusing on GWWs as individual landscape structures, rather than an ill-defined subset of raster grid cells.

The standard SCS-*CN* approach (e.g., Mockus, 1972; USDA-SCS, 1986) was modified to take into account: (i) the seasonal variation in runoff generation in the draining fields, and (ii) the location of a GWW in a watershed as well as its high infiltration capacity and hydraulic roughness, which prolongs runoff travel time after the end of a rain event. The seasonal variability in runoff generation was introduced in the standard *CN*-technique by taking the seasonal variability of soil cover and soil crusting into account (Van Oost, 2003) [Eq. (1)]:

$$CN = CN_{\max} - \left(\frac{Cc}{100} \cdot c_1\right) + \left(\frac{CR}{5} \cdot c_2\right) \quad (1)$$

where $CN_{\max}$ is the maximum *CN* derived from the USDA SCS handbook (1986), *Cc* the crop cover percentage, *CR* the crusting stage (0 =no crusting, 5 =max crusting) and $c_1$ and $c_2$ are coefficients.

The value of $c_1$ is set to get a *CN* equal to the minimum *CN* for a given crop-soil combination when the crop cover equals 100% and $c_2$ is set to reach a *CN* equal to the value for a fallow soil surface when the crop cover equals 0%. The values of $CN_{\max}$, $c_1$ and $c_2$ depend on the soil type and land use or cover, for the test site values are summarized in Table 2. In general, the *CN* values in the approach developed by Van Oost (2003) are only manipulated in the boundaries of the *CN* values used in the extensively tested original USDA SCS model. To examine the effects of GWWs for different watershed conditions two summer and one winter situation was modeled. The first summer modeling was carried out for typical July field conditions prior to the harvest of small grains (subsequently referred as summer prior to small grain harvest). For this situation an average soil cover of 80% and a crusting stage of 2.5 were assumed for all fields. The second summer model exercise represents the watershed conditions in August after harvest of small grains (subsequently referred as summer after harvest of small grains). In case of the August model runs again a soil cover of 80% and a crusting stage of 2.5 were assumed for the row corps. Following German agricultural statistics (INVEKOS inventory; Auerswald et al., 2003), on about 2/3 of the fields intercrops are planted after small grain harvest and therefore a soil cover of 60% and a crusting stage of 3 was adopted, while 1/3 of the harvested fields were assumed to be bare, hence for those a soil cover of 20% and a crusting stage of 5 was used. For the winter situation model runs were carried out with a soil cover of 10% and a crusting stage of 5. Moreover, for the summer events dry conditions with an antecedent moisture condition I (AMC I) were assumed and hence *CN*s from Eq. (1) were modified by Eq. (2). Analogously for wet conditions in the winter half-year the *CN*s from Eq. (1) were modified using Eq. (3) (Chow et al., 1988):

**Table 2. Parameter values for *CNmax*, $c_1$ and $c_2$.**

| Cover | $CN_{max}$ | $c_1$ | $c_2$ |
|---|---|---|---|
| Row crops | 88 | 6 | 3 |
| Small grains | 85 | 8 | 3 |

$$CN_I = 4.2 \cdot \frac{CN_{II}}{10 - 0.058 \cdot CN_{II}} \quad (2)$$

$$CN_{III} = 23 \cdot \frac{CN_{II}}{10 - 0.13 \cdot CN_{II}} \quad (3)$$

where $CN_I$, $CN_{II}$ and $CN_{III}$ were the *CN*s for AMC I, AMC II and AMC III, respectively.

The two summer and winter conditions thus covered about the whole range, which can realistically be expected as an average for a mesoscale watershed. Nevertheless, there might be more extreme conditions on single fields or small sub-watersheds, which were not addressed with the presented modeling exercise due to its focus on mesoscale effects of GWWs. Based on the calculated runoff volumes, peak discharge in all sub-watersheds was estimated according to SCS standard procedures (USDA-SCS, 1986), by calculating runoff travel time and using the graphical discharge method. We only modified the travel time estimation by replacing the empirical equation for shallow concentrated flow along drainage lines by the Manning's equation. For an idealized cross-section of a GWW (Figure 2), Manning's equation can be rearranged as

$$q = \frac{1}{n} \cdot S^{1/2} \cdot \left(\frac{D}{2}\right)^{8/3} \cdot \frac{4}{\tan \alpha} \quad (4)$$

where $q$ is the discharge ($m^3\ s^{-1}$), $n$ the Manning's roughness coefficient ($s\ m^{-1/3}$) dependent on soil surface conditions and vegetative cover, $S$ the slope along the drainage line, $D$ the runoff depth (m), and $\alpha$ is the side-slope of the drainage line.

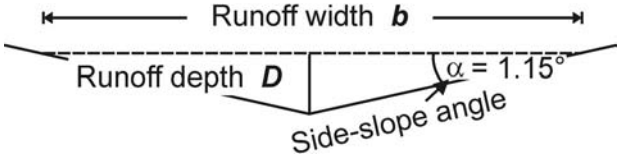


**Figure 2: Idealized cross section of modeled grassed waterways according to Fiener and Auerswald (2005).**

The average runoff depth ($D$/2) along the main drainage line of each sub-watershed was simulated for the different storms with the model. Therefore, the peak discharge mid-slope of each drainage line with a potential GWW was calculated and $D$/2 was derived from Eq. (4) and the idealized cross-section (Figure 2). The idealized cross-section, with a side-slope $\alpha$ of 1.15° was adopted from field measurements (Fiener and Auerswald, 2003a) and a physically based modeling of concentrated runoff in GWWs (Fiener and Auerswald, 2005), which underline the importance of a flat-bottomed cross-section for GWW efficiency. Based on field experiences the width of the modeled GWWs was set generally to 15 m.

A dense vegetation of typical agricultural grasses, e.g. *Elytrigia repens* L., *Dactylis glomerata* L., *Arrhenatherum elatius* L., and herbs, e.g. *Epilobium angustifolium* L., *Galeopsis aparine* L., which are mowed only once a year or let to succession was assumed in all simulations. They are typical for GWWs and measurements of hydraulic roughness carried out during field experiments can be adopted (Fiener and Auerswald, 2005). Provided vegetation in the GWWs is not flattened by high runoff velocities, a Manning's $n$ of 0.35 m $s^{-1/3}$ (e.g., Fiener and Auerswald, 2005; Jin et al., 2000) was used. Where vegetation was flattened, values of 0.05–0.01 m $s^{-1/3}$ were assumed (e.g., Kouwen, 1992). To determine the runoff depth where a failure of vegetation can be assumed we adopted an approach developed by Kouwen and Li (1980), calculating a minimum critical shear velocity $v_{crit}$ (m $s^{-1}$). This critical shear velocity depends on a combined effect of vegetation density, stiffness, and length represented by the flexural rigidity per square meter. The flexural rigidity was measured exemplarily for two grassed waterways, one let to succession the other mowed once a year (Fiener and Auerswald, 2006), applying a simple field test (Eastgate, 1969; Kouwen et al., 1981). From the critical shear velocity the critical runoff depth $D_{crit}$ (m) was calculated:

$$D_{crit} = \frac{v_{crit}^2}{g \cdot S} \tag{5}$$

where $g$ is acceleration due to gravity (m $s^{-2}$), and $S$ is the slope along the drainage line of the tested GWWs.

Combining the critical shear velocities derived from 1 yr of bi-weekly measurements (2002–2003) at 21 locations within two GWWs in Bavaria (winter: average AVR $v_{crit}$ = 0.221 m $s^{-1}$, standard deviation SD = 0.023 m $s^{-1}$; summer: AVR $v_{crit}$ = 0.276 m $s^{-1}$, SD = 0.027 m $s^{-1}$) (Fiener and Auerswald, 2006), with the slopes along the drainage lines of the potential GWWs in the Lauterbach watershed allowed to estimate $D_{crit}$. For the winter half-year on average it was 0.10 m ranging from 0.14 m for gentle slopes (3.4%) to 0.05 m for the steepest slopes (9.8%). In the summer half-year the average was 0.15m with a range between 0.23 and 0.08 m. According to these results we assumed in the modeling exercise that vegetation fails when average runoff depth in the GWWs exceeds 0.10 m in winter and 0.15 m in summer.

To take into account the high infiltration capacity and the location of the GWWs within the sub-watersheds, we estimated the amount of runoff infiltrating into the GWWs. In cases of runoff generation in the fields but not in the GWWs, the total runoff volume of the sub-watersheds was reduced by the difference between initial abstraction of the *CN*-model and rain amount in the GWWs. Moreover, the GWWs prolong runoff after the end of a rain event

compared to drainage lines without GWW, hence afterflow infiltration also increases. Based on extensive field observations and experiments with concentrated flow in two ca. 300 m long GWWs (Fiener and Auerswald, 2003a; 2005) we assumed ½ h additional afterflow infiltration per 100 m GWW length along the drainage line. As this occurs mainly in the area of concentrated flow of the GWWs, only half of the GWWs area was taken into account for afterflow infiltration. An infiltration rate of $5\times10^{-6}$ m $s^{-1}$ was assumed typical for saturated colluvial soils found along drainage lines (e.g., Blume et al., 2002).

The modeled peak discharge of each of the 15 subwatersheds was routed to the outlet of the Lauterbach watershed using the Manning's equation assuming board-full runoff within the Lauterbach (USDA-SCS, 1986). Therefore, information about the cross-section was derived from field surveys and from data of local water authorities.

**Modeled land use**

To simulate runoff and peak discharge reduction under different boundary conditions 24-h rains with a recurrence time of 2, 10, 20, and 50 yrs were applied. The 24-h rains were used under the focus of mesoscale watersheds, which typically show a similar time of runoff concentration. The rain amounts for the Lauterbach watershed were taken from regionalized maps of the National German Weather Service (DWD) presented in an 8.5 km×8.5 km grid (Bartels et al., 1997). The higher rain intensities per day measured at the meteorological station Northeast of the watershed between May and October (for 1993–2003), were confirmed by the DWD maps. Therefore, different rain intensities for the summer and winter half-year were used (Table 3).

For the field management in the watershed we assumed that all fields were planted in slope direction and no cover crops, e.g. mustard (*Sinapis alba* L.), were cultivated for soil conservation during winter. This results in a conservative estimate of the GWWs runoff control because a smaller inflow due to water-conservation measures in the watershed would increase effectiveness (Fiener and Auerswald, 2005).

**Table 3. Size of 24-h rainstorms at the test site in winter (October-April) and summer (May-September); data adopted from Bartels et al. (1997).**

| | 24-h precipitation [mm] | |
|---|---|---|
| Recurrence time [yr] | Winter (January) | Summer (July/August) |
| 2 | 30.1 | 41.2 |
| 10 | 36.3 | 61.3 |
| 20 | 38.9 | 69.9 |
| 50 | 42.4 | 81.3 |

In general the model was tested under two land use settings to evaluate the runoff control effectiveness of potential GWWs in the mesoscale Lauterbach watershed. (1) A land use dominated by arable land, which allows establishing GWWs along all drainage lines. The proportion of different agricultural land uses of this setting was taken from the Dissenbach sub-watershed

(Watershed no. 11 in Figure 1, Table 1), which is dominated by arable land. Subsequently, this land use setting is referred as predominantly arable land use. This land use was designed to determine whether there is a scale effect in runoff control moving from small agricultural watersheds, where measurements of GWW efficiency exist, to a mesoscale watershed. (2) The existing land use pattern differing between sub-watersheds was used and GWWs were established only along drainage lines where arable fields are located. Hence, the potential GWWs were widely limited to the Northern part of the watershed (Figure 3). This land use is subsequently referred as diversified land use. Comparing both land use settings allows distinguishing between land use and scale effects in case of up-scaling the efficiency in runoff control of GWWs. In both land use settings 15 m wide GWWs were assumed along drainage lines draining at least 5 ha. The locations of the GWWs were determined using a 50m×50m digital elevation model (DEM) and calculating an artificial stream network for all sub-watersheds draining at least 5 ha with an algorithm included in a the USDA Soil & Water Assessment Tool interface AVSWAT (Di Luzio et al., 2002) for Arc View 3.2 (Esri Inc., Redlands, California). Moreover, the length and slope of each potential GWW was calculated from the DEM and was used individually for modeling runoff travel time in each subwatershed. Thus, two land use settings (predominantly arable/diversified), three surface conditions (summer before and after harvest, winter) and four rain recurrence conditions (2, 10, 20, 50 yrs) were evaluated for the 16 sub-watersheds and three locations along the main watercourse.

## RESULTS

### Area demand

Under the predominantly arable land use only one subwatershed did not allow to establish a GWW due to a steep (> 10%) main drainage line. In the other sub-watersheds the GWWs occupied between 1.3% and 4.2% of the land, with an average for the whole Lauterbach watershed of 2.3% or 37.7 ha (Table 4). The individual length of the GWWs varied from 140 to 1680 m.

Under diversified land use GWWs were mainly established in the northern part of the watershed (Figure 3), which is dominated by arable land. While in seven sub-watersheds no GWW was modeled, GWWs occupied between 0.2% and 3.6% of the other sub-watershed areas. Within the total Lauterbach watershed 0.8% (12.5 ha) of the area was converted to GWWs (Table 4). The length of the GWWs varied from 120 to 1360 m. Under predominantly arable land use the GWW area was about 3-times larger than the area commonly recommended for vegetative filter strips beside third order streams, which would be 2m×10m×6700 m (13.4 ha) in case of the Lauterbach. Under diversified land use the GWW

area was smaller than the commonly recommended area for the vegetative filter strips along the Lauterbach.

**Effect during summer runoff**

Inflow volumes mid-slope of the GWWs in case of 50-yr summer storms after small grain harvest, which produce in general larger inflows than prior to small grain harvest, ranged between 1100 and 6310 $m^3$ for the predominantly arable land use with maximum inflow rates from 0.08 to 0.28 $m^3$ $s^{-1}$. Therefore, the average runoff depths of 0.06–0.10 m were always below the critical runoff depth of 0.15m in summer, and hence no vegetation failure is expected. In addition, no failure of vegetation is expected for summer storms under diversified land use.

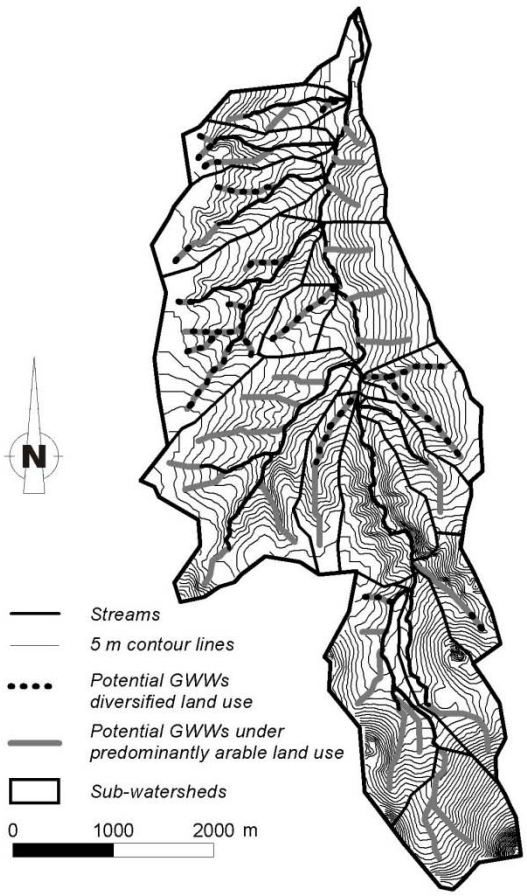


**Figure 3: Potential grassed waterways (GWWs) in the Lauterbach watershed under predominantly arable land use in all sub-watersheds and diversified land use.**

Runoff reduction by GWWs is generally governed by storm size and GWW area (Figures. 4 and 5, left). Under predominantly arable land use, in case of the smallest modeled runoffs (10-yr summer storm prior to small grain harvest), their effect in the different sub-watersheds ranged from 19% (subwatershed no. 12, 1.4% GWW area, runoff reduction 1714 $m^3$) to 88% (sub-watershed no. 7, 4.2% GWW area, runoff reduction 3296 $m^3$), while for the largest runoffs (10-yr winter storm) it was between 3% (sub-watershed no. 16, 1.5% GWW area, runoff reduction 524 $m^3$) and 21% (sub-watershed no. 7, runoff reduction 2783 $m^3$). Compared to the runoff reduction efficiency of 91% determined for a 7.8 ha watershed under soil conservation agriculture, with a 1.07 ha grassed waterway similar in cross-section and vegetation (Fiener and Auerswald, 2003b), the modeled efficiencies were clearly smaller, but seemed to be reason able due to the smaller GWW area proportion, the larger watershed sizes and the conventional agriculture, which both increase inflow volumes.

**Table 4. Area of sub-watersheds (No 1- 16) and composite watersheds (Figure 1, points A-C); length and area of potential GWWs for the modeled land use.**

| | | Diversified land use | | Predominantly arable land use | |
|---|---|---|---|---|---|
| Watershed No | Watershed area [ha] | GWWs length [m] | GWWs area [%] | GWWs length [m] | GWWs area [%] |
| 1 | 108.4 | 0 | 0.0 | 1802 | 2.5 |
| 2 | 267.3 | 294 | 0.2 | 4481 | 2.5 |
| 3 | 102.2 | 0 | 0.0 | 873 | 1.3 |
| 4 | 52.9 | 229 | 0.7 | 984 | 2.8 |
| 5 | 115.7 | 0 | 0.0 | 0 | 0.0 |
| 6 | 55.6 | 0 | 0.0 | 550 | 1.5 |
| 7 | 59.6 | 730 | 1.8 | 1674 | 4.2 |
| 8 | 79.5 | 1922 | 3.6 | 1922 | 3.6 |
| 9 | 272.3 | 0 | 0.0 | 3982 | 2.2 |
| 10 | 36.9 | 849 | 3.5 | 849 | 3.5 |
| 11 | 194.0 | 2833 | 2.2 | 2833 | 2.2 |
| 12 | 144.0 | 0 | 0.0 | 1314 | 1.4 |
| 13 | 102.2 | 825 | 1.2 | 1178 | 1.7 |
| 14 | 54.8 | 524 | 1.4 | 1107 | 3.0 |
| 15 | 45.4 | 189 | 0.6 | 705 | 2.3 |
| 16 | 87.4 | 0 | 0.0 | 899 | 1.5 |
| A | 653.4 | 1253 | 0.3 | 10364 | 2.4 |
| B | 1380.2 | 6857 | 0.8 | 21264 | 2.3 |
| C | 1670.1 | 8395 | 0.8 | 25153 | 2.3 |

For the total Lauterbach watershed runoff reduction was 2.6-times more efficient under predominantly arable land use (Figure 4, left), which allowed GWWs on 2.3% of the watershed area, than under the diversified land use (Figure 5, left), where GWWs occupied 0.8% of the area. Runoff reduction by GWWs in mesoscale watersheds is prominent in case of summer storms, which produce little runoff due to high soil cover and low crusting.

Compared to runoff reduction the efficiency of GWWs to lower peak discharge decreased less with storm size (Figures. 4–5, right). An exception was the 10-yr summer storm prior to small grain harvest, where peak discharge was strongly affected by a runoff reduction > 60% in some sub-watersheds.

Under predominantly arable land use the GWWs reduced peak discharge for the largest applied storms in summer (50-yr storm) between 30% (sub-watershed no. 16, storm after small grain harvest) and 59% (sub-watershed no. 8, storm prior to small grain harvest) (Figure 4, right). For the total Lauterbach watershed peak discharge was at least reduced by 41% in case of predominantly arable land use and by 16% for the diversified land use (50-yr summer storm after small grain harvest). In general, there was only a minor difference in peak discharge reduction between the modeled summer storms prior and after small grain harvest, because the additional inflow after small grain harvest was relatively small.

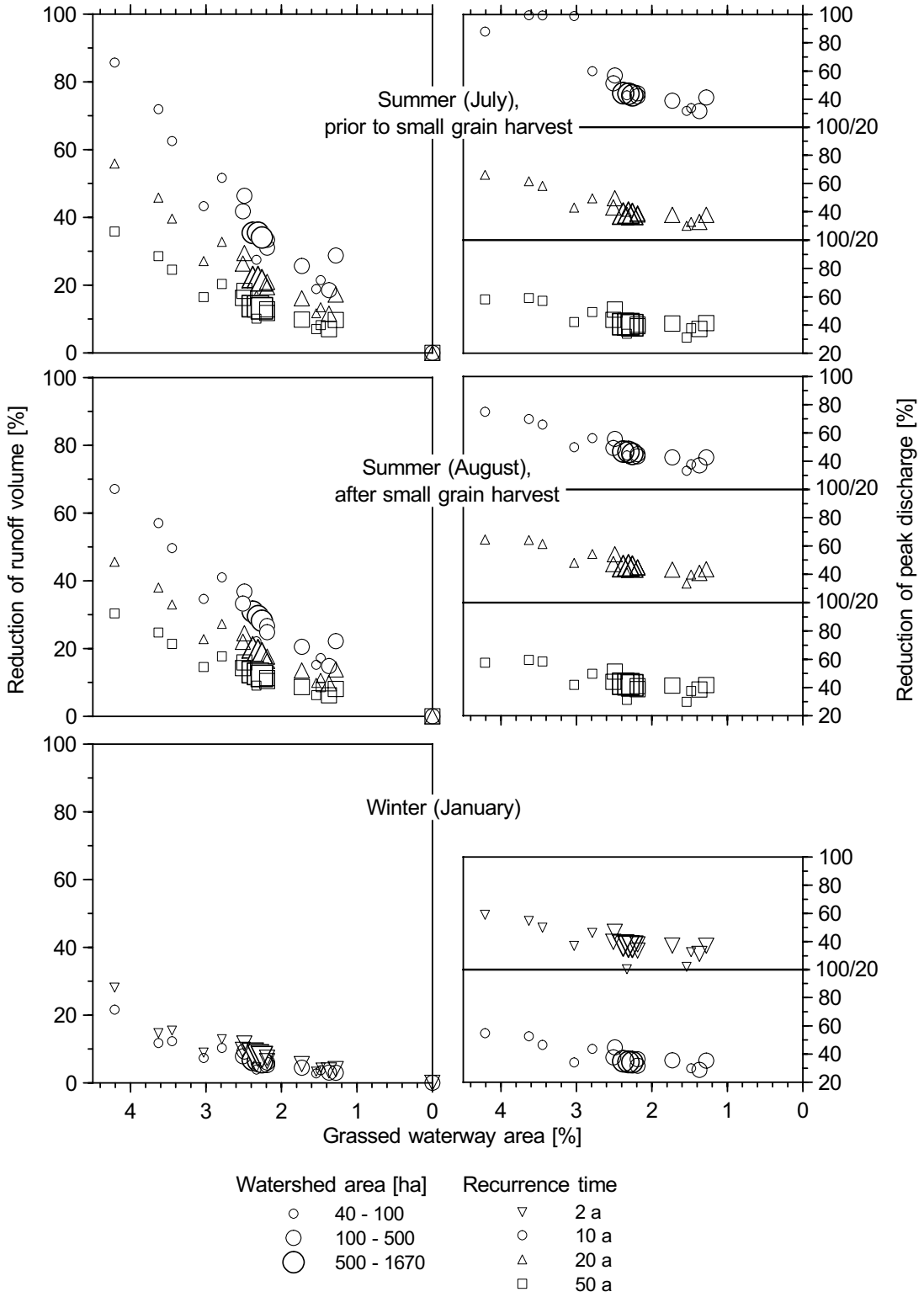


**Figure 4: Modeled reduction of runoff volume (left) and peak discharge (right) for 24-h storms for a predominantly arable land use; grassed waterways assumed in all sub-watersheds except No 5, where the drainage line was steeper than 10%; note for summer storms recurrence times of 10-50 yrs (no runoff in case of 2-yr storms), while for winter events recurrence times of 2-10 yrs are presented; winter storms > 10 yrs are excluded due to unknown vegetation behavior.**

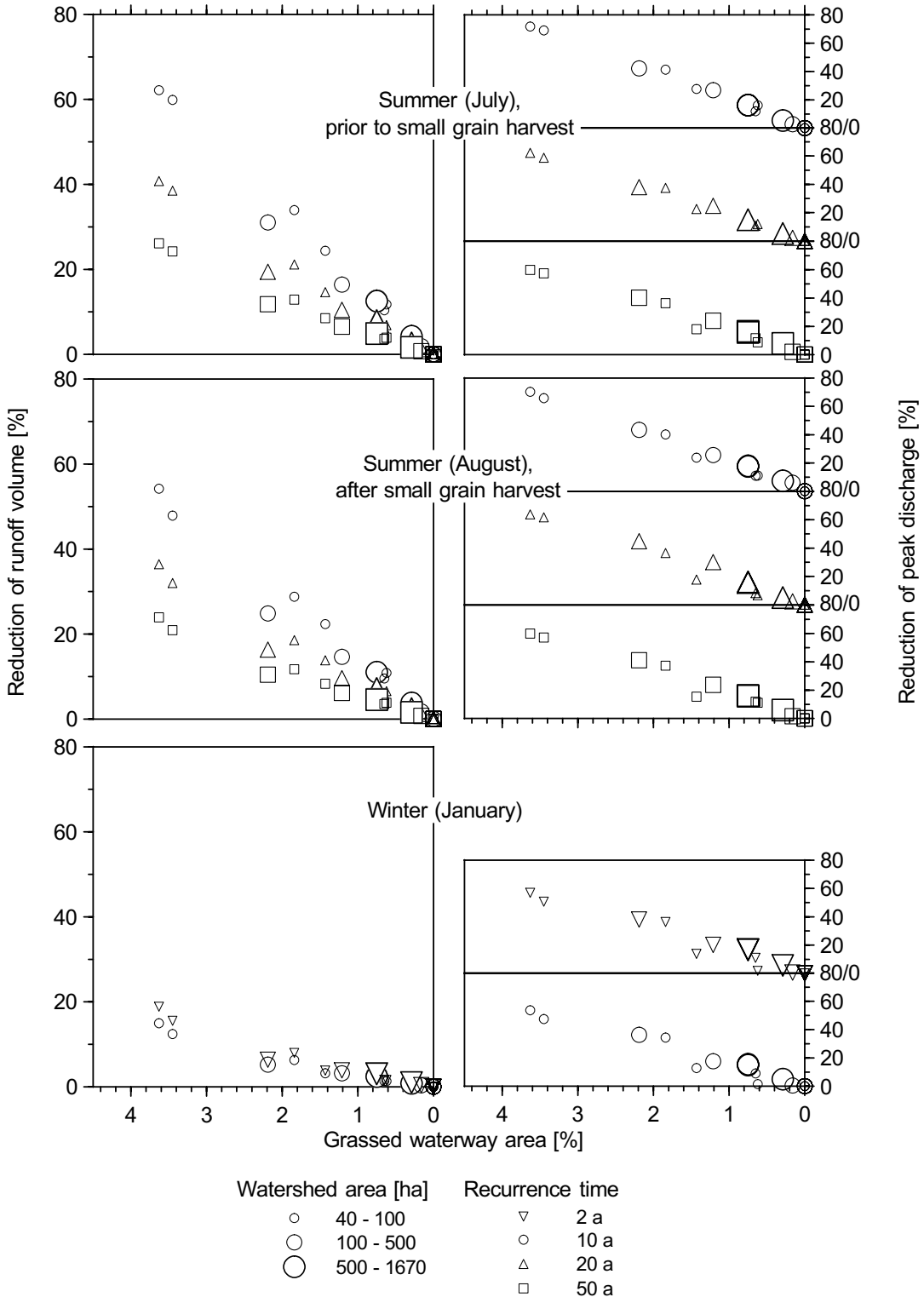


**Figure 5: Modeled reduction of runoff volume (left) and peak discharge (right) for 24-h storms for a diversified land use; grassed waterways assumed where ever possible due to topography and land use; note for summer storms recurrence times of 10-50-yrs (no runoff in case of 2-yr storms), while for winter events recurrence times of 2-10-yrs are presented; winter storms > 10-yr are excluded due to unknown vegetation behavior.**

**Effect during winter runoff**

The modeled winter events produced generally more runoff than the summer storms of equal recurrence time, even if applied summer storms are larger (Table 3). This results from insufficient cover and increased crusting on arable land in winter. Inflow volumes mid-slope of the GWWs ranged from 1430 to 8170 $m^3$ for 10-yr winter storms under predominantly arable land use, depending on sub-watershed size and GWW proportion. Taking into account gradient and length of the drainage lines simulated maximum inflow rates were 0.18-0.61 $m^3 s^{-1}$. Calculated average runoff depth for this storm size varied between 0.07 and 0.13 m. Due to high inflow rates and reduced flexural rigidity of the vegetation in winter, the average runoff depth for the 10-yr storms in case of the predominantly arable land use exceeded the critical runoff depth of 0.10 m in 5 of the 16 sub-watersheds. For the 2-yr storm this happened in one case. High runoff depths were mainly modeled in subwatersheds with long GWWs draining relatively large areas (e.g., sub-watershed no. 1 or 7), hence in case of the diversified land use the vegetation failed only in four sub-watersheds for the 10-yr winter storm. An average maximum runoff depth, which exceeds the critical runoff depth, will not automatically lead to a total failure of a GWW in increasing runoff travel time, because these high rates will not occur along the total drainage line and only after some time. Moreover, a GWW will still prevent gully erosion and the concentration of runoff within the gully by maintaining a flat-bottomed cross-section of the flow path. To take such a failure into account a more sophisticated spatially and temporally distributed model dealing with concentrated flow and gully erosion along the drainage lines would be necessary and the behavior of the vegetation after being once bent to the ground must be known. With the conceptual approach presented here this is impossible and hence winter storms with a recurrence time > 10-yr were excluded due to an increasing uncertainty because of unknown vegetation behavior. However, with a GWW management that increases flexural rigidity, e.g. by allowing succession of woody plants, a better performance during winter and rare storms can be expected although experimental evidence is missing.

Under predominantly arable land use, in case of 2-yr winter storms, the runoff reduction efficiency of the GWWs in the different sub-watersheds ranged from 3.3% (sub-watershed no. 16) to 28.1% (sub-watershed no. 7), while for the 10-yr storms it was between 2.8% and 21.6% (Figure 4, left). For the total Lauterbach watershed runoff reduction was about 2.5-times more efficient under predominantly arable compared to diversified land use (Figures 4 and 5, left).

**Table 5. Modeled runoff for different 24-h rainstorms for winter (January) and summer (July, August) events; winter storms > 10-yr not simulated due to unknown vegetation behavior.**

| | Predominantly arable land use | | | | | | Diversified land use | | | | | |
|---|---|---|---|---|---|---|---|---|---|---|---|---|
| | Winter | | Summer, prior to small grain harvest | | Summer, after small grain harvest | | Winter | | Summer, prior to small grain harvest | | Summer, after small grain harvest | |
| Storm recurrence time [yr] | without GWW† | with GWW | without GWW | with GWW | without GWW | with GWW | without GWW | with GWW | without GWW | with GWW | without GWW | with GWW |
| 2 | 16.3 | 15.1 | 1.2 | 0.0 | 1.5 | 0.0 | 14.4 | 13.8 | 1.0 | 0.0 | 1.2 | 0.0 |
| 10 | 21.6 | 20.4 | 6.5 | 4.3 | 8.3 | 6.0 | 19.4 | 19.0 | 6.2 | 5.4 | 7.2 | 6.4 |
| 20 | - | - | 9.7 | 7.6 | 12.1 | 9.8 | - | - | 9.3 | 8.6 | 10.5 | 9.8 |
| 50 | - | - | 14.7 | 12.8 | 17.7 | 15.6 | - | - | 14.1 | 13.4 | 15.7 | 15.0 |

†GWW = grassed waterway;

Similar to summer events, peak discharge decreased less with increasing storm size (Figures 4 and 5, right). Under predominantly arable land use GWWs reduced peak discharge for the largest applied winter storm (10-yr storm) between 19% (subwatershed no. 15) and 55% (sub-watershed no. 7). In case of the 10-yr storm peak discharge in the total Lauterbach watershed was reduced by 34% for predominantly arable land use and by 15% for diversified land use.

### Influence of watershed size

Increasing watershed size had no remarkable effect on runoff reduction as long as GWW area did not change with increasing watershed size. While the total watershed corresponds to the average GWW area, small sub-watersheds may have higher or lower proportions of GWW, which in turn will affect runoff reduction without being a scale effect.

The correlation between GWW area and efficiency in peak discharge reduction was less pronounced than for runoff volume reduction, because shape of watershed as well as length and slope of the main drainage line, where the GWW was established, are also important. In general, the GWWs reduced peak discharge in the predominantly arable mesoscale watershed effectively, again with no effect of scale. During summer storms in the Lauterbach watershed the peak discharge decreased at least 40% (9.2 m $s^{-1}$ without, 5.6 m $s^{-1}$ with GWW, 50-yr storm), for all applied events.

## DISCUSSION

Assuming that the average field conditions applied for the modeling are representative focusing on the GWWs efficiencies in a mesoscale watershed, it can be concluded that GWWs can be an effective measure to reduce flooding on this scale. On the scale of sub-watersheds the effects of single GWWs might differ considerably because of the large influence exhibited by an individual field of a distinct state. There might be a flooding on this small scale, reported in several studies after heavy summer storms (e.g., Verstraeten and Poesen, 1999) although already on the mesoscale summer events seem to be easier to control than winter events when all fields produce more runoff and infiltration capacities in the GWWs are small.

In summer, the effects of prolonging runoff travel time and hence to reduce peak discharge, may even increase for short rains as they are typical for heavy summer storms. Also, the prevention of gully erosion will reduce the damages of local (muddy) floods in summer. Even if these heavy storms occur in late spring or autumn (due to the general large storm sizes between May and October) when the fields produce more runoff, the GWWs should stay effective due to the high flexural rigidity of the vegetation in this period. In the winter half-year the GWWs were less effective in reducing peak discharge for storms with a recurrence interval larger than 2-yr (Figure 4). The reasons were the higher inflow rates even in case of smaller storms and the reduced flexural rigidity, which allows only a critical runoff depth of about 0.1 m without vegetation failure. The results in case of the 10-yrs storm (Figure 4) may even over estimate the GWWs effectiveness because partly a failure of vegetation can be expected. In general, in winter intensive rains often lasts for more than 1 day and hence the prolonging of runoff travel time is less prominent for a decrease of peak discharge. Nevertheless, there will be still a GWW effect by preventing gully erosion, which without GWW increases the connectivity between source of runoff and watershed outlet.

For the total Lauterbach watershed, the peak discharge reduction under present diversified land use was significantly smaller than for the predominantly arable land use but reduction was still remarkable although only some sub-watersheds had GWWs. In total the minimal reduction of peak discharge by establishing GWWs under diversified land use ranged between 15% (23.2 $m^3 s^{-1}$ without, 19.7 $m^3 s^{-1}$ with GWW, 10-yr winter storm) and 17% (2.8 $m^3 s^{-1}$ without, 2.3 $m^3 s^{-1}$ with GWW, 10-yr summer storm). Establishing GWWs only in the sub-watersheds with arable dominated land use still had a remarkable effect on peak discharge in the mesoscale watershed. It is obvious that this effect is smaller than in single sub-watersheds, which were optimal for GWW establishment, because in nearly half of the Lauterbach sub-watersheds no GWWs and in only three the optimal GWW set-up could be implemented (Table 5).

In general, the modeling exercise showed that peak discharge reduction by GWWs only slightly decreased with increasing watershed size from tens to thousands of hectare, as long as a predominant arable land use allows introducing GWWs in most drainage lines. The heterogeneity of flow pathways acts to desynchronize and thereby attenuate runoff peak volumes also on the large scales. In contrast the efficiency decreases from small sub-watersheds dominated by arable land use to a mesoscale watershed with a more heterogeneous land use. For the present diversified land use the effect of reducing peak discharge on the mesoscale is governed by some sub-watersheds in the North of the Lauterbach watershed. Therefore, the proper management of those is of major importance for mesoscale efficiency of the GWWs. Due to our results a reduction of GWWs efficiency in reducing peak discharge is mainly caused by an increasing percentage of land use not suitable for an establishment of GWWs but not by an increase of scale. The increase in the proportion of runoff bypassing the grassed area with increasing watershed size, as it was found for vegetated filter strips (Verstraeten et al., 2006), should be small because of their location close to the source of runoff production and their general design to handle concentrated runoff. Nevertheless, it must by recognized that similar efficiencies of GWWs than those presented can only be expected if they are properly designed and managed. Especially, to keep their vegetation in good condition and to shape and maintain their cross-sections flat-bottomed is of major importance (Fiener and Auerswald, 2005).

## CONCLUSIONS

The hypothesis that the efficacy of GWWs changes with scale and with land use could be verified. The decrease with scale was small, however, which was especially evident for a predominantly arable land use. Even for watershed sizes up to 1700 ha, GWWs are an efficient control of peak discharge. In contrast, the effect of land use is strong. The efficacy of GWWs is low where land use and storm size produce high amounts of inflow into the GWWs. This is especially critical in winter because then hydraulic roughness of the grass cover will drop due to a reduced flexural rigidity under these conditions. Nevertheless, even in case of a failure of vegetation GWWs will increase runoff travel time by preventing gully erosion causing a concentration of runoff and an increase in runoff velocity. The efficacy in runoff reduction is also low, where the whole area produces only very little runoff like in forested watersheds because then runoff only occurs for storms, which also produce runoff on the GWW itself. The highest efficacy, however, can be expected in watersheds of small-patterned arable land use typical for many European landscapes. Such landscapes, which suffer most from adverse off-site effects of erosion, would benefit most and over the whole range of scales tested from the installation of GWWs.

# 9. SOIL EROSION POTENTIAL OF ORGANIC VERSUS CONVENTIONAL FARMING EVALUATED BY USLE MODELING OF CROPPING STATISTICS FOR AGRICULTURAL DISTRICTS IN BAVARIA

With minor revisions published:
Karl Auerswald, Max Kainz und Peter Fiener (2003)
Soil erosion potential of organic versus conventional farming evaluated
by USLE modeling of cropping statistics for agricultural districts in Bavaria.
Soil Use and Management. 19: 305-311

***ABSTRACT.*** *Organic agriculture (OA) aims to identify a production regime that causes less environmental problems than conventional agriculture (CA). We examined whether the two systems differ in their susceptibility to soil erosion by water. To account for the large heterogeneity within the rotations practiced on different farms, we chose a statistical evaluation which modeled erosion using the USLE method from the cropping statistics for 2056 districts in Bavaria (70 547 km$^2$; 29.8% arable). Physical conditions of erosion were determined in a rectangular grid yielding 13 125 grid-cells of c. 5 km$^2$ each. For validation, erosion was measured in 10 sub-watersheds on two neighboring OA and CA farms over 8 yrs (287 erosive events). On average, about 15% less erosion on arable land was predicted for OA than for CA due to the larger area of leys, although OA occupies areas that are susceptible to erosion more often than CA. The same conclusions could be drawn from the validation data. These data also demonstrated that erosion could be reduced considerably below 1 t ha$^{-1}$ yr$^{-1}$ with best management practices under both farming systems. In contrast, at the countrywide scale, cropping did not change adequately with site conditions favoring erosion. The need for erosion control seems not to influence crop rotation decisions on erosion-prone sites.*

Soil erosion is regarded as being one of the most serious environmental problems associated with land use (Morgan, 1996). In many cases, erosion causes an almost irreversible decline in soil productivity and other soil functions (Biot and Lu, 1995; Bruce et al., 1995) and leads to environmental damage. For example, the quality of surface water bodies may be adversely affected by translocation of arable topsoil enriched in nutrients and pesticides into adjoining terrestrial and aquatic ecosystems (Verstraeten et al., 2002).

Several erosion processes are known, the most important being erosion by flowing water (‘water erosion’), wind (`wind erosion') and soil translocation by tillage (`tillage erosion'). All three damage the soil resource but only the first two additionally cause severe environmental problems because translocated soil leaves the arable area and enters neighboring ecosystems. Although water and wind erosion are different processes, they are governed by similar principles as far as land use is concerned. Soil surfaces destabilized by tillage and cov-

ered with little living or dead biomass are susceptible to erosive forces exerted by air or water. Wind erosion is mainly a problem of coastal landscapes or large plains, while water erosion is of significance more widely. Furthermore, the amount of soil lost by water erosion far exceeds the amount lost by wind erosion in most cases (Heimlich and Bills, 1986). Hence, in the following analysis we will concentrate on water erosion, although to some extent our analysis may also hold true for wind erosion due to both processes having similar agricultural impact.

Soil erosion is highly variable in time and space, which makes it difficult to base an assessment on short-term measurements only, for example over several years or on small plots. To overcome this problem many soil erosion models have been developed and are accepted tools for studying soil erosion (Nearing et al., 1990). The Universal Soil Loss Equation (Renard et al., 1994; Wischmeier and Smith, 1978) is one of the oldest models, which is still frequently used. It has a large experimental background, has been adapted to many areas in the world and is still among the best tools for long-term assessment of soil erosion by water (Nearing, 1998). The model has been extensively customized over 20 yrs using data of about 1000 rainfall simulations and 500 plot years under natural rain (summarized in Schwertmann et al., 1987) and yielded R =0.79 with measured soil losses on a field scale for six fields covering a total of 232 field years (Schwertmann and Schmidt, 1980).

Organic agriculture (OA) aims to be a production system that is in closer alignment with natural cycles and processes than conventional agriculture (CA). Hence OA should also be less conducive to erosion than CA, although this is yet to be proved. To our knowledge, there is only one study which compares soil loss on a conventional to that on an organic farm and demonstrates a smaller soil loss for OA (Reganold et al., 1987). There are also some studies comparing soil properties which influence erosion like infiltrability, aggregate stability or earthworm abundance (Mäder et al., 2002; Mulla et al., 1992; Pulleman et al., 2003; Scullion et al., 2002).

However, these attempts may be insufficient to draw firm conclusions for two reasons. First, a quantitative comparison requires that the two types of farm differ only with respect to the farming system while all other parameters match. This condition cannot be met and proven for large landscape elements like fields or farms. This is especially true for soil erosion, which depends on many site properties like soil erodibility, topography and rain erosivity - all known to change over short distances. Second, a quantitative comparison requires that the farming systems under consideration can be clearly defined. While this may be true to some degree for conventional farms in a particular landscape, this premise fails for organic farms. Each farm has to be considered unique owing to diversified strategies to incorporate N-fixing legumes in crop rotations, complicated and diversified rotations, specific adap-

tations to cope with unfavorable site conditions and exploitation of small market niches. Any extrapolation of inference from an individual organic farm to make a universal generalization about organic farms is thus inappropriate. 'Organic farming' can only be evaluated by taking into account all organic farms. Hence, in this study we compare the degree of erosion on all organic farms in Bavaria to that of all conventional farms in the same region. This comparison is based on modeling, which allows us to specify site influences on erosion when comparing the influence of farming systems.

## MATERIALS AND METHODS

### Modeling approach

The Universal Soil Loss Equation (USLE; Wischmeier and Smith, 1978) predicts long-term average, annual soil loss from the multiplication of six complex terms:

$$A = R \cdot K \cdot L \cdot S \cdot C \cdot P \quad (1)$$

where $A$ is long-term average annual soil loss (t $ha^{-1}$ $yr^{-1}$), $R$ is rainfall and runoff erosivity (N $h^{-1}$ $yr^{-1}$), $K$ is soil erodibility (t h $ha^{-1}N^{-1}$), $L$ and $S$ are dimensionless topography factors quantifying the influences of the watershed area and watershed curvature, $C$ is a dimensionless factor quantifying the influence of the cropping system, and $P$ is a dimensionless factor quantifying the influence of permanent erosion control measures like terracing and contouring.

The $C$ factor quantifies the influence of cropping. Hence whether the farming system is organic or conventional will especially have an influence on $C$. The $C$ factor is computed from the combination of the so-called soil loss ratio (SLR) with the erosivity index (EI) (Wischmeier and Smith, 1978). The EI quantifies the seasonal distribution of rainfall erosivity. The SLR quantifies the susceptibility of the soil surface relative to the conditions that occur in a freshly prepared seedbed, which is thus considered a standard. The SLR mainly depends on tillage and soil cover. It can be determined experimentally, for example, by rainfall simulator experiments (e.g., Chow and Rees, 1994) or by calculation from sub-models (Alberts et al., 1989).

The long-term average $C$ factor can only be computed for complete rotations for two reasons. First, between two main crops there is a period, sometimes of several months duration, in which considerable erosion may occur but cannot be assigned either to the previous or to the following crop. Second, carryover effects exist by which the preceding crop influences the extent of erosion during following years. This is especially true in ley-based rotations.

Sod-forming crops like clover-grass are known to stabilize the soil. This decreases soil loss up to two years after the sod has been plowed as compared to an otherwise identical system without sod (Wischmeier and Smith, 1978). These carryover effects of leys are also identified in other models like the 'prior land use factor' in EPIC (Sharpley and Williams, 1990), which is a modification of the USLE, but also in models that use a completely different prediction technology like EUROSEM (Morgan et al., 1998) or WEPP (Lane and Nearing, 1989). In the latter models the higher organic matter content, the higher aggregate stability, more earthworm channels and lower erodibility (Pulleman et al., 2003; Scullion et al., 2002; Siegrist et al., 1998) after inversion of leys would cause a similar effect.

Data on crop rotations may be raised while examining individual farms. They are not available, however, for larger areas because to our knowledge no statistical inventory of rotations exists. This is true for CA and OA. Therefore, *C* factors assumed in this study have to be computed on the basis of cropping statistics.

Auerswald (2002b) computed *C* factors of many conventional and organic rotations and combined the rotations in a Monte-Carlo simulation to simulate the effect of a combination of different farms. He showed that the *C* factor averaged over different farms can be estimated from cropping statistics. The mean absolute error between this estimation and the average from the accurately determined *C* factors of the rotations was 0.016 only. The *C* factor may hence be estimated using rather simple parameters with one equation being valid for both farming systems:

$$C = \left\{ \begin{array}{l} \left[ 830 - 15.8 \cdot \left( F_{SG} + F_{RC} + F_{SC} \right) + 0.082 \cdot \left( F_{SG} + F_{RC} + F_{SC} \right)^2 \right] \cdot \\ \left( 1 - 0.03 \cdot F_{SC} \right) + 0.1 \cdot F_{SC} - 0.5 \cdot F_{RC} + 27 \end{array} \right\} / 1000 \qquad (2)$$

Where $F_{SG}$ is the percentage of small grain (including oil seeds), $F_{RC}$ is the percentage of row crops planted in mulch tillage, $F_{SC}$ is the percentage of sod-forming crops.

Mulch tillage is the planting of row crops into a mulch cover created by the cultivation of cover crops, which are either frozen down during winter or chemically killed prior to row crop sowing or planting (Kainz, 1989). In cases where equation 2 predicts *C* factors of less than 0.01 the *C* factor has to be set to 0.01, and where it exceeds 0.45 it has to be set to 0.45 (Auerswald, 2002b).

**Study area**

Bavaria is a large state in the southern part of Germany with an area of 70 547 km$^2$, comprising 29.8% arable land, 16.7% grassland and 34.6% forest. It is characterized by a comparatively wide range of site conditions, which allows extrapolation of findings in a study such as this to other German states or to neighboring countries like Austria and Switzerland (Auerswald, 2002b). However, compared to larger areas like the United States of America, the range of site properties in Bavaria has to be regarded as limited. As far as soil erosion is concerned, however, conditions encountered in Bavaria lie right in the middle of the range found in the USA (Auerswald, 1991).

Bavaria is divided into 2050 districts. For each of these districts average cropping records exist from the INVEKOS inventory (INtegriertes VErwaltungs- und KOntrollSystem zur Kontrolle von flächengestützten Förderanträgen; integrated administration and control system for European Community aid schemes). The INVEKOS inventory covers about 97% of the agricultural area and thus provides accurate information about cropping practice, enabling the average impact to be calculated by summation of the separate impacts of the various cropping rotations. The INVEKOS data were separated into organic and conventional areas and the average *C* factor was computed for each district based on equation 2 and the respective inventory data.

We used only data from rotations but not from permanent crops like hops, grapes or asparagus and we did not compare the percentage of grassland, which may also deviate considerably between CA and OA. Not accounting for the percentage of grassland should not have affected conclusions of our study because erosion on productive grassland can be regarded close to zero in either case.

**Data evaluation**

The *C* factor alone may be insufficient to compare the erosion risk of two farming systems, when accumulations of organic farms in certain regions occur, which may be characterized by non-average erosion conditions. The *C* factors hence have to be combined with the other factors of the USLE to yield total soil loss. To guarantee a sufficiently high resolution, Bavaria was divided into a rectangular grid of 13 125 cells, each about 5 km$^2$ in size. For each of the grid cells the *R* factor was computed according to Rogler and Schwertmann (1981); the *K* factor was estimated following Auerswald (1986), and the *L* factor following Mutchler and Greer (1980). The equation by Nearing (1997) was used to compute the *S* factor from slope gradient. It is suitable also on steep land as found in alpine areas or grape-growing areas. The *P* factor is of minor importance at the district level. On average it is 0.85 in many regions of Bavaria (Kagerer and Auerswald, 1997). Methods of data acquisition and

interpretation were described by Auerswald and Schmidt (1986). By multiplying the product *RKLSP* by the respective *C* factors of OA or CA of each grid-cell we are able to predict regional and general differences in soil loss between OA and CA systems.

The average cropping conditions on either organic or conventional arable land were computed by weighting each grid-cell according to the proportion of respective arable land:

$$V_{av} = \sum_{i=1}^{13125} V_i F_i \Big/ \sum_{i=1}^{13125} F_i \qquad (3)$$

Where $V_{av}$ is the average of any variable like rain depth or rain erosivity for arable land of OA or CA, $V_i$ is the value assigned to this variable in each of the 13 125 grid-cells, and $F_i$ the area of arable land found in each grid-cell for either OA or CA.

A statistical evaluation of the difference in the averages between OA and CA is then not possible and not necessary because the averages are not computed from a sample subset of the total population but from the total population itself. Uncertainties or errors in the data cannot be quantified but should be small for such a large data set as long as there is no general bias.

**Validation**

Validation *sensu strictu* is not possible because long-term field scale measurements of erosion on many farms distributed over the country would be necessary. However, we will use data from two neighboring farms, one conventional (68 ha) the other organic (43 ha), where soil loss had been continuously measured on a field to sub-watershed scale for 8 yrs in 10 small sub-watersheds ranging in size from 0.5 to 16 ha. The sub-watersheds consisted of less than one field to a few fields because no artificial borders are allowed at this scale. The 10 sub-watersheds were selected out of 16 to have identical soil use except for the type of farming with 83.7/83.1% arable land, 10.3/10.8% grassland and permanent set-aside, 4.6/5.0% field borders, and 1.4/1.1% farm roads in the conventionally and the organically farmed watersheds, respectively. Runoff and soil loss were measured on an event base by sampling 0.5% of the runoff with Coshocton-type runoff samplers where runoff was concentrated by topography and/or field borders. For details of the measurement and validation of the measuring system, see Fiener and Auerswald (2003a). Soil loss was modeled with high resolution using the differentiated USLE (average polygon size: 13 m²; Fiener and Auerswald, 2003a). Best management practices were applied as appropriate to individual farming systems (i.e. optimized field layout with field borders acting as runoff barriers, use of ultra-

wide tires, reduction of field passes, use of intercropping, catch crops and residue management to increase surface cover, use of grassed waterways). For details of management, see Auerswald et al. (2000) and Fiener and Auerswald (2003a, b).

'Measured' *C* factors were calculated from the measured soil loss and the predicted bare fallow soil loss *RKLSP* of the instrumented watersheds after adjusting the measured soil loss for the effects of the grassed waterways and the retention ponds at field borders, as quantified by Fiener and Auerswald (2003a, b). 'Predicted' *C* factors for the specific rotations of both farms were calculated from biweekly soil cover (plants, residues, and stones) measured in 15 fields at three geodetically defined locations over four years. (For examples of data see Auerswald et al., 2000.) The SLRs were calculated from soil cover using the equation determined by Kainz (1989) with rainfall simulator experiments under similar conditions. The *C* factors were then computed from daily SLRs and the annual distribution of the erosivity index (EI) taken from Rogler and Schwertmann (1981). The carryover effect after inversion of ley on the organic farm was taken from Wischmeier and Smith (1978).

## RESULTS AND DISCUSSION

There is a tendency for OA to occupy less favorable arable sites than CA. On average, the arable OA sites receive more precipitation and have soils which are less deep and slopes with steeper gradients (Table 1). The higher annual precipitation corresponds to greater rain erosivity, *R*, and the steeper slopes to a greater *S* factor. The shallower soils of OA are also stonier, sandier or clayier and hence have 14% lower soil erodibility, *K*. This difference in *K*, however, is too small to compensate for the 27% greater *R* and 15% greater *S*.

**Table 1. Average site conditions on arable land of conventional and organic farms computed from 13125 grid-cells weighted according to their percentage of conventional or organic arable land.**

| Variable | Unit | Average, conventional farms | Average, organic farms | Difference between organic and conventional farms |
|---|---|---|---|---|
| Precipitation | mm $yr^{-1}$ | 767 | 981 | +28% |
| *R* factor | N $h^{-1}$ $yr^{-1}$ | 65.4 | 83.2 | +27% |
| Soil depth | m | 0.68 | 0.64 | -6% |
| *K* factor | t h $ha^{-1}$ $N^{-1}$ | 0.37 | 0.32 | -14% |
| Slope length | m | 185 | 150 | -19% |
| *L* factor | - | 2.41 | 2.3 | -4% |
| Slope gradient | % | 7.5 | 8.7 | +16% |
| *S* factor | - | 0.87 | 1.02 | +17% |
| *RKLSP*[a] | t $ha^{-1}$ $yr^{-1}$ | 46.9 | 53.4 | +14% |

[a]Quantifies the site-specific soil erosion potential exclusive of the influence of cropping.

Land use accounts for these more unfavorable conditions by smaller fields leading to 19% shorter erosive slope lengths. The effect on the *L* factor, however, is only 4% due to the

**Table 2. Comparison of organic and conventional agriculture based on district records for 2001.[a]**

| | | Organic farms (%) | Conventional farms (%) |
|---|---|---|---|
| Total arable land | 25% quartile | 0 | 96.4 |
| | Average | 3.6 | 96.4 |
| | 75% quartile | 3.6 | 100 |
| No. of districts | | 1965 | 1965 |
| Small grain | 25% quartile | 45.4 | 48.4 |
| | Average | 56.9 | 57.6 |
| | 75% quartile | 73.7 | 70.7 |
| No. of districts | | 1081 | 1956 |
| Row crops | 25% quartile | 7 | 23.1 |
| | Average | 20.8 | 34.5 |
| | 75% quartile | 27.4 | 43 |
| No. of districts | | 1081 | 1956 |
| Grass/legume ley | 25% quartile | 1.6 | 1.6 |
| | Average | 22.3 | 7.9 |
| | 75% quartile | 32.2 | 10.1 |
| No. of districts | | 1081 | 1956 |
| *C* factor | 25% quartile | 3.3 | 10.1 |
| | Average | 9.9 | 13.3 |
| | 75% quartile | 11.9 | 15.9 |
| No. of districts | | 1081 | 1956 |

[a] There were 2050 districts in Bavaria of which 1965 had arable land > 0.00% of total agricultural land; 1081 had organic arable land > 0.00%; and 1956 had conventional arable land > 0.00%.

low sensitivity of the *L* factor to length changes in this range of slope length. Consequently, it does not compensate for the effect of the other site-specific properties. Hence the bare fallow soil loss, *RKLSP*, is about 14% greater on organic arable land than on conventional land (Table 1).

Among all 2050 districts, 85 had no arable area and will not be considered further. OA contributed between 0 and 100% to the arable area. On average it covered 3.6% of the arable land (Table 2). Hence, it has a negligible influence on the district-wide average soil loss. The distribution between districts is very uneven, which is demonstrated by the 25% quartile being equal to 0% and the 75% quartile being equal to the mean because the mean is largely influenced by a few districts with exceptionally high percentages of OA.

The percentage of small grain on arable land is similar for CA and OA. Distinct differences occur in the percentages of row crop and sod-forming crops between the systems. Predominantly, OA is characterized by a large percentage of grass/legume ley, which is about three times greater than that for CA. This is mainly at the expense of row crops. This difference results from the need to use symbiotic N-fixation of legumes as a source of N instead of mineral N fertilizers, and to control weeds with repeated mowing. From the wide range in crop areas, a wide range in *C* factors was expected and observed (Figure 1). The *C* factors in both systems ranged from 0.01 to 0.45. The low values are restricted to regions of more than 1000 mm annual precipitation growing almost entirely grass. *C* factors of 0.45 indicate maize monocultures, which are restricted to the same regions because the maize serves to supplement the fodder from grassland. In both cases, the respective districts can be regarded as unimportant outliers in respect to the amount of arable land, although they strongly influence

the visual assessment of Figure 1. The 25% and 75% quartiles (Table 2) provide a more realistic picture of the range.

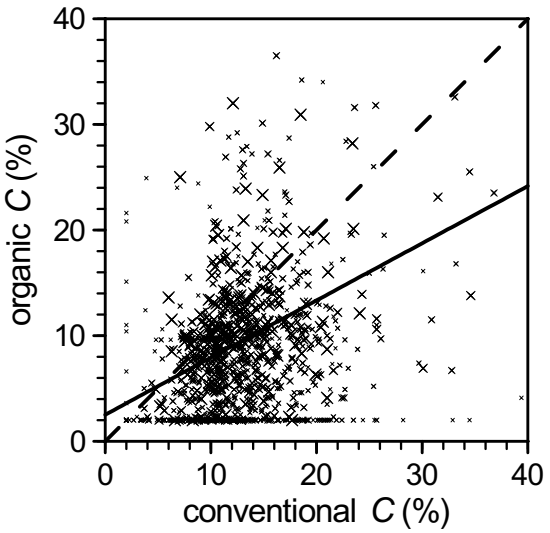


**Figure 1. Comparison of *C* factors (in % of bare fallow soil loss) between organically and conventionally farmed arable land. District averages of 1072 districts in Bavaria with > 0.00% of arable land for both organic and conventional farms; marker size increases with increasing geometric mean of arable land for organic and conventional farms; dashed line indicates unity; solid line is the regression Y = 2.5 + 0.54 X; $R^2$ = 0.128. (Regressing X on Y gives X = 10.9 + 0.24 Y.)**

The comparison of the mean *C* factors (Table 2) predicts that OA reduces soil loss by about 24% as compared to CA under identical site conditions. Due to the more erosive site conditions of OA, the soil loss is only 15% less for OA than for CA. The regression between the *C* factors of OA and CA, however, only yields $R^2$ =0.128 (for n = 1072 districts), indicating that the rotations and thus the *C* factors of both systems are governed by different influences. Given the large variability of both systems and the low correlation we should not conclude that OA decreases soil erosion, although this was true for the majority of districts. For 255 out of 1072 districts the *C* factor of OA was larger than that of CA. The large scatters show that for both systems the *C* factor, and thus soil loss, can be decreased. In both cases, the expansion of grass/legume leys would decrease soil loss far more than changing from row crop to small grain. Opportunities to increase the percentage of grass/legume leys should hence be explored in both systems.

For both systems, the average *C* factor decreases with increasing site specific erosion potential, this is quantified by RKLS:

$$C_{OA} = 13.7 - 1.1 \ln(RKLS) \qquad (4)$$
$$R^2 = 0.020 \quad (n = 6879)$$

$$C_{CA} = 17.1 - 1.0 \ln(RKLS) \qquad (5)$$
$$R^2 = 0.043 \quad (n = 10070)$$

These relationships are very weak, however. The *C* factor decreases only as logarithm of *RKLS* whereas a linear decrease would be necessary to compensate for the effect of *RKLS* on

soil loss. Slight changes in cropping thus cannot compensate for the large differences in site-specific erosion potential. This is true for both farming systems. Neither OA nor CA adequately takes into account the site-specific erosion potential in cropping decisions.

The equation used to estimate the *C* factor (equation 2) accounts for the effects created by the rotation. Organic farming differs not only in rotation but also in the use of agrochemicals. In addition to the rotation effect, absence of pesticides is sometimes claimed, which may additionally influence the *C* factor. These effects on erosion, however, have not been quantified despite attempts to do so (e.g., Auerswald, 1995) and thus have not been considered. However, it is unlikely that their effect is large; otherwise it would have been easy to quantify.

## Validation

To our knowledge, the validation data set we have used is the largest available comparing field-scale soil loss from OA and CA. During the 8-yr measuring period 287 events induced runoff and soil loss in at least one of the 10 subwatersheds. The data set, however, represents a unique situation and thus the absolute values of the different parameters for both farms differ from the country averages. Nevertheless, the relative differences between OA and CA in this data set confirm the results from the country statistics (Table 3). The organic

**Table 3. Average cropping conditions and erosion parameters on arable land (AL) of the conventional and the organic farm used for validation.[a]**

| | | | | Difference between organic and conventional farms | |
|---|---|---|---|---|---|
| Variable | Unit | Conventional farm | Organic farm | Validation (%) | All (%) |
| Small grain | % of AL | 50 | 42.9 | -7 | -1 |
| Row crops | % of AL | 50 | 20.8 | -29 | -14 |
| Ley | % of AL | 0 | 22.3 | 22 | 14 |
| Precipitation | mm $yr^{-1}$ | 804 | 804 | 0 | 28 |
| *R* factor | N $h^{-1}$ $yr^{-1}$ | 69 | 69 | 0 | 27 |
| *K* factor | t h $ha^{-1}N^{-1}$ | 0.42 | 0.32 | -24 | -14 |
| No. of fields | n.a. | 7 | 14 | 100 | n.d. |
| Field size | ha | 4.3 | 2.2 | -49 | n.d. |
| Slope length | m | 159 | 112 | 30 | -19 |
| *L* factor | n.a. | 2.69 | 2.25 | -16 | -4 |
| Slope gradient | % | 8.9 | 10.4 | 16 | 16 |
| *S* factor | n.a. | 1.04 | 1.36 | 32 | 17 |
| *RKLSP*[b] | t $ha^{-1}$ $yr^{-1}$ | 68.9 | 57.4 | -17 | 14 |
| Measured soil loss[c] | t $ha^{-1}$ $yr^{-1}$ | 0.29 | 0.04 | -86 | n.d. |

[a]High-resolution erosion modeling with a total of 52 894 cells; [b]quantifies the site-specific soil erosion potential exclusive of the influence of cropping; [c]measured soil loss is based on 2296 watershed events.
n.a.= not applicable; n.d. = not determined.

farm had more leys at the expense of row crops, which was similar to the countrywide averages. The site conditions exhibited similar differences to the country average except for long-term average precipitation and the *R* factor which are considered identical for two farms separated only by a farm road. The organic farm had soils with a smaller *K* factor. It was situated on steeper land and the *S* factor was larger, whereas the field size and the *L* factor were smaller. The bare fallow soil loss, *RKLSP*, of the organic farm in the validation study was, however, about 17% smaller due to the identical *R* factor. Finally, the measured soil loss from the organic farm was much less than the difference in *RKLSP* (86% vs. 17%), proving the lower erosion risk of land use that incorporates leys.

On the conventional farm the *C* factor determined from measured soil loss was 0.036, which matches the *C* factor predicted from soil cover measurement (0.040; range 0.028-0.049). On the organic farm the measured soil loss gave a much lower *C* factor (0.004), while from soil cover alone a higher *C* factor than on the conventional farm was obtained (0.049) because more frequent tillage reduced soil cover. Including the carry-over effect into the prediction yielded a lower *C* factor than on the conventional farm (0.032), but it was still considerably higher than that derived from the measured soil loss. This could be the result of an additional effect of organic farming reflecting the absence of mineral N fertilizers and synthetic pesticides, which until now has not been quantified. However, rigid quantification of this additional effect may not be possible, even with our data set, due to the 8-yr measuring period, which covers only one rotation on the organic farm, the limitation to one farm and the error propagation with a multitude of variables. The measured soil losses on both farms were much smaller than what could be expected on average for all conventional or organic farms. This is due to the adoption of best management practices on both farms (Auerswald et al., 2000; Fiener and Auerswald, 2003b), which have considerably lowered the soil loss. For one field, which now belongs to the organic farm, Schimmack et al. (2002) quantified the soil loss by using atomic-weapon fallout plutonium. Soil loss by sheet and rill erosion (not including tillage erosion) was more than two orders of magnitude greater than after the best management practices were introduced. Averaged over a 23-yr period the rate of soil loss was 14 t $ha^{-1}$ $yr^{-1}$ compared with substantially less than 1 t $ha^{-1}$ $yr^{-1}$ after the land use change.

## CONCLUSIONS

In Bavaria, organic farms tend to occupy the more unfavorable arable sites, which are also more at risk of erosion. The estimated site-specific bare-fallow soil loss is hence 14% greater for OA than for CA.

The district average in the proportion of row crops, small grains and grass/legume leys differed greatly between OA and CA indicating that natural site properties have little influence on rotations.

On average, OA will cause about 24% less erosion then CA under otherwise identical site conditions. This can be attributed to the larger area of grass/legume ley, which has the potential to reduce erosion markedly, even two years after inversion. The lower *C* factors more than compensate for the unfavorable site conditions. Hence, the average soil loss is about 15% less for OA than for CA.

There are large deviations on both sides of the average *C* factor indicating that erosion in both farming systems could be reduced considerably. Erosion control does not seem to influence management decisions on crop rotation in either farming type. The lower erosion in OA on average has hence to be regarded as accidental. It is a consequence of the shortage of N supply and the need for weed control, which are partly met by a greater proportion of grass/legume leys in organic rotations (Berry et al., 2002; Watson et al., 2002). The large effect of the best management practice on the soil loss in the validation exercise also demonstrates that both farming systems have much scope to reduce soil losses.

# 10. RATES OF SHEET AND RILL EROSION IN GERMANY - A META-ANALYSIS

With minor revisions published:
Karl Auerswald, Peter Fiener und Richard Dikau (2009)
Rates of sheet and rill erosion in Germany – A meta-analysis.
Geomorphology. 111. 182-193

***Abstract.*** *Knowledge of erosion rates under real conditions is of great concern regarding sustainability of landuse and off-site effects on water bodies and settlements. Experimentally derived rates of sheet and rill erosion are often biased by experimental settings, which deviate considerably from typical landuse, by short measuring periods and by small spatial extensions, which do not account for the pronounced spatio-temporal variability of erosion events. We compiled data from 27 studies covering 1076 plot years to account for this variability. Modeling was used to correct for deficiencies in the experimental settings, which overrepresented arable land and used steeper and shorter slopes as well as higher erosivity than typically found in reality. For example, the average slope gradient was 5.9° for all arable plot experiments while it is only 2.6° on total arable land in Germany. The expected soil loss by sheet and rill erosion in Germany after taking real slopes, landuse and erosivity into account averaged 2.7 t $ha^{-1}$ $yr^{-1}$. Annual crops contributed the largest proportion (90%) but hops despite its negligible contribution to landuse (0.06%) still contribute 1.0% due to its extraordinary rapid erosion, which was even faster than the measured bare fallow soil loss standardized to otherwise identical conditions. Bare fallow soil loss, which is often used as baseline, was 80 t $ha^{-1}$ $yr^{-1}$ when standardized to 5.1° slope gradient, 200 m flow path length, and average German erosivity.*

Soil erosion by water is regarded as the most important threat to the soil resources (Auerswald and Kutilek, 1998; Oldeman et al., 1991). It may be caused by water, wind, tillage or harvest of root crops. Water and tillage erosion contribute the largest proportion and affect by far the largest areas. While tillage erosion receives attention only since one to two decades ago (Lindstrom et al., 1992), water erosion has been recognized as a threat to the soil resource presumably since shortly after the onset of arable landuse. Despite this long experience with soil erosion by water and despite many attempts to quantify its extent, quantification can still be regarded as unsolved. The main reason for this deficiency is the pronounced stochastic character of erosion events. Higher and more intense rainfall is related to longer recurrence intervals. The recurrence interval, however, is only a statistical expression of highly variable rainfall events in time. Furthermore, highly erosive rains mostly cover

only small areas. The hot spots of thunderstorm cells may have several hundred meters to a few kilometers in size (Aniol, 1975; Fiener and Auerswald, 2009). Finally, most crops leave the soil surface unprotected only in a certain period of the year. It is thus highly unlikely that these rare events can be represented in a statistically correct proportion in studies of limited temporal and spatial extent. Thus, the percentage of large events is either too large or too small in an individual study. The largest event within a given measuring period often dominates the total but also the average soil loss of this period. The wrong representation of large events thus leads to significant bias of actual soil loss data in different studies. Studying vineyards in Germany for instance, Emde (1992) found a mean soil loss of 151 t $ha^{-1}$ $yr^{-1}$ averaged over 10 plot years while Richter (1991) only measured 0.2 t $ha^{-1}$ $yr^{-1}$ averaged over 144 plot years. Environmental differences between the study areas or differences in vine cultivation cannot explain this difference. It was caused by the largest event during the study by Emde (1992), which obviously was overrated as compared to the size of his data set. Such an event was entirely missing in the much larger data set of Richter (1991).

Several approaches can be applied to overcome this deficiency: (i) Long-term measurement records can be set up but they are limited to a few locations and cannot account for the large spatial variability of soil erosion phenomena. (ii) Tracer studies, especially by using $^{137}Cs$ from nuclear bomb testing in the 1960s allow quantifying soil erosion since that time and at numerous locations, and thus overcome the problems of stochastic events. Unfortunately, this technique records soil loss without adequate process considerations. Erosion processes other than water and wind erosion, namely tillage erosion (De Alba et al., 2004) and harvest erosion (Poesen et al., 2001) also contribute to total soil loss and the contribution of these different processes has to be quantified by modeling. (iii) Modeling soil erosion processes again depends on representative data for model development and parameterization. Furthermore, models are always an issue of debate, whether they sufficiently reproduce reality. In this study we follow another approach to overcome the temporal limitations of individual studies and to estimate soil erosion for different landuse in the whole of Germany. To this end, all existing measured (and published) data sets from Germany are compiled and standardized and later on used in combination with national data sets of landuse, slopes and rain erosivity.

## REGIONAL SETTING

Germany is 357,031 $km^2$ in size with highly variable natural and anthropogenic conditions for soil erosion. Rural landuse cover comprises 37% arable land, 17% grassland and 30% forests, while urban and surface water areas cover 16% (Destatis, 2002). The northern part of Germany lies in the North European Lowlands (German part called North German Lowlands), with flat to gently undulated terrain crossed by north- to north-west-flowing wa-

tercourses (Figure 1). Moving south, central Germany features a hilly countryside of low mountain ranges. The landscapes in Germany's southern part comprise upland ridges, Mesozoic escarplands, and the area of the Tertiary hills and Alpine moraines, where slopes in general are considerably steeper than in the northern lowlands. At the southern border to Austria and Switzerland, in a fringe of the Northern Alps, elevation reaches almost 3000 m and the steepest slopes occur, which are forested or occupied by pastures and natural meadows. Continental conditions increase from northwest to southeast Germany. In consequence, the frequency and severity of thunderstorms and the concentration of precipitation during summer months increase along this gradient and cause an increase in rainfall erosivity. This general trend is modified and further aggravated by topography, which induces an increase in precipitation from the flat lowlands in the North (approx. 500–800 mm $yr^{-1}$) to the mountain ridges in the centre (800–1200 mm $yr^{-1}$) and finally to the Alps in the South where precipitation peaks at more than 2000 mm $yr^{-1}$. Hence rainfall erosivity increases from 40 N $h^{-1}$ $yr^{-1}$ in the North-West to 100 N $h^{-1}$ $yr^{-1}$ in the South and even exceeds this value in the German Alps (Sauerborn, 1994).

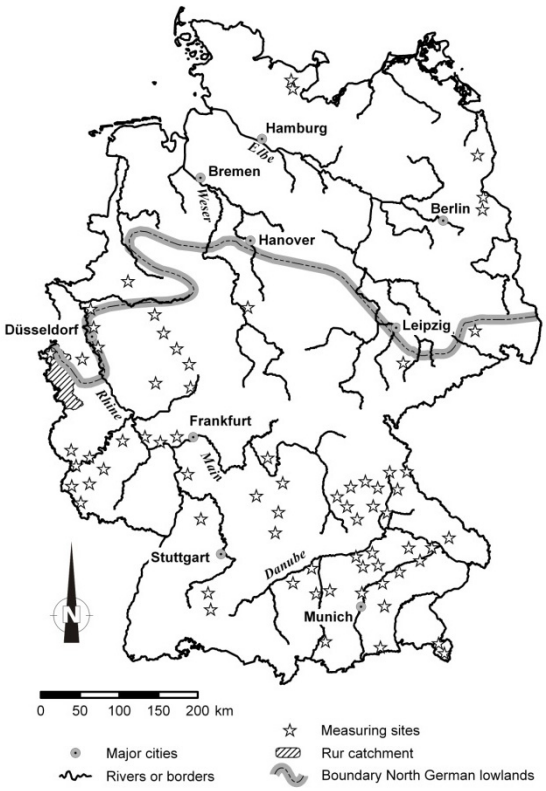


**Figure 1. Location of measuring sites; location is an approximation because most studies did not provide exact coordinates.**

## MATERIALS AND METHODS

### Collection of measured data

Data from all available studies on soil loss under natural rainfall in Germany were compiled. Most data sets were from plot experiments, but also some tracer and small watershed studies were included. As the comparison of rainfall resulting from different simulation equipments with natural rainfall is more or less impossible, rainfall simulation studies were excluded. Moreover, sediment delivery data from larger watersheds with heterogeneous

**Table 1. Measured soil losses due to sheet and rill erosion; although the table indicates comparability, this could not fully be achieved due to missing information, incomplete years of measurement, different approaches, unique situations and a lack of information about the expected return periods of the measured events in relation to the length of the observation period; to include studies with measuring periods other than one year, average monthly soil losses were calculated and multiplied by 12 to yield annual rates; no corrections were made for differences in slope gradient, plot length and size.**

| Location | Landuse | Slope (°) | Slope length (m) | Area ($m^2$) | Plot years | Type of study[1)] | Soil texture[2)] Sa /Si /Cl (%) bulk soil | Mean rainfall ($mm\ yr^{-1}$) | Mean erosion ($t\ ha^{-1}yr^{-1}$) | Reference[3)] |
|---|---|---|---|---|---|---|---|---|---|---|
| Hohenpeißenb. | arable crops | 6.8 | 8 | 16 | 24 | P | 40 / 27 / 12 | 1304 | 0.3 | J80 |
| Albacher Hof | arable crops | 5.7 | 8 | 16 | 12.0 | P | 12 / 63 / 25 | 761 | 1.1 | J80 |
| Erndtebrück | arable crops | 6.0 | 8 | 16 | 44.0 | P | 19 / 42 / 7 | 652 | 0.3 | J80 |
| Marburg | arable crops | 5.1 | 8 | 16 | 24.0 | P | 45 / 44 / 7 | 1230 | 0.6 | J80 |
| Rauischholzh. | arable crops | 4.6 | 8 | 16 | 26.0 | P | 22 / 48 / 30 | 418 | 0.1 | J80 |
| Blumberg | arable crops | 8.5 | 8 | 16 | 9.0 | P | 37 / 25 / 12 | 809 | 0.8 | J80 |
| BE2 | barley | 12.0 | 60 | 720 | 1 | W | 8 / 74 / 7 | 1100 | 0.7 | D86 |
| Müncheberg | maize | 6.8 | 65 | 293 | 2.5 | P | | 525 | 23.3 | B90 |
| EH1 | maize | 110.0 | 40 | 4 700 | 1 | W | 8 / 81 / 10 | 1100 | 36 | D86 |
| Dedelow | maize | 16.8 | 20 | 50 | 0.5 | P | | 497 | 4.5 | D89 |
| Kiel | maize | 5.7 | 5.33 | 12 | 2.3 | P | 2 soils | 750 | 4.6 | G89a, b |
| Kiel | maize + clover | 5.7 | 5.33 | 12 | 2.3 | P | 2 soils | 750 | 2.5 | G89a, b |
| Scheyern | mixed. organic farming | av. 6.5 | av. 111 | 16 000 -110 000 | 40 | W | different soils | 834 | 0.2 | A03 |
| Scheyern | mixed. with mulch tillage | av. 5.1 | av. 159 | 8 000 - 160 000 | 60 | W | different soils | 834 | 2.5 | A03 |
| EH1 | oat | 110.0 | 60 | 7 000 | 1 | W | 8 / 81 / 10 | 1100 | 1.5 | D86 |
| Taunus | rotation | 4.6-7.4 | 8 | 16 | 5 | P | 6 / 77 / 16 | 650 | 5.6 | V78 |
| Müncheberg | row crop | 5.1-5.7 | 50 | | 5 | P | | 525 | 35.2 | F98 |
| Dedelow | row crop | 6.3-8.0 | 20 | | 2.4 | P | | 497 | 5.0 | F98 |
| Dedelow | rye | 6.8 | 20 | 50 | 0.5 | P | | 497 | 0.4 | D89 |
| Obersdorf | small grain | 7.4 | 20 | 50 | 9 | P | | 531 | 1.4 | D94 |
| Dedelow | small grain | 6.3-8.0 | 20 | | 2.4 | P | | 497 | 0.4 | F98 |
| Scheyern | small grain | 11.3 | | 20 000 | 23 | T | 20 / 30 / 18 | 725 | 14 | S02 |
| Odenwald | small grain | 2.3-4.6 | 8 | 16 | 5 | P | 2 soils | 780 | 0.19 | V78 |
| Tarforst | spring barley | 4.6 | 8 | 8 | 3.0 | P | | 680 | 0.1 | R87 |
| Olewig | spring barley | 4.6 | 8 | 8 | 3.0 | P | | 465 | 0.0 | R87 |
| Kockelsberg | spring barley | 4.6 | 8 | 8 | 3.0 | P | | 718 | 0.1 | R87 |
| Bitbg. Ch. | spring barley | 4.6 | 8 | 8 | 3.0 | P | | 765 | 0.1 | R87 |
| Hungelsberg | spring barley | 4.6 | 8 | 8 | 3.0 | P | | 775 | 0.1 | R87 |
| Dickes Kreuz | spring barley | 4.6 | 8 | 8 | 3.0 | P | | 1042 | 0.0 | R87 |
| EH1 | sugar beet | 10.0 | 60 | 6 100 | 1 | W | 8 / 81 / 10 | 1100 | 458 | D86 |
| Dölzig | sugar beet | 4.6-5.1 | 85-325 | 2 000 - 9 000 | 10 | P | | 600 | 230.8 | S92 |

(continued on next page)

| Location | Landuse | Slope (°) | Slope length (m) | Area ($m^2$) | Plot years | Type of study[1)] | Soil texture[2)] Sa /Si /Cl (%) bulk soil | Mean rainfall ($mm\ yr^{-1}$) | Mean erosion ($t\ ha^{-1}yr^{-1}$) | Reference[3)] |
|---|---|---|---|---|---|---|---|---|---|---|
| ZI1 | wheat | 6.5 | 165 | 2 145 | 1 | W | 8 / 74 / 7 | 1100 | 0.2 | D86 |
| Kiel | wheat | 5.1-15.1 | 8 | 16 | 2.4 | P | | 750 | 0.7 | F00 |
| Ostrau | wheat | 2.9-11.3 | 60-250 | | 5 | P | | | 103.4 | S90 |
| Euchen | bare fallow | 4.3 | 10 | 15 | 0.9 | P | 4 / 75 / 21 | 569 | 22.1 | B91 |
| Niederkasten. | bare fallow | 2.9 | 10 | 15 | 0.9 | P | 20 / 46 / 17 | 550 | 38.0 | B91 |
| Eschmar | bare fallow | 7.7 | 10 | 15 | 0.9 | P | 71 / 14 / 10 | 632 | 140.6 | B91 |
| Saalhausen | bare fallow | 10.5 | 10 | 15 | 0.5 | P | 18 / 39 / 13 | 780 | 1.3 | B91 |
| Hochdahl | bare fallow | 4.6 | 10 | 15 | 0.6 | P | 63 / 30 / 7 | 842 | 42.1 | B91 |
| Werden | bare fallow | 2.9 | 10 | 15 | 0.8 | P | 6 / 78 / 16 | | 6.0 | B91 |
| Soest | bare fallow | 3.4 | 10 | 15 | 0.9 | P | 4 / 71 / 20 | | 0.5 | B91 |
| Nottuln | bare fallow | 3.4 | 10 | 15 | 0.7 | P | 38 / 37 / 20 | 692 | 7.7 | B91 |
| Schwäb. Alb | bare fallow | 3.4 | | | 5 | P | | | 13.9 | D68 |
| Hollmuth | bare fallow | 13.1 | 5 | 10 | 3 | P | 17 / 75 / 14 | 885 | 1.7 | D86 |
| Hollmuth | bare fallow | 13.1 | 2 | 4 | 3 | P | 17 / 75 / 14 | 885 | 49.8 | D86 |
| Hollmuth | bare fallow | 13.1 | 2 | 4 | 3 | P | 17 / 75 / 14 | 885 | 33.8 | D86 |
| Hollmuth | bare fallow | 13.2 | 5 | 10 | 3 | P | 17 / 75 / 14 | 885 | 37.2 | D86 |
| Hollmuth | bare fallow | 12.5 | 10 | 20 | 3 | P | 17 / 75 / 14 | 885 | 19.7 | D86 |
| Hollmuth | bare fallow | 12.5 | 20 | 40 | 3 | P | 17 / 75 / 14 | 885 | 18.3 | D86 |
| Dedelow | bare fallow | 6.8 | 20 | 50 | 0.5 | P | | 497 | 3.5 | D89 |
| Obersdorf | bare fallow | 7.4 | 20 | 50 | 9 | P | | 531 | 8.2 | D94 |
| Dedelow | bare fallow | 6.3-8.0 | 20 | | 2.4 | P | | 497 | 21.9 | F98 |
| Kiel | bare fallow | 5.7 | 5.33 | 12 | 2.3 | P | 2 soils | 750 | 5.4 | G89a, b |
| Hohenpeißenb. | bare fallow | 6.8 | 8 | 16 | 5 | P | 40 / 27 / 12 | 1304 | 2.5 | J80 |
| Albacher Hof | bare fallow | 5.7 | 8 | 16 | 28.0 | P | 12 / 63 / 25 | 761 | 2.2 | J80 |
| Erndtebrück | bare fallow | 6.0 | 8 | 16 | 12.0 | P | 19 / 42 / 7 | 652 | 0.7 | J80 |
| Marburg | bare fallow | 5.1 | 8 | 16 | 13.0 | P | 45 / 44 / 7 | 1230 | 6.4 | J80 |
| Rauischholzh. | bare fallow | 4.6 | 8 | 16 | 9.0 | P | 22 / 48 / 30 | 418 | 1.6 | J80 |
| Blumberg | bare fallow | 8.5 | 8 | 16 | 6.0 | P | 37 / 25 / 12 | 809 | 3.6 | J80 |
| Albacher Hof | bare fallow | 6.3 | 8 | 16 | 5 | P | 12 / 63 / 25 | 761 | 8.0 | K56 |
| Marburg | bare fallow | 5.1 | 8 | 16 | 2 | P | 45 / 44 / 7 | 1230 | 6.2 | K56 |
| Tertiary hills[4)] | bare fallow | 5.4 | 8 | 8 | 70 | P | 14 soils | 725 | 35.8 | M88, A93 |
| Escarpland[4)] | bare fallow | 5.4 | 8 | 8 | 60 | P | 12 soils | 725 | 31.2 | M88, A93 |
| Mountain ridges[4)] | bare fallow | 5.4 | 8 | 8 | 20 | P | 4 soils | 725 | 24.2 | M88, A93 |
| Moraines[4)] | bare fallow | 5.4 | 8 | 8 | 10 | P | 2 soils | 725 | 15.6 | M88, A93 |
| Mittelgebirge | bare fallow | 4.6 | | | 3 | P | | | 2.9 | P77 |
| Tarforst | bare fallow | 4.6 | 8 | 8 | 2.0 | P | | 680 | 0.5 | R87 |

(continued on next page)

| Location | Landuse | Slope (°) | Slope length (m) | Area ($m^2$) | Plot years | Type of study[1)] | Soil texture[2)] Sa /Si /Cl (%) bulk soil | Mean rainfall ($mm\ yr^{-1}$) | Mean erosion ($t\ ha^{-1}yr^{-1}$) | Reference[3)] |
|---|---|---|---|---|---|---|---|---|---|---|
| Olewig | bare fallow | 4.6 | 8 | 8 | 2.0 | P | | 465 | 1.8 | R87 |
| Kockelsberg | bare fallow | 4.6 | 8 | 8 | 2.0 | P | | 718 | 1.1 | R87 |
| Bitbg. Ch. | bare fallow | 4.6 | 8 | 8 | 2.0 | P | | 765 | 1.8 | R87 |
| Hungelsberg | bare fallow | 4.6 | 8 | 8 | 2.0 | P | | 775 | 3.2 | R87 |
| Dickes Kreuz | bare fallow | 4.6 | 8 | 8 | 0.5 | P | | 1042 | 2.6 | R87 |
| Königsbach | pasture | 19.8 | 40 | 186 | 0.4 | P | | 1065 | 0.0006 | F93 |
| Jenner | pasture | 24.2 | 40 | 182 | 0.4 | P | | 1065 | 0.012 | F93 |
| Brunnen | pasture | 19.8 | | 18 000 | 0.4 | W | | 1065 | 0.48 | F93 |
| Kaser | pasture | 19.8 | | 2 977 | 0.4 | W | | 1065 | 0.34 | F93 |
| Grat | pasture | 18.8 | | 301 | 0.4 | W | | 1065 | 0.016 | F93 |
| Königstal | pasture | 33.0 | 40 | 167 | 0.4 | P | | 1065 | 0.001 | F93 |
| Odenwald | meadow | | 8 | 16 | 5 | P | 2 soils | 780 | 0.19 | V78 |
| Tegernsee | forest | 18.8-20.8 | 40 | 200 | 8 | P | | 1700 | 0.0001 | A95 |
| Wald | forest | 30.1 | | 577 | 0.4 | W | | 1065 | 0.0002 | F93 |
| Odenwald | forest | | 8 | 16 | 5 | P | 2 soils | 780 | 0.003 | V78 |
| Steinberg | vines | 17.8 | 100 | | 14 | P | | | 28.0 | E05 |
| Geisenheim | vines | 5.7-17.8 | 100 | | 10 | P | 2 soils | 625 | 151 | E92 |
| Geisenheim | vines | 5.7-17.8 | 70 | | 1 | P | 45 / 23 / 12 | 625 | 12.4 | E92 |
| Geisenheim | vines | 5.7-17.8 | 30 | | 1 | P | 45 / 23 / 12 | 625 | 3.1 | E92 |
| Geisenheim | vines+grass | 5.7-17.8 | 100 | | 5 | P | 45 / 23 / 12 | 625 | 0.001 | E92 |
| Mertesdorf | vines | 20.8 | 8 / 16 | | 168 | P | 31 / 19 / 11 | 602 | 0.2 | R91 |
| Mainburg | hops | 2.7 | 45 | | 45 | T | 25 / 50 / 16 | 750 | 52 | S80 |
| Au | hops | 3.4 | 65 | | 34 | T | 24 / 49 / 23 | 750 | 55 | S80 |
| Au | hops | 1.4 | 70 | | 45 | T | 27/ 55 / 10 | 750 | 15 | S80 |
| Geroldshausen | hops | 2.6 | 130 | | 31 | T | 18 / 60 / 16 | 750 | 77 | S80 |
| Geroldshausen | hops | 3.6 | 210 | | 22 | T | 56 / 28 / 9 | 750 | 205 | S80 |
| Au | hops | 2.6 | 50 | | 45 | T | 28 / 50 / 14 | 750 | 24 | S80 |

[1)] P: Plots, T: Tracer, W: Fields, small watersheds; [2)] Sa: Sand > 0.63 mm, Si : Silt, Cl: Clay < 2 µm; [4)] Measurements from different landscapes in Southern Germany;

[3)] References: A03: Auerswald et al. (2003b), A93: Auerswald (1993), A95: Ammer et al. (1995), B90: Barkusky (1990), B91: Botschek (1991), D68: Dubber (1968), D86: Dikau (1986), D89: Deumlich and Gödicke (1989), D94: Deumlich and Frielinghaus (1994), E92: Emde (1992), E05: Emde et al. (2005), F00: Fleige and Horn (2000), F93: Felix and Johannes (1993), F98: Frielinghaus (1998), G89a: Goeck (1989), G89b: Goeck and Geisler (1989), J80: Jung and Brechtel (1980), K56: Kuron et al. (1956), M88: Martin (1988), P77: Preuss (1977), R87: Richter (1987), R91: Richter (1991), S80: Schwertmann and Schmidt (1980) recalculated (this article), S90: Saupe (1990), S92: Saupe (1992), S02: Schimmack et al. (2002), V78: Voss (1978);

landuse were not included as no landuse-specific identification of sediment source areas is possible in these cases. Only published data were used while internal reports and theses below Ph.D. theses level were discarded. The results of the studies are summarized in Table 1. The results were combined according to landuse and weighted according to the length of the study period. Many studies did not cover only whole-year periods but also had partial years included. These data were also used and weighted according to the months of measurement to maximize the data set. These partial years mostly covered the growing period while the dormant season is slightly underrated in the data set. No correction was applied for this bias. A correction would have to be based on an assumption on seasonal changes in erosion rates. No reliable estimate of the seasonality was available because the contribution of snowmelt erosion during winter and early spring to total soil loss is unknown (Schwertmann et al., 1987). Such an estimate of seasonality could also not be derived from the data set itself. While seasonal distribution of rain erosivity indicates that rainstorms are much more severe during summer months with more than 80% of the erosivity falling between May and September (Schwertmann et al., 1987), there are also erosion measurements showing that erosion by winter runoff can be severe, because soil cover is low and moisture content is high (Fiener and Auerswald, 2006; Saupe, 1990).

In spite of the large number of studies (27) their setup cannot be regarded representative for Germany. Four major deficiencies exist: (i) Landuse did not reflect the actual landuse. Many studies used bare fallow plots as a baseline reference, which does not exist in reality. On the other hand, grassland and forests were largely underrated. (ii) Slope gradients did not reflect reality, e.g. flat land is missing. (iii) Plots were mostly very small in size compared to real fields. (iv) Plots were predominantly located in areas with relatively large rain erosivity. Furthermore, there was a consistent bias in the data because highly erodible surfaces were more often examined on shorter plots than low erodible surfaces, e.g. weighted average slope length was 11.2 m for bare fallow plots while it was 82.3 m for annual crop plots. Field, watershed or tracer data were completely missing for bare fallow treatment (Table 1).

To overcome the limitations of individual data sets and to derive representative soil erosion rates and a soil erosion map for Germany, the following methodology was applied extending and refining an approach used by Cerdan et al. (2006) for Europe.

**Aggregation of landuse categories**

The data of the different studies were categorized to get similar landuse categories as those available on a national scale (Destatis, 2002; ECC, 1992). These landuse categories are annual arable land (including all data from annual crops), grassland and forest; and due to the specific location on steep slopes vineyards; and regarding their high erosion potential

hop gardens. As no measured data are available for urban areas and settlements, these landuse categories were excluded from further analysis.

Within landuse category 'annual arable land' most studies had a setup consisting of a plot treatment close to current landuse and additionally other treatments to achieve a wide variety of conditions. These additional treatments often included a bare fallow plot as the worst-case scenario and one or more soil conservation practices. Except for these studies aiming to determine soil erodibility (especially, Auerswald, 1993a; Martin, 1988) these bare fallow treatments did not follow the recommendations of Wischmeier (1960) and Wischmeier and Smith (1978), who did not use data of the first two years of bare fallow because these years are still heavily influenced by carryover effects of the preceding crops. Soil conservation measures applied on other plots do not occupy relevant acreages under German farming conditions. Deleting the bare fallow plots (< 2 yr fallow) and soil conservation plots from the data set would have reduced the number of years considerably while deleting only one of these two groups would have biased the averages. We hence used all arable plots to account for the range in arable landuse conditions and to base our results on a wide data set assuming that the biases caused by bare fallow and by soil conservation systems almost level out. However, studies using long-term bare fallow (> 2 yr) aiming to determine soil erodibility were deleted from the data set of annual arable land and will be reported as a separate, additional landuse category 'bare fallow', which quantifies the natural soil erosion disposition without cropping influence. These long-term bare fallow studies were available only from a few sites although they comprised a large number of plot years. To base the average soil loss for the bare fallow category on a regionally wider data set, the bare fallow plots of the annual arable landuse studies (< 2 yr) were also included but these were corrected in this case by dividing them by 0.8, which is a correction factor recommended by Wischmeier and Smith (1978) to account for prior landuse effects. The category 'bare fallow' still is dominated by studies, which followed the definition by Wischmeier and Smith (1978) and thus this assumption will introduce only small error.

**Adjustment for landuse**

To derive an areal distribution of the above categorized landuses (except hop gardens and fallow land) on a national scale, the European CORINE data set (COoRdination of INformation on the Environment; ECC, 1992) was used, which provides 44 classes of land cover data at a scale 1:100 000 mostly derived from the exploration of satellite images together with other relevant documents. The original CORINE classification for landuses found in rural areas of Germany and the aggregation of these into the categories annual arable land, grassland, forests and vineyards are shown in Table 2. Difficulties in assigning a proper landuse category arose especially for class 243 (Land principally occupied by agricul-

ture, with significant areas of natural vegetation), which contributed 2.1% of the total area. It was evenly distributed between forests and grassland. The error of this assumption should be small given the small contribution of this class to the total area and the similarity in erosion potential of forests and grasslands. Further, the class "Fruit trees and berry plantations" oc-

**Table 2: CORINE (ECC, 1992) land cover areas for Germany used to derive the landuse categories applied in this study; only those data representing rural areas were taken from the CORINE data set and are compared to German landuse statistics (Destatis, 2002); urban areas and water surfaces are not included.**

| Landuse categories | Landuse according to the CORINE data set | Area of CORINE landuses (%) | Area of landuse categories aggregated from CORINE (%) | Area of landuse categories according to statistics (%) |
|---|---|---|---|---|
| Annual arable land | Non-irrigated arable land | 39.9 | 39.9 | 36.9 |
| Grassland | Pastures and meadows | 12.0 | | |
| | Complex cultivation pattern | 5.7 | | |
| | Natural grassland | 0.1 | | |
| | Moors and heath land | 0.3 | | |
| | Land principally occupied by agriculture with significant areas of natural vegetation | 1.1 | 19.2 | 16.9 |
| Forests | Broad-leaved forest | 6.6 | | |
| | Coniferous forest | 15.9 | | |
| | Mixed forest | 6.7 | | |
| | Land principally occupied by agriculture with significant areas of natural vegetation | 1.1 | 30.3 | 29.9 |
| Vineyards | Vineyards | 0.4 | 0.4 | 0.3 |
| Hop gardens | - | - | - | 0.1 |

cupying 0.4% was evenly distributed between arable land and forests, because no measurements were available for this land use. In summary, this approach led to a distribution of rural landuse similar to the distribution derived from official statistics (Table 2; Destatis, 2002).

### Adjustment for slope gradients

To account for a slope gradient distribution throughout Germany, slope gradients were derived from the SRTM (Shuttle Radar Topography Mission) digital elevation model (Rabus et al., 2003). This digital elevation data have an absolute horizontal and vertical accuracy of 20 m (circular error at 90% confidence) and 16 m (linear error at 90% confidence), respec-

tively. The data files are freely available at a NASA file server (ftp://e0mss21u.ecs.nasa.gov/srtm/). They were processed and transformed to a raster map with 75×75 m resolution using the software package ArcGIS 9.2 (ESRI, USA). To quantify a potential bias in slopes due to a smoothening of steep and short slopes in low resolution digital elevation models (Guth, 2006) we compared the SRTM DEM with a high resolution 10×10 m laser scanner DEM (Landesvermessungsamt, North-Rhine-Westphalia) of the Rur catchment (2354 $km^2$) located southwest of Düsseldorf (Figure 1).

The slope gradients were converted to the *S* factor of the USLE, which is the dimensionless influence of slope gradient as compared to a baseline gradient of 5.1° (=9%). The equation by Nearing (1997) was used to calculate *S* because it is applicable also for steep slopes as commonly found in vineyards, grasslands and forests.

$$S = -1.5 + \frac{17}{1 + e^{2.3 - 6.1 \sin \alpha}} \quad (1)$$

where *S* is the slope factor of the USLE [–] and $\alpha$ is the slope gradient [°].

Eq. (1) was also used to standardize the measured soil losses from the individual plots to an expected loss for the baseline gradient.

**Adjustment for flow path length**

To account for the difference in flow path length between plot data and the real field situation, no appropriate data set exists. Even if one would derive data for field situations from a combination of the SRTM digital elevation model and the CORINE data set, results would be biased by the problem of missing data regarding the existing channel systems between fields and/or patchiness of fields, which both can substantially shorten flow path length. However, although no appropriate statistical data on flow path length exists, it is larger in most cases than the average plot length calculated from the evaluated studies (Table 1). Therefore, we applied a second step of standardization in correcting the measured data to a slope length of 200 m, which seems to be closer to reality under German farming conditions than the actual plot lengths. To this end, Eq. (2) provided by Wischmeier and Smith (1978) was used applying an exponent *m* of 0.5 for slopes > 2.9° and utilizing Eq. (3) from Murphree and Mutchler (1981) for smaller slopes:

$$L = \left( \frac{\lambda}{22.1} \right)^m \quad (2)$$

$$m = 1.2 \cdot (\sin\alpha)^{1/3} \quad (3)$$

where $L$ is the slope length factor of the USLE [–], $\lambda$ is slope length [m], and $\alpha$ is the slope gradient [°].

Although this procedure is unsatisfactory, it will lead to values, which should be closer to reality than the uncorrected values. The procedure will also allow adjusting the data set to reality easily once data on flow path lengths are available. For vineyards an erosive slope length of 200 m seems to be unrealistic. In a detailed study visiting all vineyards in Bavaria, Königer and Schwab (2000; 2002) identified typical slope lengths of 60 m for linkage-pull vineyards ("Steillagen") and 80 m for tractor-pull vineyards ("Direktzuglagen"), which are flatter than linkage-pull vineyards. This corresponds to $L$ factors of 1.65 and 1.90, respectively. Linkage-pull and tractor-pull vineyards contribute 17% and 83%, respectively, to total vineyard area in Germany. We hence used an area weighted average $L$ factor of 1.86 for vineyards.

**Adjustment for rain erosivity**

After standardization for slope gradient and slope length the measured data were standardized in a third step to account for regional differences in rain erosivity using an $R$ factor map of Germany based on high-resolution and long-term rainfall data measured at 139 meteorological stations (Sauerborn, 1994). As most studies did not report the $R$ factor for the measuring period or the data necessary to calculate it, this standardization could only be applied for the long-term average but not for the individual measuring period.

**Adjustment for hops**

The procedure to adjust for landuse could not be applied to hop gardens for two reasons. First, hops cannot be identified in the CORINE data set (Table 2), and second, only tracer data from fields were available from Schwertmann and Schmidt (1980), who did not distinguish between water erosion and tillage erosion at that time. However, hops are a crop especially prone to erosion and the largest hop growing area in the world (the Hallertau) is located in southern Germany (Knoll and Sieber, 1986). Hence, hops could not be omitted or assigned to any other landuse category. To distinguish between water and tillage erosion, the original data of Schmidt (1979) were used, which quantify the tracer distribution (copper in this case) over soil depth along slope transects. Accumulations at the foot slope could clearly be detected although sedimentation from water erosion is highly unlikely on these straight slopes. We assumed that the accumulations resulted from tillage erosion and are balanced by an equivalent loss from the eroding area. The total erosion reported by Schwertmann and

Schmidt (1980) could thus be attributed to a tillage-induced or water-induced portion (Table 3). To determine a slope gradient distribution, the hop gardens were identified in the official surveying and cadastral information system ATKIS (Amtliches Topographisches Kataster-Informations-System; Steudle, 1997) and the slope gradients were calculated from a more detailed 50-m grid digital elevation model, which was available for the hops area. No correction for slope length was applied assuming that the hop gardens analyzed by Schmidt (1979) reflected reality in this respect (weighted average slope length: 82 m), although they seem to be somewhat shorter than average. This may be caused by the selection of homogeneous, straight slopes in the study of Schwertmann and Schmidt (1980). On the other hand, more erosion-reducing measures are found in hop gardens now (Auerswald et al., 2003) as compared to the time when the erosion in the hop gardens was analyzed by Schwertmann and Schmidt (1980). No quantitative estimate of both effects exists but they should at least partly compensate each other. Hence we used the data from hop gardens without correction for actual slope length and actual erosion control measures.

### Combinations of adjustments in a national map

The procedures described above (Section "Aggregation of landuse categories" to Section "Adjustment for hops") were combined to derive a national soil erosion map for Germany and to calculate the average erosion rates for each land use category. To this end, standardized erosion rates of each landuse category were combined with the generalized CORINE land cover data and these standardized rates were multiplied with *S*, relative *L* (slope specific *L* factor divided by *L* factor for standard slope of 5.1°) and relative *R* (*R* factor divided by mean *R*) for each 75×75 m raster cell. To include hop gardens the standardized erosion rates of hops were multiplied with *S*, relative *R* and the proportion of hops in each raster cell. In a last step the erosion map using the CORINE data was multiplied with the proportion of landuse excluding hops, and the hops erosion map was added. No correction for soil properties was applied assuming that the measurements within the land use categories arable land, vineyards, hops, grassland and forests have been carried out on soils typical for these land uses.

## Results and discussion

### Distribution of measuring sites

Most data were derived from locations in southern and western Germany (Figure 1), while data from northern and eastern Germany were less frequent. This scarcity of data is mainly caused by the mostly flat terrain in the North German Lowlands, where comparably little sheet and rill erosion is expected due to the low slope gradients. Little error can be ex-

**Table 3. Water and tillage erosion in hop gardens as estimated from long-term copper budgets; recalculated and assigned to water and tillage erosion separately using the raw data taken from Schmidt (1979); averages are weighted for years.**

| Field No. | Number of years | Slope gradient (°) | Slope length (m) | Water erosion (t $ha^{-1}$ $yr^{-1}$) | Tillage erosion (t $ha^{-1}$ $yr^{-1}$) | Total erosion (t $ha^{-1}$ $yr^{-1}$) |
|---|---|---|---|---|---|---|
| 1 | 45 | 2.7 | 45 | 52 | 38 | 90 |
| 2 | 34 | 3.4 | 65 | 55 | 39 | 94 |
| 3 | 45 | 1.4 | 70 | 15 | 27 | 42 |
| 4 | 31 | 2.6 | 130 | 77 | 42 | 119 |
| 5 | 22 | 3.6 | 210 | 205 | 63 | 268 |
| 6 | 45 | 2.6 | 50 | 24 | 32 | 56 |
| Average | 37 | 2.7 | 95 | 58 | 38 | 96 |

pected from the scarcity of data in these areas because the correction for slope gradient and rain erosivity also predicts small soil losses. A large relative error in these areas will have little absolute effect on the country-wide averages, which are dominated by the more erosive sites.

Analogously, those landuses are also greatly underrated in the data set for which little erosion can be expected (grassland, forest). Again this should have comparably little effect on the accuracy of the country-wide average due to their small contribution to total soil loss.

**Distribution of landuse among slope gradients**

According to the SRTM and the CORINE data sets, annual arable land can be mainly found on sites with slope gradients < 4° (Figure 2). Vineyards are preferably established on slopes ranging from 10° to 30°, while hop gardens only occupy comparably flat areas with slopes around 3°. The proportion of grassland is more or less constant on slopes < 30° but increases on steeper slopes due to the steep pastures and natural meadows in mountainous and alpine areas. Forests occupy the steepest parts of the country and are in general dominating slopes > 4°.

The appearance of Figure 2 is somewhat misleading, as slope gradients larger than 4° contribute only 25% to total rural land, while Figure 2 also reports the distribution of landuse for slope gradients up to 75° and thus seems to inflate the proportion of forest and grassland. The average slopes of the landuse categories (Table 4) are hence much lower than it may be expected from Figure 2. The skew in the distribution of slope gradients also becomes obvious from the comparison of the median and mean slope (Table 4), where the median is only about half of the mean. The mean slope is largest for vineyards due to the lack of vineyards on flat terrain and it is smallest for hop gardens. From the difference in slope gradients

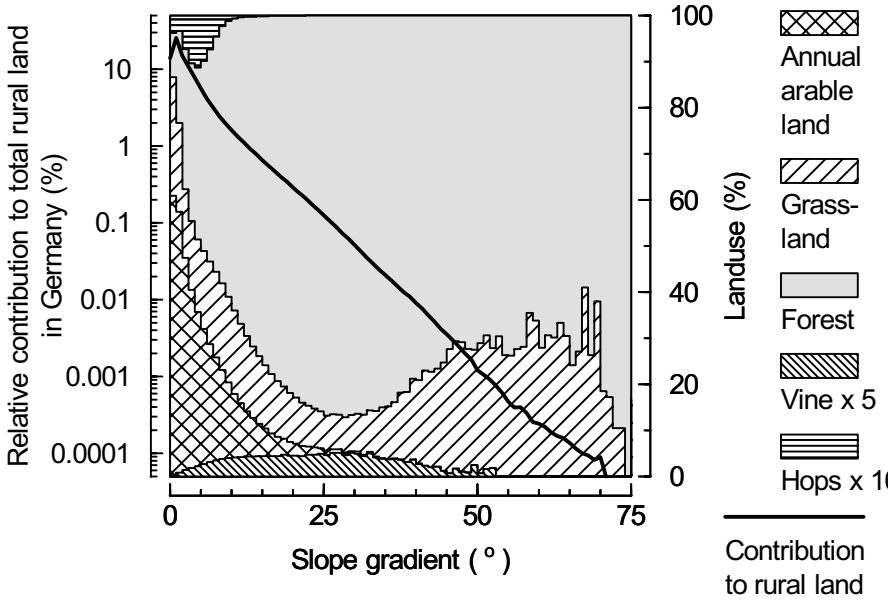


**Figure 2. Contribution of slope gradient classes to total rural land (bold line and left y axis) and distribution of landuse among slope gradient classes (right y axis and shaded areas; vine is inflated by a factor of 5, hops by 10).**

it can be expected that forest and vineyard sites are 3 to 4 times more prone to erosion than arable sites, while grassland and arable sites differ by less than a factor of 2.

The slope gradients from the plot data greatly deviate from the country averages (Table 4). Researchers mainly examined slopes which were steeper than the typical situation of a certain landuse. On the other hand, they used unrealistically short and small plots (Table 1).

There is clearly a demand for more realistic experimental setups because the extrapolation of the experimental results to reality thus depends on the applicability and accuracy of erosion models, which again are mainly developed from experiments using similar setups.

### Distribution of landuse among rain erosivity

On average the rural area in Germany has approximately an *R* factor of 58 (standard deviation SD=18 N $h^{-1}$ $yr^{-1}$). This value is later on used to standardize the plot measurements, because these measurements were, analogously to slope gradients, mostly undertaken in areas with a higher erosivity compared to the average (Table 4). In vine growing areas average erosivity is slightly lower (Average AVR=52, SD=9 N $h^{-1}$ $yr^{-1}$) while in hop gardens, which are located exclusively in southern Germany, average erosivity is slightly higher (AVR=65, SD=6 N $h^{-1}$ $yr^{-1}$). For grassland and forests average rain erosivity is approximately 62 N $h^{-1}$ $yr^{-1}$, with a more pronounced variability (SD is 21 N $h^{-1}$ $yr^{-1}$ in both cases) because these can be predominantly found in the climatically extreme sites. The German

mean erosivities deviate substantially from the means of the plot experiments (Table 4). This is especially evident for vine (52 vs. 44) and forests (63 vs. 103).

### Standardized soil loss

The standardized soil loss (slope 5.1°, slope length 200 m, average *R* factor of 58) of annual arable land was 15.2 t $ha^{-1}$ $yr^{-1}$. Soil loss from row crops without any conservation measures averaged 88.6 t $ha^{-1}$ $yr^{-1}$ (34.1 plot years) and was considerably higher than the soil loss from short-term bare fallow (34.9 t $ha^{-1}$ $yr^{-1}$, 63 plot years). Including short-term bare fallow into landuse category annual arable land, to compensate for the super proportional contribution of plots with conservation measures thus seems to be justified. These short-term bare fallow plots contribute only 14% of total plot years.

**Table 4: Characteristics of slope, slope factor *S* of the USLE, and rainfall erosivity *R* in the experimental studies and for rural land throughout Germany; nationwide data are derived from a digital elevation model with 75 m resolution and from a rain erosivity map (Sauerborn, 1994); experimental studies are weighted for plot years; bare fallow slope and rain erosivity is calculated using data of the total rural land.**

| | | | Landuse | | | | | |
|---|---|---|---|---|---|---|---|---|
| Property | Unit | Data base | Bare fallow | Arable land | Grass-land | Forests | Vine-yards | Hop gardens |
| Average slope | (°) | Experiments | 6.1 | 5.9 | 10.6 | 18.9 | 15.9 | 2.6 |
| | (°) | Germany | 4.4 | 2.6 | 3.9 | 7.0 | 7.3 | 3.4 |
| Median slope | (°) | Germany | 2.9 | 1.4 | 1.6 | 4.5 | 5.0 | 1.2 |
| Average *S* | (-) | Experiments | 0.92 | 0.46 | 1.56 | 0.77 | 1.65 | 0.6 |
| | (-) | Germany | 0.84 | 0.4 | 0.71 | 1.5 | 1.52 | 0.65 |
| Average *R* | (N $h^{-1}$ $yr^{-1}$) | Experiments | 67 | 64 | 66 | 103 | 44 | 69 |
| | (N $h^{-1}$ $yr^{-1}$) | Germany | 58 | 53 | 62 | 63 | 52 | 65 |

Bare fallow soil loss from long-term experiments (240 plot years) was considerably larger than that from short-term bare fallow (63 plot years) even after adjustment for carryover effects on the short-term plots (84.3 vs. 43.6 t $ha^{-1}$ $yr^{-1}$). This indicates that the carryover effect was underrated or that the sites of the short-term experiments were less prone to erosion although this is not evident from the available information. While the first argument would call for deleting the short-term data from the bare fallow average, the second argument calls for the opposite. We kept the short-term results in the data set considering their comparably small contribution to the total number of plot years (21%).

Site conditions (soils, climate) were almost identical for bare fallow and annual arable crops because both were often examined at the same sites. Comparing the standardized soil loss shows that annual arable crops on average reduced soil loss to 14.9% of the long-term

bare fallow soil loss. This is close to an estimate following a completely independent approach of modeling (13.2%) by Auerswald et al. (2003).

Standardized soil loss was considerably lower for vineyards than for annual arable land (Table 5), which is mainly caused by differences in soil properties (especially stoniness of vineyards) but might be also influenced by those in general different management operations.

**Table 5: Standardized erosion from plot experiments (standardization by weighting for plot years, *R* factor relative to the German average of 58 N $h^{-1}$ $yr^{-1}$, slope gradient of 5.1° and an erosive slope length of 200 m) and expected average soil loss for Germany; calculated according to the raster data of slope gradients and erosivities assuming a slope length of 200 m for annual arable land, grassland and forests, while slope lengths of 80 m and 82 m are assumed for vineyards and hops.**

| | Plot experiments | | Germany | | | |
|---|---|---|---|---|---|---|
| | Standardized erosion (200 m, 5.1° [9%], *R*=58 N $h^{-1}$ $yr^{-1}$) (t $ha^{-1}$ $yr^{-1}$) | Observation period (yr) | Average soil loss (t $ha^{-1}$ $yr^{-1}$) | Standard deviation of soil loss (t $ha^{-1}$ $yr^{-1}$) | Contribution to rural landuse (%) | Contribution to total soil loss (%) |
| Bare fallow | 79.64 | 303.0 | | | | |
| Annual arable land | 15.15 | 416.2 | 5.7 | 8.6 | 44.0 | 92.8 |
| Grassland | 0.48 | 9.4 | 0.5 | 2.3 | 20.2 | 3.7 |
| Forests | 0.01 | 13.4 | 0.2 | 2.6 | 35.7 | 2.6 |
| Vineyards | 5.44 | 175.0 | 5.2 | 5.9 | 0.34 | 0.7 |
| Hop gardens | 154.40 | 222.0 | 42.8 | 45.9 | 0.06 | 1.0 |
| Total without bare fallow | | 836.0 | 2.7[a)] | | | |

[a)] Expected average soil erosion for rural areas in Germany taking into account the area distribution of the different landuses.

In contrast, soil loss under hops was considerably higher. The data of Schwertmann and Schmidt (1980) indicated an average total soil loss of 96 t $ha^{-1}$ $yr^{-1}$ for hops for which two thirds could be attributed to water erosion and one third to tillage erosion (Table 3). The soil loss of hop gardens after adjusting to 5.1° slope gradient, 200 m slope length and average *R* factor was considerably greater than the soil loss of long-term bare fallow, which is surprising. This may be attributed to several effects: (i) It may indicate that hops even increase soil erosion above bare fallow, which, in terms of the USLE, would correspond to a *C* factor larger than 1. This could be caused by soil compaction due to frequent trafficking and by the effect of the large falling height of drops dripping off the leaves (~6 m). Especially during low-intensity rains with small drops these will be collected by the leaves and drip off as large drops (Brandt, 1989), which then gain considerable kinetic energy due to the large fall-

ing height as final crop height is 6 m with almost no leaves lower than 1 m above ground. Low-intensity rain prevail in Germany, where even the maximum 30-min intensity of erosive rains averages to only about 11 mm $h^{-1}$ (Rogler, 1981). (ii) The correction factor *L* used to adjust bare fallow soil loss may underrate the slope length effect as compared to hops. This would especially be the case if hop gardens were subject to heavy rilling (McCool et al., 1997). (iii) The sites used for hop gardens may have more erodible soils than the average erodibilities of the bare fallow plots. (iv) The computed soil loss rates of the hop gardens may still be too high even after consideration of tillage erosion as they are determined from tracer losses. In this case, copper was used as a tracer, which at that time was applied as a fungicide with a uniform treatment scheme. The copper sulphate was applied to the leaves and some copper may be washed from the leaves and lost by runoff without being associated with a corresponding soil loss (Schwertmann and Schmidt, 1980). Presently it cannot be decided to which degree these explanations contribute to the higher soil loss under hops than under bare fallow.

Soil losses from forests and grassland were less than one tenth of the soil loss from annual arable land. Whether the difference between forest and grassland holds true is questionable due to the extraordinary short experimental record for both landuse classes.

**Actual soil loss**

The expected average soil loss by sheet and rill erosion in rural areas in Germany after adjustment for real slope gradients and distribution of landuse becomes 2.7 t $ha^{-1}$ $yr^{-1}$ and is based on 836 experimental plot years (Table 5). Annual arable crops contribute the largest share to this soil loss, but hops despite their negligible contribution to landuse (0.06%) still contribute 1.0% due to their extraordinary large erosion.

The spatial distribution of soil loss in Germany (Figure 3) exhibits soil losses of 0–1 t $ha^{-1}$ $yr^{-1}$ mainly in areas covered by grassland and forest (e.g. typical for the mountain ranges in central Germany) or in flat terrain of flood plains along larger rivers. Highest erosion rates > 10 t $ha^{-1}$ $yr^{-1}$ are located in arable areas with relatively steep slopes. This causes a clear regional difference in water erosion between arable areas in the North German Lowlands and the hilly countryside of low mountain ranges in central Germany and the hilly areas of the Tertiary hills and Alpine moraines in southern Germany. The highest erosion rates concentrate in the hop growing area of Hallertau, north of Munich.

**Validity of assumptions**

The analysis is based on two assumptions. First, a long measuring period obtained by aggregating many studies can level out the pronounced variability of erosion events. Second, the

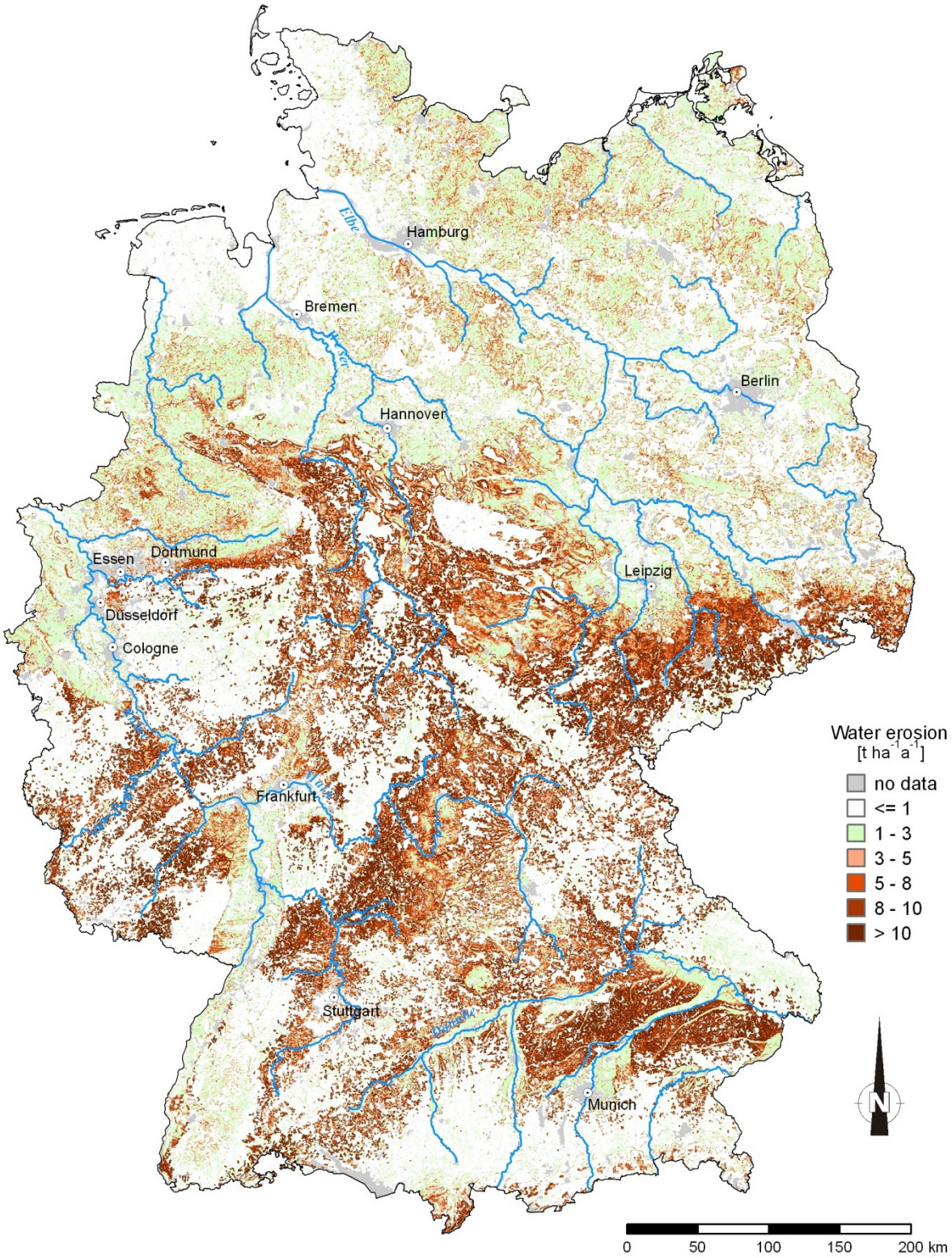


**Figure 3. Soil erosion map for Germany based on standardized soil erosion measurements of different landuse categories (836 yr of observation) and 75×75 m raster data for slope.**

soil loss rates, which were measured under non-representative conditions, can be standardized to typical conditions in Germany depending on landuse using *S*, *L* and *R* of the Universal Soil Loss Equation. It is helpful to prove both assumptions although the first is trivial and the second assumption makes use of the by far most often used soil erosion modeling tool for multi-year data. This proof cannot be conducted for the whole data set, which is statistically biased in many respects. Regarding the first assumption long-term data are mainly available for hops, while short-term data dominate for forests, which leads to an apparent but non-existing increase in soil loss with measuring period. The largest unbiased subset of data to prove the first assumption comes from annual arable crops, for which also the largest intra- and inter-annual variability can also be expected due to the varying soil cover and management. We can hence best examine the first assumption based on this subset. Short-term measurements (< 3 yr) exhibited a pronounced variability covering five orders of magnitude, which decreased to about one order of magnitude with increasing number of plot years of the individual studies (Figure 4) proving the first assumption. This convergence was still considerably weaker than what would be expected from generating long-term data by applying Monte-Carlo simulations to the short-term data. In such simulations the variability converges to less than one order of magnitude already after 20 yr (not shown). A main cause of variability results from the magnitude and timing of erosive rains. This variability cannot be covered by examining many vicinal plots over a short period of time and hence variability decreases less with the number of plot years than with the number of years. Long-term datasets covering more than 20 yr do not exist for annual arable crops in Germany and can only be created by aggregating data from several studies.

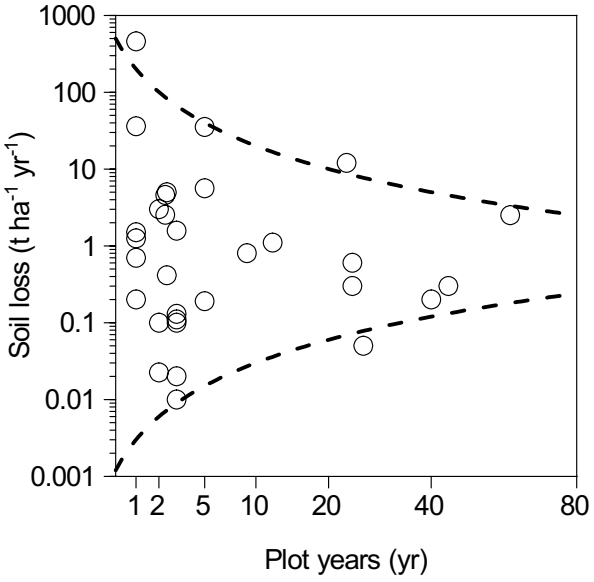


**Figure 4. Mean reported soil loss of annual arable crops of different studies (n=32) depending on the number of plot years; the lines denote arbitrarily chosen symmetrical hyperboles.**

Regarding the proof of the second assumption, the complete data set is also biased, which mainly relates to the lacking ability to measure very low or very high erosion rates. Hence, researchers aiming to measure soil surfaces with good protection select steep, long

slopes while the opposite is true for surfaces with little protection, which results in a compensation or even reversion of the apparent effects of topography in the total dataset. The influence of slope gradient and length can hence best be analyzed on long-term data under identical landuse. These conditions are perfectly met by the data from the hop gardens, which were also similar regarding soil erodibility and rain erosivity but included a considerable variation in slope length and gradient. The *L* factor varied 2.1-fold between 1.30 and 2.68 while *S* varied 2.6-fold between 0.27 and 0.67. The combination of both factors almost perfectly explained the variation in soil loss between the different hop gardens (Figure 5).

Even if the model being used to adjust the erosions rates works well, wrong estimates could still result if the data base used for the adjustment contains errors. Such errors can especially be expected for the SRTM slopes due to the coarse 75×75 m grid. Comparing slope distributions of the SRTM and the 10×10 m laser scanner DEM to determine a potential smoothening of steep slopes in the case of the low resolution data exhibited some unexpected

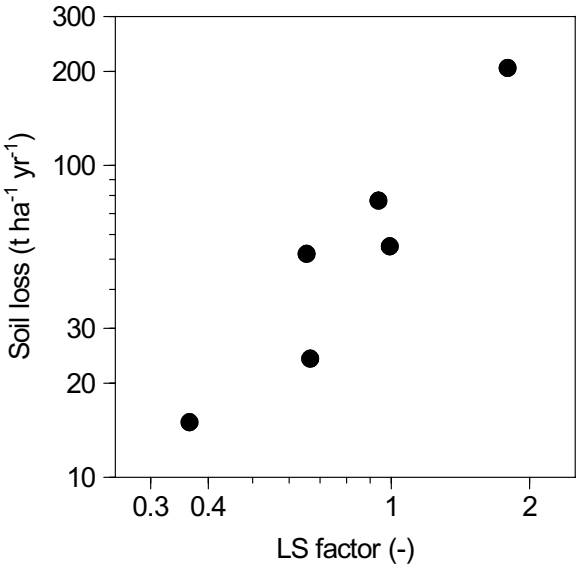


**Figure 5. Comparison between the predicted *LS* factor and long-term mean annual soil loss of hop gardens; raw data from Table 5; *R* factor is near identical for all sites 69 N $h^{-1}$ $yr^{-1}$; *K* factor varies between 0.32 and 0.45 t $ha^{-1}$ $yr^{-1}$ h $N^{-1}$; including the *K* factor slightly improves the prediction from $R^2$=0.90 to $R^2$=0.96; both axes are log scaled.**

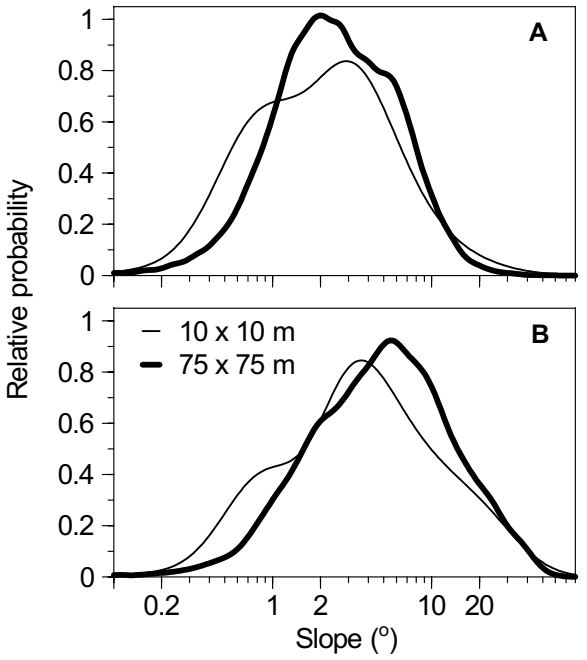


**Figure 6. Probability of slope within the Rur catchment (2354 $km^2$) depending on landuse and grid resolution; A: arable land, B: total land; shown as kernel density distribution; calculated after log transformation to account for the skewed distribution and then back transformed after kernel density estimation; to allow for comparison of differently sized data sets integral density was set equal; Silverman (1986).**

results (Figure 6). The laser scanner DEM had higher percentages of low slope gradients than the low resolution grid and no smoothening effects of steep and short slopes could be found in the SRTM data. The smaller percentage of low slope gradients in the SRTM data may result from noise in the radar data. The reason for a missing smoothing effect is unknown. Both effects are considerably smaller for arable land, which contributes most to erosion. No correction was applied considering the unknown source of the effect and the general uncertainty when retrieving slope gradients from a DEM. Warren et al. (2004) have shown that, even if the DEM is dense and accurately obtained by a geodetic survey, errors in slope calculation may cause errors in erosion by a factor of ten.

**Restrictions of the erosion data base**

Accuracy of the average soil loss from annual crops should increase considerably by accounting for the proportions of different annual crops or crop classes like small grain or row crops. This was not possible due to limitations of the experimental studies. A large proportion (about 30% of plot years) only reported soil losses averaged over the total crop rotation. Important crops were underrated in the remaining experiments reporting individual crops (e.g., rape and potato had less than five plot years while they contribute 10.8 and 2.4% respectively to annual arable land; Destatis, 2002) and experiments reporting individual crops often had treatments (cultivation techniques, crop rotations) differing considerably from reality. Moreover, measurements of erosion in case of individual crops within a crop rotation do not take into account carry-over effects of previous crops, which can be large (Fiener and Auerswald, 2007).

The expected average soil loss from annual arable land, although based on a considerable number of plot years, is strongly influenced by results from one location. This location (Scheyern) contributed 123 yr to a total of 416.2 yr (Table 6). Unfortunately, all studies carried out at Scheyern examined annual arable landuses for which comparably little soil loss can be expected. One study examined only small grain, one study examined a full soil conservation system and the third examined organic farming with soil conservation, which also produces much lower soil loss than conventional farming (Auerswald et al., 2003). Hence, average soil loss at this location was only one fourth of the German overall average and a calculation without the data from this location would increase the German average by 37%. Nevertheless, we included all data in the German average because the data from Scheyern are more realistic than most data from other studies concerning other aspects (long-term, whole-year measurements on field scale) and also all other studies must be regarded unrealistic in some aspects of their plot treatments (plots are often too small as compared to fields; they do not allow to use heavy machinery, etc.). We conclude that in spite of a considerable number of studies on soil erosion there is still little experimental evidence on soil loss under

**Table 6. Soil erosion from annual crops standardized to 5.1° slope gradient, 200 m slope length and average erosivity for studies at the Scheyern experimental farm as compared to German averages; all data weighted for plot years.**

| No. | Location | Landuse | Plot years | Erosion ($t\ ha^{-1}\ yr^{-1}$) | Study |
|---|---|---|---|---|---|
| 1 | Scheyern | conventional farming, conventional tillage, small grain | 23 | 3.6 | Schimmack et al., 2002 |
| 2 | Scheyern | conventional farming, full soil conservation, mixed rotation | 60 | 2.6 | Auerswald et al., 2003 |
| 3 | Scheyern | organic farming with soil conservation, mixed rotation | 40 | 0.1 | Auerswald et al., 2003 |
| 4 | Scheyern | arable, total | 123 | 2.0 | this study |
| 5 | Germany | arable, total | 416.2 | 15.5 | this study |
| 6 | Germany | arable, without Scheyern | 293.2 | 20.7 | this study |

realistic landuse conditions. We may further conclude that arable soil loss could be considerably lowered by soil conservation systems. If we set the German average without Scheyern as 100%, we could expect to lower soil loss by sheet and rill erosion to 17% by (unrealistically) converting all fields to small grain, to 12% by applying a full conservation system, which is more realistic, or to 1% by converting all into an organic farming system, which especially considers soil erosion in its farming decisions as it was the case at Scheyern (Auerswald et al., 2000).

The combination of 27 studies and the standardization by modeling leveled out some of the major errors of different studies. Nevertheless, many errors still exist. While some of them only contribute to the scatter, others lead to a bias, which will not level out even by including many studies. One of them can be predominantly identified, which results from publication policies. Several measuring campaigns are known to us, which were carried out but never published because (almost) no erosion occurred during the study period. Although these measurements may be the most accurate, they lead to no insight into processes or treatments and hence could not be published. Published data thus overrate erosion rates.

While the errors of the different studies are still contained in our meta-analysis, an error can result from the meta-analysis itself in the case of erosion. Long-term measurements can be regarded best because they account better for years of especially low or high erosion rates but this implies that some of the data contributing to them are rather old. Combining these data in a meta-analysis causes an additional delay. Some of the erosion events contributing to the measured soil loss of hops already occurred in the first half of the 20$^{th}$ century (Table 3). The same is true for the long-term data by Kuron et al. (1956). Agricultural and forestry

practices faced dramatic changes in many aspects during the last decades. Moreover, climate change within the last century may have increased rain erosivity in some areas of Germany. It is difficult to assess whether these old data still reflect erosion under current soil use and climatic conditions.

Hence, despite the large number of studies and plot years included in this meta-analysis and the reasonable quality of spatial input data, the calculated erosion rates still have to be regarded a rough estimate.

## CONCLUSIONS

There are a considerable number of studies reporting measured sheet and rill erosion under natural rainfall in Germany (in total 1076 plot years). However, these studies cover too short time scales to account for the large temporal variability of erosion events and hence it is impossible to derive statistically sound average erosion rates. Furthermore, a considerable number of these studies were carried out on sites that are too steep and do not represent average erosivity compared to the German average of the respective landuse. Finally arable plots were largely overrated in these studies as compared to the contribution of annual arable land to rural land in Germany. The first deficiency could be overcome by combining all studies. The second deficiency was overcome by adjusting the measured soil losses according to the slope gradients and the erosivity of a certain landuse as derived from spatially distributed national raster data sets (digital elevation model, landuse classification and erosivity map) in a 75 m resolution. The third deficiency was overcome by adjusting the measured soil erosion data according to agricultural statistics of landuse. Soil loss by sheet and rill erosion averaged over total rural land is 2.7 t $ha^{-1}$ $yr^{-1}$, where annual arable crops contribute by far the largest part (90%). Their average soil loss amounts to 5.7 t $ha^{-1}$ $yr^{-1}$ but is about twice as high if the mostly flat areas of the North German Lowlands are not taken into account. Hops, despite their negligible contribution to landuse (0.06%), still contribute 1.0% to total soil loss due to the extraordinary large erosion rates measured for this crop. These averages still have to be regarded uncertain despite the large number of studies. These uncertainties can only be overcome by better experimental studies, involving realistic, long-term, and field-scaled scenarios.

# 11. SPATIO-TEMPORAL PATTERNS IN LAND USE AND MANAGEMENT AFFECTING SURFACE RUNOFF RESPONSE OF AGRICULTURAL CATCHMENTS - A REVIEW

Submitted (10/09):
P. Fiener, K. Auerswald and K. Van Oost.
Spatio-temporal patterns in land use and management affecting
surface runoff response of agricultural catchments - a review.
Earth-Science Review.

***ABSTRACT***. *Surface runoff in and from agricultural catchments have a large number of economical and environmental on-site and off-site impacts. To develop techniques which allow mitigating such impacts requires a sound understanding of effects of spatio-temporal patterns in land use and management upon surface runoff response. A synthesis is given regarding the effects of (i) temporal patterns in land management of individual fields, and (ii) spatio-temporal interaction of several fields within catchments. Consistent effects temporal of management on surface runoff of individual fields exist, which have been incorporated in several mostly hillslope or small catchment models and allow to study temporal effects of management on surface runoff from individual fields. In contrast, the concept of patchiness, the spatial organization of patches and the effects of linear landscape structures associated with patchiness upon catchment runoff response are less well understood and less incorporated in models. The main challenge for quantifying the effects arises from the continuous change within the individual patches, with largest contrast usually occurring in mid-summer and least in mid-winter. Some studies indicate that increasing agricultural patchiness due to decreasing field sizes reduces the catchment-scale runoff disposition, especially in case of Hortonian runoff. Linear structures (e.g. field borders, ditches, ephemeral gullies) may either increasing or decreasing hydraulic connectivity within a catchment. The largest gap in research exists regarding the effects and temporal variation of patch interaction, the influence of the spatial organization of patches, and the interaction with linear structures. In view of the large changes in the structure of agricultural landscapes occurring throughout the world, it is necessary to improve our knowledge on the influences of patchiness and connectivity and to improve our respective modeling tools.*

Surface runoff in and from agricultural catchments having a large number of on-site and off-site impacts is of major concern. On-site impacts associated with the loss of water and soil have direct economical and ecological implications for farmers (Lal, 1998b). Surface runoff and sediment transport will also redistribute biochemical and chemical components attached to fines. The further matter routing into the aquatic system may result in reservoir siltation (Verstraeten and Poesen, 2000b), reduce the quality of surface waters (Sharpley et al., 1994; Wauchope, 1978) and enhance the risk of flooding and muddy floods (Boardman et al., 2003). A detailed understanding of the generation and pathways of surface runoff and sediment from agricultural catchments to aquatic environments is crucial for any integrated catchment management.

A large number of studies addressed the effects of land management on in field soil hydraulic properties and their relation to surface runoff generation in a wide range of agro-environmental settings (Ahuja et al., 2006; Green et al., 2003; Strudley et al., 2008). However, relatively few studies focus on the seasonal variation of soil hydraulic and hydromechanic properties and their importance for surface runoff generation. Based on climate, soils, crop type, and agronomic boundary conditions, farming follows a more or less clear, site-specifically predefined seasonality. The extent of the seasonal pattern in tillage operations depends on the management system, generally increasing with soil disturbance from no-till systems (NT) to conventional plowing (CT). While the extent of the pattern is similar for most crops within one system, it is shifted between crops along the time axis (Figure 1), creating a complex co-existence of, e.g. soil cover, states at the same time within a catchment. This shift in time is inherent for agricultural systems in order to optimize the use of labor and equipment capacities. The ***first objective*** of this paper is to summarize the advances made thus far in quantifying and modeling the effects of temporal patterns in land management upon in-

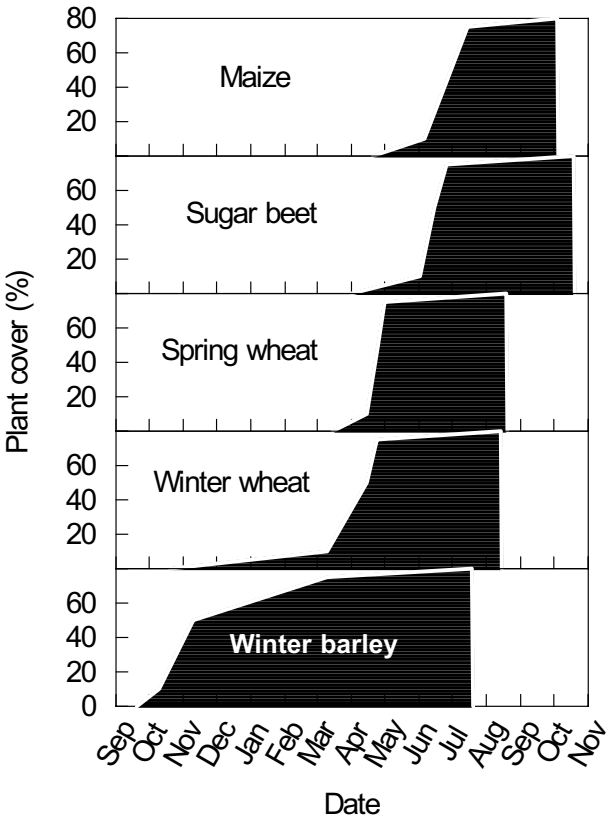


**Figure 1. Typical plant cover development of different crops under Mid-European conditions; it also indicates indirectly the timing of main tillage operations occurring between harvest and planting of the respective crop; data taken from Schwertmann et al. (1987).**

filtration and runoff processes within single fields or land use patches.

Catchments usually are not farmed uniformly but are covered by different crops or land uses. The temporal pattern in hydraulic behavior of single (field) patches hence also translates into a spatial pattern that changes over time. The different patches may interact depending on the connectivity within the catchment (Lexartza-Artza and Wainwright, 2009), which quantifies the passage of water from one part of the landscape (e.g. a single field) to another and thus influences runoff response at the catchment outlet (Bracken and Croke, 2007). The patchiness of an agricultural landscape, defined here as the number of patches with different hydrological behavior (mainly differently cropped fields and different land uses) within a given area, can hence have important implications for its surface runoff response. Moreover, the spatial organization of patches with different hydraulic behavior within a catchment and any linear structures associated with these patches, e.g. small ditches or small grass filters along field borders, will affect the passage of water through an agricultural catchment.

To address effects of patchiness, spatial organization of patches, and linear structures on surface runoff response on the catchment scale, either modeling studies or comprehensive catchment field measurements, e.g. paired-watershed experiments or landscape scale studies on different scales, are needed. This limits our scale to catchments < 10 km², where the effect of a channel network probably is less important as the time constant of the network (i.e. travel time through it) is smaller than the infiltration phase (Beven and Kirkby, 1979). Nevertheless, the effects of patchiness within such small headwater catchments with first and second order streams (equals 2/3 of total surface water drainage networks; Leopold et al., 1964) may also have large-scale consequences (Freeman et al., 2007). The ***second objective*** of this review is therefore to synthesize the knowledge regarding the effects of the interaction between field and land-use patches on surface runoff response of agricultural catchments and especially focus on the overall effects of patchiness.

## MATERIALS AND METHODS

In this review we compare effects of a wide variety of cropping and management operations upon surface runoff response. A direct comparison of results from different studies is biased by the problem that dates even of the same cropping and management operations vary considerably between sites throughout the world. In order to avoid absolute dates and to quantify the degree of variation in time caused by a certain management regime within an individual field we quantify the extent of temporal variation and the length of temporal autocorrelation by semivariograms (Kyriakidis and Journel, 1999; Rouhani and Myers, 1990), which will be calculated from measured data taken from literature. Analogously to the temporal description of data we will also use semivariograms to quantify the degree of variation

in space resulting from landscape patchiness assuming virtual agricultural landscapes determined by a varying number of fields per area (1.56 to 64 fields per km²; Figure 2).

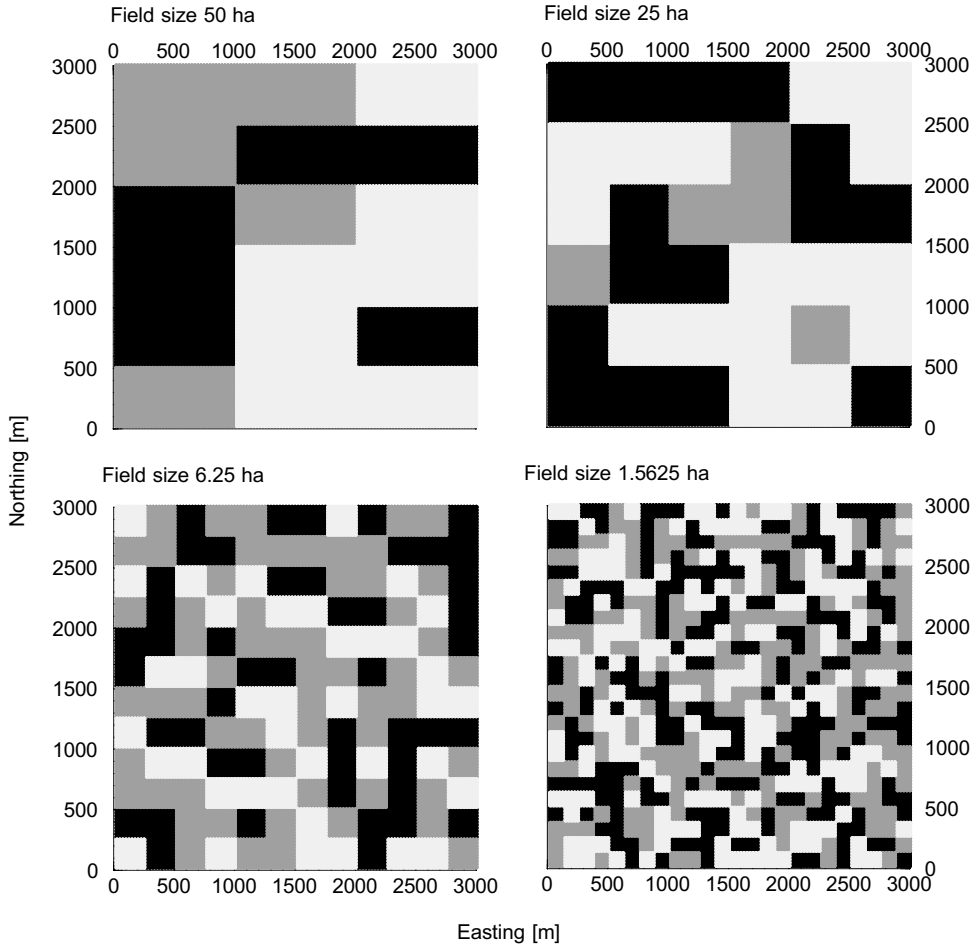


**Figure 2. Patchiness in a virtual 9 x 9 km landscape segment with a 3-year crop rotation and different field sizes (1.56 - 50.0 ha); distribution of the position of each field within the crop rotation was determined using a random generator (GraphPad Software Inc., USA).**

In general, these semivariograms express the variance in data with increasing lag in time (or space). They allow to determine three major characteristics of temporal (or spatial) data: (i) the short-term (or short distance) variability of a property and the accuracy of applied measuring technique is represented in the nugget effect (N) of the semivariogram indicated at a time (or space) lag of zero; (ii) the maximum variability of a property in time (or space) is given by the sill (S); and (iii) the time (or space) lag at which two states of a property become independent from each other is denoted as range (R). The extent of seasonality (or spatial variability) is hence given by the partial sill (sill minus nugget) and the temporal (or spatial) range.

However, it is important to note that second-order stationarity assumed for semivariograms (Rossi et al., 1992) will not always be sufficiently met on smaller time scales as sud-

den breaks occur that exceed the general behavior, e.g. soil cover may change by almost 100% from one day to another if plowing is applied, while the semivariogram indicates a mean change in soil cover of only 3.6% for a lag of one day within a rotation. The semivariogram at short time lags thus underrates the true variation at such breaks and overrates it in-between but still allows to generalize a rotation sufficiently well and to compare between different land-use systems. The same restriction as for the temporal data is true when semivariograms are applied to spatial data. The semivariogram at short spatial lags underrates the true variation at field borders and overrates it within fields but it also should still allow to generalize catchments and to compare between different degrees of patchiness.

All semivariograms were determined using the GNU R version 2.6 (R Development Core Team, 2007) and the supplementary geostatistical package gstat (Pebesma, 2004).

## WITHIN-FIELD SEASONAL PATTERNS IN SURFACE RUNOFF DISPOSITION

### Soil bulk density

Tillage disturbs the soil and thus influences soil hydraulic properties. The most intensively investigated soil properties in this context are soil bulk density and soil porosity. In general, tillage decreases bulk density of the tilled soil layer and subsequently soils reverts back to approximately its original density (e.g. Ahuja et al., 2006; Franzluebbers et al., 1995; Onstad et al., 1984). The temporal changes of bulk density are more pronounced in case of CT than NT, although NT may causes a long term increase in macroporosity by faunal activity, which in some cases may even cause a larger total porosity under NT than under CT (e.g. Benjamin, 1993; Katsvairo et al., 2002). The seasonality of bulk density is low for NT and pronounced for CT. In the example shown in Figure 3, NT exhibits a pure nugget effect indicating that bulk density varies randomly during the year by about 0.045 Mg $m^{-3}$ while CT produces a clear seasonal pattern yielding a periodic semivariogram (0.055 Mg/m³ partial sill) in addition to the same random variation (nugget) as found for NT. The pattern ranges over one year reflecting the rotation consisting of annual crops.

Despite the difficulties to fully represent the interactions between tillage operations, soil properties and environmental conditions during tillage (Alberts et al., 1995), there are empirical modeling approaches in use to relate bulk density and tillage operations with different tillage implements (Chen et al., 1998; Williams et al., 1984). The approach of Williams et al. (1984) was originally developed for the EPIC model and is similarly implemented in the model WEPP (Alberts et al., 1995).

$$\rho_t = \rho_{t-1} - \left[ \left( \rho_{t-1} - \frac{2}{3}\rho_c \right) T_{ds} \right] \quad (1)$$

where $\rho_t$ is the bulk density after tillage [kg m$^{-3}$; for all $\rho$], $\rho_{t-1}$ is bulk density before tillage, $\rho_c$ is the consolidated soil bulk density at 0.033 MPa of tension, $T_{ds}$ is the fraction of the soil surface disturbed by the tillage implement. This fraction depends on the implement and the crop residue type (Alberts et al., 1995). Consolidated soil bulk density $\rho_c$ represents the bulk density without any tillage effect depending on texture, soil organic matter, and cation exchange capacity of clay.

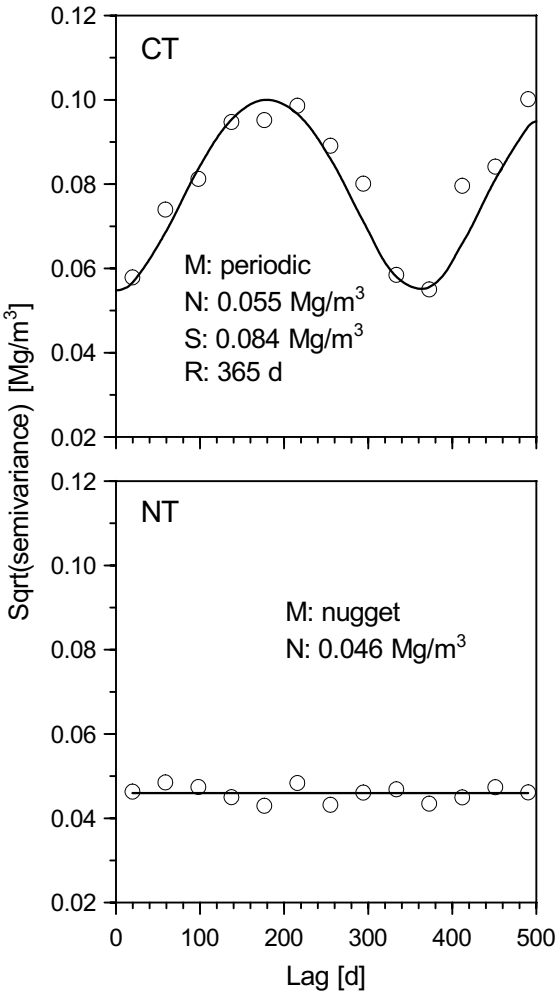


**Figure 3. Semivariogram of seasonal variation of bulk density in 0-50 cm depth for conventional tillage CT (mean density: 1.19 Mg/m³) and no-tillage NT (mean density: 1.27 Mg/m³); planted cops are sorghum (*Sorghum bicolor* L.), wheat (*Triticum aestivum* L.), and soybean (*Glycine max* L.); bulk density was measured 57 times during a 2-years period from July 1991 to June 1993 (Franzluebbers et al., 1995); the square root of the semivariance is displayed to yield the unit of bulk density; M, N, S, and R are model type, nugget , sill, and range of the theoretical semivariograms.**

Continuous simulation must also model the reconsolidation, which happens after tillage mainly associated with subsequent rainfall events. Most studies report that a maximum bulk density in the topmost soil layer (< 100 mm soil depth) is reached after approximately 100 mm of rainfall (Fohrer et al., 1999; Knapen et al., 2008; Onstad et al., 1984; Schiettecatte et al., 2005), which seems to underrate the range in Figure 3. For deeper layers (> 100 mm soil depth) only a slight reconsolidation due to rainfall (Rousseva et al., 1998) or even no effects were found (Karunatilake and Van Es, 2002). For the upper most soil layer one of the most frequently used equations, originally developed by Onstad et al. (1984), is implemented in the EPIC (Williams et al., 1984) and the WEPP (Alberts et al., 1995) model:

$$\rho_d = \rho_t + \Delta\rho_{mx} \frac{R_c}{0.01 + R_c} \quad (2)$$

where $\rho_d$ is the bulk density after rainfall, $\rho_t$ is the bulk density after tillage, and $\Delta\rho_{mx}$ is the maximum increase in soil bulk density with rainfall, which can be estimated from $\rho_t$ and the soil clay content (Alberts et al., 1995), and $R_c$ is the cumulative rainfall since tillage [m].

Such empirical approaches are typically only implemented in erosion models like EPIC and WEPP, which are mostly applied in catchments of up to several square kilometers while soil disturbance by tillage usually is not taken into account in hydrological modeling at larger scales. Technically it would be possible to implement such approaches in larger scale models either by directly determining the effects of tillage on soil-water-retention characteristics (Diiwu et al., 1998; Ndiaye et al., 2007; Van Es et al., 1999) or by combining bulk density algorithms of the type of Eq. 1 and 2 with pedotransfer functions developed to predict water retention characteristics, using soil texture, soil organic matter content and bulk density (e.g. Gupta and Larson, 1979; 2003; Scheinost et al., 1997; Wösten et al., 2001). However, such an implementation on larger scales has to face the week data availability regarding tillage operations on different fields.

**Soil sealing**

Infiltration into agriculturally used soils is often governed by the development of a thin seal or crust of low permeability (Duley, 1939) resulting from raindrop impact on uncovered soil surfaces evaluated in many studies. In general, sealing (used here synonymous to the term crusting) decreases infiltration rates rapidly and pronouncedly, often by more than one order of magnitude (Horton, 1939) and hence increases runoff coefficients.

Seal development is on the one hand governed by a number of site-specific, more or less time invariant parameters, like soil texture, soil organic carbon, slope steepness etc. (Bradford and Huang, 1992) and on the other hand depends on the seasonality of (i) rainfall, (ii) soil surface conditions due to tillage, and (iii) soil cover by living and dead biomass. Moreover, crusts are removed by tillage. Regarding surface sealing and associated surface runoff site-specific seasonality in both rain energy, which causes sealing (Mualem et al., 1990), and rainfall amounts, which leads to runoff, must be considered. Although connected, both rain properties differ in their seasonal distribution, which becomes obvious, when comparing the seasonal distribution of rainfall and the seasonal distribution of rain erosivity, which mainly

depends on rain energy (Figure 4A). In general, rain erosivity or kinetic energy is less evenly distributed than rainfall, which should lead to a corresponding seasonality in the sealing initiation. Seasonality in rain erosivity may differ to a larger extent between different areas (Figure 4B) than the difference between field conditions of the same areas. In consequence of the discrepancy in the seasonality of rainfall and rain kinetic energy, similar amounts of rain can cause different runoff depending on the time of the year, even if the seasonality of the soil surface conditions due to agricultural operations are not considered. The most pronounced variation in sealing potential due to agricultural operations results from varying soil cover. Cover under CT has a more pronounced seasonality than mulch tillage, organic farming (Figure 5) or NT, where soils are kept more evenly covered either by living or dead biomass. Compared to soil cover, the variation of soil properties affecting potential seal development like aggregate stability are less pronounced (Figure 6), and their effect on seal development is less clear.

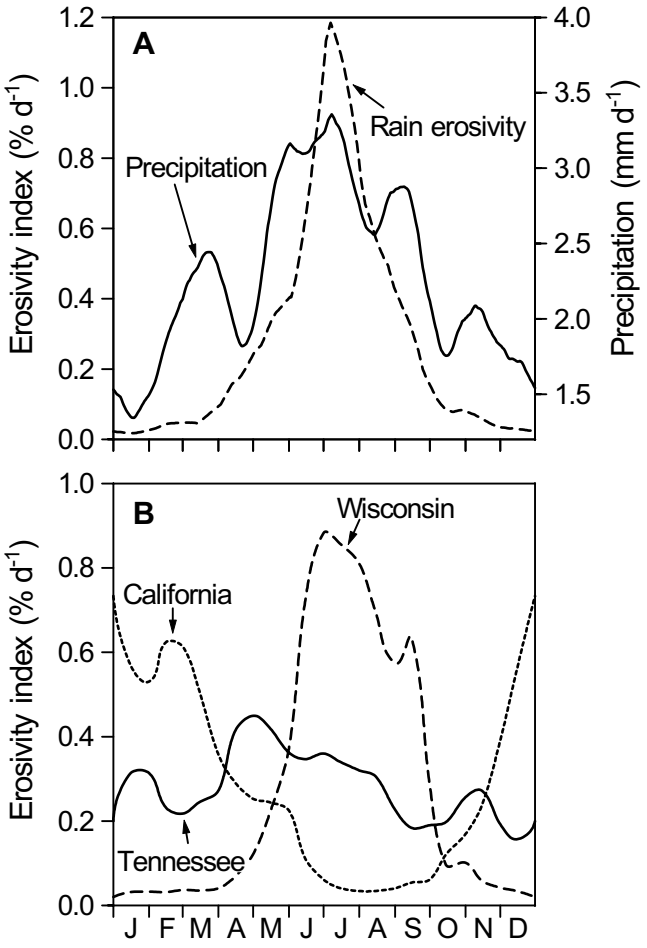


**Figure 4. A: Comparison of seasonal variation of precipitation and erosivity index for a location in Germany (data taken from Fiener and Auerswald, (2006); B: Comparison of the seasonal erosivity index distributions for three locations in the United States (San Luis Obispo in California, Memphis in Tennessee and Madison in Wisconsin; data taken from Wischmeier and Smith, (1978); erosivity index = erosivity per day/erosivity per year (EI would be 0.27 % $d^{-1}$ in case of equal distribution).**

The change of infiltration rate due to sealing is most often modeled by negative exponential equations (Assouline and Mualem, 1997; Horton, 1939; Morin and Benyamini, 1977; Schröder and Auerswald, 2000) depending on rain amount or rain energy, more or less empirical parameters representing soil properties and soil cover. General versions of the mostly used equations are given in Eq. 3 and Eq. 4:

$$K_{cr} = K_f + (K_0 - K_f) \cdot e^{-C \cdot Ekin_{eff}} \qquad (3)$$

where $K_{cr}$, $K_f$, and $K_0$ are the hydraulic conductivity of the sealed/crusted soil, the final hydraulic conductivity of $K_{cr}$, and the hydraulic conductivity of an unsealed soil (beginning of an event), $C$ is a constant representing soil properties determined either individually from, e.g. rainfall experiments or derived from empirical relations to soil properties, and $Ekin_{eff}$ is the effective rainfall energy at the soil surface.

$$Ekin_{eff} = Ekin \cdot (1 - Cover) \qquad (4)$$

where $Ekin$ is the kinetic rainfall energy and $Cover$ gives the relative soil cover by plants and plant residues. Some authors included surface roughness either in Eq. (3) (e.g. Risse et al., 1995) or take roughness into account when calculation $Ekin_{eff}$ in Eq. (4) (e.g. Linden, 1979).

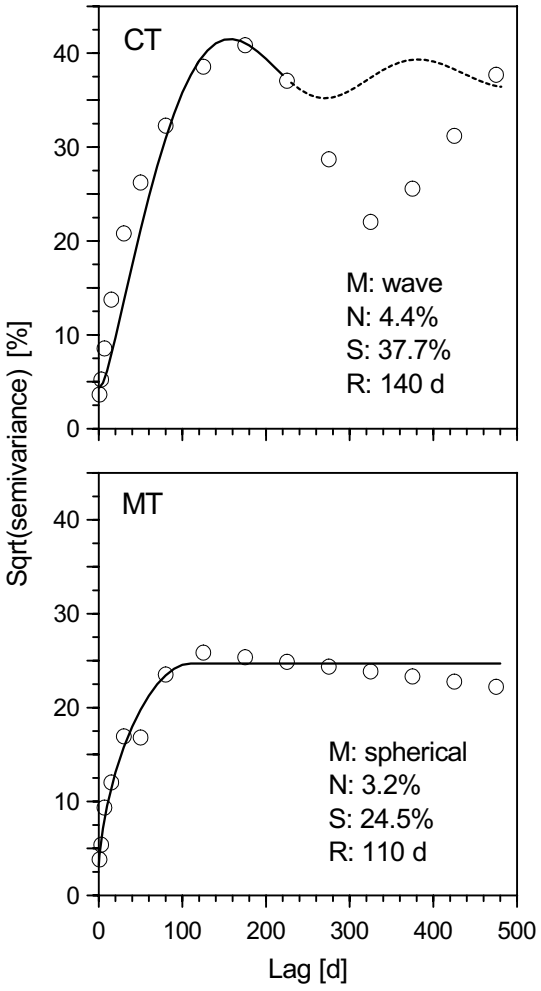


**Figure 5. Semivariogram of seasonal variation of soil cover for rotations with two tillage systems (conventional farming CT, mean cover = 26%; mulch tillage MT, mean cover = 49%); data taken from Auerswald et al. (2000); The lower cover of conventional farming is caused by the pronounced seasonality, where crops provide similar cover as in the mulch tillage cases, but low cover characterizes the periods between two crops. The square root of the semivariance is displayed to yield the unit of soil cover; M, N, S, and R are model type, nugget, sill, and range of the theoretical semivariograms.**

While these kinds of models were successfully applied to describe rainfall experiments, their application for continuous modeling is limited by the difficulty to predict $K_f$, $K_0$ and $C$ and the crust recovery due to soil cracks, earthworm activity and plant-soil interactions etc. which are again variable in respect of climate and season. Potentially applicable approaches to quantify such recovery effects would be a model to determine the patterns of cracks in crusted soils due to shrinkage processes (Valette et al., 2008) or the work by Bronswijk (1989; 1998) on subsidence and shrinking of soils. Introducing sealing in

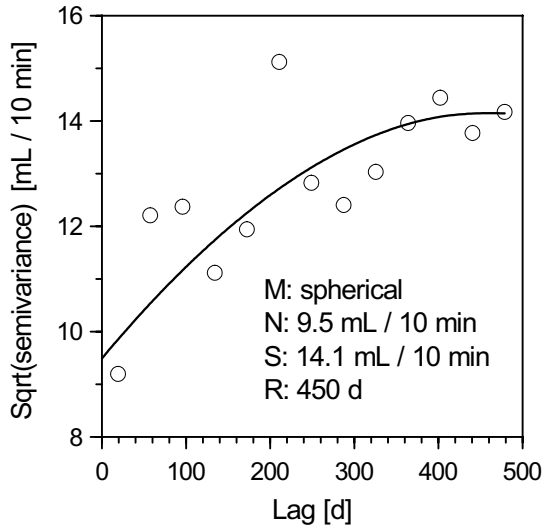


**Figure 6. Semivariogram of seasonal variation of aggregate stability (expressed as percolation stability) for mulch tillage taken from Fiener and Auerswald (2007); Aggregate stability varies rather rapidly, e.g. due to tillage operations. This leads to a large nugget effect (square root of about 9), while the square root of the partial sill is only about 5 ml/10 min for a mean percolation stability of 30.8 ml/10 min); the square root of the semivariance is displayed to yield the unit of percolation stability; M, N, S, and R are model type, nugget, sill, and range of the theoretical semivariograms.**

catchment-scale models is additionally hindered by the large spatial heterogeneity of seal development resulting from small scale differences in soil properties, soil cover, microtopography, management, etc. Nevertheless, some applications of hydrological or erosion models successfully integrated sealing processes as one of the dominate drivers of surface runoff (e.g. Cerdan et al., 2001; Fiener et al., 2008).

### Surface roughness and detention storage

Surface roughness in agricultural fields may either result from tillage operations or from residues at the surface (Gilley et al., 1991) and subsequently decays again causing a clear seasonality depending on cropping and management system. Tillage creates an oriented roughness due to the direction of tillage and a random roughness (Govers et al., 2000). This differentiation is important insofar as oriented roughness in general is more pronounced than random roughness (Figure 7 and 8) but most of its effects depend on its orientation relative to the main slope (Foster et al., 1997). It is fully effective when oriented perpendicular to the main slope and ineffective in slope direction. In contrast, random roughness is much smaller but acts independently of the slope aspect. Roughness decay is governed by the stability of the soil depending on cohesive substances namely clay (Kemper and Rosenau, 1984), organic matter (Tisdall and Oades, 1982), soil moisture (Auerswald et al., 1994; Cousen and Farres, 1984; Kemper and Rosenau, 1984), roots and mycelia (Marinissen and Dexter, 1990; Oades, 1987; Thomas et al., 1993) , the extent of forces interfere the surface, which mainly result from rain (Zobeck and Onstad, 1987) and wind (Saleh and Fryrear, 1999) and the protection of the roughness from these forces, which mainly results from soil cover. Tillage thus creates roughness but by destroying the soil cover and weakening the aggregates (Auerswald, 1993b) also promotes its subsequent decay.

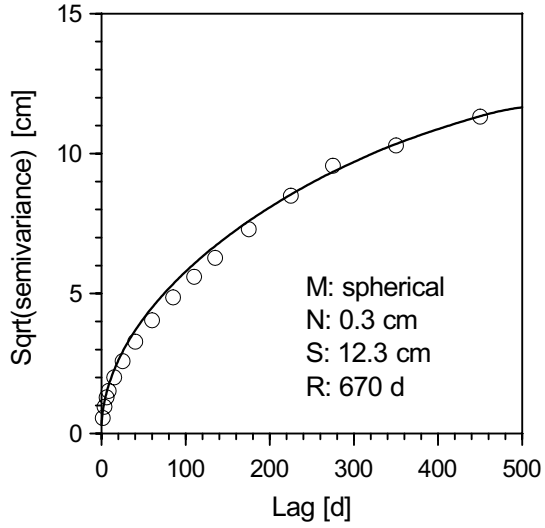


**Figure 7. Semivariogram of seasonal variation of orientated roughness; data of orientated roughness of different soil management from Takken et al. (2001b) combined with management data representing a potato (*Solanum tuberosum* L.), winter wheat (*Triticum aestivum* L.), maize (*Zea mays* L.), and winter wheat rotation (Fiener et al., 2008); especially due to the included potato the orientated roughness varied substantially with a square root of the partial sill of 12.0 cm for a mean orientated roughness of 8.0 cm; the square root of the semivariance is displayed to yield the unit orientated roughness; M, N, S, and R are model type, nugget, sill, and range of the theoretical semivariograms.**

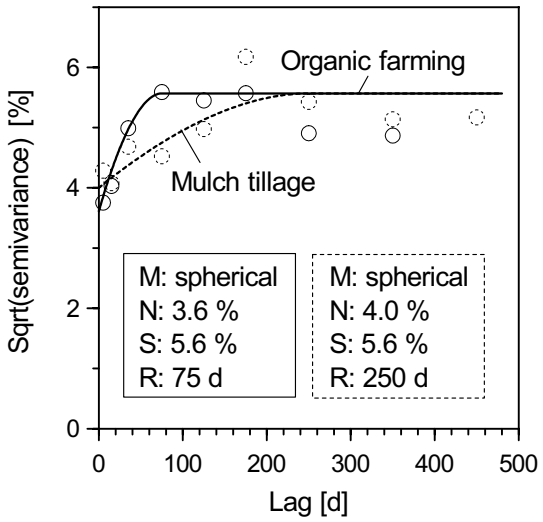


**Figure 8. Semivariogram of random roughness measure RFR used in the runoff and erosion model EUROSEM (Morgan et al., 1998); RFR calculated from a 3-year data set of fields under a potato, winter wheat, maize, and winter wheat rotation (Kaemmerer, 2000); the square root of the semivariance is displayed to yield the unit RFR; M, N, S, and R are model type, nugget, sill, and range of the theoretical semivariograms.**

Roughness in turn affects (i) runoff direction due to oriented roughness (Govers et al., 2000), (ii) seal development, (iii) runoff velocities (Figure 9), and (iv) detention storage. Modeling assumes that seal development is retarded in case that tillage operations create a random roughness larger than 40 mm (Rawls et al., 1990) but otherwise tillage removes residues, which protect soils from raindrop impact, and thus indirectly increases the potential of subsequent seal development.

The effect of surface roughness on runoff velocity is mostly integrated in hydrological modeling by relating surface roughness and residue cover to hydraulic roughness coefficients in one of the common kinematic wave equations (e.g. Weisbach, Chezy, and Manning equations). Data needed to calculate hydraulic roughness from empirical relationships (e.g. Gilley et al., 1991; Gilley and Finkner, 1991; Roels, 1984) are either measured (e.g. Figure 9) or modeled via residue decay approaches, empirical relationships between tillage implements and roughness (Alberts et al., 1995) or random roughness decay as a function of

amount of rainfall or rainfall kinetic energy (e.g. Burwell and Larson, 1969; Johnson et al., 1979; Magunda et al., 1997).

Detention storage is the part of the rain which remains on the ground surface during rain and is absorbed by infiltration after a rain ends (Horton, 1933). The extent of detention storage can be approximated based on slope and surface rougness due to tillage (Huang and Bradford, 1990; Mwendera and Feyen, 1992; Onstad, 1984). Detention storage can exceed 20 mm for a freshly moldboard plowed soil surface with zero slope (Moore and Larson, 1979) but in most cases it is one order of magnitude lower (Govers et al., 2000). The effects of a residue cover on detention storage are more difficult to address, as they depend on type and location of residues (within tillage furrows or on ridges) and their location can change during runoff events. The effects of an anisotropy in tillage roughness on runoff direction and hence duration (e.g. Soucherè et al., 1998) was also integrated into models focusing on surface runoff and erosion on hillslopes or in small catchments (Takken et al., 2001a/b/c), which allowed predicting the pattern of rill and ephemeral gully erosion much more accurate than using topography alone.

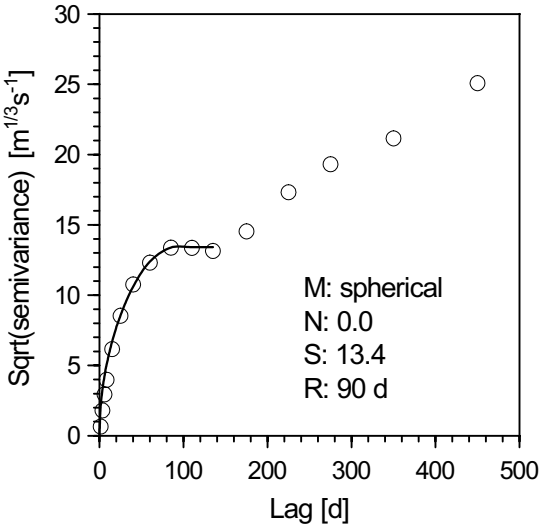


**Figure 9. The semivariogram of the seasonal variation in residue induced hydraulic roughness shows an almost twofold (mean Strickler coefficient $K$ = 39) variation in runoff velocity within a crop (lag < 150 d) and an even stronger variation between crops (lag > 200 d); residue cover data from a potato, winter wheat, and maize cropping sequence applying mulch tillage were taken from Fiener et al. (2008) to calculate roughness according to Gilley et al. (1991); Strickler's $K$ (Dyck and Peschke, 1995), which is the inverse of Manning's $n$, was used; it is superior to $n$ in this analysis because it relates linearly to runoff velocity; the square root of the semivariance is displayed to yield values directly comparable to K; M, N, S, and R are model type, nugget, sill, and range of the theoretical semivariograms.**

## CATCHMENT SCALE INTERACTION BETWEEN PATCHES, PATCHINESS AND SURFACE RUNOFF RESPONSE

When moving from the field to the catchment scale, generally, surface runoff response is governed by areas differing in land use, called patches from now on to include different fields but also other land use types, and in their interaction depending on their spatial organization. The asynchronous temporal variation in their runoff disposition and the temporal and spatial variation of rain events cause a complex behavior, which does not allow to scale up results from homogenous plots directly to catchment scale. Moreover, linear structures play

an important role for catchment runoff response. Such structures can either be associated with patch borders, e.g. ditches or grass filters, or affected by patch sizes, e.g. episodic linear erosion. To address the effects of man-made patchiness in agricultural catchments on runoff response it is therefore necessary to evaluate the effects of patch number per area, of the spatial organization of these patches, and of the linear structures typically associated with (field) patches.

**Effects of field size**

Rain excess differs depending on rainfall characteristics and infiltration characteristics of the patches. While some fields/patches produce runoff, run-on infiltration can occur in others. Patches differing in hydraulic roughness and detention storage will affect runoff velocity, peak discharge and run-on infiltration, which depend on runoff travel time. Run-on infiltration reduces runoff volume and peak discharge (e.g. Assouline and Mualem, 2006; Corradini et al., 1998). Also mulch cover (e.g. Greb et al., 1967; Steiner, 1994) and tillage direction (e.g. Takken et al., 2001b; 2001c) can increase in detention storage, slow down runoff and hence prolong runoff duration. However, to our knowledge there are no studies evaluating the effects of patch size (or patchiness) on agricultural catchment runoff response.

The effects of patchiness are more evident and easier to study in situations, where the temporal variation is smaller than the spatial variation and thus causes a spatial pattern, which is almost constant in time. Such situations especially can be found in heterogeneous natural vegetation like in semi-arid landscapes, where vegetated and bare patches co-occur. Many studies showed that runoff generated on bare areas re-infiltrates in the vegetation patches and hence reduces catchment outflow (Dunkerley, 1999; Puigdefabregas, 2005; Sanchez and Puigdefabregas, 1994; Valentin et al., 1999). For example, a loss of landscape patchiness lead to an overall 25% loss of plant available soil water and banded vegetation was more effective (plus 8%) in capturing run-on water compared to a stippled pattern in the studies by Ludwig et al. (1999; 2005). Bracken and Croke (2007) concluded that in these environments the loss of patchiness has the greatest influence on the ability of hillslopes to reduce surface runoff and hence to capture rainfall for biomass development.

In general, these results should also apply to agricultural catchments but the spatial heterogeneity in agricultural catchments is often caused and equivalent to their temporal variability, e.g. where all fields are cropped with the same rotation but differ in their position within the rotation. Under such conditions, research is mainly focused on the temporal variation within homogenous plots, which is a prerequisite to understand the spatial variation, while the influence of patchiness itself is less proven for such a consistently changing pattern of runoff and run-on patches following the asynchronous seasonality of cropping in different

fields. Experience from land reconsolidation projects shows that a reduction in patchiness in case of increasing field sizes increases runoff volume and peak discharge (Bucher and Demuth, 1985; Luft et al., 1981) although the multitude of changes associated with land reconsolidation leaves some uncertainty regarding the contribution of different measures to the overall effect (Bronstert et al., 1995).

This restriction does not apply for changes in the opposite direction associated with strip cropping, where patchiness is increased to reduce soil loss and runoff for soil conservation purposes (Natural Resources Conservation Service, 2004; Smith et al., 1991) proving the influence of patchiness. This restriction would also not apply for modeling studies, but there are no modeling studies that explicitly focus on the effects of patchiness. In most cases land use and/or management change are simultaneously evaluated (e.g. Bormann et al., 2008; Fohrer et al., 2001; Souchère et al., 2005; Srivastava et al., 2002). Nevertheless, there is some indication that decreasing field sizes and hence increasing patchiness reduces surface

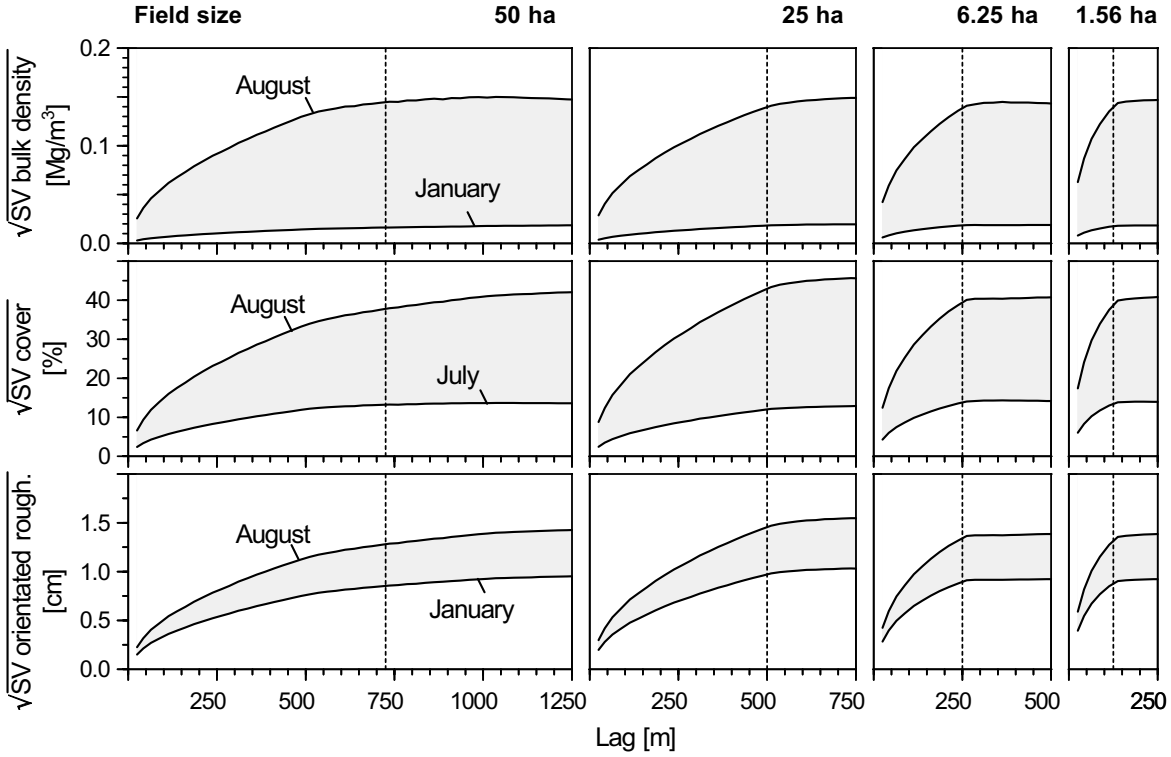


**Figure 10. Semivariograms of bulk density, soil cover, and orientated roughness in a 3-year crop rotation (sugar beet [*Beta vulgaris* L.], winter wheat and winter barley [*Hordeum vulgare* L.]) depending on patchiness of an artificial 9 x 9 km agricultural landscape segment (see Figure 2); data of bulk density, soil cover, and orientated roughness taken from Franzluebbers et al. (1995), Schwertmann et al. (1987), and Takken et al. (2001b), respectively; timing of tillage according to Schwertmann et al. (1987; Figure 1); the square root of the semivariances (SV) are displayed to yield the same unit as the parameter to be evaluated; dotted lines indicate the edge length of the different field sizes; only the months with the largest and the lowest variance of the individual parameter are shown.**

runoff (Bormann et al., 2007; Fohrer et al., 2005) although the opposite can also be true. In an abandoned mediterranean environment small sized terraced patches produced more saturation runoff than large land patches due to the combined effect of enhanced saturation in parts of the abandoned terraces and accelerated runoff in an old ditch system associated with the terraces (Gallart et al., 1994).

In general, effects of patchiness of agricultural landscapes should be most pronounced where hydrologically relevant parameters differ pronouncedly in time and thus between patches. A large temporal variability can be expected under CT for bulk density, soil cover, and orientated roughness, while under NT (or mulch tillage) orientated roughness and soil cover (plants and residues) are important (Figure 3, 5-9).

Due to spatial semivariograms, as expected, the spatial autocorrelation length increases with increasing field size for all tested parameters (Figure 10). The increase was linear as indicated by an increasing range from approximately 170 m (1.56 ha fields) up to approximately 1900 m (50 ha fields [Table 1]) and also independent from season, which indicates that fields cultivated with different crops differ during all seasons although the extent of var-

**Table 1. Theoretical semivariograms (spherical model) of the experimental semivariances for the months with the highest and the lowest spatial variability as shown in Figure 10; semivariances are given as square roots to allow for a comparison with the original data.**

| | | Nugget | Partial sill | Range | Nugget | Partial sill | Range |
|---|---|---|---|---|---|---|---|
| | | | | **Bulk density** | | | |
| Field size | Edge length | | August | | | January | |
| [ha] | [m] | [Mg/m³] | [Mg/m³] | [m] | [Mg/m³] | [Mg/m³] | [m] |
| 50 | 707 | 0.00 | 0.145 | 839 | 0.01 | 0.019 | 1912 |
| 25 | 500 | 0.00 | 0.147 | 733 | 0.00 | 0.019 | 724 |
| 6.25 | 250 | 0.00 | 0.140 | 320 | 0.00 | 0.018 | 296 |
| 1.565 | 40 | 0.00 | 0.145 | 167 | 0.00 | 0.018 | 170 |
| | | | | **Soil cover** | | | |
| | | | August | | | July | |
| | | [%] | [%] | [m] | [%] | [%] | [m] |
| 50 | 707 | 2.41 | 44.2 | 1341. | 0 | 13.4 | 850 |
| 25 | 500 | 0.00 | 45.0 | 721 | 0 | 12.7 | 744 |
| 6.25 | 250 | 0.00 | 39.6 | 306 | 0 | 13.8 | 310 |
| 1.565 | 40 | 0.00 | 40.5 | 171 | 0 | 13.8 | 165 |
| | | | | **Orientated roughness** | | | |
| | | | August | | | January | |
| | | [cm] | [cm] | [m] | [cm] | [cm] | [m] |
| 50 | 707 | 0.37 | 1.46 | 1510 | 0.2481 | 0.98 | 1509 |
| 25 | 500 | 0.00 | 1.53 | 721 | 0 | 1.02 | 721 |
| 6.25 | 250 | 0.00 | 1.35 | 305 | 0 | 0.90 | 305 |
| 1.565 | 40 | 0.00 | 1.37 | 171 | 0 | 0.92 | 171 |

iation (sill) varies.

The spatial variance of bulk density is least in January (close to the pure nugget) and most pronounced in August with the square root of the partial sill being 0.15 Mg $m^{-3}$. Analogously the most pronounced variation in soil cover can be found in August (partial sill about 40 to 45%) when some crops are already harvested, while – opposite to bulk density – in July difference between fields are smallest as all crops exhibit a larger amount of biomass (partial sill about 13%). Compared to soil cover and bulk density seasonal differences in spatial variance of orientated roughness are small. It is most pronounced in August (square root of partial sill about 1.4 cm) because of the large differences between already harvested fields (OR = 0 cm) and fields under sugar beet (OR = 3 cm). In general the spatial variation of roughness is moderate in the presented crop rotation (average in January and August is 1.3 and 1.1 cm, respectively) but could be much larger if potato (OR = 25 cm) would be included in a rotation.

The maximum relative variance of all evaluated parameters (square root of partial sill relative to the average over all fields) increased from bulk density (12%) to soil cover (135%) and orientated roughness (140%). The hydraulic effect of orientated roughness, however, also depends on the relation of tillage direction to direction of slope, which was not considered in this evaluation. In general the spatial variation of all hydrologically important parameters was most pronounce in case of partly harvested agricultural areas (August) and hence effects of patchiness upon surface runoff response should be most pronounced in case of heavy summer storms.

**Effects of spatial organization of land-use patches**

Within the last decades increasing attention was set to the effect of spatial organization of land-use patches on hillslope or catchment surface runoff response. Most studies were carried out under an engineering perspective, e.g. to evaluate the best location of buffer strips for soil and water conservation (e.g. Correll, 2005; Dabney et al., 2006), but also on the general runoff response following different arrangement of patches (or raster cells in models). For example, Western et al. (2001) have modeled the effect grid of cells high in soil moisture on saturated surface runoff of a grassland catchment. The grid cells produced surface runoff significantly earlier if connected along the drainage pathway than if randomly distributed. This effect leveled out in case of larger (30-40 year) rainstorms. Ziegler et al. (2007) quantified the effects of patchiness and optimized arrangement of patches of six land use categories (abandoned field, young secondary vegetation, upland field, intermediate secondary vegetation, forest, and grassland) to reduce surface runoff in two upland catchments in Vietnam. Independent from modeled event size an increasing patchiness and an optimized

patch arrangement, which maximizes the number of transfers between patches of different hydrological behavior, substantially reduced catchment outflow without changing proportions of different land uses.

However, optimum patch arrangement can only be found in case of permanent differences in hydrological behavior of patches. In arable landscapes where fields are shifted annually in a rotation such optimizations might be only possible if arable fields are combined with permanently buffering land uses, like forest or grass buffers.

**Effects of linear structures**

In agriculturally used catchments relatively small linear structures, either intentionally constructed or just side-products of field management are often associated with field borders. Some of these linear structures are more or less stable while others vary in space and time. As these are often associated with microtopograhical elevations or depressions they cause runoff concentration, and affect hydraulic connectivity and surface runoff response of catchments (e.g. Van Dijk et al., 2005; Van Oost et al., 2000).

Common stable linear structures in agricultural areas are (i) field margins, (ii) field roads often interrupting flow pathways and concentrating runoff, (iii) ditches along field borders used to drain agricultural land, and (iv) any kind of vegetated filters either perpendicular to flow direction, e.g. grass filter strips at the downslope end of fields, or along the drainage pathway, e.g. grassed waterways. Even if these structures are more or less stable in space, their hydrological behavior may change in time. For example, ditches in a 0.91 $km^2$ agriculturally used catchment reduced runoff in summer due to an increased infiltration, while they increased runoff in winter due to ground water exfiltration into the ditches (Moussa et al. (2002). Also the vegetation properties of linear structures changes seasonally. For example grassed waterways reduce runoff less in winter due to a reduced hydraulic roughness of the dormant vegetation (Fiener and Auerswald, 2006).

In general, linear structures can increase hydraulic connectivity if concentrated runoff is promoted, e.g. a ditch system following field borders can increase peak runoff rates up to 30% (Moussa et al., 2002). On the other hand, surface runoff can be slowed down and lowered if the linear structures increase the flow length of the runoff as in constructed terrace systems (Lal, 1982; Mockus et al., 2002) or if runoff cross section and hydraulic roughness are optimized to slow down runoff and facilitate infiltration like in a long-term landscape experiment where peak runoff rate was reduced by 25% in case of a flat-bottomed compared to a slightly incised grassed waterway cross section (Fiener and Auerswald, 2005).

Despite the importance of stable linear structures shown in many small catchment studies their integration into modeling studies intended to evaluate the overall effects of patchiness

on surface runoff response is missing jet. This partly results from a lack of detailed data regarding location and temporal behavior as well as the difficulties to adequately represent such small structures by commonly used fixed raster cell sizes (Anderton et al., 2002). At least the second problem might be partly solved using nested approaches to representing topography, where areas of concentrated flow are represented in higher spatial resolution (Heathwaite et al., 2005), or in triangulated irregular networks (TINs) that explicitly account for linear features in the landscape (Vivoni et al., 2005).

The effect of linear structures variable in time like those associated with field management is even more difficult. Typical structures are plow furrows or back furrows along field border (Soucherè et al., 1998; Takken et al., 2001a/b/c), and ephemeral gullies, which will be removed during the following tillage operations (Morgan et al., 1998; Nearing et al., 1989). However, in hydrological modeling the seasonal and/or event based change of runoff concentrating structures is commonly not accounted for even though such changes might be a major source of model uncertainty. In general, the effect of complex linear structures associated with field layout, despite shown in many experimental studies (e.g. Fiener and Auerswald, 2005; Moussa et al., 2002) seems to be underrepresented in most hydrological models.

## CONCLUSIONS AND SUMMARY

The overview of the advances and challenges regarding the effects of spatio-temporal patterns in land use and management on surface runoff response of agricultural catchments at first focused on temporal patterns within individual fields, necessary to understand the spatio-temporal effects of combining several fields within a catchment. The most important relations with more or less consistent behavior are: (i) bulk density decreases within the plow layer after tillage, which could be successfully used in pedotransfer functions to calculate vertical soil hydraulic properties, (ii) random and orientated roughness increase due to tillage, which affects detention storage and runoff direction, (iii) hydraulic roughness increases with increasing plant residues on the soil surface, (iv) soil cover either by living or dead plant material decreases soil crusting, (v) soil crust are removed by tillage operations, and (vi) plant transpiration influences soil moisture (not treated in this paper). In general, the fastest changes occur for soil cover and random roughness while aggregate stability and oriented roughness change slowly. The temporal variability of runoff disposition in single fields decreases with decreasing management intensity.

The knowledge from the field and laboratory studies has been incorporated in several, mostly hillslope or small catchment scale hydrological models. However, a full seasonality of field scale management effects on hydraulic behavior is still difficult to model for some

processes, e.g. the recovery of soil crust. However, even if there is further work needed to improve and rigorously test these small scale modeling tools they already have a great potential to study the temporal effects of management on runoff disposition of single fields.

The second part of this overview treated the combined spatio-temporal patterns of land use and management and their effect on surface runoff response on a catchment scale, with a special focus on the concept of patchiness, the spatial organization of patches and the effects of linear landscape structures associated with (field) patches. The concept of patchiness is not well established and tested in hydrological sciences and studies on the effects of patchiness on surface runoff response of agricultural landscapes are relatively rare. Nevertheless, several studies indirectly address this topic indicating that increasing patchiness due to decreasing field sizes reduces the runoff disposition, especially in case of Hortonian runoff. The effects of patchiness among fields are least during winter, when many fields are in similar condition, and largest during summer, when some fields are already harvested while other still carry crops. The influence of linear structures, which can either promote or dampen runoff response, is less treated in studies and much less incorporated in models.

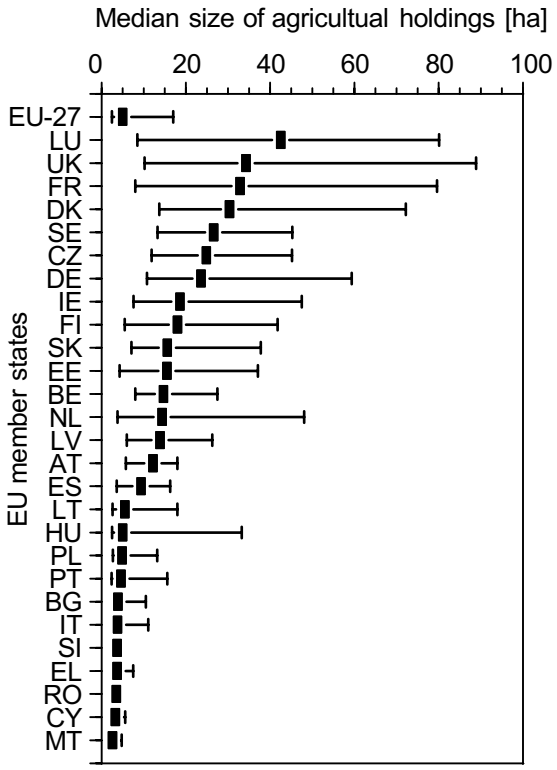


**Fig. 11. Median size with the 25% and 75% percentiles (bars) of agricultural holdings in 2005 within the EU (EUROSTAT Pocketbooks - Agricultural Statistics - Main Results 2006-2007). The median and the 25% and 75% percentiles were calculated from the five categories given in statistics by linear interpolation within each category; abbreviations of EU member states following ISO 3166 code list (ISO, 2009).**

It can be concluded that patchiness and its associated structures substantially affect (mostly reduce) surface runoff disposition of agriculturally used catchments. Differences in runoff behavior in different agricultural regions can be expected due to the large regional differences in field sizes. However, field sizes are commonly not part of official statistics and large scale studies are missing that determine field sizes from other data sources, e.g. remote sensing. Nevertheless, a first hint, for example for the European Union, could be derived from statistics of the median size of agricultural holdings (Figure 11).

Clearly, the largest gap in surface runoff (and erosion) research is on the effects and temporal variation of patch interaction, the influence of the spatial organization of patches, the interaction with linear structures often dominating the hydraulic connectivity on the catchment scale. While large changes in the structure of agricultural landscapes occur throughout the world, our knowledge on the consequences and the availability of (modeling) tools to predict the effects are still limited.

## SUMMARY OF RESULTS

The pattern and process interactions of lateral water and matter fluxes in agricultural landscapes were evaluated in a series of eleven studies published or submitted to scientific journals in the field of geography, hydrology, agronomy, soil science, geomorphology and related environmental sciences. The first four studies focused on the *effects of spatio-temporal patterns of land use and management on lateral fluxes*. This work was mainly based on continuous long-term monitoring of processes on different scales within small watersheds under market-oriented agricultural practice including several soil and water conservation measures. This research contributes to closing the gap in knowledge between plot studies, which neither represent real-world conditions nor allow for an evaluation of pattern interactions, and uncontrolled hydrological watershed studies focusing more or less exclusively on watershed output.

In the second set (two papers), *existing soil patterns in agricultural landscapes were analyzed* and the *processes creating these patterns were evaluated*. These papers explicitly focus on short-term process analysis in combination with long-term pattern effects. The studies use sub-kilometer scale measurements and different available modeling approaches as analytical tools to improve system understanding and extend experimental results.

In the third part, an *erosion, transport, and deposition model* was developed and tested against an extensive long-term watershed data set. This model explicitly focuses on the simulation of processes following soil and water conservation techniques and introduced a new technique to represent deposition processes.

In the fourth part, field data and modeling experience were used to *up-scale the results* of the more detailed studies *to the mesoscale and macroscale*. Therefore, robust modeling tools were combined with detailed own data and extensive data from statistics and literature.

The thesis closes with an extended *review* regarding the advances made thus far in quantifying the effects of *spatio-temporal patterns in land use and management on surface runoff* response in agricultural watersheds. It demonstrates that spatial and temporal patterns cannot be viewed in isolation but as the sum of both parts, yielding a new quality.

### *Effects of spatio-temporal patterns in land use and management on lateral fluxes*

The land use at the Scheyern experimental farm, located about 40 km north of Munich in the Tertiary hills, followed the principal hypothesis that economically and ecologically sustainable land use can be established under different management systems and hence the research farm could act as a prototype of future agriculture. As part of the concept, a number

of soil and water conservation measures were established. These included optimization of land use patterns, management with less soil disturbing field operations, and single linear or point measures to reduce hydraulic connectivity and improve biotic connectivity. This made the research farm a prominent case to examine the influence of spatio-temporal patterns on lateral fluxes, which were monitored in long-term, controlled watershed measurements on multiple scales.

The spatial patterns of rainfall on the 1-km$^2$ scale of the research farm were measured for 4 years. During the hydrological summer half-years, 38 out of 115 events (> 5.0 mm) had a highly significant spatial trend. Gradients in rainfall ranged from 1.0 to 15.7 mm km$^{-1}$ with a mean of 4.2 mm km$^{-1}$ (median 3.3 mm km$^{-1}$). Gradients mainly developed during short bursts of rain and thus gradients were even larger for rain intensities and caused a variation in event-based rain erosivity of up to 255%. The trends did not have a single primary direction and thus level out spatially on the long term. Yet for short-time periods or for single events, the assumption of spatially uniform rainfall is invalid on the sub-kilometer scale. Moreover, it could be shown that the strength of the spatial trend increases with rain intensity, hence lateral water and matter fluxes – often dominated by single large rain events – cannot be sufficiently analyzed without taking spatial patterns of rainfall in relation the land use patterns into account.

As a first management option to reduce watershed connectivity at the Scheyern experimental farm, four small detention ponds were created by raising down-slope field borders at the point of discharge. Their effects upon lateral water and matter fluxes were evaluated during the long-term monitoring. The detention ponds trapped 54–85% of the incoming sediment. The trapped sediment was insignificantly to slightly depleted (5–25%) in organic carbon, phosphorus, nitrogen and clay as compared to the eroding topsoil, but strongly depleted compared to the eroded topsoil. The detention ponds temporarily stored 200–500 m$^3$ of runoff. A failure never occurred. Infiltration and evaporation reduced runoff by less than 10% for large events due to the siltation of the pond bottom, the short filling time (maximum 1-5 days) and the small area covered with water. Peak discharge during heavy rains was lowered by a factor of three. Peak concentration of an agrochemical (Terbutylazin) was lowered by a factor of two. Thus, the detention ponds efficiently reduced adverse erosion effects downslope. According to long-term watershed-scale measurements, which allowed taking the interaction with surrounding field patterns into account, the ponds proved their potential for soil conservation and water quality management.

A second measure to reduce hydraulic connectivity (and improve biotic connectivity) at the research farm was to introduce hydraulic rough grassed surfaces along the thalwegs during the land use redesign of the research farm in 1993. In earlier studies (Fiener and Auers-

wald, 2005; 2003a), the effectiveness of such grassed waterways to reduce runoff volume, peak discharge and sediment delivery could be shown. However, the question if these structures, which are highly effective in trapping particulate phosphorus, also enrich runoff in dissolved reactive phosphorous (DRP) was open to debate. Hence, the DRP concentrations were measured along the flow pathway, namely in open field precipitation, in canopy throughfall of different crops and grass, in surface runoff interacting with topsoil and mulch cover, and lastly in runoff of paired watersheds with and without grassed waterways. DRP concentrations in throughfall for the different cover and grass types showed a clear temporal pattern with the highest concentrations (up to 2.8 mg $L^{-1}$) occurring during flowering of the respective crop and after frost events. DRP concentrations in runoff from straw-covered surfaces were slightly higher compared with those from bare soil. On average, there was a small difference in DRP concentrations between throughfall under growing crops and grass and in runoff from bare or straw covered soil surfaces. Hence, the introduction of relatively small grassed areas within a watershed had little effect on the DRP concentration in surface runoff from the total watershed. This finding was supported by the watershed data, where runoff from watersheds with and without grassed waterways showed similar DRP concentrations. As the grassed waterways do not increase DRP concentrations, they reduce DRP loads analogously to runoff reduction as shown in an earlier study (Fiener and Auerswald, 2003a).

To optimize land management regarding soil conservational and economical aspects, appropriate market-oriented crop rotation with acceptable erosion potential is essential. For economic reasons, a crop rotation that included potato (winter wheat, potato, winter wheat, maize rotation under no-till) was established in Scheyern and its effects on soil erosion was monitored. However, when comparing crops with respect to their erosion potential, we tend to focus on the effects within the year the crop was planted, while neglecting carryover effects from one crop in a rotation to the next crop. Such carryover effects are largely unknown and hence the effect of the temporal pattern (succession) of crops is unclear. The carryover effects within the crop rotation practiced in Scheyern were evaluated in four small watersheds (0.8–4.2 ha in size) during 198 rainfall–runoff events (1994–2001). Sediment delivery from potato and maize during their respective vegetation periods differed only slightly (monthly average: 17.3 and 19.8 kg $ha^{-1}$, respectively), while significantly smaller deliveries were measured with winter wheat (monthly average: 5.7 kg $ha^{-1}$). However, using this crop-specific information in modeling approaches or for land use and management planning would be misleading, as soil loss from winter wheat clearly depended on the preceding crop (either potato or maize). The difference was especially large during the first months after the preceding crop, when the protection by the wheat crop itself was missing or small (ratio between potato–winter wheat and maize–winter wheat sequence of 3.9 for the average sediment delivery of November and December), but it was still detectable under full-grown

wheat (ratio of 2.1 for the average between May and August). This could be explained by little residue cover, disintegration of large aggregates, and low stability of small aggregates following the potato crop. Carry-over effects must be taken into account in an optimization of crop rotations and they are essential while developing and testing modeling tools.

In general, all four studies from the Scheyern experimental farm furthered the understanding of the effects that result from complex spatial and temporal patterns in land use and management upon event-based lateral water and matter fluxes. This was made possible by using long-term, controlled watershed studies, while simultaneously quantifying the drivers and their effects on the underlying processes with high resolution. Understanding these effects as well as such data sets are major prerequisites for model development and application to better represent complex real-world systems in environmental assessments.

*Effects of lateral fluxes on patterns of soil properties*

Patterns, e.g. in land use, which affect different kind of processes, will also create or modify patterns, e.g. in soil properties, if the conditions remain effective over a sufficiently long period of time. A typical case is the pattern in soil organic carbon (SOC) content within fields. As SOC patterns – and hence the processes, which create these patterns – have substantial effects upon carbon cycling, we evaluated the layer-specific patterns of SOC in a 4.2 ha test site and analyzed associated processes by using terrain attributes and erosion modeling results. Our data indicated that different processes were at play from which these patterns emerged. In general, SOC contents decreased (average 1.10, 0.76, and 0.34 % kg $kg^{-1}$, respectively) with depth (< 0.25, 0.25-0.5, and 0.5-0.9 m, respectively), while the coefficients of variation in SOC increased (13.5, 36.3, and 62.6%, respectively). The pronounced SOC variation in the deepest soil layer clearly corresponds to the spatial location of a colluvial area. The spatial patterns in the top soil layer were less clear as patterns emerging from redistribution processes were probably weakened by the homogenizing effects of tillage. The soil layer in-between exhibited a somewhat intermediate spatial variability. Correlation analyses between SOC and various covariables indicated the importance of soil redistribution processes. Water and tillage erosion patterns correlated highly significantly with SOC patterns, with an increasing correlation with depth. However, it remained unclear if the correlation with soil redistribution only results from the redistribution processes itself or if soil moisture patterns and especially erosion and deposition by water additionally induce or attenuate the spatial variability of in-situ carbon mineralization or sequestration.

The potential relationship between soil deposition and SOC mineralization was addressed in a laboratory study. Soil disposition was initiated using a combination of an erosion flume and a down-slope depositional area under three treatments (medium and high

deposition of aggregated soil and high deposition of dispersed soil). After the experiments, soil respiration was measured in the depositional areas and in controls for approximately 100 days. For all treatments, most of the eroded sediment accumulated in the depositional area (97% on average of the aggregated high deposition runs and 83% in case of the dispersed runs). This sediment was slightly depleted in SOC indicating a preferential transport of carbon with runoff leaving the system (total export of eroded C with runoff 10–25%). Compared to the controls without erosion or deposition, $CO_2$-efflux increased in the depositional areas (additional loss of C of 2-12%), most pronounced in the case of the (high) deposition of aggregated soil. The patterns of SOC within agricultural fields thus result from the complex interaction of the redistribution processes itself with partial depletion of SOC during deposition and additional respiration in depositional areas. This is an important step in understanding the effects of soil erosion and deposition on soil carbon cycling.

*Model building*

The Multi-Class Sediment Transport (MCST) model was developed for three main purposes: (i) modeling of surface runoff formation and concentration as affected by agricultural land use, while using 'simple', transferable algorithms, (ii) simulating size-selective erosion, transport, and deposition, explicitly taking into account re-entrainment during net-deposition, (iii) and accounting for the effects of soil and water conservation measures on these processes. The model was tested against 8 yrs of measurements from two small watersheds (0.7 and 3.7 ha, respectively) at the Scheyern experimental farm. For runoff events > 3 mm, the model simulated runoff accurately. The results for smaller events are relatively weak due to the threshold driven behavior of the model and the difficulty in parameterizing runoff behavior of conservation structures such as vegetated filter strips for small runoff volumes. The overall results of the runoff module are promising as large events generally dominate erosion and deposition within the watersheds. The relatively simple hydrological model structure allows a wide range of application of the model. The model also performed reasonably well for sediment delivery (Nash-Sutcliffe-coefficient = 0.62; $n$=37). For large events, modeled interrill, rill and sedimentation patterns agree well with qualitative field observations. Taking into account effects of plant and plant residue cover, the model adequately represented soil conservation measures in most cases. Hence, the model is easy to use in watersheds under soil conservation, if soil cover data are available or can be estimated. However, the model results could be substantially improved if better data regarding rill erodibility were available. The sediment size-specific modeling successfully reproduced the clay enrichment at the watershed outlet. As such, the model is one of the first 2-D models to have the potential to dynamically model the delivery of size-specific sediment-bound sub-

stances to water courses, while taking re-entrainment processes in areas of net-deposition into account.

*Up-scaling*

Up-scaling of findings from small watershed-scale studies to the regional or even continental scale is a major research issue. In this thesis, up-scaling was realized by combining measurements and modeling and was carried out for three purposes: (i) To investigate the scale dependency of runoff response following different land use scenarios with and without grassed waterways, (ii) to analyze if soil erosion rates under organic farming (subsidized in addition to higher product costs) differ from those under conventional framing in Bavaria, and (iii) to determine total erosion and erosion patterns in rural areas in Germany.

The scale dependency of the efficacy of grassed waterways (GWWs) in reducing runoff volume and peak discharge was tested under two land use scenarios in watersheds between 37 and 1670 ha. In cases of primarily arable land use (80% of total area under arable use) including GWWs along most thalwegs (2.3% of total area), modeling indicated only a slight decrease in GWW efficiency with increasing spatial scale. GWWs reduced runoff volume and peak discharge during summer events (reoccurrence interval of rain up to 50 yr) by at least 30 and 40%, respectively, independent of scale. This efficiency decreased for winter events, when fields produce more inflow to the GWWs and the prolonged infiltration in the grassed areas is less important. In cases of diversified land use similar to the real land use in the tested area (45% of total area under arable use), the efficiency of the GWWs decreased from arable dominated sub-watersheds to the mesoscale watershed, where only a small proportion of the thalwegs are suitable for the establishment of GWWs (0.8% of total area). In this case, runoff volume was reduced by less than 5%, whereas a reduction in peak discharge of at least 15% was still simulated. The modeled scenarios showed that GWWs can significantly contribute to flood control in small mesoscale watersheds (< 50 km²). Most pronounced effects can be expected in mainly agriculturally used watersheds (where most thalwegs are suitable for grassed waterways) and in areas where flooding is mainly caused by heavy summer storms.

The comparison of soil erosion rates under organic and conventional agriculture in Bavaria indicated two opposing effects. On the one hand organic farms tended to occupy preferentially more unfavorable arable sites (with higher rain erosivity, steeper slopes and only slightly smaller soil erodibility), which increased their risk of erosion. The estimated site-specific bare-fallow soil loss was hence 14% greater for organic agriculture than for conventional agriculture. On the other hand, the district average in the proportion of row crops, small grains and grass/legume leys differed between organic and conventional agriculture.

Hence, on average, organic agriculture will cause about 24% less erosion than conventional agriculture under otherwise identical site conditions. This can be attributed to the larger area of grass/legume leys, which has the potential to reduce erosion markedly, even two years after inversion. In consequence of both opposing effects, the average soil loss was predicted to be about 15% less for organic as compared to conventional agriculture. These results were verified by validation data from the Scheyern experimental farm. However, there was little correlation between natural conditions favoring erosion and the cropping pattern being practiced. Erosion control does not seem to influence management decisions on crop rotation in either farming type. Hence the lower erosion in organic agriculture on average has to be regarded as accidental. Furthermore, large deviations on both sides of the average *C* factor (representing soil management effects according to the USLE) were found for both farming types, indicating that erosion in both farming systems could be reduced considerably. The large effect of the best management practice on the soil loss in the validation exercise also demonstrates that both farming systems have ample opportunity to reduce soil losses.

Erosion under real conditions is of great concern on a national scale regarding sustainability of land use and off-site effects on water bodies and settlements. However, experimentally derived rates of sheet and rill erosion are often biased by short measuring periods and by experimental settings, which deviate considerably from typical land use, and typical spatial extensions. To overcome these deficiencies, we compiled data from 27 studies covering 1076 plot years and accounted for deficiencies in experimental settings by a model based correction method. Soil loss by sheet and rill erosion, averaged over total rural land, was 2.7 t $ha^{-1}$ $yr^{-1}$, whereby annual arable crops contributed by far the largest part (90%). The average soil loss for the latter land use type amounted to 5.7 t $ha^{-1}$ $yr^{-1}$, but was about twice as high when the mostly flat areas of the North German Lowlands were not taken into account. Hops, despite their negligible contribution to land use (0.06%), still contributed 1.0% to total soil loss due to the extraordinary large erosion rates measured for this crop. These average values still have to be regarded as uncertain despite the large number of studies. These uncertainties can only be overcome by better experimental studies, involving realistic, long-term, and field-scaled scenarios.

*Review – spatio-temporal patterns in land use and management affecting surface runoff*

This review provides an overview of the advances and challenges in quantifying the effects of spatio-temporal patterns in land use and management on surface runoff response of agriculturally used watersheds. The first part focuses on the respective temporal patterns in land management of individual fields. The results from field and laboratory studies show consistent effects of management upon surface runoff disposition for the following relation-

ships: (i) a decrease in bulk density in the plow layer after tillage operations, (ii) an increase in random and orientated roughness due to tillage operations, which affects detention storage and runoff direction, (iii) an increase of hydraulic roughness with increasing plant residues on the soil surface, (iv) a decrease in soil crusting potential with increasing soil cover either by living or dead plant material, (v) a removal of soil crust due to tillage operations, and (vi) the importance of crop-specific transpiration regarding soil moisture dynamics. These temporal effects within fields must be taken into account when analyzing spatio-temporal interactions of several fields within a watershed. The second part of the review focuses on the runoff response of watersheds as a result of these interactions, with a special focus on the concept of landscape patchiness, spatial organization of patches and effects of linear landscapes structures associated with land use patches. The concept of patchiness is not well established and tested in hydrological sciences and hence studies focusing on effects of patchiness on runoff response of agricultural landscapes are not widely available. Nevertheless, several studies that indirectly address this topic indicated that increasing agricultural patchiness due to decreasing field sizes reduces the runoff disposition of agricultural watersheds, especially in case of Hortonian runoff. The aspects of spatial organization of patches were investigated in more studies, which mainly focused on the spatial organization of areas with high (e.g. vegetated filters) and low (e.g. areas tending to saturation runoff) infiltration capacities. In general, an increasing number of transitions between areas of different infiltration capacity and surface roughness decrease surface runoff response. There were also several studies focusing on the effects of stable or variable linear structures on hydraulic connectivity. It was shown that these structures may have either important increasing or decreasing effects upon hydraulic connectivity, depending upon the kind of the linear structure (e.g. field borders, ditches, ephemeral gullies). Nevertheless, in contrary to their importance, especially in agricultural watersheds, there is only limited awareness in hydrological modeling literature regarding their effects.

# CONCLUSIONS

The analysis of the effects of pattern and process interactions upon lateral water and matter fluxes in agricultural landscapes calls for a multi-spatial and multi-temporal approach. Detailed measurements of system inputs, outputs and internal processes from the pore or sediment grain to the small watershed scale are needed. Such a multi-scale approach can close the gap between plot-scale process studies, which neither represent 'real-world' conditions nor allow for an evaluation of pattern interactions, and process-integrating hydrological studies focusing on watershed outputs only. The research at the Scheyern experimental farm is a prominent case of such an approach that allows determining the influences of spatio-temporal patterns upon lateral fluxes in controlled watersheds. Results from this research are presented in the first part of this thesis:

The assumption of spatial homogeneity of rainfall on an event basis is invalid on the sub-kilometer scale. Event-based spatial heterogeneity is even more pronounced for rainfall intensity, erosivity and rain excess. Gradients of these parameters tend to increase with increasing recurrence intervals of rainfall events. Hence, any event-based experimental and/or modeling studies on lateral water and matter fluxes, especially if the investigated processes are dominated by single rare extreme events and if studies carried out in areas where convective storms predominate, need to take spatial heterogeneity of rainfall into account.

Based on multi-scale data, an evaluation of the combined and interacting effects of optimized land use patterns, optimized field management and structures affecting concentrated flow and hence land-water connectivity was carried out. These combined effects were explicitly shown for small detention ponds at field borders and grassed waterways along thalwegs. Both structures effectively trap sediments and reduce peak discharges. Moreover, the ponds prevent down-slope linear erosion, which would increase hydraulic connectivity to surface water bodies in case of large events, and decrease peak concentrations of agrochemicals due to mixing processes within the ponds. The grassed waterways also reduce runoff volumes (shown in earlier studies) and - as they did not increase dissolved reactive phosphorus concentrations - these structures also effectively reduced outflow of particulate and dissolved phosphorus. In general, both studies improve the understanding of complex interactions between spatio-temporal patterns in land use and management and conservation potential of measures established in areas of concentrated flow. Moreover, the results also underline the importance of taking pattern-process interactions into account in successful land use planning, and generally emphasize the importance of small structures that affect watershed connectivity.

A market-oriented crop rotation and field management that simultaneously conserves with respect to water and soil resources is essential in supporting sustainable economical and ecological agro-ecosystem services. To demonstrate that both goals can be met simulta-

neously, a mulch tillage system with a new crop rotation (including potato) was established in Scheyern, which improved the economic returns and allowed the reduction of soil disturbances. To evaluate the effects of introducing the mulch tillage system, including the erosion prone potato crop, calls for long-term continuous measurements, as a failure of the conservation system might be restricted to rare events and the effects of a single crop might be carried over into the following crops. It could be shown that single soil conservation measures, e.g. mulch tillage with potato, reduced erosion event frequency, but can fail to sufficiently decrease magnitude of extremes. This is an important finding insofar as it indicates that a combination of measures is more appropriate to prevent unwanted runoff, sediment and matter delivery to surface water bodies, and it generally shows a shift in the frequency-magnitude relationship of the system, which is rarely addressed in soil conservation planning. Moreover, while the erosion potential of potato and maize differed only slightly, substantially higher erosion was measured under winter wheat following potato compared to winter wheat following maize. Hence, such carry-over effects must be taken into account while optimizing crop rotations and they are also essential for successful model development and testing.

In general, long-term and multi-scale data are also needed to improve and rigorously test modeling approaches that simulate watershed output and watershed internal processes. In this study, the Multi-Class Sediment Transport model (MCST) was modified to account for soil-conservation agriculture. MCST focuses on runoff formation processes as affected by field management, and it is one of the first 2-D realizations to model size-selective re-entrainment in case of net-deposition. The model was successfully tested against runoff, watershed internal erosion, sediment delivery, and clay enrichment of two watersheds under soil and water conservation in Scheyern. The successful modeling of size-selectivity, which was validated by measured clay enrichment, points to its potential for modeling the transport of sediment-bound substances. In general, MCST is a powerful tool for further model-based research, especially for the detailed analysis of soil and water conservation measures and for scenario modeling to analyze effects of patchiness, spatial organization of patches and linear structures affecting hydraulic conductivity.

Especially in hydrological modeling studies, analyzing the effects of pattern-process interactions upon lateral water and matter fluxes in agricultural landscapes often focuses on the effects of spatial and temporal patterns *upon* processes. Changes in spatial patterns, especially in soil properties, that emerge from processes in land use and management are often not accounted for as a recognizable change in patterns mostly is a relatively slow process. However, slow changes over decades or more have important implications for present lateral water and matter fluxes. These implications are often underrepresented in soil data that is not regularly updated. Processes leading to changes in soil properties, here soil organic carbon

(SOC), were evaluated in a first study following a statistical approach relating measured SOC patterns in a small agriculturally used watershed with terrain attributes and results from water and tillage erosion modeling. In a second study, the effects of soil deposition by water on $CO_2$-effluxes were analyzed according to a laboratory experiment. The first study showed the strong relation between patterns in water and especially tillage erosion and patterns in SOC in agriculturally used landscapes. Especially the accumulation of SOC in depositional areas corresponded to modeled soil redistribution. However, the second study indicated an increase of $CO_2$ respiration in case of the deposition of aggregated soils, typically following heavy erosion events in summer. Hence, long-term SOC accumulation in depositional areas due to water and tillage erosion is counterbalanced to some extent by increasing respiration in these areas. Such detailed information is needed to improve our understanding of the combined effects of soil redistribution and carbon cycling. Ongoing and future research on weather soil redistribution functions a source or a sink of $CO_2$ relies on these data and respective models.

Up-scaling results from detailed investigations at individual research locations to mesoscale or macroscales is a major challenge in environmental science. Regarding soil and water conservation measures there is an on-going debate, if (and to which extent) the effectiveness of single measures, e.g. reducing peak discharge, decreases when moving from farm-scale to mesoscale watersheds. In this study, we tested the hypothesis that the effectiveness of grassed waterways in reducing runoff volume and peak discharge decreases with increasing watershed size. We used a model simulating runoff through potential grassed waterways while accounting for their typical cross sections (which would be impossible with raster based modeling). It was shown that especially in case of heavy summer storms, the effectiveness of grassed waterways in reducing runoff volume and especially peak discharge only slightly decreases if up-scaling from a microscale (< 0.4 km²) to a mesoscale watershed (~ 17 km²) occurs. Such results are of growing importance in cases of a likely increase of the intensity of summer storms under global climate change. Therefore, such measures should be taken into account in integrated watershed management, as it is for example required in the European Water Framework Directive. Moreover, it should be recognized that grassed waterways along thalwegs (within fields) are more effective in trapping sediments and prevent sedimentation in stream networks than the typical narrow grass filters along streams.

A further increase in scale to the macroscale again calls for other, suitable concepts to evaluate lateral fluxes. To analyze soil erosion in macroscale areas, data regarding land use and especially timing of management (which often dominates erosion processes) that are necessary for event based modeling are not available and model testing against watershed outputs alone is not appropriate to evaluate internal dynamics. Bridging the gap between a

detailed understanding of processes that implies high data demand that can only be met in a few areas of intensive research and usual data availability is necessary. Two research questions regarding soil erosion on the macroscale were addressed in this study:

The first was, as to whether organic farming shows a lower erosion risk as compared to conventional agriculture. While the question is complex, data availability is restricted to cropping statistics. However, detailed understanding of the underlying processes, which not only applies to the erosion processes itself, but also to agricultural restrictions and mechanisms, provided reasonable estimates. The restriction of such an approach based on generalized statistical data is that it can only give a statistical answer (e.g., long-term average soil loss; county average soil loss). On average, organic farming in Bavaria causes 15% less erosion compared to conventional farming, although organic farms are, on average, situated in more erosion prone locations. The lower erosion rates in organic farming are due to larger areas of grass/legume leys and do not result from special soil conservation measures. Therefore, the reduction in erosion can be regarded as accidental. However in both farming types, erosion control does not seem to influence management decisions on crop rotations (indicated by the extensive range of *C* factors with no correlation to the site-specific erosion potential).Thus both systems exhibit a huge soil conservation potential under best management practice, which is an important information for any conservation planning.

The second question was, if it is possible to determine realistic soil erosion rates for all of the Germany, if the erosion plot data that were published within the last 50 years are compiled together. We utilized 1076 erosion plot years measured throughout the country and combined these with moderate modeling. According to the developed approach, we determined an average erosion rate under rural land use in Germany of 2.7 t $ha^{-1}$ $yr^{-1}$, where annual arable crops contribute by far the largest part (90%, average 5.7 t $ha^{-1}$ $yr^{-1}$). Nevertheless, these estimates are biased due to systematic deficits in erosion experiments. The data were mainly collected on plots that were too small, slopes that were too steep, and arable land was over-represented compared to overall rural land use in Germany. Therefore, the study underlines the need for measurements under more realistic conditions and points to major deficits in model parameterizations when scaling up to large areas. However, the results also emphasize importance and benefit of combining data of different case studies representing (very) side-specific conditions to come up with more general results and conclusions that are highly recommended by regional planners and politicians.

Despite the importance of lateral water and matter fluxes in and from agricultural landscapes for many environmental topics, such as water quality or carbon balance, there are still deficits in addressing the interaction between man-made patterns in land use and management and associated processes on the landscape scale. Aspects of patchiness of these landscapes, spatial organization of patches, and effects of small linear structures affecting land to

surface water connectivity are mostly underrepresented. This is partly a result of disciplinary boundaries between agronomy related science focusing on in-field processes and watershed hydrology related sciences focusing on in-stream relations. However, there is a huge potential in optimizing agricultural landscapes to reduce lateral water and matter fluxes, which is of growing common interest in the context of global climate and land use change. Such optimizations should be set into practice while also balancing other functions and services of agro-ecosystems. In general, it seems to be one of the major challenges for future environmental research to come to a more holistic view on the multi-functionality of our 'man-made' landscapes.

## REFERENCES


Abu-Zreig, M., Rudra, R.P., Whiteley, H.R., Lalonde, M.N., Kaushik, N.K., 2003. Phosphorus removal in vegetated filter strips. J. Environ. Qual. 32: 613-619.

Adami, A., Da Deppo, L., 1986. On the systematic errors of tipping bucket recording rain gauges. pp. 27-30. *In* Sevruk B. (Editor). Correction of precipitation measurements. ETH/IAHS/WMO workshop on the correction of precipitation measurements. Zürich.

Ahmed, S., DeMarsily, G., 1987. Comparison of geostatistical methods for estimating transmissivity using data on transmissivity and specific capacity. Wat. Resourc. Res. 23: 1717-1737.

Ahuja, L.R., Ma, L., Timlin, D.J., 2006. Trans-disciplinary soil physics research critical to synthesis and modeling of agricultural systems. Soil Sci. Soc. Am. J. 70: 311-326.

Alberts, E.E., Nearing, M.A., Weltz, M.A., Risse, L.M., Pierson, F.B., Zhang, X.C., Laflen, J.M., Simanton, J.R., 1995. Soil component. *In* Flanagan D.C., Nearing M.A. (Editors). USDA - Water Erosion Prediction Project hillslope profile and watershed model documentation. USDA-ARS National Soil Erosion Research Laboratory, West Lafayette, Indiana, pp. 7.1-7.47.

Alberts, E.E., Weltz, M.A., Ghidey, F., 1989. Plant growth component. *In* NSERL Report. Washington DC, pp. 8.1-8.38

Amundson, R., 2001. The carbon budget in soils. Annu. Rev. Earth Pl. Sc. 29: 535-562.

Anderton, S.P., Latron, J., White, S.M., Llorens, P., Gallart, F., Salvany, C., O'Connell, P.E., 2002. Internal evaluation of a physically-based distributed model using data from a Mediterranean mountain catchment. Hydrol. Earth Syst. Sci. 6: 67-83.

Aniol, R., 1975. Flächenausdehnung kurzer Starkregen in einem dichten Regenschreibernetz. Interpraevent: 149-158.

Arora, M., Singh, P., Goel, N.K., Singh, R.D., 2006. Spatial distribution and seasonal variability of rainfall in a mountainous basin in the Himalayan region. Wat. Resourc. Manag. 20: 489-508.

Arriaga, F.J., Lowery, B., 2005. Spatial distribution of carbon over an eroded landscape in southwest Wisconsin. Soil Tillage Res. 81: 155-162.

Assouline, S., Mualem, Y., 1997. Modeling the dynamics of seal formation and its effect on infiltration as related to soil and rainfall characteristics. Wat. Resourc. Res. 33: 1527-1536.

Assouline, S., Mualem, Y., 2006. Runoff from heterogeneous small bare catchments during soil surface sealing. Wat. Resourc. Res. 42: W12405.

Auerswald, K., 1986. Einstufung der Bodenerodibilität (K-Faktor) nach dem Klassenbeschrieb der Reichsbodenschätzung für Südbayern. Z. Kulturtechn. Flurber. 27: 344-351.

Auerswald, K., 1991. Significance of erosion determining factors in the USA and in Bavaria. Z. Geomorph. Suppl. N. F. 83: 155-160.

Auerswald, K., 1993a. Bodeneigenschaften und Bodenerosion - Wirkungswege bei unterschiedlichen Betrachtungsmaßstäben. Borntraeger, Berlin, 208 pp.

Auerswald, K., 1993b. Influence of initial moisture and time since tillage on surface structure breakdown and erosion of a loessial soil. Catena Suppl. 24: 93-101.

Auerswald, K., 1995. Percolation stability of aggregates from arable topsoils. Soil Sci. 159: 142-148.

Auerswald, K., 2002a. Landnutzung und Hochwasser. *In* Kommision für Ökologie (Editor). Katastrophe oder Chance? Hochwasser und Ökologie. Friedrich Pfeil Verlag, München, pp. 67-76.

Auerswald, K., 2002b. Schätzung des C-Faktors aus Fruchtartenstatistiken für Ackerflächen in Gebieten mit subkontinentalem bis subatlantischem Klima nördlich der Alpen. Landnutz. Landentwick. 43: 269-273.

Auerswald, K., Albrecht, H., Kainz, M., Pfadenhauer, J., 2000. Principles of sustainable land-use systems developed and evaluated by the Munich Research Alliance on agroecosystems (FAM). Petermanns Geogr. Mitt. 144: 16-25.

Auerswald, K., Becher, H.H., Vogl, W., Hafez, M., 1984. Ein Laborregner zur Erodibilitätsbestimmung von Böden. Z. Kulturtechn. Flurber. 25: 300-307.

Auerswald, K., Gerl, G., Kainz, M., 2006. Influence of cropping system on harvest erosion under potato. Soil Tillage Res. 89: 22-34.

Auerswald, K., Haider, J., 1996. Runoff curve numbers for small grain under German cropping conditions. J. Environ. Manag. 47: 223-228.

Auerswald, K., Kainz, M., Fiener, P., 2003. Soil erosion potential of organic versus conventional farming evaluated by USLE modelling of cropping statistics for agricultural districts in Bavaria. Soil Use Manag. 19: 305-311.

Auerswald, K., Kainz, M., Scheinost, A.C., Sinowski, W., 2001. The Scheyern experimental farm: research methods, the farming system and definition of the framework of site properties and characteristics. *In* Tenhunen J.D., Lenz R., Hantschel R. (Editors). Ecosystem Approaches to landscape management in central Europe. Berlin, Heidelberg, New York, pp. 183-194.

Auerswald, K., Kutilek, M., 1998. An European view to the protection of the soil resource. Soil Tillage Res. 46: 9-11.

Auerswald, K., Mutchler, C.K., McGregor, K.C., 1994. The influence of tillage-induced differences in surface moisture content on soil erosion. Soil Tillage Res. 32: 41-50.

Auerswald, K., Schmidt, F., 1986. Atlas der Erosionsgefährdung in Bayern - Karten zum flächenhaften Bodenabtrag durch Regen. GLA-Fachberichte 1, München, 74 pp.

Auerswald, K., Weigand, S., 1996. Ecological impact of dead-wood hedges: release of dissolved phosphorus and organic matter into runoff. Ecol. Eng. 7: 183-189.

Auerswald, K., Weigand, S., 1999. Eintrag und Freisetzung von P durch Erosionsmaterial in Oberflächengewässern. VDLUFA-Schriftenreihe 50: 37-54.

Bajracharya, R.M., Lal, R., Kimble, J.M., 2000. Diurnal and seasonal $CO_2$-C flux from soil as related to erosion phases in central Ohio. Soil Sci. Soc. Am. J. 64: 286-293.

Barfield, B.J., Belvins, R.L., Fogle, A.W., Madison, C.E., Inamdar, S., Carey, D.I., Evangelou, V.P., 1998. Water quality impacts of natural filter strips in karst areas. Trans. ASAE 41: 371-381.

Bartels, H., Malitz, G., Asmus, S., Albrecht, F.M., Dietzer, B., Günther, T., Ertel, H., 1997. Starkniederschlaghöhen für Deutschland - KOSTRA. Deutscher Wetterdienst, Offenbach a. Main, 82 pp.

Bastin, G., Lorent, B., Duque, C., Gevers, M., 1984. Optimal estimation of the average areal rainfall and optimal selection of rain-gauge locations. Wat. Resourc. Res. 20: 463-470.

Becher, H.H., Muller, K., Schneider, E., 1990. Determination of the bulk-density of small single aggregates by submersed weighing following paraffining. Z. Pflanzenernähr. Bodenkd. 153: 369-371.

Becher, H.H., Schäfer, R., Schwertmann, U., Wittmann, O., Schmidt, F., 1980. Experiences in determining the erodibility of soils following Wischmeier in some areas of Bavaria. *In* De Boodt M., Gabriels D. (Editors). Assessment of Erosion. Wiley & Sons, Chichester, pp. 203-206.

Bechmann, M.E., Kleinman, P.J.A., Sharpley, A.N., Saporito, L.S., 2005. Freeze-thaw effects on phosphorus loss in runoff from manured and catch-cropped soils. J. Environ. Qual. 34: 2301-2309.

Benjamin, J.G., 1993. Tillage effects on near-surface soil hydraulic properties. Soil Tillage Res. 26: 277-288.

Berhe, A.A., Harte, J., Harden, J.W., Torn, M.S., 2007. The significance of the erosion-induced terrestrial carbon sink. BioScience 57: 337-346.

Berne, A., Delrieu, G., Creutin, J.D., Obled, C., 2004. Temporal and spatial resolution of rainfall measurements required for urban hydrology. J. Hydrol. 299: 166-179.

Berry, P.M., Sylvester-Bradley, R., Philipps, L., Hatch, D.J., Cuttle, S.P., Rayns, F.W., Gosling, P., 2002. Is the productivity of organic farms restricted by the supply of available nitrogen? Soil Use Manag. 18: 248-255.

Beuselinck, L., Govers, G., Steegen, A., Hairsine, P.B., Poesen, J., 1999a. Evaluation of the simple settling theory for predicting sediment deposition by overland flow. Earth Surf. Process. Landforms 24: 993-1007.

Beuselinck, L., Govers, G., Steegen, A., Quine, T.A., 1999b. Sediment transport by overland flow over an area of net deposition. Hydrol. Proc. 13: 2769-2782.

Beuselinck, L., Hairsine, P.B., Sander, G.C., Govers, G., 2002. Evaluating a multiclass net deposition equation in overland flow conditions. Wat. Resourc. Res. 38: 10.1029/2001WR000248.

Beuselinck, L., Steegen, A., Govers, G., Nachtergaele, J., Takken, I., Poesen, J., 2000. Characteristics of sediment deposits formed by intense rainfall events in small catchments in the Belgian Loam Belt. Geomorphology 32: 69-82.

Beven, K., Kirkby, M., 1979. A physically based, variable contributing area model of basin hydrology. Hydrol. Sci. Bull. 24: 43-69.

Beyer, L., Frund, R., Schleuss, U., Wachendorf, C., 1993. Colluvisols under cultivation in Schleswig-Holstein. 2. Carbon distribution and soil organic-matter composition. Z.Pflanzenernähr.Bodenkd. 156, 213-217.

Bielders, C.L., Ramelot, C., Persoons, E., 2003. Farmer perception of runoff and erosion and extent of flooding in the silt-loam belt of the Belgian Walloon Region. Environ. Sci. Policy 6: 85-93.

Bilotta, G.S., Brazier, R.E., Haygarth, P.M., 2007. Processes affecting transfer of sediment and colloids, with associated phosphorus, from intensively farmed grasslands: Erosion. Hydrol. Proc. 21: 135-139.

Biot, Y., Lu, X.X., 1995. Loss of yield caused by soil erosion on sandy soils in the UK. Soil Use Manag. 11: 157-162.

Bisdom, E.B.A., Dekker, L.W., Schoute, J.F.T., 1993. Water repellency of sieve fractions from sandy soils and relationships with organic material and soil structure. Geoderma 56: 105-118.

Blanco-Canqui, H., Gantzer, C.J., Anderson, S.H., 2006. Performance of grass barriers and filter strips under interrill and concentrated flow. J. Environ. Qual. 35: 1969-1974.

Blöschl, G., 2006. Hydrologic synthesis: across processes, places, and scales. Wat. Resourc. Res. 42: 1-3.

Blöschl, G., Sivapalan, M., 1995. Scale issues in hydrological modelling: A review. Hydrol. Proc. 9: 251-290.

Blume, H.-P., Brümmer, G., Schwertmann, U., Horn, R., Kögel-Knabner, I., Stahr, K., Auerswald, K., Beyer, L., Hartmann, A., Litz, N., Scheinost, A., Stanjek, H., Welp, G., Wilke, B.-M., 2002. Scheffer/Schachtschabel - Lehrbuch der Bodenkunde. Enke, Stuttgart, 593 pp.

Boardman, J., Evans, R., Ford, J., 2003. Muddy floods on the South Downs, southern England: problems and responses. Environ. Sci. Policy 6: 69-83.

Boardman, J., Ligenau, L., De Roo, A.P., Vandaele, K., 1994. Flooding of property by runoff from agricultural land in northwestern Europe. Geomorphology 10: 183-196.

Borga, M., 2002. Accuracy of radar rainfall estimates for streamflow simulation. J. Hydrol. 267: 26-39.

Borga, M., Vizzaccaro, A., 1997. On the interpolation of hydrologic variables: Formal equivalence of multiquadratic surface fitting and kriging. J. Hydrol. 195: 160-171.

Borin, M., Vianello, M., Morari, F., Zanin, G., 2005. Effectiveness of buffer strips in removing pollutants in runoff from a cultivated field in North-East Italy. Agric. Ecosys. Environ. 105: 101-114.

Bormann, H., Breuer, L., Gräff, T., Huisman, J.A., 2007. Analysing the effects of soil properties changes associated with land use changes on the simulated water balance: A comparison of three hydrological catchment models for scenario analysis. Ecol. Mod. 209: 29-40.

Bormann, H., Breuer, L., Gräff, T., Huisman, J.A., Croke, B., 2008. Assessing the impact of land use change on hydrology by ensemble modelling: IV. Model sensitivity to data aggregation and spatial (re-)distribution. Adv. Wat. Resour. 31: 674-695.

Bracken, L.J., Croke, J., 2007. The concept of hydrological connectivity and its contribution to understanding runoff-dominated geomorphic systems. Hydrol. Proc. 21: 1749-1763.

Bradford, J.M., Huang, C., 1992. Mechanisms of crust formations: Physical components. *In* Sumner M.E., Stewart B.A. (Editors). Soil crusting - chemical and physical processes. Lewis, Boca Raton, pp. 55-72.

Brandt, C.J., 1989. The size distribution of throughfall drops under vegetation canopies. Catena 16: 507-524.

Brazier, R.E., Beven, K., Anthony, S., Rowan, J.S., Quinn, P., 2001. Implications of complex model uncertainty for the mapping of hillslope scale soil erosion predictions. Earth Surf. Process. Landforms 26: 1333-1352.

Brazier, R.E., Beven, K., Freer, J., Rowan, J.S., 2000. Equifinality and uncertainty in physically based soil erosion models: Application of the GLUE methodology to WEPP-the water erosion prediction project-for sites in the UK and USA. Earth Surf. Process. Landforms 25: 825-845.

Briggs, J.A., Whitwell, T., Riley, M.B., 1999. Remediation of herbicides in runoff water from container plant nurseries utilizing grassed waterways. Weed Technol. 12: 157-164.

Bronstert, A., Bárdossy, A., 2003. Uncertainty of runoff modelling at the hillslope scale due to temporal variations of rainfall intensity. Phys. Chem. Earth 28: 283-288.

Bronstert, A., Niehoff, D., Bürger, G., 2002. Effects of climate and land-use change on storm runoff generation: present knowledge and modelling capabilities. Hydrol. Proc. 16: 509-529.

Bronstert, A., Vollmer, S., Ihringer, J., 1995. Die Bedeutung von Flurbereinigungsmaßnahmen für das Abflussverhalten von Starkniederschlägen in ländlichen Gebieten. Wasser & Boden 47: 29-46.

Bronswijk, J.J.B., 1989. Prediction of actual cracking and subsidence in clay soils. Soil Sci. 148: 87-93.

Bronswijk, J.J.B., 1998. Modeling of water balance, cracking and subsidence of clay soils. J. Hydrol. 97: 199-212.

Bruce, R.R., Langdale, G.W., West, L.T., Miller, W.P., 1995. Surface soil degradation and soil productivity restoration and maintenance. Soil Sci. Soc. Am. J. 59: 654-660.

Bucher, B., Demuth, S., 1985. Vergleichende Wasserbilanz eines flurbereinigten und eines nicht flurbereinigten Einzugsgebietes im Ostkaiserstuhl für den Zeitraum 1977-1980. Dt. Gewässerkundl. Mitt. 29: 1-4.

Burwell, R.E., Larson, W.E., 1969. Infiltration as influenced by tillage-reduced random roughness and pore space. Soil Sci. Soc. Am. Proc. 33: 449-452.

Buytaert, W., Celleri, R., Willems, P., De Bievre, B., Wyseure, G., 2006. Spatial and temporal rainfall variability in mountainous areas: A case study from the south Ecuadorian Andes. J. Hydrol. 329: 413-421.

Cambardella, C.A., Moorman, T.B., Novak, J.M., Parkin, T.B., Karlen, D.L., Turco, R.F., Konopka, A.E., 1994. Field-scale variability of soil properties in central Iowa soils. Soil Sci. Soc. Am. J. 58: 1501-1511.

Cerdan, O., Poesen, J., Govers, G., Saby, N., Le Bissonnais, Y., Gobin, A., Vacca, A., Quinton, J.N., Auerswald, K., Klik, A., Kwaad, F.J., Roxo, M.J., 2006. Sheet and rill erosion. *In* Boardman J., Poesen J. (Editors). Soil erosion in Europe. Wiley, Chichester, pp. 501-514.

Cerdan, O., Soucherè, V., Lecomte, V., Couturier, A., Le Bissonnais, Y., 2001. Incorporating soil surface crusting processes in an expert-based runoff and erosion model: Sealing and Transfer by Runoff and Erosion related to Agricultural Management. Catena 46: 189-205.

Chai, X., Shen, C., Yuan, X., Huang, Y., 2008. Spatial prediction of soil organic matter in the presence of different external trends with REML-EBLUP. Geoderma 148: 159-166.

Chaubey, I., Edwards, D.R., Daniel, T.C., Moore, P.A.jr., Nichols, D.J., 1994. Effectiveness of vegetative filter strips in retaining surface-applied swine manure constituents. Trans. ASAE 37: 845-850.

Chaubey, I., Edwards, D.R., Daniel, T.C., Moore, P.A.jr., Nichols, D.J., 1995. Effectiveness of vegetative filter strips in controlling losses of surface-applied poultry litter constituents. Trans. ASAE 38: 1687-1692.

Chen, F., Kissel, D.E., West, L.T., Adkins, W., 2000. Field-scale mapping of surface soil organic carbon using remotely sensed imagery. Soil Sci. Soc. Am. J. 64: 746-753.

Chen, Y., Tessier, S., Rouffignat, J., 1998. Soil bulk density estimation for tillage systems and soil textures. Trans. ASAE 41: 1601-1610.

Chow, T.L., Rees, H.W., 1994. Effects of potato hilling on water runoff and soil-erosion under simulated rainfall. Can. J. Soil Sci. 74: 453-460.

Chow, T.L., Rees, H.W., Daigle, J.L., 1999. Effectiveness of terraces/grassed waterway systems for soil and water conservation: A field evaluation. J. Soil Water Conserv. 3: 577-583.

Chow, V.T., Maidment, D.R., Mays, L.W., 1988. Applied hydrology. McGraw-Hill, New York, 572 pp.

Ciesiolka, C.A.A., Yu, B., Rose, C.W., Ghadiri, H., Lang, D., Rosewell, C., 2006. Improvement of soil loss estimation in USLE type experiments. J. Soil Water Conserv. 61: 223-230.

Cole, J.J., Caraco, N.F., 2001. Carbon in catchments: connecting terrestrial carbon losses with aquatic metabolism. Marine Freshwater Resear. 52: 101-110.

Cole, J.T., Baird, J.H., Basta, N.T., Huhnke, R.L., Storm, D.E., Johnson, G.V., Payton, M.E., Smolen, M.D., Martin, D.L., Cole, J.C., 1997. Influence of buffers on pesticide and nutrient runoff from bermudagrass turf. J. Environ. Qual. 26: 1589-1598.

Cooper, C.M., 1993. Biological effects of agriculturally derived surface water pollutant on aquatic systems - A review. J. Environ. Qual. 22: 402-408.

Corradini, C., Morbidelli, R., Melone, F., 1998. On the interaction between infiltration and Hortonian runoff. J. Hydrol. 204: 52-67.

Correll, D.L., 2005. Principles of planning and establishment of buffer zones. Ecol. Eng. 24: 433-439.

Cousen, S.M., Farres, P.J., 1984. The role of moisture content in the stability of soil aggregates from a temperate silty soil to raindrop impact. Catena 11: 313-320.

Cowen, W.F., Lee, G.F., 1973. Leaves as sources of phosphorus. Environ. Sci. Technol. 7: 853-854.

Dabney, S.M., Moore, M.T., Locke, M.A., 2006. Integrated management of in-field, edge-of-field, and after-field buffers. J. Am. Wat. Resour. Assoc. 42: 15-24.

Dalal, R.C., 1979. Mineralization of carbon and phosphorus from carbon-14 and phosphorus-32 labeled plant material added to soil. Soil Sci. Soc. Am. J. 43: 913-916.

Datta, S., Jones, W.L., Roy, B., Tokay, A., 2003. Spatial variability of surface rainfall as observed from TRMM field campaign data. J. Appl. Meteo. 42: 598-610.

Davidson, E.A., Belk, E., Boone, R.D., 1998. Soil water content and temperature as independent or confounded factors controlling soil respiration in a temperate mixed hardwood forest. Global Change Biol. 4: 217-227.

De Alba, S., Lindstrom, M., Schumacher, T.E., 2004. Soil landscape evolution due to soil redistribution by tillage: a new conceptual model of soil catena evolution in agricultural landscapes. Catena 58: 77-100.

De Gryze, S., Bossuyt, H., Six, J., Van Meirvenne, M., Govers, G., Merckx, R., 2007. Factors controlling aggregation in a minimum and a conventionally tilled undulating field. Europ.J.Soil Sci. 58: 1017-1026.

De Roo, A.P., Offermans, R.J.E., Cremers, H.D.T., 1996a. LISEM: A single-event, physically based hydrological and soil erosion model for drainage basins. II: Sensitivity analysis, validation and application. Hydrol. Proc. 10: 1119-1126.

De Roo, A.P., Wesseling, C.G., Ritsema, C.J., 1996b. LISEM: A single-event physically based hydrological and soil erosion model for drainage basins. I: Theory, input and output. Hydrol. Proc. 10: 1107-1117.

Deletic, A., 2001. Modelling of water and sediment transport over grassed areas. J. Hydrol. 248: 168-182.

Deletic, A., Fletcher, T.D., 2006. Performance of grass filters used for stormwater treatment - A field and modelling study. J. Hydrol. 317: 261-275.

Desa, M.N.M., Niemczynowicz, J., 1997. Dynamics of short rainfall storms in a small scale urban area in Coly Limper, Malaysia. Atmos. Res. 44: 293-315.

Desmet, P.J.J., Govers, G., 1996. A GIS procedure for automatically calculating the USLE LS factor on topographically complex landscape units. J. Soil Water Conserv. 51: 427-433.

Destatis, 2002. http://www.destatis.de/basis/d/umw/ugrtab7.htm (Statistisches Bundesamt Deutschland, verified 28 May 2003).

Di Luzio, M., Srinivasan, R., Arnold, J.G., Neitsch, S.L., 2002. ArcView interface for SWAT2000 - User's Guide. TWRI Report TR-193, Temple, Texas, USA, 351 pp.

Di Stefano, C., Ferro, V., 2002. Linking clay enrichment and sediment delivery processes. Biosystems Eng. 81: 465-479.

Diggle, P.J., Ribeiro Jr, P.J., 2007. Model-based geostatistics. Springer, New York. 228 pp.

Diiwu, J.Y., Rudra, R.P., Dickinson, W.T., Wall, G.J., 1998. Tillage and heterogeneity effects on the performance of soil water characteristic models. J. Agric. Eng. Res. 71: 307-313.

Dillaha, T.A., Reneau, R.B., Mostaghimi, S., Lee, D., 1989. Vegetative filter strips for agricultural nonpoint source pollution control. Trans. ASAE 32: 513-519.

Dorioz, J.M., Wang, D., Poulenard, J., Visan, D., 2006. The effect of grass buffer strips on phosphorus dynamics-A critical review and synthesis as a basis for application in agricultural landscapes in France. Agric. Ecosys. Environ. 117: 4-21.

Duley, F.L., 1939. Surface factors affecting the rate of intake of water by soils. Soil Sci. Soc. Am. Proc. 4: 60-64.

Dunkerley, D.L., 1999. Banded chenopod shrublands of arid Australia: modelling responses to interannual rainfall variability with cellular automata. Ecol. Mod. 201: 127-138.

Dyck, S., Peschke, G., 1995. Grundlagen der Hydrologie. Verlag für Bauwesen, Berlin, 536 pp.

Eastgate, W., 1969. Vegetated stabilization of grassed waterways and dam bywashes. Water Research Foundation of Australia, Kingsford, Australia, 16 pp.

ECC (European Communities-Commission), 1992. CORINE land cover project - technical guide. No. EUR 12585.

Emde, K., 1992. Experimentelle Untersuchungen zu Oberflächenabfluß und Bodenaustrag in Verbindung mit Starkregen bei verschiedenen Bewirtschaftungssystemen in Weinbergsarealen des oberen Rheingaus., 248 pp.

Faurès, J.-M., Goodrich, D.C., Woolhiser, D.A., Sorooshian, S., 1995. Impact of small-scale spatial rainfall variability on runoff modeling. J. Hydrol. 173: 309-326.

Fiener, P., Auerswald, K., 2001. Eight years of economical and ecological experience with soil-conserving land use. *In* Helming K. (Editor). Multidisciplinary approaches to soil conservation strategies. pp. 121-126.

Fiener, P., Auerswald, K., 2003a. Effectiveness of grassed waterways in reducing runoff and sediment delivery from agricultural watersheds. J. Environ. Qual. 32: 927-936.

Fiener, P., Auerswald, K., 2003b. Concept and effects of a multi-purpose grassed waterway. Soil Use Manag. 19: 65-72.

Fiener, P., Auerswald, K., 2005. Measurement and modeling of concentrated runoff in a grassed waterway. J. Hydrol. 301: 198-215.

Fiener, P., Auerswald, K., Weigand, S., 2005. Managing erosion and water quality in agricultural watersheds by small detention ponds. Agric. Ecosys. Environ. 110: 132-142.

Fiener, P., Auerswald, K., 2006. Seasonal variation of grassed waterway effectiveness in reducing runoff and sediment delivery from agricultural watersheds in temperate Europe. Soil Tillage Res. 87: 48-58.

Fiener, P., Auerswald, K., 2007. Rotation effects of potato, maize and winter wheat on soil erosion by water. Soil Sci. Soc. Am. J. 71: 1919-1925.

Fiener, P., Govers, G., Van Oost, K., 2008. Evaluation of a dynamic multi-class sediment transport model in a catchment under soil-conservation agriculture. Earth Surf. Process. Landforms 33: 1639-1660.

Fiener, P., Auerswald, K., 2009. Spatial variability of rainfall on a sub-kilometre scale. Earth Surf. Process. Landforms 34: 848-859.

Fierer, N., Allen, A.S., Schimel, J.P., Holden, P.A., 2003. Controls on microbial $CO_2$ production: a comparison of surface and subsurface soil horizons. Global Change Biol. 9: 1322-1332.

Flacke, W., Auerswald, K., Neufang, L., 1990. Combining a modified Universal Soil Loss Equation with a digital terrain model for computing high resolution maps of soil loss resulting from rain wash. Catena 17: 383-397.

Flanagan, D.C., Nearing, M.A., (Editiors) 1995. USDA Water Erosion Predition Project: Hillslope profile and watershed model documentation. NSERL report No. 10. USDA-ARS National Soil Erosion Research Laboratory, West Lafayette, Indiana, USA.

Fohrer, N., Berkenhagen, J., Hecker, J.-M., Rudolph, A., 1999. Changing soil and surface conditions during rainfall single rainstorm / subsequent rainstorms. Catena 37: 355-375.

Fohrer, N., Haverkamp, S., Eckhardt, K., Frede, H.-G., 2001. Hydrologic response to land use changes on the catchment scale. Phys. Chem. Earth B 26: 577-582.

Fohrer, N., Haverkamp, S., Frede, H.-G., 2005. Assessment of the effects of land use patterns on hydrologic landscape functions: development of sustainable land use concepts for low mountain range areas. Hydrol. Proc. 19: 659-672.

Foster, G.R., (Editor) 2005. Science documentation: Revised Universal Soil Loss Equation Version 2 (RUSLE2). USDA - Agricultural Research Service, Washington D.C., 286 pp.

Foster, G.R., Meyer, L.D., 1972. Transport of soil particles by shallow flow. Trans. ASAE 15: 99-102.

Foster, G.R., Meyer, L.D., 1975. Mathematical simulation of upland erosion by fundamental erosion mechanics. *In* ARS-S-40 USDA-Sci.Educ.Adm. (Editor). Present and Prospective Technology for Predicting Sediment Yields and Sources. pp. 190-204.

Foster, G.R., Weesies, G.A., Renard, K.G., Yoder, D.C., McCool, D.K., Poster, J.P., 1997. Support practice factor (P). *In* Renard K.G., Foster G.R., Weesies G.A., McCool D.K., Yoder D.C. (Editors). Predicting soil erosion by water: A guide to conservation planning with the revised universal soil loss equation (RUSLE). U.S. Dep. Agric., Washington, pp. 183-251.

Fox, D.M., Le Bissonnais, Y., Bruand, A., 1998. The effect of ponding depth on infiltration in a crusted surface depression. Catena 32: 87-100.

Franzluebbers, A.J., Hons, F.M., Zuberer, D.A., 1995. Tillage-induced seasonal changes in soil physical properties affecting soil $CO_2$ evolution under intensive cropping. Soil Tillage Res. 34: 41-60.

Freeman, M.C., Pringle, C.M., Jackson, C.R., 2007. Hydrologic connectivity and the contribution of stream headwaters to ecological integrity at regional scales. J. Am. Wat. Resour. Assoc. 43: 5-14.

Gallart, F., Llorens, P., Latron, J., 1994. Studying the role of old agricultural terraces on runoff generation in a small Mediterranean mountainous basin. J. Hydrol. 159: 291-303.

Gat, J.R., 1996. Oxygen and hydrogen isotopes in the hydrologic cycle. Annu. Rev. Earth Pl. Sc. 24: 225-262.

Gharabaghi, B., Rudra, R.P., Goel, P.K., 2006. Effectiveness of vegetative filter strips in removal of sediments from overland flow. Water Qual. Res. J. Can. 41: 275-282.

Gilley, J.E., Finkner, S.C., 1991. Hydraulic roughness coefficients as affected by random roughness. Trans. ASAE 34: 897-903.

Gilley, J.E., Finkner, S.C., Spomer, R.G., Mielke, L.N., 1986. Runoff and erosion as affected by corn residue: Part I. Total losses. Trans. ASAE 29: 157-160.

Gilley, J.E., Kottwitz, E.R., Wieman, G.A., 1991. Roughness coefficients for selected residue materials. J. Irr. Drain. Eng. -ASCE 117: 503-514.

Gimenez, R., Govers, G., 2002. Flow detachment by concentrated flow on smooth and irregular beds. Soil Sci. Soc. Am. J. 66: 1475-1483.

Giménez, R., Govers, G., 2008. Short term effects of incorporated straw residue on rill erosion and hydraulics. Catena 72: 214-223.

Goodrich, D.C., Faures, J.M., Woolhiser, D.A., Lane, L.J., Sorooshian, S., 1995. Measurement and analysis of small-scale convective storm rainfall variability. J. Hydrol. 173: 283-308.

Govers, G., 1985. Selectivity and transport capacity of thin flows in relation to rill erosion. Catena 12: 35-49.

Govers, G., 1986. Soil erosion process research: A state of the art. Academiae Analecta 58(1). Mededelingen van de Koniklijke Academie voor Wetenschappen, Letteren en Schone Konsten van België, Brussel, Belgium.

Govers, G., 1990. Empirical relationships for the transport capacity of overland flow. pp. 45-63. *In* Jerusalem Workshop 1987. Jerusalem.

Govers, G., 1991. Time-dependency of runoff velocity and erosion: the effect of the initial soil moisture profile. Earth Surf. Process. Landforms 16: 713-729.

Govers, G., 1992a. Evaluation of transporting capacity formulae for overland flow. *In* Parsons A.J., Abrahams A.D. (Editors). Overland flow - Hydraulics and erosion mechanics. UCL Press, London, pp. 243-271.

Govers, G., 1992b. Relationship between discharge, velocity and flow area for rills eroding loose, non-layered materials. Earth Surf. Process. Landforms 17: 515-528.

Govers, G., Everaert, W., Poesen, J., Rauws, G., De Ploey, J., Lautridou, J.P., 1990. A long flume study of the dynamic factors affecting the resistance of a loamy soil to concentrated flow erosion. Earth Surf. Process. Landforms 15: 313-328.

Govers, G., Giménez, R., Van Oost, K., 2007. Rill erosion: exploring the relationship between experiments, modelling and field observations. Earth-Sci. Rev. 84: 87-102.

Govers, G., Quine, T.A., Walling, D.E., 1993. The effect of water erosion and tillage movement on hillslope profile development: a comparison of field observation and model results. *In* Wicherek S. (Editor). Farm land erosion in temperate plains environments and hills. Elsevier, Amsterdam, pp. 285-300.

Govers, G., Takken, I., Helming, K., 2000. Soil roughness and overland flow. Agronomie 20: 131-146.

Govers, G., Vandaele, K., Desmet, P., Poesen, J., Bunte, K., 1994. The role of tillage in soil redistribution on hillslopes. Europ. J. Soil Sci. 45: 469-478.

Grayson,R.B., Blöschl,G., (Editors) 2000. Spatial patterns in catchment hydrology - observations and modelling. Cambridge University Press, Cambridge, 397 pp.

Greb, B.W., Smika, D.E., Black, A.L., 1967. Effect of straw mulch rates on soil water storage during summer fallow in the Great Plains. Soil Sci. Soc. Am. Proc. 31: 556-559.

Green, T.R., Ahuja, L.R., Benjamin, J.G., 2003. Advances and challenges in predicting agricultural management effects on soil hydraulic properties. Geoderma 116: 3-27.

Gregorich, E.G., Greer, K.J., Anderson, D.W., Liang, B.C., 1998. Carbon distribution and losses: erosion and deposition effects. Soil Tillage Res. 47: 291-302.

Grunwald, S., Frede, H.-G., 1999. Using the modified agricultural non-point source pollution model in German watersheds. Catena 37: 319-328.

Gupta, S.C., Larson, W.E., 1979. Estimating soil water retention characteristics from particle size distribution, organic matter percent, and bulk density. Wat. Resourc. Res. 15: 1633-1635.

Guth, P.L., 2006. Geomorphometry from SRTM: comparision to NED. Photogramm. Eng. Rem. S. 72: 269-277.

Hairsine, P.B., Beuselinck, L., Sander, G.C., 2002. Sediment transport through an area of net deposition. Wat. Resourc. Res. 38: Art. No. 1086 JUN.

Hairsine, P.B., Rose, C.W., 1992a. Modeling water erosion due to overland flow using physical principles. 1. Sheet flow. Wat. Resourc. Res. 28: 237-243.

Hairsine, P.B., Rose, C.W., 1992b. Modeling water erosion due to overland flow using physical principles. 2. Rill flow. Wat. Resourc. Res. 28: 245-250.

Haith, D.A., Tubbs, L.J., Pickering, N.B., 1984. Simulation of pollution by soil erosion and soil nutrient loss. Purdoc, Wageningen, NL, 77 pp.

Hansen, N.C., Daniel, T.C., Sharpley, A.N., Lemunyon, J.L., 2002. The fate and transport of phosphorus in agricultural systems. J. Soil Water Conserv. 57: 408-416.

Harden, J.W., Sharpe, J.M., Parton, W.J., Ojima, D.S., Fries, T.L., Huntington, T.G., Dabney, S.M., 1999. Dynamic replacement and loss of soil carbon by eroding cropland. Global Biogeochem. Cycles 13: 885-901.

Hawkins, R.H., Hjelmfeldt, A.T., Zevenbergen, A.W., 1985. Runoff probability, storm depth, and curve numbers. J. Irr. Drain. Eng. -ASCE 111: 330-340.

Haygarth, P.M., Bilotta, G.S., Bol, R., Brazier, R.E., Butler, P.J., Freer, J., Gimbert, L.J., Granger, S.J., Krueger, T., Macleod, C.J.A., Naden, P., Old, G., Quinton, J.N., Smith, B., Worsfold, P., 2006. Processes affecting transfer of sediment and colloids, with associated phosphorus, from intensively farmed grasslands: An overview of key issues. Hydrol. Proc. 20: 4407-4413.

Heathwaite, A.L., Quinn, P.F., Hewett, C.J.M., 2005. Modelling and managing critical source areas of diffuse pollution from agricultural land using flow connectivity simulation. J. Hydrol. 304: 446-461.

Hedeker, D., Gibbons, R.D., 2006. Longitudinal data analysis. John Wiley & Sons, Hoboken, New Jersey, 360 pp.

Heimlich, R.E., Bills, N.L., 1986. An improved soil erosion classification: Update, comparision, and extension. *In* Committee on Conservation (Editor). Soil conservation: Assessing the national resources inventory. Nat. Academy Press, Washington, D.C., pp. 1-20.

Helming, K., Auzet, A.V., Favis-Mortlock, D., 2005. Soil erosion patterns: Evolution, spatio-temporal dynamics and connectivity. Earth Surf. Process. Landforms 30.

Hengl, T., Heuvelink, G.B.M., Rossiter, D.G., 2007. About regression-kriging: From equations to case studies. Comput. Geosci. 33: 1301-1315.

Hengl, T., Heuvelink, G.B.M., Stein, A., 2004. A generic framework for spatial prediction of soil variables based on regression-kriging. Geoderma 120: 75-93.

Herbst, M., Hellebrand, H.J., Bauer, J., Huisman, J.A., Simunek, J., Weihermüller, L., Graf, A., Vanderborght, J., Vereecken, H., 2008. Multi-year heterotrophic soil respiration: Evaluation of a coupled $CO_2$ transport and carbon turnover model. Ecol. Mod. 214: 271-283.

Hernandez, M., Miller, S.N., Goodrich, D.C., Goff, B.F., Kepner, W.G., Edmonds, C.M., Jones, K.B., 2000. Modeling runoff response to land cover and rainfall spatial variability in semi-arid watersheds. Environ. Monitor. Asses. 64: 285-298.

Hill, R.D., Peart, M.R., 1998. Land use, runoff, erosion and their control: a review for southern China. Hydrol. Proc. 12: 2029-2042.

Hjelmfelt, A., Wang, M., 1997. Using modelling to investigate impacts of grass waterways on water quality. pp. 1420-1425. *In* Proc. 27th Congress Internat. Assoc. Hydraulic Research. San Francisco. 1-15 Aug. 1997. Am. Soc. of Civil Eng. San Francisco, California.

Hoffmann, T., Erkens, G., Cohen, K.M., Houben, P., Seidel, J., Dikau, R., 2007. Holocene floodplain sediment storage and hillslope erosion within the Rhine catchment. Holocene 17: 105-118.

Honisch, M., Hellmeier, C., Weiss, K., 2002. Response of surface and subsurface water quality to land use changes. Geoderma 105: 277-298.

Horton, R.E., 1933. The role of infiltration in the hydrological cycle. Trans. Am. Geophys. Union 14: 446-460.

Horton, R.E., 1939. Analysis of runoff plat experiments with varying infiltration capacity. Trans. Am. Geophys. Union Part IV: 693-694.

Huang, C., Bradford, J.M., 1990. Depressional storage for Markov-Gaussian surfaces. Wat. Resourc. Res. 26: 2235-2242.

Isaaks, E.H., Srivastava, R.M., 1989. Applied geostatistics. Oxford University Press, New York, 592 pp.

ISO, 2009. Country short names code ISO 3166. http://www.iso.org/iso/country_codes/iso_3166_code_lists.htm.

Jacinthe, P.A., Lal, R., Kimble, J.M., 2001. Organic carbon storage and dynamics in croplands and terrestrial deposits as influenced by subsurface tile drainage. Soil Sci. 166: 322-335.

Jacinthe, P.A., Lal, R., Kimble, J.M., 2002. Carbon dioxide evolution in runoff from simulated rainfall on long-term no-till and plowed soils in southwestern Ohio. Soil Tillage Res. 66: 23-33.

Jacinthe, P.A., Lal, R., Owens, L.B., Hothem, D.L., 2004. Transport of labile carbon in runoff as affected by land use and rainfall characteristics. Soil Tillage Res. 77: 111-123.

Jensen, N.E., Pedersen, L., 2005. Spatial variability of rainfall: Variations within a single radar pixel. Atmos. Res. 77: 269-277.

Jester, W., Klik, A., 2005. Soil surface roughness measurement-methods, applicability, and surface representation. Catena 64: 174-192.

Jetten, V., Boiffin, J., De Roo, A.P., 1996. Defining monitoring strategies for runoff and erosion studies in agricultural catchments: a simulation approach. Europ. J. Soil Sci. 47: 579-592.

Jetten, V., Govers, G., Hessel, R., 2003. Erosion models: quality of spatial predictions. Hydrol. Proc. 17: 877-900.

Jin, C.X., Römkens, M.J.M., Griffioen, F., 2000. Estimating Manning's roughness coefficient for shallow overland flow in non-submerged vegetative filter strips. Trans. ASAE 43: 1459-1466.

Jobbagy, E.G., Jackson, R.B., 2000. The vertical distribution of soil organic carbon and its relation to climate and vegetation. Ecol. Appl. 10: 423-436.

Johannes, B., 2001. Ausmaß und Ursachen kleinräumiger Niederschlagsvariabilität und Konzequenzen für die Abflussbildung. Shaker, Aachen, 163 pp.

John, M.K., 1970. Colorimetric determination of phosphorus in soil and plant materials with ascorbic acid. Soil Sci. 109: 214-220.

Johnson, C.B., Mannering, J.V., Moldenhauer, W.C., 1979. Influence of surface roughness and clod size and stability on soil and water losses. Soil Sci. Soc. Am. J. 43: 772-777.

Kachanoski, R.G., Carter, M.R., 1999. Landscape position and soil redistribution under three soil types and land use practices in Prince Edward Island. Soil Tillage Res. 51: 211-217.

Kaemmerer, A., 2000. Raum-Zeit-Variabilität von Aggregatstabilität und Bodenrauhigkeit. Shaker, Aachen, 207 pp.

Kagerer, J., Auerswald, K., 1997. Erosionsprognose-Karten im Maßstab 1:5.000 für Flurbereinigungsverfahren und Landwirtschaftsberatung. Bayerische Landesanstalt für Bodenkultur und Planzenbau (LBP), Munich, 43 pp.

Kainz, M., 1989. Runoff, erosion and sugar beet yields in conventional and mulched cultivation. Results of the 1988 experiment. Soil Technol. Ser. 1: 103-114.

Karunatilake, U.P., Van Es, H.M., 2002. Rainfall and tillage effects on soil structure after alfalfa conversion to maize on a clay loam soil in New York. Soil Tillage Res. 67: 135-146.

Katsvairo, T., Cox, W.J., Van Es, H.M., 2002. Tillage and rotation effects on soil physical characteristics. Agron. J. 94: 299-304.

Kemper, W., Rosenau, R., 1984. Soil cohesion as affected by time and water content. Soil Sci. Soc. Am. J. 48: 1001-1006.

Kemper, W.D., Rosenau, R., Nelson, S., 1985. Gas displacement and aggregate stability of soils. Soil Sci. Soc. Am. J. 49: 25-28.

Kerry, R., Oliver, M.A., 2007a. Determining the effect of asymmetric data on the variogram. I. Underlying asymmetry. Comput. Geosci. 33: 1212-1232.

Kerry, R., Oliver, M.A., 2007b. Determining the effect of asymmetric data on the variogram. II. Outliers. Comput. Geosci. 33: 1233-1260.

Kirkby, M.J., Bracken, L.J., Shannon, J., 2005. The influence of rainfall distribution and morphological factors on runoff delivery from dryland catchments in SE Spain. Catena 62: 136-156.

Kleinman, P.J.A., Sharpley, A.N., Veith, T.L., Maguire, R.O., Vadas, P.A., 2004. Evaluation of phosphorus transport in surface runoff from packed soil boxes. J. Environ. Qual. 33: 1413-1423.

Knapen, A., Poesen, J., De Baets, S., 2008. Rainfall-induced consolidation and sealing effects on soil erodibility during concentrated runoff for loess-derived topsoils. Earth Surf. Process. Landforms 33: 444-458.

Knoll, G., Sieber, H., 1986. Die Hallertau. Frisinga Verlag, Freising, 142 pp.

Königer, S., Schwab, A., 2000. Application of a Geographical Information System (GIS) for the determination of soil erosion risk in Franconian vineyards, northwestern Bavaria, Germany. pp. 155-159. *In* Congress on Regional Geological Cartography and Information Systems. Munich.

Königer, S., Schwab, A., 2002. Anwendung eines Geographischen Informationssystems (GIS) zur Planung verbesserter Bodenschutzmassnahmen in Weinbaugebiet Franken (NW-Bayern, Deutschland). Z. geol. Wiss. 30: 351-364.

Kouwen, N., 1992. Modern approach to design of grassed channels. J. Irr. Drain. Eng. - ASCE 118: 733-743.

Kouwen, N., Li, R.-M., 1980. Biomechanics of vegetative channel linings. J. Hydraulics Div. Proc. ASCE 106: 1085-1103.

Kouwen, N., Li, R.M., Simons, D.B., 1981. Flow resistance in vegetated waterways. Trans. ASAE 24: 684-690.

Kruizinga, S., Yperlaan, G.J., 1978. Spatial interpolation of daily totals of rainfall. J. Hydrol. 36: 65-73.

Kuhn, N.J., Hoffmann, T., Schwanghart, W., Dotterweich, M., 2009. Agricultural soil erosion and global carbon cycle: controversy over? Earth Surf. Process. Landforms DOI: 10.1002/esp.1796.

Kuron, H., Jung, L., Schreiber, H., 1956. Messungen von oberflächlichem Abfluß und Bodenabtrag auf verschiedenen Böden Deutschlands. *In* Schriftenreihe des Kuratoriums für Kulturbauwesen. Vol. 5. Wasser und Boden/Hamburg. Hamburg.

Kyriakidis, P.C., Journel, A.G., 1999. Geostatistical space-time models: A review. Math. Geol. 31: 651-684.

La Barbera, P., Lanza, L.G., Stagi, L., 2002. Tipping bucket mechanical errors and their influence on rainfall statistics and extremes. Wat. Sci. Technol. 45: 1-9.

Lado, M., Ben-Hur, M., Shainberg, I., 2004. Soil wetting and texture effects on aggregate stability, seal formation, and erosion. Soil Sci. Soc. Am. J. 68: 1992-1999.

Lal, R., 1982. Effects of slope length and terracing on runoff and erosion on a tropical soil. IAHS Publ. 137: 23-31.

Lal, R., 1998a. Soil erosion research methods. St. Lucie Press, Boca Raton, FL, 244 pp.

Lal, R., 1998b. Soil erosion impact on agronomic productivity and environment quality. Crti. Rec. Plant Sci. 17: 319-464.

Lal, R., 2001. Soil degradation by erosion. Land Degrad. Dev. 12: 519-539.

Lal, R., 2003. Soil erosion and the global carbon budget. Environ. Int. 29: 437-450.

Lane, L.J., Nearing, M.A., 1989. USDA-Water Erosion Predicting Project: Hillslope profile model documentation. USDA-ARS, National Soil Erosion Research Laboratory, West Lafayette.

Lark, R.M., Cullis, B.R., Welham, S.J., 2006. On spatial prediction of soil properties in the presence of a spatial trend: the empirical best linear unbiased predictor (E-BLUP) with REML. Europ. J. Soil Sci. 57: 787-799.

Le Bissonnais, Y., 1996. Aggregate stability and assessment of soil crustability and erodibility: I. Theory and methodology. Europ. J. Soil Sci. 47: 425-437.

Le Bissonnais, Y., Benkhadra, H., Chaplot, V., Fox, D., King, D., Daroussin, J., 1998. Crusting, runoff and sheet erosion on silty loamy soils at various scales and upscaling from m2 to small catchments. Soil Tillage Res. 46: 69-80.

Le Bissonnais, Y., Lecomte, V., Cerdan, O., 2004. Grass strip effects on runoff and soil loss. Agronomie 24: 129-136.

Léonard, J., Ancelin, O., Ludwig, B., Richard, G., 2006. Analysis of the dynamics of soil infiltrability of agricultural soils from continuous rainfall-runoff measurements on small plots. J. Hydrol. 326: 122-134.

Leopold, L.B., Wolman, M.G., Miller, J.P., 1964. Fluvial processes in Geomorphology. W.H. Freeman and Company, San Francisco. 522 pp.

Lexartza-Artza, I., Wainwright, J., 2009. Hydrological connectivity: Linking concepts with pratical implications. Catena 79: 146-152.

Linden, D.R., 1979. A model to predict soil water storage as affected by tillage practices. PhD thesis, University of Minnesota, St. Paul, MN. 320 pp.

Lindstrom, M.J., Nelson, W.W., Schumacher, T.E., 1992. Quantifying tillage erosion rates due to moldboard plowing. Soil Tillage Res. 24: 243-255.

Littell, R.C., Henry, P.R., Ammerman, C.B., 1998. Statistical analysis of repeated measures data using SAS procedures. J. Anim. Sci. 76: 1216-1231.

Little, J.L., Nolan, S.C., Casson, J.P., Olson, B.M., 2007. Relationships between Soil and Runoff Phosphorus in Small Alberta Watersheds. J. Environ. Qual. 36: 1289-1300.

Liu, S.G., Bliss, N., Sundquist, E., Huntington, T.G., 2003. Modeling carbon dynamics in vegetation and soil under the impact of soil erosion and deposition. Global Biogeochem. Cycles 17: 43-1-43-24.

Loftis, J.C., MacDonald, L.H., Streett, S., Iyer, H.K., Bunte, K., 2001. Detecting cumulative watershed effects: the statistical power of pairing. J. Hydrol. 251: 49-64.

Lohila, A., Aurela, M., Regina, K., Laurila, T., 2003. Soil and total ecosystem respiration in agricultural fields: effect of soil and crop type. Plant Soil 251: 303-317.

Ludwig, J.A., Tongway, D.J., Marsden, S.G., 1999. Stripes, strands or stipples: Modelling the influence of three landscape banding patterns on resource capture and productivity in semi-arid woodlands, Australia. Catena 37: 257-273.

Ludwig, J.A., Wilcox, B.P., Breshears, D.D., Tongway, D.J., Imeson, A.C., 2005. Vegetation patches and runoff-erosion as interacting ecohydrological processes in semiarid landscapes. Ecology 86: 288-297.

Luft, G., Morgenschweis, G., Keller, R., 1981. Auswirkungen von Großterrasierung auf hydrologische Prozesse im Ostkaiserstuhl. Wasser und Boden 9: 436-442.

Mabit, L., Bernard, C., Makhlouf, M., Laverdière, M.R., 2008. Spatial variability of erosion and soil organic matter content estimated from $^{137}$Cs measurements and geostatistics. Geoderma 145: 245-251.

Mäder, P., Fließbach, A., Dubois, D., Gunst, L., Fried, P., Niggli, U., 2002. Soil fertility and biodiversity in organic farming. Science 296: 1694-1697.

Magunda, M.K., Larson, W.E., Linden, D.R., Nater, E.A., 1997. Changes in microrelief and their effects on infiltration and erosion during simulated rainfall. Soil Technol. 10: 57-67.

Marinissen, J.C.J., Dexter, A.R., 1990. Mechanisms of stabilization of earthworm casts and artificial casts. Biology and Fertility of Soils 9: 97-100.

Martin, W., 1988. Die Erodierbarkeit von Böden unter simulierten und natürlichen Regen und ihre Abhängigkeit von Bodeneigenschaften. PhD thesis, Technische Universität München, Freising-Weihenstephan, Germany. 160 pp.

Matheron, G., 1963. Principles of geostatistics. Econ. Geol. 58: 1246-1266.

Mbagwu, J.S.C., Auerswald, K., 1999. Relationship of percolation stability of soil aggregates to land use, selected properties, structural indices and simulated rainfall erosion. Soil Tillage Res. 50: 197-206.

McCool, D.K., Foster, G.R., Weesies, G.A., 1997. Slope length and steepness factors (LS). *In* Renard K.G., Foster G.R., Weesies G.A., McCool D.K., Yoder D.C. (Editors). Predicting soil erosion by water: A guide to conservation planning with the revised universal soil loss equation (RUSLE). U.S. Dep. Agric., Washington, pp. 101-141.

Meyer, L.D., Line, D.E., Harmon, W.C., 1992. Size characteristics of sediment from agricultural soils. J. Soil Water Conserv. 47: 107-111.

Minasny, B., McBratney, A.B., 2007a. Spatial prediction of soil properties using EBLUP with the Mátern covariance function. Geoderma 140: 324-336.

Minasny, B., McBratney, A.B., 2007b. Corrigendum to "Spatial prediction of soil properties using EBLUP with the Mátern covariance function" [Geoderma 140 (2007) 324-336]. Geoderma 142: 357-358.

Mishra, S.K., Jain, M.K., Singh, V.P., 2004. Evaluation of the SCS-CN-based model incorporating antecedent moisture. Wat. Resourc. Manag. 18: 567-589.

Mitasova, H., Hofierka, J., Zlocha, M., Iverson, L.R., 1996. Modelling topographic potential for erosion and deposition using GIS. Int. J. Geogr. Info. Sys. 10: 629-641.

Mockus, V., 1972. Estimation of direct runoff from storm rainfall. *In* SCS National Engineering Handbook. Sektion 4. Hydrology. USDA, pp. 10.1-10.24.

Mockus, V., Woodward, D.E., Neilsen, R.D., Kluth, R., Plummer, A., Van Mullem, J.A., Conaway, G., Gburek, B., Cooley, K.R., Hawkins, R.H., (Editors) 2002. Land use and treatment classes. National Engineering Handbook, Part 630 Hydrology. USDA - Natural Resources Conservation Service, Washington D.C.

Molini, A., Lanza, L.G., La Barbera, P., 2005. Improving the accuracy of tipping-bucket rain records using disaggregation techniques. Atmos. Res. 77: 203-217.

Moore, I.D., Gessler, P.E., Nielsen, G.A., Peterson, G.A., 1993. Soil attribute prediction using terrain analysis. Soil Sci. Soc. Am. J. 57: 443-452.

Moore, I.D., Larson, C.L., 1979. Estimating micro-relief surface storage from point data. Trans. ASAE 22: 1073-1077.

Morgan, R.P.C., 1996. Soil erosion and conservation. Addison-Wesley Pub Co., Reading, MA, 198 pp.

Morgan, R.P.C., Quinton, J.N., Smith, R.E., Govers, G., Poesen, J.W.A., Auerswald, K., Chisci, G., Torri, D., Styczen, M.E., 1998. The European soil erosion model (EURO-SEM): A dynamic approach for predicting sediment transport from fields and small catchments. Earth Surf. Process. Landforms 23: 527-544.

Morin, J., Benyamini, Y., 1977. Rainfall infiltration into bare soils. Wat. Resourc. Res. 13: 813-817.

Moussa, R., Voltz, M., Andrieux, P., 2002. Effects of the spatial organization of agricultural management on the hydrological behaviour of a framed catchment during flood events. Hydrol. Proc. 16: 393-412.

Mualem, Y., Assouline, S., Rohdenburg, H., 1990. Rainfall induced soil seal: A critical review of observations and models. Catena 17: 185-203.

Mueller, T.G., Pierce, F.J., 2003. Soil carbon maps: Enhancing spatial estimates with simple terrain attributes at multiple scales. Soil Sci. Soc. Am. J. 67: 258-267.

Mulla, D.J., Huyck, L.M., Reganold, J.P., 1992. Temporal variation in aggregate stability on conventional and alternative farms. Soil Sci. Soc. Am. J. 56: 1620-1624.

Munoz-Carpena, R., Parsons, J.E., Gilliam, J.W., 1999. Modeling hydrology and sediment transport in vegetative filter strips. J. Hydrol. 214: 111-129.

Murphree, C.E., Mutchler, C.K., 1981. Verification of the slope factor in the universal soil loss equation for low slopes. J. Soil Water Conserv. 36: 300-302.

Mutchler, C.K., Greer, J.D., 1980. Effect of slope length on erosion from low slopes. Trans. ASAE 23: 866-869.

Mwendera, E.J., Feyen, J., 1992. Estimation of depression storage and Manning's resistance coefficient from random roughness measurements. Geoderma 52: 235-250.

Nash, J.E., Sutcliffe, J.V., 1970. River flow forecasting through conceptual models: Part I. A discussion of principles. J. Hydrol. 10: 282-290.

Natural Resources Conservation Service, 2004. Conservation Practice Standard - Stripcropping. Code 585. Natural Resources Conservation Service, Washington D.C.

Ndiaye, B., Molénat, J., Hallaire, V., Gascuel, C., Hamon, Y., 2007. Effects of agricultural practices on hydraulic properties and water movement in soils in Brittany (France). Soil Tillage Res. 93: 251-263.

Nearing, M.A., 1997. A single, continuous function for slope steepness influence on soil loss. Soil Sci. Soc. Am. J. 61: 917-919.

Nearing, M.A., 1998. Why soil erosion models over-predict small soil losses and under-predict large soil losses. Catena 32: 15-22.

Nearing, M.A., 2006. Can soil erosion be predicted? *In* Owens P.N., Collins A.L. (Editors). Soil erosion and sediment redistribution in river catchments: measurement, modelling and management. Wallingford, pp. 145-152.

Nearing, M.A., Foster, G.R., Lane, L.J., Finkner, S.C., 1989. A process-based soil erosion model for USDA-water erosion prediction project technology. Trans. ASAE 32: 1587-1593.

Nearing, M.A., Govers, G., Norton, D.L., 1999. Variability in soil erosion data from replicated plots. Soil Sci. Soc. Am. J. 63: 1829-1835.

Nearing, M.A., Lane, L.J., Alberts, E.E., Laflen, J.M., 1990. Prediction technology for soil erosion by water: Status and research needs. Soil Sci. Soc. Am. J. 54: 1702-1711.

Nielsen, D.R., Wendroth, O., 2003. Spatial and temporal statistics: Sampling field soils and their vegetation. Catena Verlag, Reiskirchen, 398 pp.

Niemczynowicz, J., 1982. Areal intensity-duration-frequency curves for short-term rainfall events in Lund. Nordic Hydrol. 13: 193-204.

Nyssen, J., Vandenreyken, H., Poesen, J., Moeyersons, J., Deckers, J., Haile, M., Salles, C., Govers, G., 2005. Rainfall erosivity and variability in the Northern Ethiopian Highlands. J. Hydrol. 311: 172-187.

Oades, J.M., 1987. Aggregation in soils. pp. 74-101. *In* Rengasamy P. (Editor). Soil structure and aggregate stability. Dept. of Agriculture and Rural Affairs, Victoria.

Odeh, I.O.A., McBratney, A.B., Chittleborough, D.J., 1994. Spatial prediction of soil properties from landform attributes derived from a digital elevation model. Geoderma 63: 197-214.

Odeh, I.O.A., McBratney, A.B., Chittleborough, D.J., 1995. Further results on prediction of soil properties from terrain attributes: heterotrophic cokriging and regression-kriging. Geoderma 67: 215-226.

Oldeman, L.R., Hakkeling, R.T.A., Sombroek, W.G., 1991. World map of the status of human-induced soil degradation. Global Assessment of soil degradation. ISRIC and UNEP, Wageningen.

Onstad, C.A., 1984. Depressional storage on tilled soil surfaces. Trans. ASAE 27: 729-732.

Onstad, C.A., Wolfe, M.L., Larson, C.L., Slack, D.C., 1984. Tilled soil subsidence during repeated wetting. Trans. ASAE 27: 733-736.

Overgaard, S., El-Shaarawi, A.H., Arnbjerg-Nielsen, K., 1998. Calibration of tipping bucket rain gauges. Wat. Sci. Technol. 37: 139-145.

Owens, P.N., Duzant, J.H., Deeks, L.K., Wood, G.A., Morgan, R.P.C., Collins, A.J., 2007. Evaluation of contrasting buffer features within an agricultural landscape for reducing sediment and sediment-associated phosphorus delivery to surface waters. Soil Use Manag. 23: 165-175.

Papamichail, D.M., Metaxa, I.G., 1996. Geostatistical analysis of spatial variability of rainfall and optimal design of a rain gauge network. Wat. Resourc. Manag. 10: 107-127.

Papy, F., Douyer, C., 1991. Influence des états de surface du territoire agricole sur le déclenchement des inondations catastrophiques. Agronomie 11: 201-215.

Parson, J.E., Thomas, D.L., Huffman, R.L., 2001. Agricultural non-point source water-quality models: their use and application. Southern Cooperative Series Bulletin No. 398.

Parsons, A.J., Wainwright, J., Powell, D.M., Brazier, R.E., 2004. A conceptual model for determining soil erosion by water. Earth Surf. Process. Landforms 29: 1293-1302.

Pebesma, E.J., 2004. Mutivariable geostatistics in S: the gstat package. Comput. Geosci. 30: 683-691.

Phillips, J.D., 1991. Fluvial sediment budget in the North Carolina Piedmont. Geomorphology 4: 231-241.

Ping, J.L., Dobermann, A., 2006. Variation in the precision of soil organic carbon maps due to different laboratory and spatial prediction methods. Soil Sci. 171: 374-387.

Poesen, J.W.A., Verstraeten, G., Soenens, R., Seynaeve, L., 2001. Soil losses due to harvesting of chicory roots and sugar beet: an underrated geomorphic process? Catena 43: 35-47.

Polyakov, V.O., Lal, R., 2004. Soil erosion and carbon dynamics under simulated rainfall. Soil Sci. 169: 590-599.

Puigdefabregas, J., 2005. The role of vegetation patterns in structuring runoff and sediment fluxes in drylands. Earth Surf. Process. Landforms 30: 130-147.

Pulleman, M., Jongmans, A., Marinissen, J., Bouma, J., 2003. Effects of organic versus conventional arable farming on soil structure and organic matter dynamics in a marine loam in the Netherlands. Soil Use Manag. 19: 157-165.

Quinn, P.F., Beven, K., Chevallier, P., Planchon, O., 1991. The prediction of hillslope flow paths for distributed hydrological modelling using digital terrain models. Hydrol. Proc. 5: 59-79.

Quinton, J.N., Catt, J.A., 2004. The effects of minimal tillage and contour cultivation on surface runoff, soil loss and crop yield in the long-term Woburn Erosion Reference Experiment on sandy soil at Woburn, England. Soil Use Manag. 20: 343-349.

Quirmbach, M., Schultz, G.A., 2002. Comparison of rain gauge and radar data as input to an urban rainfall-runoff model. Wat. Sci. Technol. 45: 27-33.

R Development Core Team, 2007. R: A language and environment for statistical computing. http://www.R-project.org.

Rabus, B., Eineder, M., Roth, A., Bamler, R., 2003. The shuttle radar topography mission - a new class of digital elevation models acquired by spaceborne radar. ISPRS J. Photogramm. 57: 241-262.

Raich, J.W., Potter, C.S., 1995. Global patterns of carbon-dioxide emissions form soils. Global Biogeochem. Cycles 9: 23-36.

Rasmussen, K.J., 1999. Impact of ploughless soil tillage on yield and soil quality: A Scandinavian review. Soil Tillage Res. 53: 3-14.

Rawls, W.J., Brakensiek, D.L., Simanton, J.R., Kohl, K.D., 1990. Development of a crust factor for a Green Ampt model. Trans. ASAE 33: 1224-1228.

Rawls, W.J., Pachepsky, Y.A., Ritchie, J.C., Sobecki, T.M., Bloodworth, H., 2003. Effect of soil organic carbon on soil water retention. Geoderma 116: 61-76.

Reganold, J.P., Elliott, L.F., Unger, Y.L., 1987. Long-term effects of organic and conventional farming on soil erosion. Nature 330: 370-372.

Renard, K.G., Foster, G.R., Weesies, G.A., McCool, D.K., Yoder, D.C., 1996. Predicting soil erosion by water: A guide to conservation planning with the Revised Universal Soil Loss Equation (RUSLE). USDA, Agricultural Research Service, Washington, DC, 119 pp.

Renard, K.G., Foster, G.R., Weesies, G.A., Porter, J.P., 1991. RUSLE - Revised universal soil loss equation. J. Soil Water Conserv. 46: 30-33.

Renard, K.G., Foster, G.R., Yoder, D.C., McCool, D.K., 1994. RUSLE revisited: Status, questions, answers, and the future. J. Soil Water Conserv. 49: 213-220.

Richter, D., 1995. Ergebnisse methodischer Untersuchungen zur Korrektur des systematischen Meßfehlers des Hellmann-Niederschlagsmessers. DWD Offenbach Selbstverlag, 93 pp.

Richter, G., 1991. The Soil Erosion Measurement Station and its program. Foschungsstelle Bodenerosion 10: 97-108.

Risse, L.M., Liu, B.Y., Nearing, M.A., 1995. Using curve numbers to determine baseline values of Green-Ampt effective hydraulic conductivities. Water Resources Bull. 31: 147-158.

Ritchie, J.C., McCarty, G.W., 2003. $^{137}$Cesium and soil carbon in a small agricultural watershed. Soil Tillage Res. 69: 45-51.

Ritchie, J.C., McCarty, G.W., Venteris, E.R., Kaspar, T.C., 2007. Soil and soil organic carbon redistribution on the landscape. Geomorphology 89: 163-171.

Roberson, T., Bundy, L.G., Andraski, T.W., 2007. Freezing and drying effects on potential plant contributions to phosphorus in runoff. J. Environ. Qual. 36: 532-539.

Roels, J.M., 1984. Flow resistance in concentrated overland flow on rough slope surfaces. Earth Surf. Process. Landforms 9: 541-551.

Rogler, H., 1981. Die Erosivität der Niederschläge in Bayern. Master-Thesis. TU München, Lehrstuhl f. Bodenkunde. Freising-Weihenstephan, Germany.

Rogler, H., Schwertmann, U., 1981. Erosivität der Niederschläge und Isoerodentkarte Bayerns. Z. Kulturtechn. Flurber. 22: 99-112.

Rossi, R.E., Mulla, D.J., Journel, A.G., Franz, E.H., 1992. Geostatistical tools for modeling and interpreting ecological spatial dependence. Ecol. Monogr. 62: 277-314.

Roth, C., 1992. Die Bedeutung der Oberflächenverschlämmung für die Auslösung von Abfluß und Abtrag. Institut für Ökologie, TU Berlin, Berlin, 179 pp.

Rouhani, S., Myers, D.E., 1990. Problems in space-time kriging of geohydrological data. Math. Geol. 22: 611-623.

Rousseva, S.S., Ahuja, L.R., Heathman, G.C., 1998. Use of a surface gamma-neutron gauge for in-situ measurements of changes in bulk density. Soil Tillage Res. 12: 235-251.

Rozanski, K., Froehlich, K., Mook, W.G., Stichler, W., 2001. Environmental isotopes in the hydrological cycle - principles and applications. Technical Documents in Hydrology 39, 117 pp.

Rushton, B.T., Bahk, B.M., 2001. Treatment of stormwater runoff from row crop farming in Ruskin, Florida. Wat. Sci. Technol. 44: 531-538.

Ruysschaert, G., Poesen, J., Verstraeten, G., Govers, G., 2006. Soil losses due to mechanized potato harvesting. Soil Tillage Res. 86: 52-72.

Saleh, A., 1993. Soil roughness measurement: Chain method. J. Soil Water Conserv. 48: 527-529.

Saleh, A., Fryrear, D.W., 1999. Soil roughness for the revised wind erosion equation (RWEQ). J. Soil Water Conserv. 54: 473-476.

Samiuddin, M., 1970. On a test for an assigned value of correlation in a bivariate normal distribution. Biometrika 57: 461-464.

Sanchez, G., Puigdefabregas, J., 1994. Interactions of plant growth and sediment movement on slopes in a semi-arid environment. Geomorphology 9: 243-260.

Sander, G.C., Hairsine, P.B., Beuselinck, L., Govers, G., 2002. Steady state sediment transport through an area of net deposition: multi-size class solutions. Wat. Resourc. Res. 38: 1087. DOI: 10.1029/2001 WR000323.

Sauerborn, P., 1994. Die Erosivität der Niederschläge in Deutschland - Ein Beitrag zur quantitativen Prognose der Bodenerosion durch Wasser in Mitteleuropa. *In* Bonner Bodenkundliche Abhandlungen. Vol. 13. Institut für Bodenkunde, Bonn, 189 pp..

Saupe, G., 1990. Winterweizen - unterschätzte Erosionsgefahren? Feldwirtsch. 31: 367-368.

Schäuble, H., 2004. HydroTools 1.0 for ArcView 3.x. http://www.terracs.de/Hydrotools_eng.pdf.

Scheinost, A.C., Schwertmann, U., 1995. Predicting phosphate adsorption-desorption in a soilscape. Soil Sci. Soc. Am. J. 59: 1575-1580.

Scheinost, A.C., Sinowski, W., Auerswald, K., 1997. Regionalization of soil water retention curves in a highly variable soilscape, I. Developing a new pedotransfer function. Geoderma 78: 129-143.

Schiettecatte, W., Gabriels, D., Cornelis, W., Hofinan, G., 2008. Impact of deposition on the enrichment of organic carbon in eroded soil. Catena 72: 340-347.

Schiettecatte, W., Ke, J., Yao, Y., Cornelis, W.M., Junjie, L., Huijun, W., Verbist, K., Dianxiong, C., Gabriels, D., Hartmann, R., 2005. Influence of simulated rainfall on physical properties of a conventionally tilled loess soil. Catena 64: 209-221.

Schimmack, W., Auerswald, K., Bunzl, K., 2002. Estimation of soil erosion and deposition rates at an agricultural site in Bavaria, Germany, as derived from fallout radiocesium and plutonium as tracers. Naturwissenschaften 89: 43-46.

Schjonning, P., Thomsen, I.K., Moldrup, P., Christensen, B.T., 2003. Linking soil microbial activity to water- and air-phase contents and diffusivities. Soil Sci. Soc. Am. J. 67: 156-165.

Schlesinger, W.H., 2005. The global carbon cycle and climate change. Adv. Econ. Environ. Resour. 5: 31-53.

Schmidt, F., 1979. Die Abschätzung des Bodenabtrages in Hopfengärten mit Hilfe der Kupferbilanz. PhD thesis, TU München, Freising-Weihenstephan.

Schmitt, T.J., Dosskey, M.G., Hoagland, K.D., 1999. Filter strip performance and processes for different vegetation, widths, and contaminants. J. Environ. Qual. 28: 1479-1489.

Schreiber, J.D., 1985. Leaching of nitrogen, phosphorus, and organic carbon from wheat straw residues: II. Loading rate. J. Environ. Qual. 14: 256-261.

Schreiber, J.D., Duffy, P.D., McDowell, L.L., 1990. Nutrient leaching of a loblolly pine forest floor by simulated rainfall. I. Intensity effects. Forest Sci. 36: 765-776.

Schreiber, J.D., McDowell, L.L., 1985. Leaching of nitrogen, phosphorus, and organic carbon from wheat straw residues: I. Rainfall intensity. J. Environ. Qual. 14: 251-256.

Schröder, R., 2000. Modellierung von Verschlämmung und Infiltration in landwirtschaftlich genutzten Einzugsgebieten. *In* Bonner Geographische Abhandlungen. Vol. 101. Geographisches Institut. Bonn, 175 pp.

Schröder, R., Auerswald, K., 2000. Modellierung des Jahresgangs der verschlämmungsinduzierten Abflussbildung in kleinen landwirtschaftlich genutzten Einzugsgebieten. Z. Kulturtechnik Landentw. 41: 167-172.

Schülein, J., 1998. Untersuchungen zum lateralen Transport von Herbiziden und Herbizidmetaboliten in einem Agrarökosystem. Technische Universität München, 145 pp.

Schüller, H., 1969. Die CAL-Methode, eine neue Methode zur Bestimmung des pflanzenverfügbaren Phosphats in Böden. Z. Pflanzenernähr. Bodenkd. 123: 48-63.

Schuurmans, J.M., Bierkens, M.F.P., Pebesma, E.J., Uijlenhoet, R., 2007. Automatic prediction of high-resolution daily rainfall fields for multiple extents: The potential of operational radar. J. Hydrometeorol. 8: 1204-1224.

Schwab, G.O., Fangmeier, D.D., Elliot, W.J., 1993. Soil and water management systems. John Wiley & Sons, New York. 372 pp.

Schwertmann, U., Schmidt, F., 1980. Estimation of long term soil loss using copper as a tracer. *In* De Boodt M., Gabriels D. (Editors). Assessment of Erosion. Wiley, pp. 203-206.

Schwertmann, U., Vogl, W., Kainz, M., 1987. Bodenerosion durch Wasser - Vorhersage des Abtrags und Bewertung von Gegenmaßnahmen. Ulmer Verlag, Stuttgart, 64 pp.

Scullion, J., Neale, S., Philipps, L., 2002. Comparisons of earthworm populations and cast properties in conventional and organic arable rotations. Soil Use Manag. 18: 293-300.

Sharpley, A.N., 1981. The contribution of phosphorus leached from crop canopy to losses in surface runoff. J. Environ. Qual. 10: 160-165.

Sharpley, A.N., 1993. Estimating phosphorus in agricultural runoff available to several algae using iron-oxide paper strips. J. Environ. Qual. 22: 678-680.

Sharpley, A.N., Chapra, S.C., Wedepohl, R., Sims, J.T., Daniel, T.C., Reddy, K.R., 1994. Managing agricultural phosphorus for protection of surface waters: Issues and options. J. Environ. Qual. 23: 437-451.

Sharpley, A.N., Daniel, T.C., Edwards, D.R., 1993. Phosphorus movement in the landscape. J. Prod. Agric. 6: 492-500.

Sharpley, A.N., Kleinman, P.J.A., McDowell, R.W., Gitau, M., Bryant, R.B., 2002. Modeling phosphorus transport in agricultural watersheds: Processes and possibilities. J. Soil Water Conserv. 57: 425-439.

Sharpley, A.N., Robinson, J.S., Smith, S.J., 1995. Bioavailable phosphorus dynamics in agricultural soils and effects on water quality. Geoderma 67: 1-15.

Sharpley, A.N., Smith, S.J., Berg, W.A., Williams, J.R., 1985. Nutrient runoff losses as predicted by annual and monthly sampling. J. Environ. Qual. 14: 354-360.

Sharpley, A.N., Smith, S.J., Jones, O.R., Berg, W.A., Coleman, G.A., 1992. The transport of bioavailable phosphorus in agricultural runoff. J. Environ. Qual. 21: 30-35.

Sharpley, A.N., Smith, S.J., Menzel, R.G., 1989. Phosphorus dynamics in agricultural runoff and reservoirs in Oklahoma. Lake Reservoir Manag. 5: 75-81.

Sharpley, A.N., Williams, J.R., (Editors) 1990. EPIC - Erosion/Productivity Impact Calculator: 1. Model documentation., U.S. Dep. Agric., Techn. Bull. 1768, 235 pp.

Siegrist, S., Schaub, D., Pfiffner, L., Mader, P., 1998. Does organic agriculture reduce soil erodibility? The results of a long-term field study on loess in Switzerland. Agric. Ecosys. Environ. 69: 253-264.

Silverman, B.W., 1986. Density estimation for statistics and data analysis. Chapman and Hall / CRC, London, 176 pp.

Simbahan, G.C., Dobermann, A., Goovaerts, P., Ping, J., Haddix, M.L., 2006. Fine-resolution mapping of soil organic carbon based on multivariate secondary data. Geoderma 132: 471-489.

Sinowski, W., Auerswald, K., 1999. Using relief parameters in a discriminate analysis to stratify geological areas with different spatial variability of soil properties. Geoderma 89: 113-128.

Sinowski, W., Scheinost, A.C., Auerswald, K., 1997. Regionalization of soil water retention curves in a highly variable soilscape, II. Comparison of regionalization procedures using a pedotransfer function. Geoderma 78: 145-159.

Sivakumar, M.V.K., Hatfield, J.L., 1990. Spatial variability of rainfall at an experimental station in Niger, West Africa. Theor. Appl. Climatol. 42: 33-39.

Six, J., Paustian, K., Elliot, E.T., Combrink, C., 2000. Soil structure and organic matter: I. Distribution of aggregate-size classes and aggregate-associated carbon. Soil Sci. Soc. Am. J. 64: 681-689.

Smith, K.A., Ball, T., Conen, F., Dobbi, K.E., Massheder, J., Rey, A., 2003. Exchange of greenhouse gases between soil and atmosphere: interactions of soil physical factors and biological processes. Europ. J. Soil Sci. 54: 779-791.

Smith, R.E., Goodrich, D.C., Woolhiser, D.A., Unkrich, C.L., 1995. KINEROS - A kinematic runoff and erosion model. *In* Singh V.P. (Editor). Computer models of watershed hydrology. Water Resources Publications, Collins, pp. 697-732.

Smith, R.J., Hancock, N.H., Ruffini, J.L., 1991. Strip cropping - development of guidelines for the selection of strip spacing. Agric. Water Manag. 20: 1-16.

Smith, S.V., Sleezer, R.O., Renwick, W.H., Buddemeier, R.W., 2005. Fates of eroded soil organic carbon: Mississippi basin case study. Ecol. Appl. 15: 1929-1940.

Souchère, V., Cerdan, O., Dubreuil, N., Le Bissonnais, Y., King, C., 2005. Modelling the impact of agri-environmental scenarios on runoff in a cultivated catchment (Normandy, France). Catena 61: 229-240.

Soucherè, V., King, D., Daroussin, J., Papy, F., Capillon, A., 1998. Effects of tillage on runoff directions: consequences on runoff contributing area within agricultural catchments. J. Hydrol. 206: 256-267.

Srivastava, P., Hamlett, J.M., Robillard, P.D., Day, R.L., 2002. Watershed optimization of best management practices using AnnAGNPS and a genetic algorithm. Wat. Resourc. Res. 38: 31-314.

Stallard, R., 1998. Terrestrial sedimentation and the carbon cycle: Coupling weathering and erosion to carbon burial. Global Biogeochem. Cycles 12: 231-257.

Steegen, A., 2001. Sediment deposition in and export from small agricultural catchments. PhD thesis, K.U. Leuven, Leuven, Belgium. 220 pp.

Steegen, A., Govers, G., Takken, I., Nachtergaele, J., Poesen, J., Merckx, R., 2001. Factors controlling sediment and phosphorus export from two Belgian agricultural catchments. J. Environ. Qual. 30: 1249-1258.

Steiner, J.L., 1994. Crop residue effects on water conservation. *In* Unger P.W. (Editor). Managing agricultural residues. Lewis Publishers, pp. 41-76.

Steudle, G., 1997. Surveying and mapping Germany. GIS Europe 6: 22-24.

Stevens, A., Van Wesemael, B., Bartholomeus, H., Rosillon, D., Tychon, B., Ben-Dor, E., 2008. Laboratory, field and airborne spectroscopy for monitoring organic carbon content in agricultural soils. Geoderma 144: 395-404.

Stow, C.D., Dirks, K.N., 1998. High-resolution studies of rainfall on Norfolk Island: Part 1: The spatial variability of rainfall. J. Hydrol. 208: 163-186.

Strudley, M.W., Green, T.R., Ascough II, J.C., 2008. Tillage effects on soil hydraulic properties in space and time: State of the science. Soil Tillage Res. 99: 4-48.

Sumfleth, K., Duttmann, R., 2008. Prediction of soil property distribution in paddy soil landscapes using terrain data and satellite information as indicators. Ecol. Indic. 8: 485-501.

Syed, K.H., Goodrich, D.C., Myers, D.E., Sorooshian, S., 2003. Spatial characteristics of thunderstorm rainfall fields and their relation to runoff. J. Hydrol. 271: 1-21.

Syversen, N., 2005. Effect and design of buffer zones in the Nordic climate: The influence of width, amount of surface runoff, seasonal variation and vegetation type on retention efficiency for nutrient and particle runoff. Ecol. Eng. 24: 483-490.

Syversen, N., Borch, H., 2005. Retention of soil particle fractions and phosphorus in cold-climate buffer zones. Ecol. Eng. 25: 382-394.

Takata, Y., Funakawa, S., Akshalov, K., Ishida, N., Kosaki, T., 2007. Spatial prediction of soil organic matter in northern Kazakhstan based on topographic and vegetation information. Soil Sci. Plant Nutr. 53: 289-299.

Takken, I., Govers, G., Jetten, V., Nachtergaele, J., Steegen, A., Poesen, J., 2001a. Effects of tillage on runoff and erosion patterns. Soil Tillage Res. 61: 55-60.

Takken, I., Govers, G., Steegen, A., Nachtergaele, J., Guerif, J., 2001b. The prediction of runoff flow directions on tilled fields. J. Hydrol. 248: 1-13.

Takken, I., Jetten, V., Govers, G., Nachtergaele, J., Steegen, A., 2001c. The effect of tillage-induced rouhgness on runoff and erosion patterns. Geomorphology 37: 1-14.

Tang, J.W., Baldocchi, D.E., Qi, Y., Xu, L.K., 2003. Assessing soil $CO_2$ efflux using continuous measurements of $CO_2$ profiles in soils with small solid-state sensors. Agr. Forest Meteorol. 118: 207-220.

Taupin, J.D., 1997. Characterization of rainfall spatial variability at a scale smaller than 1 km in a semiarid area (region of Niamey, Niger). Comptes Rendus de l Academie des Sciences Serie Ii Fascicule A-Sciences de la Terre et des Planetes 325: 251-256.

Terra, J.A., Shaw, J.N., Reeves, D.W., Raper, R.L., van Santen, E., Mask, P.L., 2004. Soil carbon relationships with terrain attributes, electrical conductivity, and a soil survey in a coastal plain landscape. Soil Sci. 169: 819-831.

Thomas, R.S., Franson, R.L., Bethlenfalvay, G.J., 1993. Separation of vesicular-arbuscular mycorrhizal fungus and root effects on soil aggregation. Soil Sci. Soc. Am. J. 57: 57-81.

Tisdall, J.M., Oades, J.M., 1982. Organic matter and water-stable aggregates in soils. J. Soil Sci. 33: 141-163.

Tsanis, I.K., Gad, M.A., Donaldson, N.T., 2002. A comparative analysis of rain-gauge and radar techniques for storm kinematics. Adv. Wat. Resour. 25: 305-316.

Tufekcioglu, A., Raich, J.W., Isenhart, T.M., Schultz, R.C., 2001. Soil respiration within riparian buffers and adjacent crop fields. Plant Soil 229: 117-124.

Turner, M.G., 1989. Landscape ecology: The effect of pattern on process. Annu. Rev. Ecol. Evol. Syst. 20: 171-197.

USDA-SCS, 1986. Urban hydrology for small watersheds. Technical release 55, USDA-SCS, Washington DC, 164 pp.

Uusi-Kämppä, J., 2007. Effects of freezing and thawing on DRP losses from buffer zones. *In* Heckarth G., Rubæk G.H., Kornvang B. (Editors). Diffuse phosphorus loss: Risk assessment, mitigation options and ecological effects in river basins. pp. 169-172.

Uusi-Kämppä, J., Braskerud, B., Jansson, H., Syversen, N., Uusitalo, R., 2000. Buffer zones and constructed wetlands as filters for agricultural phosphorus. J. Environ. Qual. 29: 151-158.

Uusi-Kämppä, J., Turtola, E., Hartikainen, H., Yläranta, T., 1997. The interactions of buffer zones and phosphorus runoff. *In* Haycock N.E., Burt T.P., Goulding K.W.T., Pinay G. (Editors). Buffer zones: Their processes and potential in water protection. Quest Environment, Harpenden, GB, pp. 43-53.

Valentin, C., d`Herbes, J.M., Poesen, J., 1999. Soil and water components of banded vegetation patterns. Catena 37: 1-24.

Valette, G., Prévost, S., Laurent, L., Leónard, J., 2008. A dynamic model of cracks development based on a 3D discrete shrinkage volume propagation. Computer Graphics Forum 27: 47-62.

Van Dam, D., Heil, F.W., Heijne, B., 1987. Throughfall chemistry of grassland vegetation: a new method with ion-exchange resins. Functional Ecol. 1: 423-427.

Van Dijk, P.M., Auzet, A.V., Lemmel, M., 2005. Rapid assessment of field erosion and sediment transport pathways in cultivated catchments after heavy rainfall events. Earth Surf. Process. Landforms 30: 169-182.

Van Es, H.M., Ogden, C.B., Hill, R.L., Schindelbeck, R.R., Tsegaye, T., 1999. Integrated assessment of space, time, and management-related variability of soil hydraulic properties. Soil Sci. Soc. Am. J. 63: 1599-1608.

Van Oost, K., 2003. Spatial modelling of soil redistribution processes in agricultural landscapes. PhD thesis, K.U. Leuven, Leuven, Belgium, 250 pp.

Van Oost, K., Beuselinck, L., Hairsine, P.B., Govers, G., 2004. Spatial evaluation of multiclass sediment transport and deposition model. Earth Surf. Process. Landforms 29: 1027-1044.

Van Oost, K., Govers, G., Desmet, P., 2000. Evaluating the effects of changes in landscape structure on soil erosion by water and tillage. Landscape ecol. 15: 577-589.

Van Oost, K., Quine, T.A., Govers, G., De Gryze, S., Six, J., Harden, J.W., Ritchie, J.C., McCarty, G.W., Heckrath, G., Kosmas, C., Giraldez, J.V., Marques da Silva, J.R., Merckx, R., 2007. The impact of agricultural soil erosion on the global carbon cycle. Science 318: doi:10.1126/science.1145724.

Van Rompaey, A.J.J., Verstraeten, G., Van Oost, K., Govers, G., Poesen, J., 2001. Modelling mean annual sediment yield using a distributed approach. Earth Surf. Process. Landforms 26: 1221-1236.

Verstraeten, G., Poesen, J., 1999. The nature of small-scale flooding, muddy floods and retention pond sedimentation in central Belgium. Geomorphology 29: 275-292.

Verstraeten, G., Poesen, J., 2000a. Estimating trap efficiency of small reservoirs and ponds: methods and implications for the assessment of sediment yield. Progress Phys. Geogr. 24: 219-251.

Verstraeten, G., Poesen, J., 2000b. The importance of sediment characteristics and trap efficiency in assessing sediment yield using retention ponds. Phys. Chem. Earth 26: 83-87.

Verstraeten, G., Poesen, J., Gillijns, K., Govers, G., 2006. The use of riparian vegetated filter strips to reduce river sediment loads: an overestimated control measure? Hydrol. Proc. 20: 4259-4267.

Verstraeten, G., Poesen, J., Govers, G., Gillijns, K., Van Rompaey, A., Van Oost, K., 2003. Integrating science, policy and farmers to reduce soil loss and sediment delivery in Flanders, Belgium. Environ. Sci. Policy 6: 95-103.

Verstraeten, G., Van Oost, K., Van Rompaey, A., Poesen, J., Govers, G., 2002. Evaluating an integrated approach to catchment management to reduce soil loss and sediment pollution through modelling. Soil Use Manag. 19: 386-394.

Vivoni, E.R., Teles, V., Ivanov, V.Y., Bras, R.L., Entekhabi, D., 2005. Embedding landscape processes into triangulated terrain models. Int. J. Geogr. Inf. Sci. 19: 429-457.

Voltz, M., Webster, R., 1990. A comparison of kriging, cubic splines and classification for predicting soil properties from sample information. J. Soil Sci. 41: 473-490.

Warren, S.D., Hohmann, M.G., Auerswald, K., Mitasova, H., 2004. An evaluation of methods to determine slope using digital elevation data. Catena 58: 215-233.

Watson, C.A., Atkinson, D., Gosling, P., Jackson, L.R., Rayns, F.W., 2002. Managing soil fertility in organic farming systems. Soil Use Manag. 28: 239-247.

Wauchope, R.D., 1978. The pesticide content of surface water draining from agricultural fields - A review. J. Environ. Qual. 7: 459-472.

Webster, R., Oliver, M.A., 2001. Geostatistics for environmental scientists. Wiley, Chichester, 271 pp.

Werner, W., Olfs, H.W., Auerswald, K., Isermann, K., 1991. Stickstoff- und Phosphoreintrag in Oberflächengewässer über "diffuse Quellen". *In* Hamm A. (Editor). Studie über Wirkungen und Qualitätsziele von Nährstoffen in Fließgewässern. Academia Verlag, Sankt Augustin, pp. 665-764.

Western, A.W., Blöschl, G., Grayson, R.B., 2001. Toward capturing hydrologically significant connectivity in spatial patterns. Wat. Resourc. Res. 37: 83-97.

Wiens, J.A., 1976. Population responses to patchy environments. Annu. Rev. Ecol. Evol. Syst. 7: 81-120.

Williams, J.R., 1985. The physical components of the EPIC model. *In* El-Swaify S.A., Moldenhauer W.C., Lo A. (Editors). Soil Conservation Society of America, Ankeny, IA, pp. 272-284.

Williams, J.R., Jones, C.A., Dyke, P.T., 1984. A modeling approach to determining the relationship between erosion and soil productivity. Trans. ASAE 27: 129-144.

Wischmeier, W.H., 1959. A rainfall erosion index for a universal soil-loss equation. Soil Sci. Soc. Am. Proc. 23: 246-249.

Wischmeier, W.H., 1960. Cropping-management factor evaluations for a universal soil-loss equation. Soil Sci. Soc. Am. Proc. 24: 322-326.

Wischmeier, W.H., 1975. Estimating the soil loss equations' cover and management factor for undisturbed areas. *In* US Agr.Res.Ser. (Editor). Present and prospective technology for predicting sediment yields and sources. pp. 118-124.

Wischmeier, W.H., Smith, D.D., 1958. Rainfall energy and its relationship to soil loss. Trans. Am. Geophys. Union 39: 285-291.

Wischmeier, W.H., Smith, D.D., 1960. A universal soil-loss equation to guide conservation farm planning. *In* Proceedings 7th Intern. Congress of Soil Science. Madison, Wisc.

Wischmeier, W.H., Smith, D.D., 1978. Predicting rainfall erosion losses - a guide to conservation planning. USDA Agric. Handbook 537, U.S. Gov. Print Office, Washington, D.C.

Wösten, J.H.M., Pachepsky, Y., Rawls, W.J., 2001. Pedotransfer functions: Bridging the gap between available basic soil data and missing soil hydraulic characteristics. J. Hydrol. 251: 123-150.

Yoder, D.C., Poster, J.P., Laflen, J.M., Simanton, J.R., Renard, K.G., McCool, D.K., Foster, G.R., 1997. Cover-management factor (C). *In* Renard K.G., Foster G.R., Weesies G.A., McCool D.K., Yoder D.C. (Editors). Predicting soil erosion by water: A guide to conservation planning with the revised universal soil loss equation (RUSLE). U.S. Dep. Agric., Washington D.C., pp. 143-181.

Yoo, K., Amundson, R., Heimsath, A.M., Dietrich, W.E., 2005. Erosion of upland hillslope soil organic carbon: Coupling field measurements with a sediment transport model. Global Biogeochem. Cycles 19: GB 3003, doi:10.1029/2004GB002271.

Young, R.A., Onstad, C.A., Bosch, D.D., 1995. AGNPS: An agricultural nonpoint source model. *In* Singh V.P. (Editor). Computer models of watershed hydrology. Water Resources Publications, Morris, pp. 1001-1020.

Young, R.A., Onstad, C.A., Bosch, D.D., Anderson, W.P., 1989. AGNPS: A nonpoint-source pollution model for evaluating agricultural watersheds. J. Soil Water Conserv. 44: 168-173.

Zhang, J.N., Quine, T.A., Ni, S., Ge, F., 2006. Stocks and dynamics of SOC in relation to soil redistribution by water and tillage erosion. Global Change Biol. 12: 1834-1841.

Ziegler, A.D., Giambelluca, T.W., Plondke, D., Leisz, S., Tran, L.T., Fox, J., Nullet, M.A., Vogler, J.B., Minh Troung, D., Tran, D., V, 2007. Hydrological consequences of land-scape fragmentation in mountainous northern Vietnam: Buffering of Hortonian overland flow. J. Hydrol. 337: 52-67.

Zobeck, T.M., Onstad, C.A., 1987. Tillage and rainfall effects on random roughness: a review. Soil Tillage Res. 9: 1-20.